



EUROPEAN
COMMISSION

Community research

BELBaR

(Contract Number: 295487)

Deliverable D6.14

**Proceedings from second workshop, final conference of the
BELBaR project.
Berlin, 3-4 February 2016**

Date of issue of this report: 2016-02-19

Start date of project: 01/03/12

Duration: 48 Months

Project co-funded by the European Commission under the Seventh Euratom Framework Programme for Nuclear Research & Training Activities (2007-2011)		
Dissemination Level		
PU	Public	X
RE	Restricted to a group specified by the partners of the BELBaR project	
CO	Confidential, only for partners of the BELBaR project	

BELBaR



DISTRIBUTION LIST

Name	Number of copies	Comments
Christophe Davies (EC) BELBaR participants		

BELBaR

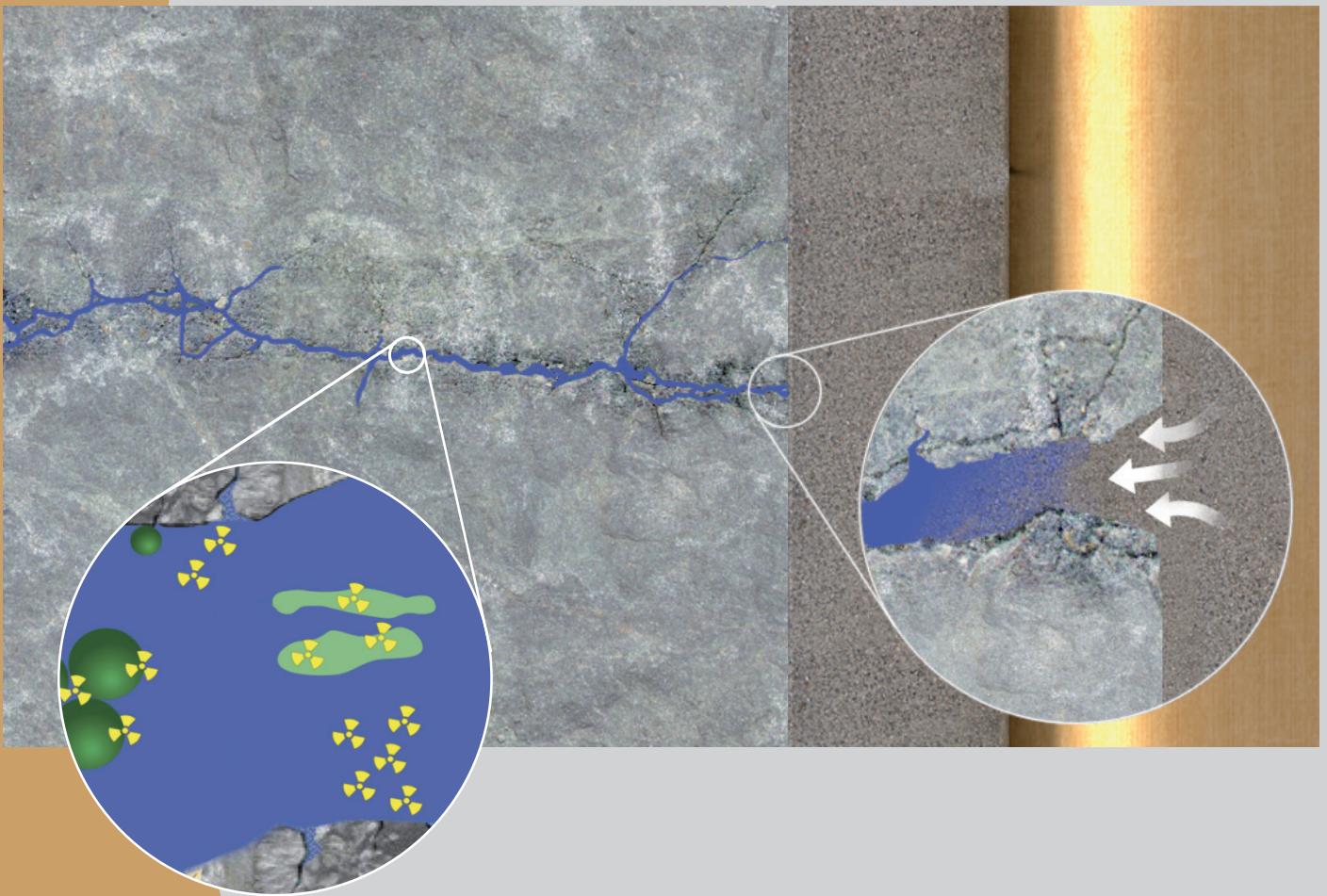
(D-N°:D6.14) – Proceedings from second workshop, final conference of the BELBaR project,
Berlin, 3-4 February 2016
Dissemination level: PU
Date of issue of this report: **19/02/2016**



The BELBaR project has received funding from the European Atomic Energy Community's (EURATOM) 7th Framework Programme (FP7/2007-2011) under the grant agreement No. 295487

Final conference

Clay Colloids in Aqueous Systems



Stability of clay colloids
Sorption/desorption of pollutants on colloids
Erosion of clay
Modelling of clay colloids

3 and 4 February 2016
Seminaris CampusHotel Berlin

Partners

No.	Acronym	Name	Country
1	SKB	Svensk Kärnbränslehantering	SE
2	CIEMAT	Centro de Investigatigaciones Energeticas, Medioambientales y Technologicas	ES
3	NRI	Nuclear Research institute Rez plc	CZ
4	KIT	Karlsruhe Institut of Technology	GE
5	POSIVA	Posiva OY	FI
6	VTT	Technical Research Institute of Finland	FI
7	ClayTech	Clay Technology	SE
8	JYU	University of Jyväskylä	FI
9	KTH	Kungliga Tekniska Högskolan	SE
10	NDA/RWM	Nuclear Decommissioning Authority/ Radioactive Waste Management	GB
11	B+Tech	B+Tech	FI
12	UNIMAN	University of Manchester	GB
13	HU	Helsinki University	FI
14	MSU	Lomonosov Moscow State University	RU

WELCOME to the BELBaR End Conference Clay Colloids in Aqueous Systems

BELBaR

The main aim of the BELBaR project has been to increase the knowledge of the processes that controls clay colloid stability, generation and ability to transport radionuclides. The overall purpose of the project will be to suggest a treatment of the issues in long-term safety/performance assessment.

Nature and scope of the project

Partners include national radioactive waste management organisations (WMOs) from a number of countries, research institutes, universities and commercial organisations working in the radioactive waste disposal field. The Collaborative Project is based on the desire to improve the long-term safety assessments for repository concepts that combine a clay Engineered Barrier System (EBS) with a fractured rock. The formation and stability of colloids from the EBS may have a direct impact of assessed risk from the repository in two aspects:

- Generation of colloids may degrade the engineered barrier
- Colloid transport of radionuclides may reduce the efficiency of the natural barrier. An increased understanding of processes will have an effect on the outcome of future assessments.

Activities

The main aim of BELBaR has been to reduce the uncertainties in the description of the effect of clay colloids on the long term performance of the engineered barrier and on radionuclide transport. This has been done by:

- Improving the understanding on when bentonite colloids are unstable. For a given site/site evolution, this is critical information, since it determines whether or not clay colloids need to be included in the long-term assessment.
- Improving the quantitative models for erosion on the bentonite barrier for the cases when the colloids are stable
- Improving the understanding of how radionuclides attach to clay colloids. This information will be used to formulate improved transport models for the assessment of radionuclide transport in the Geosphere.

To meet the main aim and number of experimental and modelling activities will be undertaken within the project. Another objective is to take full advantage of the collaborative project structure. Key issues in BELBaR are therefore interaction, communication and cooperation. Since a large part of the work within project will be of interest for a more general community, the objective is to, as far as reasonably possible, publish the results in peer-reviewed journals.

Results

There is a large pool of knowledge about colloid stability both from the general scientific literature and from national and international projects within the nuclear waste management community. However, there was still at the start of the project a large gap of knowledge in the ability to transfer the scientific understanding into a useful abstraction for long term performance assessment for real systems. The main contribution of BELBaR will be:

- Development of experimental programmes that are tailor-made to resolve the issues that are important in safety assessment
- Development of quantitative models, founded on sound science and verified by relevant experiments, for the assessment of erosion and radionuclide transport
- An increased knowledge about bentonite colloid stability in realistic systems that can be used in safety assessments as well as in the formulation of site investigation/site modelling programmes Formulation of a joint understanding of the issues within and outside the project, which will aid future license applications and R&D programmes.

Societal impact

The primary target audience of the outcome of the project is the national waste management organisations. The key use is reduction of uncertainties in the understanding of a process that has been shown to have a direct impact on the assessed dose/risk from a repository for high level nuclear waste. The reduction of uncertainties in the understanding may lead to:

- Reduction of the assessed overall risk from a repository
- The possibility to totally neglect the process in assessments under some circumstances
- Guidance to future site selection and site characterization programmes
- Aid in the selection of engineered barriers for a nuclear waste repository A uniqueness of the project is that the step from fundamental science to “industrial application” is short. This means that many of the results from the project will be of significant value to the scientific community as a whole, especially for the fields of surface and colloid chemistry.

End User Review Board Evaluation Report
Evaluation of presentations from the final conference of the project
Berlin, 3-4 February 2016

Jinsong Liu and Jarmo Lehtikoinen

19/02/2016



The BELBaR project has received funding from the European Atomic Energy Community's (EURATOM) 7th Framework Programme (FP7/2007-2011) under the grant agreement No. 295487

Introduction

In this evaluation report, the outcomes (deliverables) from the EU-project within the framework of Euratom FP7, *Bentonite Erosion: effects on the Long term performance of the engineered Barrier and Radionuclide transport* (BELBaR), will be reviewed and evaluated. The focus of the evaluation is on the scientific quality of the various deliverables, including the soundness of the scientific basis, the initiative of the research and the reliability of the achieved results. The researches' potential contribution to the long-term safety performance assessment of a nuclear waste repository will be commented as well.

A brief description of the project's aims, scope and activities will be given. The partners will be listed out and the different Work Packages of the project outlined. It follows evaluation of the different deliverables package for package.

Aims of the project

The main aim of the BELBaR project is to increase the knowledge of the processes that controls clay colloid stability, generation and ability to transport radionuclides. The overall purpose of the project will be to suggest a treatment of the issues in long-term safety and performance assessment.

Scope and activities of the project

The project is based on the desire to improve the long-term safety assessments for repository concepts that combine a clay Engineered Barrier System (EBS) with a fractured rock. The formation and stability of colloids from the EBS may have a direct impact of assessed risk from the repository in two aspects:

- Generation of colloids may degrade the engineered barrier ,
- Colloid-mediated transport of radionuclides may reduce the efficiency of the natural barrier.

The outcome of the project is expected to have an effect on future performance assessment, through an increased understanding of the processes related to clay colloid. It is also expected that the uncertainties can be reduced in the description of the effect of clay colloids on the long term performance of the engineered barrier and on radionuclide transport mediated by clay colloid.

The major activities of project are:

- To improve the understanding on when bentonite colloids are unstable,
- To improve the quantitative models for erosion on the bentonite barrier for the cases when the colloids are stable,
- To improve the understanding of how radionuclides attach to and are transported together with clay colloids.

The activities are undertaken through a number of experimental and modelling approaches within the project. Key issues in BELBaR are interaction, communication and cooperation. Since a large part of the work within project will be of interest for a more general community, the objective is to, as far as reasonably possible, publish the results in peer-reviewed journals

Participants

- Svensk Kärnbränslehantering AB, SE
- CIEMAT Centro de Investigaciones Energeticas, Medioambientales y Technologicas, ES
- NRI Nuclear Research institute Rez plc, CZ
- KIT Karlsruhe Institut of Technology, GE
- POSIVA Posiva OY, FI
- VTT Technical Research Institute of Finland, FI
- ClayTech Clay Technology, SE
- JYU University of Jyväskylä, FI
- KTH Kungliga Tekniska Högskolan, SE
- B+Tech B+Tech, FI
- NDA Nuclear Decommissioning Authority, GB
- RWM Radioactive Waste Management Ltd, GB
- UNIMAN University of Manchester, GB
- MSU Lomonosov Moscow State University, RU
- HU Helsinki University, FI.

Work Packages

The project consists of the following Work Packages:

- WP1: Safety Assessment
- WP2: Erosion
- WP 3: Colloid radionuclide and host rock interaction
- WP4: Colloid stability
- WP5: Conceptual and mathematical models
- WP6: Knowledge spreading and communication
- WP7: Coordination

WP6 and WP7 are not subject to this evaluation

Evaluation, End User Review Board

The End User Review Board consists of:

Jinsong Liu, Analyst, Section of Disposal of Radioactive Waste, Dept. of Radioactive Materials at SSM – The Swedish Radiation Safety Authority

Jarmo Lehtikainen, Senior Inspector Nuclear Waste and Material Regulation and Nuclear Waste Safety Assessment at STUK - Radiation and Nuclear Safety Authority.

Summary of the presentations during the last annual meeting of the project, Work packages 2, 3, 4 and 5 (WP2, WP3, WP4 and WP 5).

The last annual meeting of the project, *Final Conference, Clay Colloids in Aqueous Systems*, is held in Berlin, Germany, on February 3-4, 2016. The End User Review Board's evaluation of the presentations is based the materials presented in the abstract collections of the meeting.

The main objective of WP 2 will be to understand the main mechanisms of erosion of clay particles from the bentonite surface and to quantify the (maximum) extent of the possible erosion under different physico-chemical conditions. Additionally, these studies will point out under what conditions compacted bentonite is able to produce colloidal particles, free to move into the contacting aqueous phase and to determine the bentonite colloids "source term".

The aim of WP3 is to

1. improve the understanding of processes controlling colloid mobility, and their appropriate description;
2. study the role of sorption reversibility on clay colloid mobility; and
3. identify additional retention processes, such as matrix diffusion.

WP3 also has the responsibility to ensure that the parameters selected for experimental and modelling work enable, as far as possible, appropriate consideration of the conditions expected in a spent-fuel repository.

WP 4 deals with clay colloid stability. Clay colloid stability is one of the key questions for prediction of their potential influence on erosion of bentonite buffer/backfill material (see WP2) and migration of radionuclide carried by colloids (see WP3). Clay colloid stability in aquatic environments is primarily driven by groundwater geochemistry such as salinity (ionic strength) and edge charge, which is a function of pH. Also other factors should be taken into account within the colloid stability such as water flow rate, filtration effects, heterogeneity of solid phase surface charge and time. The stability of clay colloids in the site-specific host rock conditions is important for assessments of long-term performance of radioactive waste repositories.

The objective of WP 5 is to validate and advance the conceptual and mathematical models used to predict mass loss of clay in dilute waters and clay colloid generation as well as clay colloid facilitated radionuclide transport relevant to geological disposal of higher level radioactive waste. Validation of the current conceptual as well as mathematical models is pending. The target is to obtain validated advanced model(s) for the purposes of geological disposal of higher level radioactive waste.

The following is a summary of the presentations during the meeting. The presentations are grouped into the following topics: characterisation, process study and mechanism understanding, colloid mobility and radionuclide sorption (ir)reversibility, as well as modelling.

Characterisation

Fossum (pp. 3-4)¹ presented new sedimentation experiments by using electric fields together with flow for characterising the nano-structures in detail, and for studying the interplay of van der Waals and electrostatic forces screened by ions at the nanoscale. **Filella's** (pp. 5-7) presentation focused on characterisation of inorganic colloids from glacier abrasion in lakes that drain glacier-melt waters. The properties studied include particle size distribution, coagulation and sedimentation behaviour, mineralogical composition, etc. of the colloid particles. These two presentations have brought the project to a wider perspective of the issues the project is dealing with.

Segad (p.13) used several spectroscopic and other analytical techniques to study the effect of platelet size, pH, temperature and electrostatic interactions on swelling, flocculation and aggregation phenomena. **Brázda and Červinka** (pp. 61-54) introduced the method for measurement of specific area by using polar liquids. 28 different clay samples were used in the experiment for measuring their specific area by using EGME (ethylene glycol monoethyl ether, or 2-methoxyethanol). Some of the known correlations between specific area and other geochemical properties of clay, such as cation exchange capacity, type of cation in the interlayer or smectite content, have been confirmed.

Eriksson and Schatz (pp. 31-33) employed optical and rheological methods to gain information about the detachment mechanism of clay colloids. The optical coherence tomography imaging shows that there exists a domain of sedimented colloidal material extended radially outwards from the perimeter of the inner gel-like phase, in the swelling tests inside an artificial fracture. Important observations are initial generation of colloidal materials at the gel/sol interface that later aggregates downstream of the source, Ca-clay displays no gel-like character, at high electrolyte concentrations the gel-like, elastic response for any clay is significantly reduced or disappears entirely.

Missana et al. (pp. 73-76) conducted experimental characterisation of the colloids as dispersed from the raw bentonite of different types from different places (FEBEX from Spain, IBECO from Mylos island in Greece, Wyoming MX-80 from USA, Rokle Na-activated bentonite from Czech, and a Russian bentonite from Khakassia deposit). Stability tests were carried out after characterisation. The main findings are that generated colloid concentration correlates well with the quantity of Na at the cation exchange sites. The accessory minerals may lead to aggregation that otherwise does not occur and thus affect the colloid stability.

Pacovský et al. (pp.81-82) presented the hot mock-up experiments in the framework of the Czech program. In the geochemical part, the study into colloids, their chemistry and potential changes in their chemistry, migration abilities, transport potential and sorption capacity of respective colloids, their interactions with the surrounding rock and bentonite (erosion and alteration abilities) certainly represent a big challenge. **Mikes and Spacek** (pp. 87-90) presented novel microbiological methods in clay colloid studies. In commercial montmorillonite the number of all cultural microorganisms was detected by cultivation methods based on most probable number quantification.

Fernández et al. (pp. 117-120) characterised mineralogical and geochemical composition, physic-chemical properties such as ion exchange, external and total surface area of a variety

¹ The page numbering refers to the book of abstracts for the final conference.

of raw bentonites and clay minerals, which have different structural characteristics: 2:1 (TOT) or 1:1 (TO) layer type, di- or tri-octahedral sites, TOT layer with low or high layer charge, charge location at tetrahedral or octahedral sites, dioctahedral clay minerals with cis- or trans-vacant position.

Nilsson and Hedström (pp. 129-131) experimentally characterised the shear strength of the gel formed of Kutch bentonite at different clay concentrations and a number of solutions of different NaCl concentrations (5 to 100 mM). The technique used was rotating vane rheometry. The results indicate that it is importance to distinguish between paste and gel. The swelling ability of pastes causes self-healing after a strong disturbance but gel does not. It is also observed that the yield stress increases substantially above the critical concentration of about 4 mM, which could be due to edge-face interactions. The gel strength increases proportionally to the square of the volume fraction of the clay material. The experiments support the argument that a gel will be formed at the swelling front and strongly limited penetration of bentonite into water-bearing fractures.

Eriksson and Haavisto (pp. 137-140) studied experimentally the rheological properties of dilute montmorillonite suspension subjected to small amplitude oscillatory shear at varying amplitudes and frequencies. The results show that montmorillonite suspensions prepared under free swelling conditions are dynamic systems that will relax in response to a small applied strain, such as flowing groundwater, and therefore the system behaves like a viscous liquid rather than a gel. It has been argued that gel-like behaviour of clay suspensions can possibly be achieved in laboratory with sufficient mechanical agitation. The environment of a disposal repository can be much more complicated so that viscous liquid forms instead of gel. **Eriksson** (pp. 141-143) conducted potentiometric and conductometric titrations on dilute Na-montmorillonite suspensions and corresponding supernatants at NaCl and CaCl₂ concentrations between 0.0001 – 1 M. The results are explained as that montmorillonite particles are not inert, especially in the presence of high electrolyte concentrations.

Matusewicz et al. (pp. 155-157) studied the microstructure of pure Ca- and Na-montmorillonite, as well as MX-80 bentonite at different compaction levels and different salinity conditions. The methods used in the study include small-angle X-ray scattering (SAXS), nuclear magnetic resonance (NMR), ion exclusion (IE) and transmission electron microscopy imaging (TEM). The TEM studies showed a clear difference in the microstructure of the MX-80 bentonite and the montmorillonite obtained by the purification of MX-80. Apart from removing the accessory minerals, clusters and aggregates of clay layers have been destroyed and montmorillonite layers organized in a different way. The platelets seem to be more oriented in the purified clay, whereas in the MX-80 their orientation appears to be more random. Combining the information from SAXS, NMR and IE quantification of interlamellar pores has been made and compared with the total pore volume. A clear tendency of forming larger stacked structures is visible for the calcium montmorillonite than for the predominantly sodium MX-80 bentonite.

Process study and mechanism understanding

Schatz et al. (pp. 9-11) presented experimental results using artificial fracture setups to study the erosion processes of compacted Na-montmorillonite at different flow velocities. The results show clearly that the extrusion and erosion behaviour are different at different flow velocities. **Reijonen et al.** (pp. 15-18) considered how representative the experiments made with purified mono-ionic smectite are for application in the performance assessment of waste

repository. Several mechanisms that may possibly destabilise colloid of smectite particles have been discussed. **Friedrich et al.** (pp. 57-60) used techniques of environmental scanning electron microscopy coupled with digital image analysis to study the swelling behaviour of bentonite at different relative humidities. The results show that the hydration isotherms of various cation exchanged Febex bentonite have an exponential form with strongly increased swelling at high relative humidities.

Hansen and Hedström (pp. 23-26) conducted both theoretical and experimental studies to explore the gelling process and the effect of the positive charge at edges. The spillover of negative potential from the surface charge to the edges and the electrostatic screening has been studied by means of the Poisson-Boltzmann equation. An enthalpy of edge-to-face binding has been determined by experimentally by studying the yield point temperature in relation to colloid concentration. **Alonso et al.** (pp. 65-68) studies the erosion behaviour of a variety of smectite as well as other relevant clay minerals. The minerals contain different contents of the smectite group, including montmorillonite, saponite beidellite and nontronite, with different structural properties, such as di- or trioctahedral smectite, and exchanged with different cations (Na, Ca-Mg, Ca, Fe). The other relevant minerals include illite and kaolinite. The minerals have been obtained from different places in the world. Erosion behaviour has been observed to be more related to the smectite clay content than to the exchangeable cation.

Thuresson et al. (pp.77-80) studied the temperature response of the swelling of both natural and refined clays, both theoretically and experimentally. An anomalous temperature behaviour which depends on the valency of the counterion has observed. It has also been showed that (i) the increase in swelling pressure with increasing temperature for monovalent counterions can be understood from entropic reasons, and (ii) the decrease in swelling pressure with increasing temperature for divalent counterions can be understood from ionic correlations that are important when multivalent ions are present. The key point is that the product the dielectric constant of water and temperature, $\epsilon_r T$, decreases as the temperature increases in aqueous solutions, hence, the net effect is an increased coupling.

Suorsa and Hölttä (pp. 91-94) experimentally studied the stability of montmorillonite colloid in different groundwaters (Allard, ionic strength (IS) = 4.2 mM; and OLSO, IS = 0.517 M; diluted OSLO, NaCl and CaCl₂ with IS = 0.1 to 100 mM) by analysing particle size distribution using the photon correlation spectroscopy, as well as by measuring Zeta potential applying the dynamic electrophoretic mobility. The results show that the colloid stability depends strongly on the ionic strength of the medium and the valence of the cation. At saline conditions, like at Finnish repository site in Olkiluoto, the colloids are unstable and therefore do not affect the radionuclide transport. The possible post-glacial diluting of the groundwater may still have to be taken into account.

Reid et al. (pp.95-98) performed both variable and uniform aperture cell tests with MX 80 bentonite samples as they were delivered. Filtration by the accessory minerals that mitigates erosion has been observed. **Hildebrand et al.** (pp. 99-100) presented experimental studies of the stability and transport of actinide(IV)-silica colloid, using packed columns with crushed granite. Positron emitting zirconium radionuclides are planned to be used to mimic the actinide(IV), since the transport of positron emitters can be readily visualised by means of positron emission tomography. **Svensson** (p. 101) studied the swelling properties of three montmorillonites (Wyoming, Milos and Kutch) with divalent interlayer cations with free access to water, using synchrotron X-ray diffraction and small angle X-ray scattering.

Hansen et al. (pp. 103- 106) studies the erosion behaviour of Wy-Na and Wy-Na-Ca bentonite in artificial fractures. Hysteresis behaviour of erosion process was observed when starting from high ionic strengths followed by a decrease of the ionic strength of the solute concentration. It has also been observed that gel formation stops the swelling into the fracture, while swelling into stagnant deionised water is substantial and leads to a paste/sol transition. The rate of such transition may limit the erosion rate. Another result is that erosion in sloped fractures was substantially higher. **Schatz** (pp. 107- 109) demonstrated that accessory minerals within bentonite remain behind and form layers, following the erosive loss of colloidal montmorillonite through contact with dilute groundwater at a transmissive fracture interface. The accessory phases have either been mixed into purified Na-montmorillonite or by using MX-80 montmorillonite washed free of soluble minerals and thorough exchanged with Na cation.

Fossum (p. 115) reported experiments which show that gaseous CO₂ can intercalate into the interlayer nano-space of a smectite clay at conditions close to ambient causing crystalline swelling. **Harjupatana et al.** (pp.121-122) used desk-top X-ray tomographic scanner to study the swelling/expansion properties of bentonite with different initial water ratios. The results indicate that the displacement is different at different axial positions of the sample, with the largest displacement being in the position in direct contact with water. **Rinderknecht et al.** (pp. 145-147) studied the erosion process by using synthetic Ni-labelled montmorillonite in the ring form and Grimsel groundwater. Erosion rates normalised to the contact area have been obtained. **Dohrmann** (p. 177) conducted studies to identify the differences of stability of bentonite in deionised water. The studies show that the colloid stability depends not only on the amount of exchangeable Na⁺, but also on pH. The effect of alkalinity on detachment of colloidal particles has been observed. This can be either due to the increase of solubility of aluminosilicate at high pH or due to the stabilisation of the dispersion.

Colloid mobility and radionuclide sorption (ir)reversibility

In the study by **Mayordomo et al.** (pp. 19–21), a clear indication of aggregation-disaggregation hysteresis was observed within the time frame of the experiment. The results of the study showed that disaggregation of bentonite colloids is effectively promoted by the decrease in the electrolyte ionic strength. The process was found partly irreversible even at lower ionic strength and in the absence of Ca²⁺. The mean particle hydrodynamic size was always greater than the initial stable one. The stable fraction of disaggregated colloids compared to the primary sample in the presence Ca²⁺ was considerably less than in its absence. The authors left open the possibility for further disaggregation of partly aggregated colloidal particles at longer times.

In the study by **Romanchuk et al.** (pp. 35–38), sorption of Np(V) on suspended bentonite samples from Russian and Indian deposits was investigated as a function of different experimental parameters. An effort was also made to identify the role of different constituent minerals in the bentonite in Np(V) sorption; for this purpose local distribution of neptunium on clay was determined by α -track analysis.

In the study by **Kolomá and Červinka** (pp. 39–41), the transport of radionuclides through the granite matrix in a synthetic ground water was found significantly faster than in deionized water in the absence of colloids. The results from dynamic column experiments showed that the radionuclide transport was accelerated by the presence of bentonite colloids. The sorption of the radionuclides on bentonite was fully (Sr²⁺) or partially (Cs⁺) reversible. Overall, the

transport of the radionuclides was influenced by sorption mechanism on bentonite colloids and also by solution phase composition.

In the study by **Schäfer et al.** (pp. 43–45), all the experiments performed so far for U(VI), Np(V), Pu(IV) and Am(III) showed desorption kinetics from the clay nanoparticles; for trivalent actinides in batch-type studies, a rate that was almost three orders of magnitude smaller than that in column experiments with crushed granite. These studies indicated full reversibility for trivalent actinides/lanthanides but much slower desorption rate for tetravalent actinides. A technique that enables the detection of all the radionuclides in the long tails of the breakthrough curves has been developed. However, no unambiguous interpretation of the interplay of the factors affecting radionuclide transport is currently possible. According to the authors, the knowledge gained about forward and backward rate constants could enable more reliable predictions of the long-term behaviour of radionuclides.

In the study by **Missana et al.** (pp. 47–50), filtration of bentonite colloids was always observed below a threshold residence time, which was somewhat specific to colloids and ground water chemistry. The bentonite colloid recovery was found to strongly decrease with the Ca^{2+} concentration in the solution. Also, the colloid recovery was found to decrease with the water flow rate and the transport of the mobile fraction of bentonite colloids was always unretarded relative to the water. Sorption linearity and reversibility of several radionuclides was investigated; only Cs^+ displayed clearly irreversible retardation behaviour. While colloids had a significant effect on Cs transport in the Grimsel water, the breakthrough of Cs was only slightly affected by colloids in the more saline Äspö water. Generally, bentonite colloids did not significantly enhance radionuclide transport but, rather, slightly increased the net retardation in the fracture. Unexpectedly, small elution, which was clearly attributable to the presence of mobile colloid particles, of very highly sorbing radionuclides, like Eu, was observed.

In the study by **Hölttä et al.** (pp. 83–86), radionuclide adsorption on the clays was found to increase with the pH and to decrease with the ionic strength. The transport of colloids was affected by the extent of rock alteration, the type and length of the column, water flow rate and colloid size. In both types of column, Eu-152 was significantly retarded. Sr-85 was also retarded without colloids. In the presence of colloids, slow elution of Sr-85 was observed. The sorption of Eu-152 was not fully reversible on bentonite colloids and mineral surfaces. However, the measured zeta-potentials suggested purely electrostatic and reversible sorption for Sr. The column experiments showed that colloids have an effect of radionuclide transport. The transport of colloids was, in turn, affected by their size, the water flow rate, and column material and type. The authors concluded the main uncertainties to still remain in the quantification of colloids in actual repository conditions and the mobility of colloids.

In the study by **Elo et al.** (pp. 111–114), a non-sorbing tracer (Cl-36) was found to elute through the drill-core column faster than through the crushed-granite column owing likely to a less tortuous transport path through the former. A potential explanation offered for the fairly low sorption of Np-237 over the pH range considered was the variability in the size of bentonite colloids. Also, the recovery of bentonite colloids was greater in the drill-core columns than in the crushed-rock column. The results obtained at different water flow rates through the columns indicate that bentonite colloids have the potential to enhance the transport of Np-237.

In study by **Rinderknecht et al.** (pp. 149–151), the concentration of the conservative tracer, which was detectable after 100 d in an observation borehole at the Grimsel Test Site (GTS), steadily increased at constant pH. The Zn and Al concentrations in the ground water samples were taken indicative of bentonite colloids. High Mg concentrations and reversed Mg-to-Al-ratios in the effluents suggested cation exchange of Mg and Ca on bentonite. No significant activity of sulphate-reducing bacteria was not observed in the experiments. The sole radionuclide that was found in the effluent was Tc-99, the concentration of which correlated with that of the conservative tracer and the Eh and pH in the near-field of the CFM.

In the study by **Bouby et al.** (pp. 159–162), the erosion was found to be clearly correlated with the initial chemical composition of the bentonite; the highest erosion occurred for the Na-exchanged pellets while virtually no erosion was observed for Ca-exchanged ones and it was much more limited when using raw or the Na-Ca-pellets. The sizes of the material eroded after about 1 month agreed with the sizes previously reported. A tentative estimate of the Eu sorbed on the eroded bentonite was given; lower sorption occurred on material eroded from the raw MX-80 bentonite pellets. Using the methods applied in the study it is possible to take into consideration the natural radionuclides originating from the bentonite material itself, which enables setting a the baseline for the interpretation of the results.

In the study by **Norrfors et al.** (pp. 163–166), the presence or absence of organic matter, like fulvic acids (FAs), did not have an effect on the stability of clay colloidal size fractions. The colloid size did not seem to play a role in the radionuclide (Th, U, Np, Tc and Pu) sorption. The main implication of the results was that implementation of an average distribution coefficient for all colloid sizes would be acceptable. Sorption reversibility of radionuclides was not guaranteed in the colloidal system investigated. When reversibility did occur, it greatly depended on the geochemical parameters (pH, ionic strength, competing ligand). Specific important observations included; at low pH, the U sorption was reversible and that of Th partly reversible, and the Pu remained associated to clay material in the absence of FA while the presence of FA increased the labile Pu fraction.

In the study by **Bouby et al.** (pp. 167–171), the chemical composition of the aqueous solution was found to strongly influence the clay colloid generation. The mean hydrodynamic diameter of clay colloids was found significantly larger in the calcium-dominant system owing to particle aggregation. The presence of FA might have slowed down this process. Irrespective of the aqueous media in which the clay colloids are formed, they presented the same coagulation behaviour at moderate to high ionic strength in Na-, Ca- or Mg- electrolytes in the short term. At the lowest salinity in the sodium system, the coagulation rate slowed down, possibly due to FA. In the long-term study, the clay colloids underwent slow agglomeration under conditions representative of a glacial melt water, even in the presence of organic matter.

In the study by **Krupskaya et al.** (pp. 173–175), the relative transformation susceptibility of the two clay samples was taken attributable to the proportion of octa- and tetrahedral charge in the clay structure. Even after exposure that is far more aggressive than ever to be expected in repository conditions, montmorillonites were stated to retain their ability to adsorb cations, including Cs, at a very high level. The authors concluded that the results can be used in assessing the transformation of the montmorillonite structure and stability of bentonite-based barriers.

Modelling

Liu (pp. 27-29) has developed an extension of the weighted correlation approach within the framework of the density function theory of statistical mechanics. The approach was extended to include solvent-solvent and ion-solvent interaction using the solvent primitive model. The modelling results revealed the importance of hydration of counter-ion (the size of the hydrated ions in comparison with the solvent molecules, i.e. water molecules) and ion valence for swelling of smectite and aggregation of its colloid. **Neretnieks et al.** (pp. 51-54) further developed their previous model for bentonite expansion and erosion by incorporating a two-region sub-model to improve the resolution of flow velocity and smectite concentration in the very thin rim zone. The two regions are a Bingham fluid region and a viscous fluid region. The model has been further extended by accounting for floc formation that increases erosion in sub-vertical fractures. The model was successfully validated by simulating a series of experiments.

Leroy et al. (pp. 69-72) proposed a new electrophoretic mobility model to interpret the electrophoretic mobility measurements of the basal planes of Na-montmorillonite dispersion in a NaCl aqueous solution. The electrophoretic model is combined with a triple layer model, a surface conductivity model of the Stern and diffuse layer of the clay/water interface. It is observed that the surface conductivity effect is increasingly important with decreased solution salinity.

Yang et al. (pp.123-126) presented a novel density function approach of a planer electrical double layer with the primitive model. The approach has been applied to calculate the interaction forces between smectite (montmorillonite) particles and the Gaines-Thomas selectivity coefficient of the Ca/Na ion exchange equilibrium. Excellent agreement with the results of Monte Carlo simulations and experimental results from the literature has been obtained. Of special interest are the predictions that the colloid interaction can be switched from attraction to repulsion with increasing of the diameter of counterions from standard to hydrated ionic size; and that Ca^{2+} is preferentially taken up into the surface exchange site for compacted clay system with smaller interlayer separation.

Molinero et al. (pp. 127-128) propose a numerical technique to study the erosion of bentonite buffer embedded in rock as it extrudes into a water-conducting fracture. The numerical technique couples the discrete element method, used to model the colloidal particles, to the finite element method, which is used to solve the modelling equations for the suspending fluid. **Olin et al.** (pp. 133-135) developed a modified version of Neretnieks' model to handle the scaling issues. The model focused on Péclet number and computed the steady state solution as a function of diameter and groundwater velocity. The modelling experiences revealed the difficulties of maintaining relative accuracy and achieving system stability. A major finding is that the total erosion flux obtained from the model fitted to exponent Péclet number. **Huber et al.** (p. 153) studied the effect of flow field/fracture heterogeneity on the bentonite erosion by using the "KTH model". Lognormal distribution of fracture aperture and the "cubic law" relating aperture and hydraulic conductivity are assumed.

Evaluation of presentations by the End-User Review Board

The presentations belonging to each of the WPs and presented at the fourth, and final, annual BELBaR meeting in Berlin on February 3–4, 2016, were evaluated. Instead of focusing on the scientific and technical aspects of the project outcomes, this review rather evaluated their merits and usefulness from the end-user (here, regulatory) point of view. It is, however, safe to say that, for example, the expertise of the consortium and the set of state-of-the-art experimental techniques used in the project BELBaR project were truly impressive.

The project outcomes have the potential to pave way for new investigations where the most critical uncertainties are mitigated and managed, and bits and pieces of information gained not only from the BELBaR project are put together systematically to expand the knowledge base for months and years to come. Such improved knowledge would also enable the construction of refined conceptual models and to more credibly bound the potential risk posed by clay colloid formation and phenomena associated with it.

The following are specific evaluations of the presentations during the meeting.

Characterisation

The End-User Review Board considers it very positive that a variety of analytical techniques, which had not previously been widely used in this area, have now been used to characterise the properties of bentonite and the colloid it forms. A large amount of information, such as cation exchange capacity, external and total surface areas, microstructure of the layered clay, etc. has been obtained for a variety of different bentonite and clay minerals through such study in the project and the information is valuable for performance assessment of a final repository. The difference of microstructure (i.e. the platelets seem to be more oriented in the purified clay samples) between samples of natural clay and purified clay may have significance for performance assessment.

The aggregation and sedimentation behaviour of clay colloid particles have been much better understood, which can be of great importance for evaluation of the conservativeness of the different modelling approaches used in the performance assessment. The finding that the accessory minerals may lead to aggregation that otherwise does not occur is of great importance for the performance assessment and probably need to be further confirmed.

While characterising the rheological properties of clay suspensions the project reveals several interesting phenomena that may require further attention to be paid when the results are incorporated in performance assessment. To distinguish between gel and paste that is formed, to consider the effect of edge-face interaction, as well as to unambiguously define a gel phase can be some of the challenges.

Process study and mechanism understanding

The End-User Review Board has the opinion that the understanding of the mechanisms involved in the erosion process has been greatly deepened through this project. The erosion tests using artificial fracture have both confirmed some of the previous gained understanding of the mechanisms and revealed new ones. It has been confirmed, at least qualitatively, that bentonite erosion is influenced by water flow rate, that the hydration/water-saturation is related to relative humidity, that the colloid stability depends on ionic strength of the solution

and on the cation exchange properties of the bentonite, as well as that particles of the accessory minerals are left behind during the erosion process and are also capable to mitigate erosion.

It is of special interest that many new phenomena and processes related to the bentonite erosion have been discovered during the project. It has been observed that the swelling of bentonite has different temperature dependences for swelling in monovalent and divalent counterion solutions. It has also been shown that the displacement along the axis of the sample is uneven during swelling, with largest displacement occurring at the end of the sample in direct contact with solution.

Regarding the colloid stability, several new findings possibly of great importance for performance assessment have been obtained. The temperature dependence of the yielding of the gel has been shown to have an origin from edge-face interaction and enthalpy for such interaction has been obtained. It has been observed that the colloid stability depends not only on solution type and ionic strength, but also on pH. Could this be considered as evidence for edge-face interaction?

Some relative new observations concerning the erosion behaviour of bentonite are: the erosion behaviour is more related to the smectite clay content than to the exchangeable counterion; erosion in sloped fractures is substantially increased. The last mentioned phenomenon need definitely to be considered in performance assessments where Na-montmorillonite is assumed to form a conservative case, as it is known that Na-montmorillonite is more sensible to erosion. But Ca-montmorillonite has been observed to readily form stacks of platelets, making it more sensitive to sedimentation under gravitation.

Intercalation of CO₂ into the interlayer of nano-space of smectite clay may lead to swelling. Can this phenomenon have significant for performance assessment?

Colloid mobility and radionuclide sorption (ir)reversibility

The End-User Review Board have the opinion that the WP3 was successful in meeting its objectives. Thanks to the BELBaR project, those carrying out safety assessments certainly are in a better position to make more informed choices in a safety case to argue for the long-term performance of the bentonite-based barriers and the host rock and, ultimately, for the post-closure safety. The results and new insight gained from the project also enables both an implementor and a regulator to better identify, mitigate and manage the uncertainties thought to pose the greatest risk to the performance of a disposal system and to the post-closure safety.

Apart from one of the studies that indicated full sorption reversibility for trivalent actinides/lanthanides, the results gained from the project still beg the question of full reversibility of radionuclides in actual repository conditions. The key role in attaining sorption reversibility was found to be played by the experimental time; given this time is long enough, a system may approach a condition indicative of full sorption reversibility. Also, the much slower desorption rate for tetravalent actinides begs the question of a conservative assumption regarding the reversibility of their sorption; would full irreversibility be such an assumption? When sorption reversibility did occur, it greatly depended on the geochemical parameters (pH, ionic strength, competing ligand²). Improved knowledge of the rates involved in the

² Here, fulvic acid (FA).

radionuclide desorption from bentonite colloids enables more credible assessments of the role of colloid-mediated radionuclide transport to affect the post-closure safety under vastly varying flow conditions, i.e., in systems with considerably different residence times. An implication of the results presented in WP3 was that implementation of an average radionuclide distribution coefficient for all colloid sizes could be acceptable, which serves to facilitate safety analyses.

Bentonite erosion was found to be clearly correlated with the chemical composition of the influent or the bentonite itself; the erodibility decreased with an increase in calcium concentration. Less disaggregation of bentonite colloids in calcium-dominant systems than in sodium systems is a direct indication of its lesser erodibility, and hence better performance robustness, compared to Na-bentonite. Also, the lower affinity of radionuclides towards a dominantly divalent-cation form of bentonite than towards sodium form would, in turn, imply less colloid-mediated radionuclide transport. Organic matter (FA) did not have an effect on the stability of clay colloidal size fractions. The transport of colloids eroded from bentonite was affected by their size, the influent flow rate and the experimental setup. When bentonite colloids were found to have a non-negligible mobility, their potential to enhance radionuclide transport was evident. Clearly, this should have implications for whether or not colloid-mediated radionuclide transport should be considered in a safety case.

The way one of the partners (Norrfors et al.) presented the main implications of their work is considered a good practice recommendable to all future projects. Such practice can also be extremely useful to a regulator, or any other interested party, to be able to focus in their appraisal on the most critical factors anticipated to affect the post-closure safety.

One aspect that was not touched upon by WP3 concerns the role of biocolloids (e.g. bacteria), which are ubiquitous in natural aquifers, to mediate radionuclide transport. Although the scope of the project was limited to consideration of bentonite colloids, it would have been informative to learn about the importance of bentonite colloids to mediate the radionuclide transport relative to biocolloids. The less explored field of biocolloids could be a potential topic for future investigations.

While the End-User Review Board tend to agree with one of the partners in that the main uncertainties still remain in the quantification of colloids in actual repository conditions and in the mobility of colloids, WP3 certainly has succeeded in mitigating these uncertainties to be managed in a safety case in attempts to argue for the post-closure safety. It would also seem that the results from WP3 regarding radionuclide sorption (ir)reversibility and the role colloids may have in mediating radionuclide transport do have implications for some of the issues in Chapter 4 in D1.2 that WP3 was planning to revisit.

Modelling

The End-User Review Board can give the comment that the modelling of bentonite erosion has made a large progress during the project, which has both increased the number of processes dealt with in the model, and enriched the tool-kit for performance assessment to select suitable models.

The classical “KTH-model” has been expanded and the numerical methods have been improved. The scaling approach has been developed based on the “KTH-model” by focusing on the system’s Péclet number.

Attempted has been made to model the ion-ion interaction, by using the weighted correlation approach in the framework of density function theory of statistic mechanics. The model may have significance in performance assessment for a better understanding and quantification of the erosion of Ca-smectite. The novel density function approach to describe the selectivity of cation exchange process has paved the way for theoretical prediction of selectivity constants.

The electrophoretic mobility model has been introduced into the study of several processes related to erosion, such as surface conductivity effect.

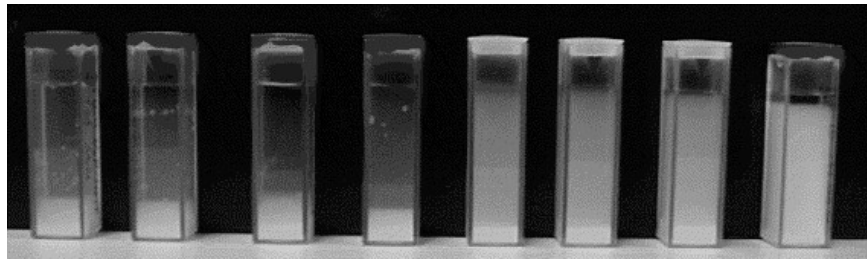
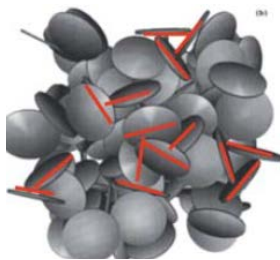
FLOW OF CLAYS

Jon Otto Fossum (jon.fossum@ntnu.no)

Department of Physics
Norwegian University of Science and Technology - NTNU
Trondheim
Norway

Clays or clay based composite materials is an expanding activity in the context of modern materials science¹. In this presentation we briefly discuss this, illustrated through the rich behaviour displayed by clays as a physical model system for soft materials².

In order to understand macroscopic flow behaviours in clay systems³, it is crucial to characterize the underlying nano-structures in detail. We will discuss the interplay of van der Waals and electrostatic forces screened by ions at the nanoscale, with the result that clays may either form glass-like or gel-like materials⁴, which in turn can be related to questions related to materials aging flow dynamics⁵.



Two alternatives for sedimented and compacted clay structures?

Left panel: Simplistic sketch of clay house-of-card structure (From ref. 4).

Right panel: Layered structuring of clay particles sedimented in saline water with increasing salt contents from left to right containers (From ref. 10).

With the nano-structural base at hand, we can discuss clay systems from the geological example of quick clay sedimentation, flows and avalanches⁶, via fracturing of clay gels, to materials science and the stability, strength and flow of smart electrorheological clay structures^{7,8}. Quick clays are often referred to as hours-of-card structures at their nano-/meso-scale⁹, although the existence of such house-of-card structures is still debated. Our sedimentation experiments¹⁰ may point to other possibilities. In the context of materials science, the use of electric fields together with flow in order to improve the processing of clay composite materials may open new unexplored avenues¹¹.

¹ *Handbook of Clay Science*, Edited by F. Bergaya, B.K.G. Teng and G. Lagaly, Elsevier Ltd. (2006)

² *Physical Phenomena in Clays*, J.O. Fossum, *Physica A* 270, 270 (1999)

³ *Flow of Clays*, Jon Otto Fossum, *European Physical Journal Special Topics* 204, 41-56 (2012)

⁴ *A fresh look at the Laponite phase diagram*, B. Ruzicka and E. Zaccarelli, *Soft Matter* 7, 1268 (2011)

⁵ *Prediction of Long and Short Time Rheological Behavior in Soft Glassy Materials*, A. Shahin, Y.M. Joshi, *Phys. Rev. Lett.* 106, 038302 (2011)

⁶ *Quickclay and Landslides of Clayey Soils*, A. Khaldoun, P.Moller, A. Fall, G.Wegdam, B. De Leeuw, Y. Meheust, J.O. Fossum, D. Bonn, *Phys.Rev.Lett.* 103, 188301 (2009)

⁷ *Intercalation-enhanced electric polarization and chain formation of nano-layered particles*, J.O. Fossum, Y. Méheust, K.P.S. Parmar, K.D. Knudsen, K.J. Måløy and D. d.M.Fonseca, *Europhys. Lett.* 74, 438-444 (2006)

⁸ *Active structuring of colloidal armour on liquid drops*, P Dommersnes, Z Rozynek, A Mikkelsen, R Castberg, K Kjerstad, K Hersvik & J O Fossum, *Nature Communications* 4:2066, DOI: 10.1038/ncomms3066 (2013)

⁹ *An Introduction to Clay Colloid Chemistry*, H. van Olphen, Wiley, New York, 1977.

¹⁰ *Observations of orientational ordering in aqueous suspensions of a nano-layered silicate*, J.O. Fossum, E. Gudding, D. d.M.Fonseca, Y. Meheust, E. DiMasi, T. Gog and C. Venkataraman, *Energy The International Journal*, Volume 3, 873 (2005)

¹¹ *Polypropylene-organoclay nanocomposites under different electric field strengths*, Z. Rozynek; S. M. de Lima Silva; J. O. Fossum; G. J. da Silva; E. Novais de Azevedo; H. Mauroy; T. Plivelic, *Appl. Clay Science* 96, 67-72 (2014).

BACK TO THE PROJECT ON INORGANIC COLLOIDAL PARTICLES IN LAKE BRIENZ (SWITZERLAND) TEN YEARS AFTER

Montserrat Filella (montserrat.filella@unige.ch), Institute F.-A. Forel, University of Geneva, Boulevard Carl-Vogt 66, CH-1205 Geneva, Switzerland

Lakes that drain glacier-melt waters have high turbidities due to the suspension of inorganic particles from glacier abrasion. As a result of the high concentration of suspended particles, which backscatter a portion of the incident solar radiation, these lakes are characterised by a smaller trophogenic zone and cooler summer water temperatures compared to non-glacial lakes. High mineral turbidity modifies food webs through direct and indirect effects at all trophic levels. Although the extent suspended clays influence lake trophic organisation depends mineral particle size and mineralogy, this issue has been little studied.

Within the framework of an extensive research project into the causes and consequences of the ultraoligotrophic status of Lake Brienz, Switzerland, the fate of mineral colloid particles was studied in the lake and its tributary rivers over 16 months (June 2004 to October 2005). Quantitative studies of colloid behaviour at the scale of a whole water body (e.g. a lake) are rare because of the lack of adequate measuring techniques and the need for intensive field work. Most existing studies either give only qualitative information or are devoted to a specific aspect of colloid behaviour. The working strategy adopted in this study included the use of many different complementary techniques in the field and in the laboratory. This required significant method development. To test the hypothesis that an increase in lake productivity would favour colloid coagulation and particle removal, special attention was paid to the presence of different types of natural organic matter in the lake.

Some of the methodological developments concerned:

- the evaluation of the MBTH method for carbohydrate determination in freshwaters [1],
- the development of a simple, very sensitive voltammetric method for the determination of refractory organic substances in freshwaters [2],
- the development of a non-perturbing scheme for the mineralogical characterization and quantification of inorganic colloids in natural waters [3],
- the measurement of particle size distributions in natural surface waters from 15 nm to 2 μm by a combination of LIBD and Single Particle Counting [4].

Direct results of the project were the study of:

- the particle size distribution and mineralogical composition of inorganic colloids in Lake Brienz [5],
- their coagulation and sedimentation behaviour [6],
- the particle size distribution and mineralogical composition of inorganic colloids in glacier-melting water and overlying ice [7],
- the composition and sources of organic carbon in the submicron (colloidal plus dissolved) range [8],
- the spectromicroscopy mapping of colloidal/particulate organic matter [9].

The project also allowed:

- the appraisal of the role of colloids in the variability of the measured molybdate reactive phosphorous concentrations in freshwaters [10],
- the evaluation of the effect of the filter feeder *Daphnia* on the particle size distribution of inorganic colloids in lake Brienz [11].

The methodology developed was also applied to a different system: draining waters of the adit of an abandoned antimony mine [12].

All these issues will be presented in this communication and the work put into context. The scientific echo of this research will also be discussed.

References

- [1] V. Chanudet and M. Filella, The application of the MBTH method for carbohydrate determination in freshwaters revisited. *INTERN. J. ENVIRON. ANAL. CHEM.*, 86, 693-712 (2006). doi:10.1080/03067310600585936
- [2] V. Chanudet, M. Filella and F. Quentel, Application of a simple voltammetric method to the determination of refractory organic substances in freshwaters. *ANAL. CHIM. ACTA*, 596, 244-249 (2006).doi:10.1016/j.aca.2006.03.097
- [3] V. Chanudet and M. Filella, A non-perturbing scheme for the mineralogical characterization and quantification of inorganic colloids in natural waters. *ENVIRON. SCI. TECHNOL.*, 40, 5045-5051 (2006). doi:10.1021/es060255y
- [4] C. Walther, S. Büchner, M. Filella and V. Chanudet, Probing particle size distributions in natural surface waters from 15 nm to 2 μ m by a combination of LIBD and Single Particle Counting. *J. COLLOID INTERFACE SCIENCE*, 301, 532-537 (2006). doi:10.1016/j.jcis.2006.05.039
- [5] V. Chanudet and M. Filella, Size and composition of inorganic colloids in a peri-alpine, glacial flour-rich lake. *GEOCHIM. COSMOCHIM. ACTA*, 72, 1466-1479 (2008). doi:10.1016/j.gca.2008.01.002
- [6] V. Chanudet and M. Filella, The fate of inorganic colloidal particles in Lake Brienz. *AQUATIC SCIENCES*, 69, 199-211 (2007). doi:10.1007/s00027-007-0877-2
- [7] V. Chanudet and M. Filella, Particle size and mineralogical composition of inorganic colloids in glacier-melting water and overlying ice in an Alpine glacier, the Oberaargletscher, Switzerland. *JOURNAL OF GLACIOLOGY*, 52, 473-475 (2006). doi:10.3189/172756506781828485
- [8] V. Chanudet and M. Filella, Submicron organic matter in a peri-alpine, ultra-oligotrophic lake. *ORG. GEOCHEM.*, 38, 1146-1160 (2007). doi:10.1016/j.orggeochem.2007.02.011

- [9] T. Schäfer, V. Chanudet, F. Claret and M. Filella, Spectromicroscopy mapping of colloidal/particulate organic matter in Lake Brienz, Switzerland. *ENVIRON. SCI. TECHNOL.*, 41, 7864-7869 (2007). doi:10.1021/es071323z
- [10] M. Filella, C. Deville, V. Chanudet and D. Vignati, Variability of the colloidal molybdate reactive phosphorous concentrations in freshwaters. *WATER RESEARCH*, 40, 3185-3192 (2006). doi:10.1016/j.watres.2006.07.010
- [11] M. Filella, C. Rellstab, V. Chanudet, P. Spaak, Effect of the filter feeder *Daphnia* on the particle size distribution of inorganic colloids in freshwaters. *WATER RESEARCH*, 42, 1919-1924 (2008). doi:10.1016/j.watres.2007.11.021
- [12] M. Filella, V. Chanudet, S. Filippo and F. Quentel, Particle size and mineralogical composition of inorganic colloids in draining waters of the adit of an abandoned mine, Goesdorf, Luxembourg. *APPL. GEOCHEM.*, 24, 52-61 (2009). doi:10.1016/j.apgeochem.2008.11.010

Benchmarking Exercise of Clay Erosion in Artificial Fracture Tests

Tim Schatz^a, Ursula Alonso^b, Tiziana Missana^b, Christopher Reid^c,
Frank Friedrich^d, Franz Rinderknecht^d & Kari Koskinen^e

^a*B+Tech Oy, Helsinki, Finland*

^b*CIEMAT, Environmental Department, Physico-Chemistry of Actinides and Fission Products Unit, Madrid, Spain*

^c*Department of Civil and Environmental Engineering, University of Strathclyde, Glasgow, United Kingdom*

^d*KIT, INE, Karlsruhe, Germany*

^e*Posiva Oy, Olkiluoto, Finland*

In deep, geological repositories in crystalline rock, bentonite buffer material may be eroded by contact with dilute groundwater flowing through intersecting, transmissive fractures. The assessment of this possibility will include the use of data from artificial fracture tests. These tests are performed in systems featuring shimmed, transparent plates (providing a fracture plane between them of known aperture) allowing the imposition of solution (flow and composition) boundary conditions. Most importantly, the test systems incorporate buffer material samples which are intersected by the fracture planes.

The BELBaR Project includes work by several partners performed using artificial fracture tests to examine aspects of the clay erosion process. Insofar as the analysis of clay erosion in artificial fracture systems does not have a long, recorded history by which to judge its efficacy, reliability or accuracy, it was decided to include a benchmarking exercise in the BELBaR Project. The aim of this exercise was 1) to perform artificial fracture tests in different partner laboratories using identical clay samples and experimental parameters and similar methods of analysis and 2) to aid in model development.

The artificial fracture benchmark tests were conducted using a commercial sodium montmorillonite product (Nanocor, PGN grade) emplaced at a dry density of 1400 kg/m³. Although different, custom-designed artificial fracture systems were used by each laboratory (varying in the size of the fracture planes and sample dimensions), a fixed fracture aperture of 0.1 mm was employed in every case. Three of the benchmark tests were performed with similarly-sized, cylindrical samples of approximately 20 mm in diameter and from 10 to 20 mm in height; a fourth benchmark test was initiated using a ring block sample with an inner diameter of 40 mm, an outer diameter of 80 mm and a height of 25 mm. Experiments were carried out in three subsequent phases: 1) stagnant conditions (no flow), 2) low-flow conditions ($\sim 10^{-5}$ to 10^{-6} m/s) and 3) high-flow conditions ($\sim 10^{-4}$ m/s) using 1 mM NaCl solution. Measured data included penetration distance of the solid phase interface into the fracture as a function of time, effluent solids concentration, swelling pressure (in two cases) and post-mortem analysis of penetrated mass and mass remaining in emplacement volume.

Images from the three benchmark tests performed with the similarly-sized samples are displayed in Figure 1 and extrusion distances into the 0.1 mm fractures during these tests are plotted as a function of time in Figure 2. As indicated, phase 1 of the tests (stagnant period) was characterized by somewhat symmetric extrusion to steady-state distances; phase 2 of the tests (low flow velocity) was characterized by rather abrupt increases in average extrusion distances and the formation of distinct solid material regions; phase 3 (high flow velocity) of the tests was characterized by further development of the sharp boundary between the inner continuous solid material zones (used to determine extrusion distance) and the outer discontinuous particulate

material zones which, in the cases of tests A and C, translated into overall decreases in the average extrusion diameters. Clear flow patterns of entrained, eroding solid material from around the extrudates are also visible during the high flow velocity phase.

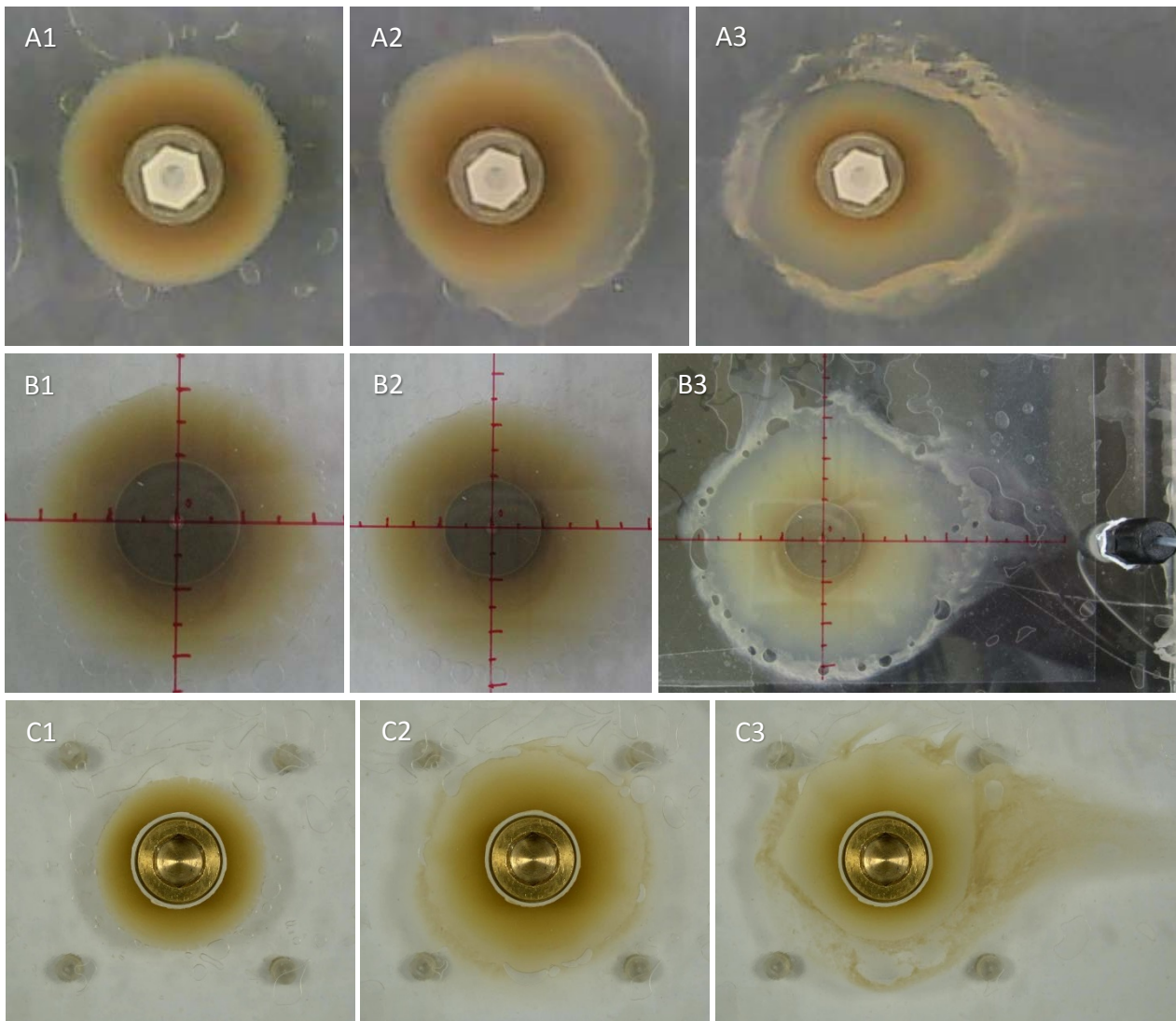


Figure 1. Appearance of the three benchmark tests (A, B and C) performed with similarly-sized samples shown at the end of phase 1, phase 2 and phase 3.

Overall benchmark tests A, B and C showed extrusion distances, considered as average diameters of the extruding phase into the fracture volumes, ranging from 3.8 to 4.6 cm at the end of phase 1, from 4.9 to 5.3 cm at the end of phase 2 and from 4.4 to 5.9 cm at the end of phase 3.

In terms of effluent solids content measurements performed during the active flow phases of the benchmark tests, concentrations ranging from 8 to 30 ppm during phase 2 (for tests A and B at $\sim 1.3 \times 10^{-6}$ m/s) and from 56 to 108 ppm during phase 3 (for tests A, B and C at $\sim 1.2 \times 10^{-4}$ m/s) were measured. These results are in accord with a positive dependence between groundwater velocity and erosion rate. Phase 3 erosion was accompanied by a measured 40% drop in swelling pressure for test C.

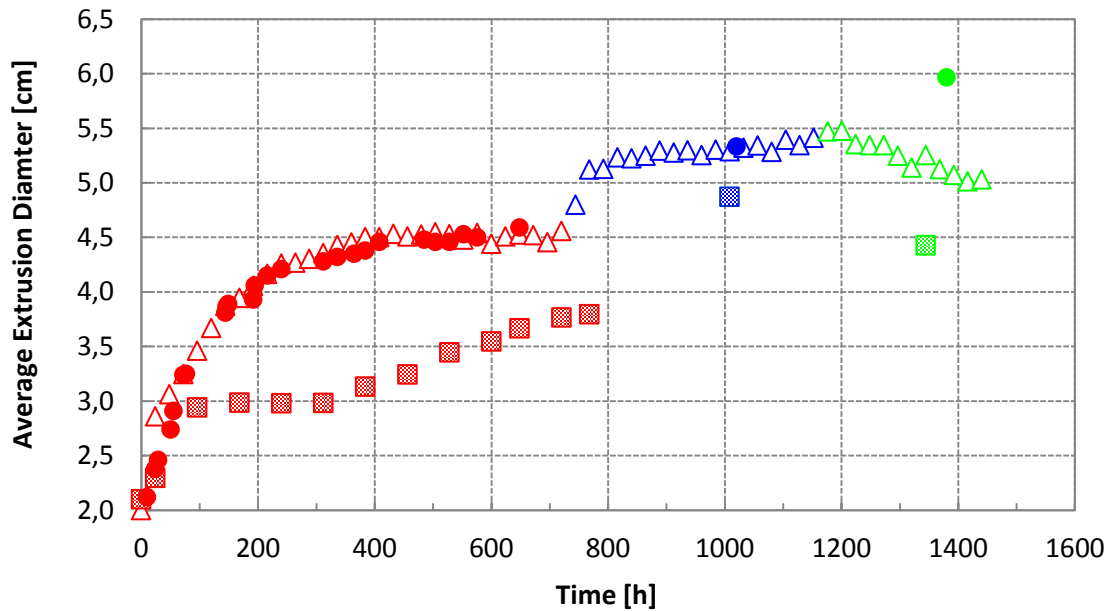


Figure 2. Extrusion behavior over the course of the benchmark tests. Tests A, B and C (see Figure 1) correspond to the open triangle, solid circle and pattern-filled square symbols, respectively. Specific test phases are indicated with distinct symbol colors (phase 1 data is red, phase 2 data is blue and phase 3 data is green). Average extrusion diameters were determined by the same image analysis technique for all of the phase 2 and phase 3 values.

Post-mortem analyses of mass remaining in the emplacement volume and extruded mass relative to original emplacement mass indicates a total loss of 2 to 11% with respect to the benchmark test conditions.

Naturally this first attempt at benchmarking artificial fracture tests was not without associated procedural ambiguities, practical difficulties and other uncertainties. Of particular interest is the experience of the fourth benchmark test which was conducted at a four times larger sample scale than tests A, B and C. The behavior of this test was markedly different than the tests with similarly-sized, smaller samples as the onset of extrusion was significantly delayed and its subsequent growth was greatly reduced to the extent that phases 2 and 3 of the test could not be performed.

Size of Clay Platelets, pH and Temperature Matter

M. Segad

Advanced Light Source, Lawrence Berkeley National Laboratory,
1 Cyclotron Rd, Berkeley, CA 94720, USA

Clay mineral plays an essential role in many environmental and industrial processes e.g. gas and nuclear waste storages. However, little is known regarding the microstructure and the forces involved in clay-water systems. Hybrid X-ray techniques such as wide/small-angle X-ray scattering (WAXS/SAXS), X-ray absorption spectroscopy (XAS) and X-ray photon correlation spectroscopy (XPCS) and some other methods as dynamic light scattering (DLS), nuclear magnetic resonance (NMR), transmission electron microscopy (TEM) and Cryogenic-TEM have been used to provide direct information about the structure of natural and synthetic clay dispersions that in equilibrium with a bulk solution of given ionic composition, temperature and pH. Multi-scale theoretical approach has also been used to predict the osmotic pressure as well as the colloidal behaviors of single and multi-component systems. In this talk, I will describe the effect of platelet size, pH, temperature and electrostatic interactions on swelling, flocculation and aggregation phenomena. I will also present a number of factors that control the aggregation process, so that the results can be generalized.

References

- [1] M. Segad, B. Cabane and Bo Jönsson, *Nanoscale* 7 (2015) 16290.
- [2] M. Segad, *J. Appl. Cyst.* 46 (2013) 1316.
- [3] M. Segad, T. Åkesson, B. Cabane and Bo Jönsson, *PCCP* 17 (2015) 29608.

UNDERSTANDING THE MECHANISMS OF CHEMICAL EROSION OF BENTONITE – NEED FOR A HOLISTIC APPROACH

Heini Reijonen (Heini.reijonen@sroy.fi), Nuria Marcos, Saanio & Riekkola Oy, Barbara Pastina, Posiva Oy

Introduction

Geologic repositories in crystalline rock rely on the swelling properties of clays sealing the open volumes after emplacement of high-level radioactive waste. Chemical erosion is a process that has been suggested to challenge the stability of clays in presence of dilute groundwater (i.e. total charge equivalent of cations <4mM, SKB 2011 and Posiva 2012). Hence there is a need to better understand all the mechanisms that can potentially affect the potential for erosion of bentonite in repository conditions.

Chemical erosion has been observed mostly in laboratory conditions in rather simplified experimental setups involving artificial fractures and mostly purified montmorillonite. These laboratory tests showed that Ca-bentonite is more resistant to erosion than Na bentonite. However, when looking at bentonite deposits in previously glaciated terrains (i.e. areas within the boundaries of the last glacial maximum), dilute water does not seem to be responsible for erosion. Furthermore, montmorillonite occurs as an ancient alteration mineral in locations where the surrounding hydrogeochemical conditions are dilute (according to the above definition). In fact, smectites are actually formed in surface soils affected by the infiltration of meteoric waters. All these observations suggest that chemical erosion of montmorillonite and other smectites is not a simple process and it cannot be easily studied in laboratory conditions using the current simplified systems. Understanding the underlying mechanisms of smectite-water interaction in more realistic boundary conditions is of great importance to be able to construct a realistic conceptual model for the chemical erosion process, i.e. define the boundary conditions for the occurrence and extent of the process.

To expand the knowledge base and improve the understanding of the mechanisms of chemical erosion, ideas and examples are provided here for further consideration from:

- in situ experiments,
- geological formations, and
- experimental studies from other fields of expertise, such as colloid sciences or geotechnical engineering.

Modelling development and understanding of the groundwater evolution are beyond the scope of this presentation, although these are important factors as well from the performance assessment point of view.

Sources of information

Of all reported in-situ experiments (at full or reduced scale) in dilute groundwater conditions, none has been done with Na-bentonite. Because no in-situ experiments have been attempted so far with Na-bentonite, it is unclear whether this type of bentonite is really more prone to erosion than Ca-bentonite, as suggested by laboratory tests. Na-bentonite is also found in nature alongside with Ca-bentonites in relatively dilute conditions (surficial exposures, e.g. in Wyoming), so there may be a common factor that limit to a large extent chemical erosion. As also observed in laboratory

conditions, bentonites are, in general, more resistant to chemical erosion compared with purified montmorillonite minerals. Unfortunately, detailed investigations on natural bentonite formations and their interactions with local groundwater are rather scarce (e.g. Laine & Karttunen 2010).

Smectites, including montmorillonite, are the main components of bentonite. They have been observed also in fracture systems of crystalline bedrock (e.g. Gehör 2007 and Marcos 2002) as well as in weathering profiles (e.g. Vartiainen 2005) and larger intrusive rock bodies that have pervasively altered to smectite (Laine & O'Brien 2008). These fracture minerals are a result of hydrothermal late stage alteration and seem to have been preserved in situ, also at previously glaciated terrains. Currently, there is no detailed information on the properties of these montmorillonites (see Reijonen & Alexander 2015). However, studying their mode-of-occurrence in open and closed fracture systems could shed light on the long-term erosion resistance of these materials. Notably, at Kivetty site in Finland, montmorillonites are present in fractures (Gehör et al. 1997) where, according to the groundwater analyses, the water composition is more dilute than at Olkiluoto (Pitkänen et al. 1998). Similar observations were gathered from the Hyrkkölä site, where smectite has been observed from open fractures in dilute conditions (Marcos 2002, Marcos and Ahonen 1999) (Fig.1).

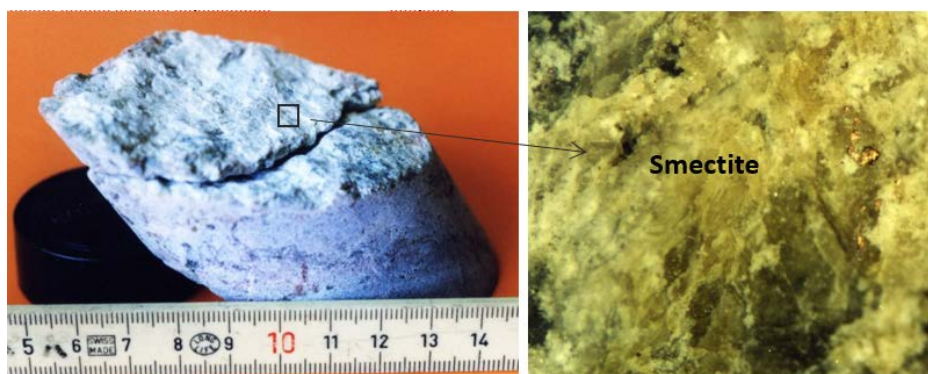


Fig. 1. Drill core and close up from Hyrkkölä, Finland at about 80 m depth in dilute conditions (Marcos 2002).

The colloid stability of bentonites as well as the chemical reactions and parameters affecting it have been thoroughly studied in colloidal science. In order to produce colloidal solutions, purification of natural bentonite is needed. The presence of iron oxides and organic materials affects the properties of colloidal suspensions and prevent optimal peptization, i.e. the formation of a stable dispersion of colloidal particles (Lagaly and Dékány 2013). It is well known in colloidal sciences that the carbonate and silica present in bentonite destabilize colloid dispersions, the former due to potential Ca and Mg release and consequent reduction of peptization and the latter due to cementing process caused by amorphous silica (Lagaly and Dékány 2013). Hence, carbonate and silica are responsible for at least some of the differences in the ability to form stable colloids observed between natural bentonites and purified montmorillonites.

Certain compounds, such as phosphates and oxides also destabilize colloidal particles (see Lagaly and Dékány 2013). These are all compounds found in natural groundwaters.

Furthermore, the sedimentation of dispersed bentonite particles should be considered in more detail when studying colloidal systems. In colloidal science, at least two sedimentation types (free and structural) have been observed in laboratory conditions (see Lagaly and Dékány 2013). It seems that in addition to the type of dispersion, sedimentation is affected also by chemical factors, such as

cation composition and pH. Filter cake formation is known from colloid clay science and could also be studied in more detail, to better understand how potentially eroded bentonite might settle in repository conditions. In geological formations, re-sedimentation of bentonites is rarely reported but this may be due to lack of studies with a specific focus on this process. Nonetheless, sedimentation is a process utilised in many geotechnical solutions.

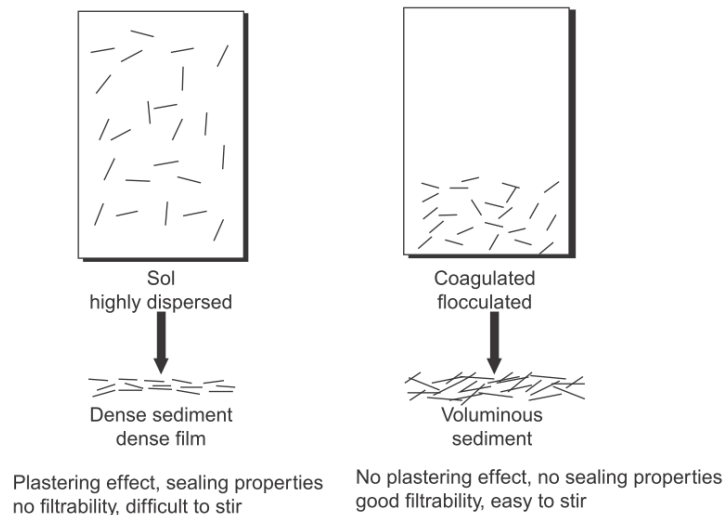


Fig. 1. Two types of sedimentation defined for well dispersed clay colloids (left) and aggregates (right) (Lagaly and Dékány 2013).

Geotechnical solutions utilising bentonite often use also techniques that are based on coating reactions. Coating may be a relevant process in the KBS-3 system, since the possible reactions that occur at the bentonite-fracture interface may occur over a limited surface areas and bentonite acts, in practice, as coating material. For example, the cation exchange process will alter the buffer bentonite at the buffer-groundwater interface, but it is unclear whether this will occur throughout the buffer mass.

Summary and conclusions

Considering the current data available, it can be said that the experimental set ups currently used to study chemical erosion may be overly simplified. A more holistic approach is needed to perform a reliable assessment of the bentonite stability in repository conditions. The mismatch between laboratory experiments and observations in nature is due to a lack of understanding of the parameters and processes affecting the erodability of smectite and how these interact with each other. This has four main implications:

1. all the information in the scientific literature should be considered, including additional field of expertise such as geotechnical sciences and colloid sciences,
2. the experimental set ups to study chemical erosion should cover also more complex groundwater compositions (accounting for more complex anion/cation compositions) and smectite/bentonite compositions (including presence of various types of accessory minerals)
3. natural formations of montmorillonites should be further studied to understand their mode of occurrence as stable phases in natural repository relevant environments.

4. the scaling effects of the process should be better understood when moving from laboratory scale to in-situ conditions. The lack of underground research laboratories providing data on the larger scale is an obvious challenge.

If such a holistic approach were to be implemented, the overall understanding of the stability of the bentonite buffer in the repository conditions can then be based on a conceptual model that is backed up by experimental and geological data.

References

- Gehör, S. 2007. Mineralogical Characterization of Gouge Fillings in ONKALO Facility at Olkiluoto. Posiva Working Report 2007-33. Posiva Oy, Olkiluoto, Finland.
- Gehör, S. Kärki, A., Suoperä, S. & Taikina-aho, O. 1997. Kivetty, Äänekoski: Petrology and low temperature minerals in the K1-K11 drill core samples. Posiva Working Report 97-16. Posiva Oy, Helsinki, Finland.
- Lagaly, G. and Dékány, I. 2013. Colloid clay science. *Developments in clay science*, 5, 243–345.
- Laine, H. & Karttunen, P. 2010. Long-Term Stability of Bentonite- A Literature Review. Posiva WR 2010-53. Posiva Oy, Eurajoki, Finland.
- Laine, H. & O'Brien, H. 2008. Alteration and primary kimberlite rock type classification for Lahtojoki kimberlite, Finland. 9th International Kimberlite Conference Extended Abstract No. 9IKC-A-00348, 2008.
- Marcos, N. 2002. Lessons from nature – the behaviour of technical natural barriers in the geological disposal of spent nuclear fuel. *Acta Polytechnica Scandinavica, Civil Engineering and Building Construction Series*, Espoo 2002. Published by the Finnish Academy of Technology, 39p.
- Marcos, N. and Ahonen, L. 1999. New data on the Hyrkkölä U-Cu mineralization: The behaviour of native copper in a natural environment. Posiva 99-23. Posiva Oy, Helsinki, Finland.
- Pitkänen, P., Luukkonen, A., Ruotsalainen, P., Leino-Forsman, H. & Vuorinen, U. 1998. Geochemical modelling of groundwater evolution and residence time at the Kivetty site. POSIVA 98-07. Posiva Oy, Helsinki, Finland.
- Posiva 2012. Safety case for the disposal of spent nuclear fuel at Olkiluoto – Design Basis 2012. POSIVA 2012-03. Posiva Oy, Eurajoki, Finland.
- Reijonen, H.M. & Alexander, W.R. 2015. Bentonite analogue research related to geological disposal of radioactive waste: current status and future outlook. *Swiss Journal of Geosciences*, 2015, 108 (1), 101-110.
- SKB 2011. Long-term safety for the final repository for spent nuclear fuel at Forsmark Main report of the SR-Site project, Volume I. SKB TR-11-01. SKB, Stockholm, Sweden.
- Vartiainen, R. 2005. Teollisuusmineraali- ja rakennuskivitutkimukset Pohjois-Suomessa vuosina 2002–2004 (in Finnish with English abstract). M 10.4/2005/4. Geological Survey of Finland.

IRREVERSIBILITY OF BENTONITE COLLOID AGGREGATION UNDER DIFFERENT ENVIRONMENTS

Natalia Mayordomo, Ursula Alonso (ursula.alonso@ciemat.es) and Tiziana Missana. CIEMAT Department of Environment, Avenida Complutense 40, CP 28040, Madrid (Spain).

Bentonite colloids generated from the backfill barrier in nuclear waste repositories may act as radionuclide carriers if they are stable and mobile. The stability of bentonite as a function of several chemical and physical parameters, such as pH, ionic strength, temperature and presence of different multivalent ions, or organic ligands, has been widely analysed. Stability studies analyse whether or not colloids aggregate and the main measurable consequence of aggregation is the increase of particle mean size. It is well established that colloids are aggregated and unstable when pH is acidic and ionic strength is high [1-2].

Negligible colloid concentration is therefore predicted in repository scenarios with high saline groundwater but, in the time frame of repositories, groundwater conditions may evolve. Recharge water (i.e. rivers, lakes, rain or water from melting ice sheet) may reduce groundwater salinity promoting particle disaggregation and stabilization.

Within the frame of a nuclear waste repository, especially considering the Scandinavian scenario, the possible disaggregation of clay particles, due to water glacial melting, is of concern. Under saline conditions colloids are aggregated but the possible disaggregation processes have been scarcely investigated.

Therefore the objective of this work is to study the irreversibility of clay colloid aggregation.

Within BELBAR EC project, bentonite colloids disaggregation was analysed by different approaches, in Na^+ , Na^+ - Ca^{2+} mixed and Ca^{2+} electrolytes, and considering experimental times from hours to months [3]. Aggregation and disaggregation was induced by ionic strength changes. Photon Correlation spectrometry (PCS) and Single Particle Counter (SPC) technique were used to measure the mean hydrodynamic diameter, the size distribution and the concentration of bentonite particles.

All experiments were carried out starting from a stable suspension of bentonite colloids prepared from FEBEX bentonite in NaClO_4 0.5 mM as described in [2-3]. All suspensions were maintained at $\text{pH } 6.5 \pm 0.5$. The mean hydrodynamic particle diameter of the stable suspension, measured by PCS, was around 300 nm.

Bentonite colloid aggregation was promoted by increasing the ionic strength from 0.5 mM up to 0.1 M in the different electrolytes. Particles start aggregation when the repulsive forces weaken or become attractive, in our case promoted by increasing the ionic strength of the suspensions.

By increasing the ionic strength, fast aggregation occurred and hydrodynamic diameters over 1 μm were measured at 0.1M in case of NaClO_4 and for ionic strengths higher than 10 mM in the case of Na^+ - Ca^{2+} electrolytes, as consequence of the aggregating effect of Ca^{2+} , as Schulze-Hardy rule predicts.

Main aim of our experiments was to verify if colloids, once aggregated, could return to the fully disaggregated state by turning chemical conditions favourable to their stability. Some disaggregation experiments were carried out by dialysis method, maintaining bentonite colloid concentration thorough progressive ionic strength decrease. Figure 1 presents the hydrodynamic diameter measured on bentonite samples aggregated at 0.1 M in Na^+ or Na-Ca mixed electrolytes and later subjected to progressive ionic strength decrease in the same electrolyte. In both electrolytes it was observed that the average hydrodynamic size decreases

as ionic strength decreases, but disaggregation is clearly favoured at the lowest ionic strength and in absence of Ca^{2+} . It is noteworthy that hydrodynamic diameter of the initial stable suspension at 0.5 mM (plotted as continuous lines in Figure 1) was not recovered in any case. Once bentonite colloids are aggregated, disaggregation is not complete within the time frame of our experiments, even in Ca^{2+} free environments. This clearly indicates a hysteresis in the aggregation/disaggregation process.

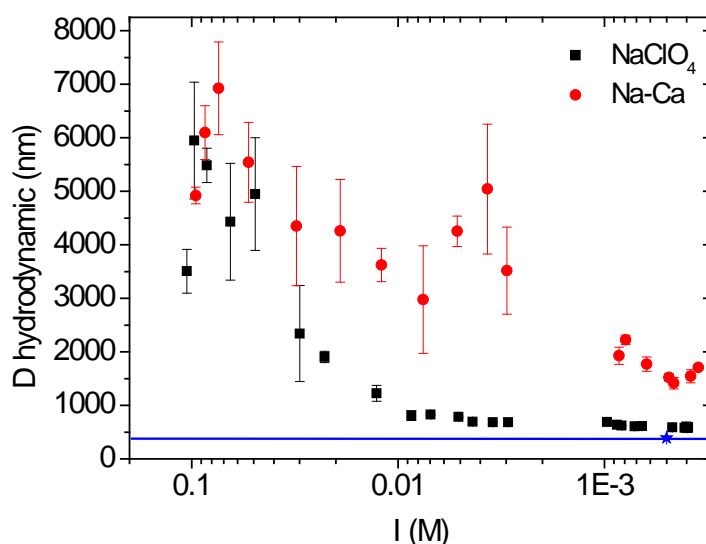


Figure 1. Hydrodynamic diameter measured on aggregated bentonite samples subjected to progressive ionic strength decrease, by dialysis method, in (■) Na^+ or (●) Na-Ca mixed electrolytes. Average hydrodynamic diameter of the initial bentonite colloid suspension in NaClO_4 0.5 mM is plotted as continuous line.

Other experiments were focused in comparing the kinetics of aggregation and disaggregation, carried out by time resolved measurements during 60 minutes. Aggregation was induced by increasing ionic strength up to 0.1 M as well, in different background electrolytes (NaClO_4 and $\text{Na}^+-\text{Ca}^{2+}$ and CaCl_2). Disaggregation in this case was promoted by fast dilution at lower ionic strengths (10 mM, 1 mM, and 0.5 mM).

By dilution to lower ionic strength, disaggregation occurred in less than five minutes. Figure 2 presents the final hydrodynamic diameter measured, after 60 minutes, upon dilution in the different electrolytes for sample previously aggregated at 0.1 M in Na (Figure 2a), Na-Ca mixed (Figure 2b) and Ca (Figure 2c) electrolytes. Colloids aggregated in Na electrolyte (Figure 2a) are disaggregated by decreasing ionic strength both in Na and mixed Ca-Na electrolytes. Colloids aggregated in mixed Na-Ca electrolytes (Figure 2b) are appreciably disaggregated only in Ca free electrolytes. And colloids aggregated in Ca electrolytes are not significantly disaggregated in any case. This means that the history of aggregation plays a role on future disaggregation.

Single Particle Counter (SPC) was applied to analyse in depth the size distribution of the stable fraction recovered in the bentonite suspensions after disaggregation [3]. It is remarkable that, even at high ionic strengths, and in presence of Ca , small colloids are detected in disaggregated samples. The most populated fraction of stable colloids recovered in Na^+ electrolyte was found within 50-100 nm size detector, while in the $\text{Na}^+-\text{Ca}^{2+}$ was within 50 to 300 nm, higher in diameter ranges > 200 nm, as Ca^{2+} hinders disaggregation. Nevertheless, it should be noted that the total particle concentration measured by SPC in disaggregated samples is lower than the one in 0.5 mM NaClO_4 , which is the initial stable suspension. Suspensions disaggregated in NaClO_4 had a concentration ratio very close to that of primary

suspension (about 0.91 average), but in presence of Ca^{2+} , the ratio of concentration of disaggregated particles is low compared to the primary (0.3 in the best situation).

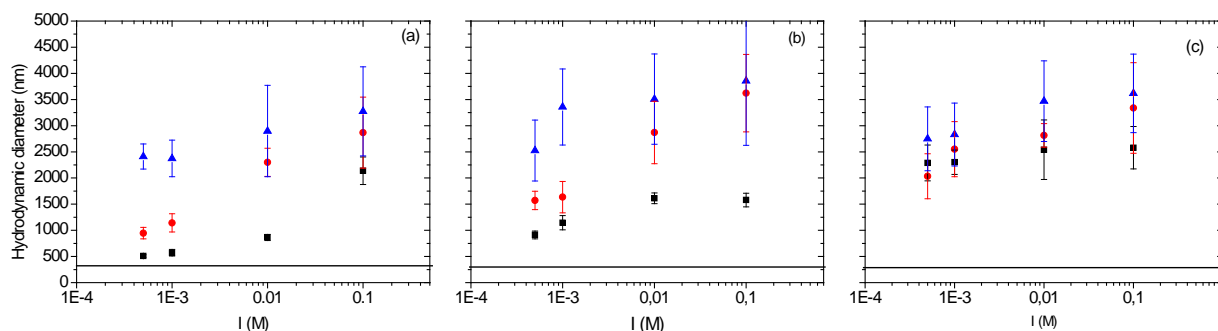


Figure 2. Hydrodynamic diameter measured on aggregated bentonite samples in (a) Na^+ or (b) Na-Ca mixed and (c) Ca electrolytes, upon fast dilution lower ionic strength in different electrolytes (■) Na^+ or (●) Na-Ca mixed and (▲) Ca electrolytes. Average hydrodynamic diameter measured on the initial bentonite colloid suspension in NaClO_4 0.5 mM is plotted as continuous line.

Overall, our results showed that disaggregation of bentonite colloids is effectively promoted by decreasing ionic strength, but the process is not fully reversible and initial stable hydrodynamic diameter is not recovered, even at lower ionic strength and in the absence of divalent cations. Mean particle size recovered is in most cases over $1 \mu\text{m}$, SPC results indicated that fast and great dilution of aggregated colloids to low ionic strength provided as well smaller colloids. Pareto values obtained indicated that a population of stable colloids is present, but their concentration was low compared to the initial values.

In presence of divalent cations, the stable portion of disaggregated colloids was very low compared to the primary sample ($< 10\%$) even at the lowest ionic strength, but it was around a 70% in the absence of Ca. Not fully disaggregated particles would have restricted mobility, but further disaggregation at longer times is not discarded.

This work was supported by the EU FP7/2007-2011 program, under the EC-BELBAR project (N° 295487). N. Mayordomo acknowledges the FPI BES-2012-056603 grant from MINECO (Spain).

- [1] Lagaly, G. & Ziesmer, S. (2003) Colloid chemistry of clay minerals: The coagulation of montmorillonite dispersions. *Advances in Colloid and Interface Science*, 100-102, 105–128.
- [2] Missana, T., Alonso, U. & Turrero, M.J. (2003) Generation and stability of bentonite colloids at the bentonite/granite interface of a deep geological radioactive waste repository. *Journal of contaminant hydrology*, 61, 17–31.
- [3] Mayordomo, N., Degueldre C., Alonso, U. and Missana, T. (2015). *Clay Minerals* (In press, accepted manuscript).

INFLUENCE OF TEMPERATURE ON SMECTITE CLAY GELS

Emelie Ekvy Hansen, Magnus Hedström (mh@claytech.se)

Clay Technology AB, IDEON Science Park, SE-223 70 Lund, Sweden

Understanding gelation of smectite clay is important for many industrial applications. While undesirable in some cases, gel formation may be necessary to ascertain long-term safety for the use of bentonite in high-level nuclear waste repositories. The forces responsible for gelling in smectite gels have been under debate. At high ionic strength, of the order of 100 mM and above the van der Waals interaction may play the dominating role in the coagulation process. But at low ionic strength, a different mechanism is needed to explain gelation. The strong influence of pyrophosphate and other polyphosphates on clay gel formation has been interpreted as evidence of electrostatic edge-to-face attraction. In recent rheological measurements on bentonite slurries (7% w/w) it was found that the addition of polyphosphates totally removed the yield strength over the pH range 5-10 and drastically reduced the yield strength below pH 4 (Goh et al., 2011). Without adding polyphosphate, the yield strength was significant ~30 Pa even at pH 10, which led the authors to further draw the conclusion that: “The nature of the clay particle edge charge must still be positive at this high pH level”.

However, adding polyphosphates to a clay suspension leads to a modification of the edge of the clay particles. In the present study (Ekvy Hansen and Hedström, 2016), we aim at investigation the nature of the gelling process in smectite clays without changing the particles. We therefore develop a protocol where smectite gels are heated in a water bath and their response to temperature is recorded. Under some combinations of clay concentration and ionic strength the gels exhibit thermoreversible behaviour: They melt while heated, i.e, transform into a sol, and return to the gel state when the temperature falls. With other combinations of clay concentration and ionic strength the gels do not undergo a complete phase transformation but may exhibit yield (Figure 1). The temperature at which yield is first observed is recorded as the yield-point temperature. The gel strength, presumably reflected in the yield-point temperature, was found to depend on salinity, clay concentration, and aging. Especially at the lower end of investigated ionic strengths aging increased the yield-point temperature, while for high ionic strength where presumably van der Waals interactions dominate, the yield-point temperature was relatively insensitive to gel age.

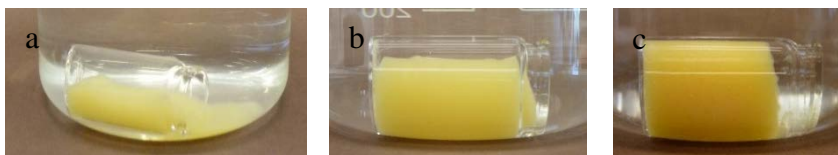


Figure 1 Three gels after rapid heating to 75 °C. (a) Ku-Na gel (10 g/l) in 5 mM NaCl solution. The gel underwent almost complete melting transition during heating to 75 °C and solidified as the temperature was lowered. (b) Ku-Na gel (10 g/l) in 6 mM NaCl-solution. The gel experienced large deformation (partial melting) during heating to 75 °C. (c) Ku-Na gel (20 g/l) in 200 mM NaCl-solution. The gel showed no sign of change.

Gelling of sodium smectite dispersions do not occur unless the sodium salt (here we limit the study to NaCl) concentration is above a critical value (CCC). It seems that the positive edges are not discernible to the negative faces at concentrations below the CCC. This observation has been interpreted in terms of a spillover of the negative potential of the particle face into the edge region. By numerically solving the Poisson-Boltzmann equation for a thin disc, mimicking the aspect ratio and the edge and face charge densities of montmorillonite, it was found that the spillover of the negative potential depends strongly on the NaCl concentration (Secor and Radke, 1985). Above the CCC the spillover is reduced to such extent that the potential emanating from the edge region is positive and thereby attraction with the negative surface of a second clay particle becomes possible. However, electrostatic screening also influences the attraction between positive and negative charges so at some ionic strength further above the CCC the smectite gel is expected to get weaker.

We recorded the variation of the yield point temperature with NaCl concentration and the result are in accordance with the prediction of the spillover and electrostatic screening model (Figure 2)

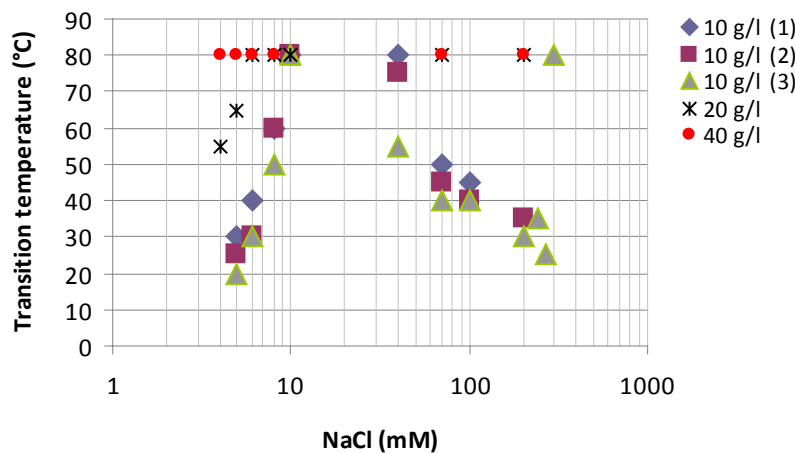


Figure 2 Transition (yield point) temperatures of Ku-Na gel (10-40 g/l) at varying salinity. Samples that showed no change upon heating to 75 °C (the maximum temperature in the test) are plotted at 80 °C.

We also investigated the variation of yield point temperature, T_y with clay concentration, C_{clay} keeping the salinity constant at 5 mM. The results are shown in Figure 3 and suggest that the relation

$$\ln C_{\text{clay}} = \Delta H / RT_y + \text{constant}, \quad (1)$$

holds. In Eq. (1) ΔH is the enthalpy of edge-to-face binding. Eq. (1) follows from percolation theory and was first tested and confirmed for gelatin gels in the 1950s (Eldridge and Ferry, 1954).

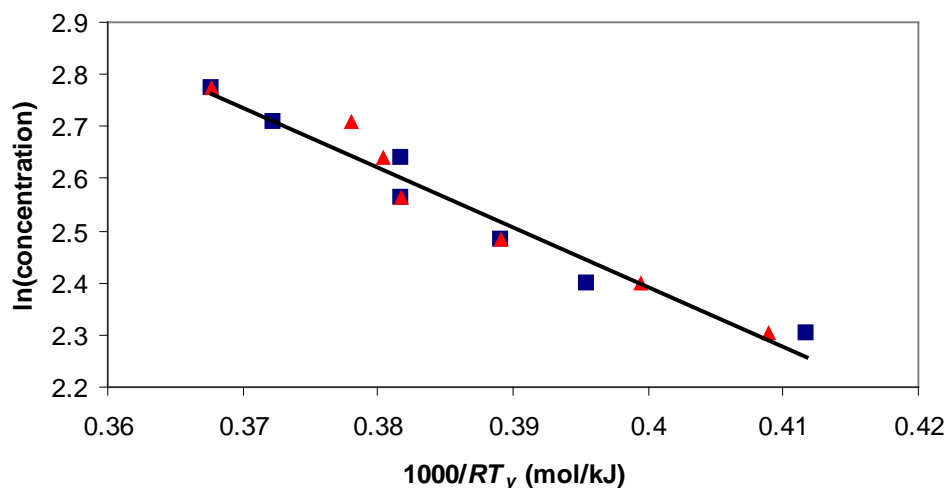


Figure 3 Relation between \ln (clay concentration) vs. inverse transition temperature for Ku-Na montmorillonite at NaCl concentration of 5 mM. Regression analysis of the data from both test series gave the enthalpy of formation of edge-to-face junctions to -11.5 ± 0.7 kJ/mol corresponding to $-4.6 \pm 0.3 k_B T$ at room temperature.

The experiments presented here provide novel evidence that Coulombic attraction between the positive edges and the negative faces of the clay particles is the dominating force at relatively dilute saline conditions. By heating smectite gels, a non-trivial variation of the yield-point temperature was observed as a function of NaCl concentration. This salt concentration dependence on the yield-point temperature is in agreement with Poisson-Boltzmann theory that includes edges and electrostatic screening.

From the yield-point temperature variation with clay concentration, under constant salinity, the enthalpy of edge-face bonds was evaluated, using a relation that was derived using ideas from percolation theory. In particular for Ku-Na montmorillonite at 5 mM NaCl the edge-to-face binding enthalpy was evaluated to -11.5 ± 0.7 kJ/mol or equivalently $-4.6 \pm 0.3 k_B T$ at room temperature.

A consequence of the present results is that in order to model the phase diagram of smectite clay and ultimately the evolution of a bentonite buffer in a nuclear waste repository, attractive edge-face interactions need be included besides the conventional DLVO forces. The evaluated binding enthalpy may serve a guideline to the strength of edge-face attraction.

Acknowledgements

The research leading to these results has received funding from the European Atomic Energy Community's Seventh Framework Programme (FP7/2007-2011) under Grant Agreement

no295487, the BELBaR project, and from the Swedish Nuclear Fuel and Waste Management Company (SKB).

References

- Goh, R., Leong, Y.-K., Lehane, B., 2011. Bentonite slurries—zeta potential, yield stress, adsorbed additive and time-dependent behaviour. *Rheol. Acta* 50, 29–38.
- Ekvy Hansen, E., Hedström, M., 2016. Smectite clay gel behaviour during heating: Evidence of electrostatic edge-to-face attraction. Submitted to *J. Colloid Interface Sci.*
- Eldridge, J.E., Ferry, J.D., 1954. Studies of the Cross-linking Process in Gelatin Gels. III. Dependence of Melting Point on Concentration and Molecular Weight. *J. Phys. Chem.* 58, 992–995.
- Secor, R.B., Radke, C.J., 1985. Spillover of the diffuse double layer on montmorillonite particles. *J. Colloid Interface Sci.* 103, 237–244.

INTERACTION PRESSURE BETWEEN CHARGED PLATE-LIKE PARTICLES IN ELECTROLYTE SOLUTIONS: AN APPLICATION OF DENSITY FUNCTIONAL THEORY WITH THE SOLVENT PRIMITIVE MODEL

Longcheng Liu

Department of Chemical Engineering and Technology
 Royal Institute of Technology, KTH
 S-100 44, Stockholm, Sweden
lliu@ket.kth.se

Within the BELBaR project, we have developed a weighted correlation approach (WCA) [1, 2] to the density functional theory (DFT) of statistical mechanics. This approach has been applied previously [1-3] to study homo-interaction between parallel charged plates, like clay particles, immersed in electrolytes in the framework of the restrictive primitive model (RPM). It is now extended to include solvent-solvent and ion-solvent interactions using the solvent primitive model (SPM), which was not accounted for in the classical DLVO theory of colloid stability. The objective is to explore the steric effects of the neutral solvent molecules on the interaction pressure between clay particles and to see when the RPM is applicable.

As exemplified in Figs. 1 and 2, the analysis shows that the WCA approach is excellent in describing the structural and thermodynamic properties of the SPM of electrical double layers (EDLs) over a wide range of electrolyte concentrations as well as surface charge densities, in comparison with the results of Monte Carlo simulations [4, 5]. It is superior to both the modified Poisson-Boltzmann approach [5] and the reference fluid density (RFD) theory [6], giving more accurate predictions.

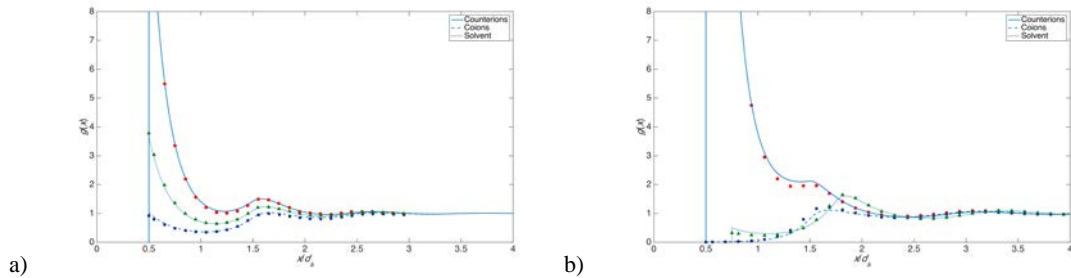


Fig. 1. Singlet distribution functions for a 1:1 electrolyte at $c = 1.0$ M in the cases involving a) the surface charge density $\sigma = 0.1$ C m⁻², the total packing fraction $\eta = 0.3$, and the diameters $d_+ = d_- = d_s = 0.4$ nm; and b) $\sigma = 0.5$ C m⁻², $\eta = 0.32$, $d_+ = d_- = 0.4$ nm, and $d_s = 0.6$ nm, respectively, using the SPM. The Monte Carlo data [4,5] are given by symbols while the WCA results by lines.

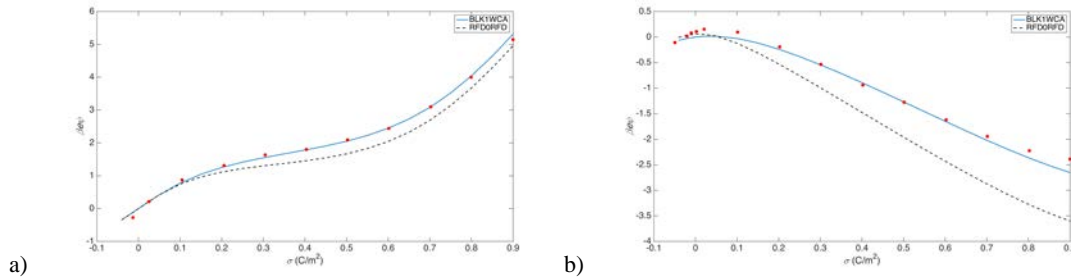


Fig. 2. Mean electrostatic potential at the contact distance $\psi(d/2)$ as a function of the surface charge density for the cases involving a) 1:1 electrolyte and b) 1:2 electrolyte, respectively, with $c = 1.0$ M, $d_+ = d_- = d_s = 0.4$ nm, and $\eta = 0.3$ at $\sigma = 0.1$ C m⁻² using the SPM. The Monte Carlo data [4] are given by symbols while the WCA and the RFD results by lines.

Of great importance, we found that the hard-core exclusions of solvent molecules play a dominant role in determining the interaction pressure between charged plates in an electrolyte solution, especially in the cases where the sizes of hydrated ions are comparable to those of solvent molecules. As shown in Fig. 3, the strongly oscillatory force that results from the presence of the neutral solvent molecules was found to be largely independent of the properties of the electrolyte in the cases when the solvent molecules have the same diameter as the ions. This behavior has never been seen in the RPM of electrolytes, but consistent with experimental observations of the interaction between mica surfaces in non-polar liquid [7].

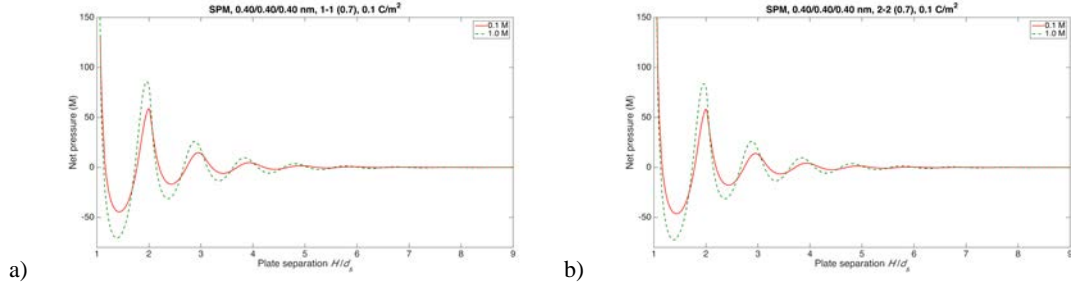


Fig. 3. Interaction pressure between charged plates as a function of the plate separation for the cases involving a) 1:1 electrolyte and b) 2:2 electrolyte, respectively, with $d_+ = d_s = 0.4 \text{ nm}$, and the solvent packing fraction $\eta_s = 0.3665$ at $\sigma = 0.1 \text{ C m}^{-2}$ using the SPM.

When the solvent molecules are slightly smaller than the ions, however, the interaction pressure becomes less oscillatory, but still very different from the results obtained from the RPM of electrolytes, as seen in Figs. 4 and 5. In such cases, a negative shallow minimum can also be observed in 1:1 electrolytes at large concentration and surface charge densities. The valence of counterions then turns out to be an important parameter: the attractive interaction when the counterions are divalent is much stronger than that when the counterions are monovalent.

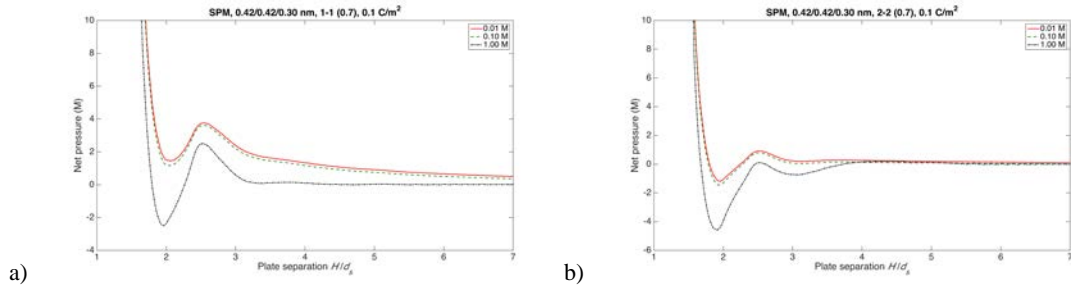


Fig. 4. Interaction pressure between charged plates as a function of the plate separation for the cases involving a) 1:1 electrolyte and b) 2:2 electrolyte, respectively, with $d_+ = d_s = 0.42 \text{ nm}$, $d_s = 0.3 \text{ nm}$, and $\eta_s = 0.3665$ at $\sigma = 0.1 \text{ C m}^{-2}$ using the SPM.

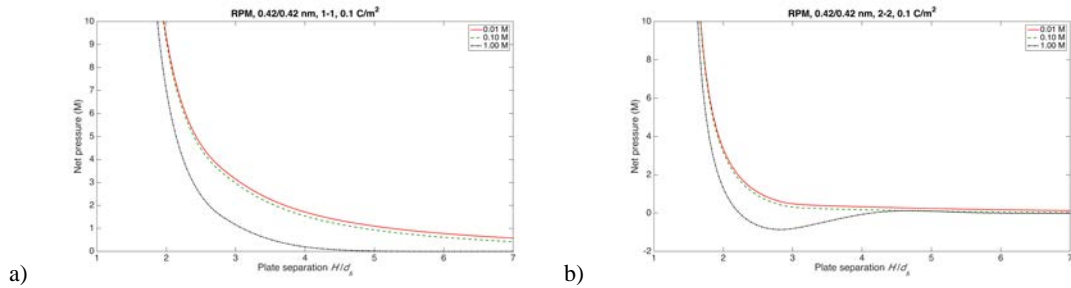


Fig. 5. Interaction pressure between charged plates as a function of the plate separation for the cases involving a) 1:1 electrolyte and b) 2:2 electrolyte, respectively, with $d_+ = d_s = 0.42 \text{ nm}$ at $\sigma = 0.1 \text{ C m}^{-2}$ using the RPM.

When the counterions have been fully hydrated, a prehensive diameter for Na^+ and Ca^{2+} ions would be 0.72 nm and 0.84 nm , respectively. They are far larger than the size

of water molecules, and therefore it is of great interest to see if the effects of the hard-core exclusions of water molecules are still pronounced in these cases in determining the behavior of interaction between charged plates. Clearly, the results shown in Figs. 6 and 7 indicate that the dependences of the interaction pressure on the surface charge density, the electrolyte concentration, and the separation distance in the SPM of electrolytes are qualitatively the same as those identified in the RPM of electrolytes where the molecular nature of water has been totally ignored. The major difference exhibits only in short separations, smaller than the thickness of 4 or 5 water layers.

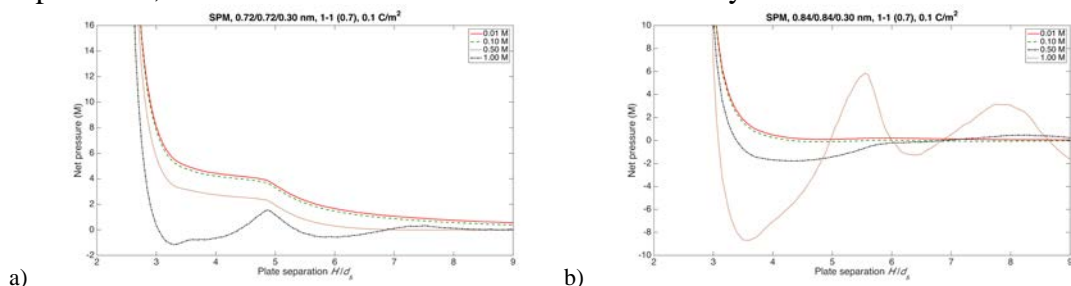


Fig. 6. Interaction pressure between charged plates as a function of the plate separation for the cases involving a) 1:1 electrolyte with $d_+ = d_- = 0.72$ nm and b) 2:2 electrolyte with $d_+ = d_- = 0.84$ nm, respectively, with $d_s = 0.3$ nm and $\eta_s = 0.3665$ at $\sigma = 0.1$ C m $^{-2}$ using the SPM.

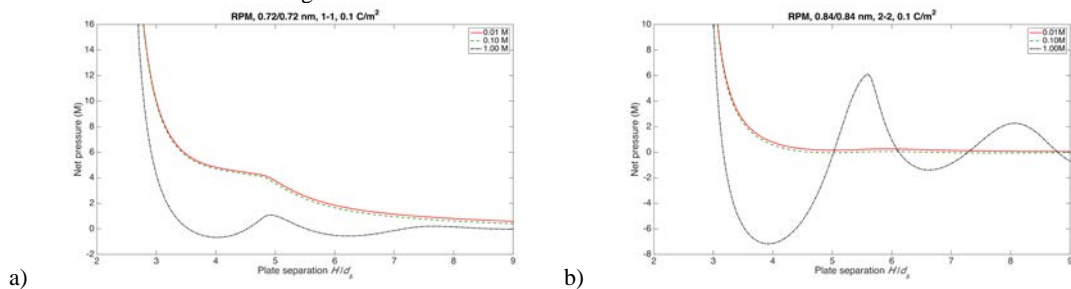


Fig. 7. Interaction pressure between charged plates as a function of the plate separation for the cases involving a) 1:1 electrolyte with $d_+ = d_- = 0.72$ nm and b) 2:2 electrolyte with $d_+ = d_- = 0.84$ nm, respectively, at $\sigma = 0.1$ C m $^{-2}$ using the RPM.

These findings signify the importance of the sizes of hydrated counterions in comparison with those of solvent molecules on crystalline swelling [8] of bentonite-based materials upon water uptake, and may be used to explain the mechanisms governing the formation and breakup of stacked montmorillonite particles or flocs, and to describe the interaction between spherical agglomerates in studies of dense colloidal dispersions.

References

- ¹Z. Wang, L. Liu, and I. Neretnieks, *J. Phys.: Condens. Matter* **23**, 175002 (2011).
- ²Z. Wang, L. Liu, and I. Neretnieks, *J. Chem. Phys.* **135**, 244107 (2011).
- ³L. Liu, *J. Chem. Phys.* **143**, 064902 (2015).
- ⁴S. Lamperski, and A. Zydor, *Electrochimica Acta* **52**, 2429 (2007).
- ⁵M. Pluciennik, C. W. Outhwaite, and S. Lamperski, *Mol. Phys.* **112**, 165 (2014).
- ⁶D. Gillespie, W. Nonner, and R. S. Eisenberg, *J. Phys.:Condens. Matter* **14** 12129 (2002).
- ⁷Y. Liang, N. Hilal, P. Langston, and V. Starov, *Adv. Collid Interface Sci.* **134-135** 151 (2007).
- ⁸L. Liu, *Colloids Surf. A: Physicochem. Eng. Aspects* **434**, 308 (2013).

DETACHMENT OF COLLOIDS AT THE CLAY SOLID/LIQUID INTERFACE

Rasmus Eriksson (rasmus.eriksson@btech.fi) and Tim Schatz, B+Tech Oy, Laulukuja 4, 00420 Helsinki, Finland

Introduction

One scenario of interest for the long-term safety assessment of a spent nuclear fuel repository involves the loss of bentonite barrier material through contact with dilute groundwater at a transmissive fracture interface. Small-scale, flow-through, artificial fracture experiments demonstrated that the quasi-free swelling of compacted montmorillonite into thin, horizontal fractures in the presence of dilute aqueous solutions leads to the formation of an inner, rigid gel-like phase and an outer, colloidal phase, with a distinct interface separating these two phases (Schatz, et al., 2012). However, the exact mechanism leading to the formation of the colloidal phase, followed by erosive loss of material due to flowing (ground)water, has not been determined.

Aim of the study

Employ optical and rheological methods to gain information about the detachment mechanism of clay colloids. The rheological properties of batch montmorillonite suspensions of differing composition (in terms of solids content and electrolyte concentration) designed to cover a range of predicted physicochemical states of the swelling clay inside an artificial fracture were investigated.

Results and discussion

Optical Coherence Tomography (OCT) imaging of the interface between the inner and the outer phase of swelling clay material inside an artificial fracture revealed that a domain of sedimented colloidal material extends radially outwards from the perimeter of the inner gel-like phase (see Figure 1).

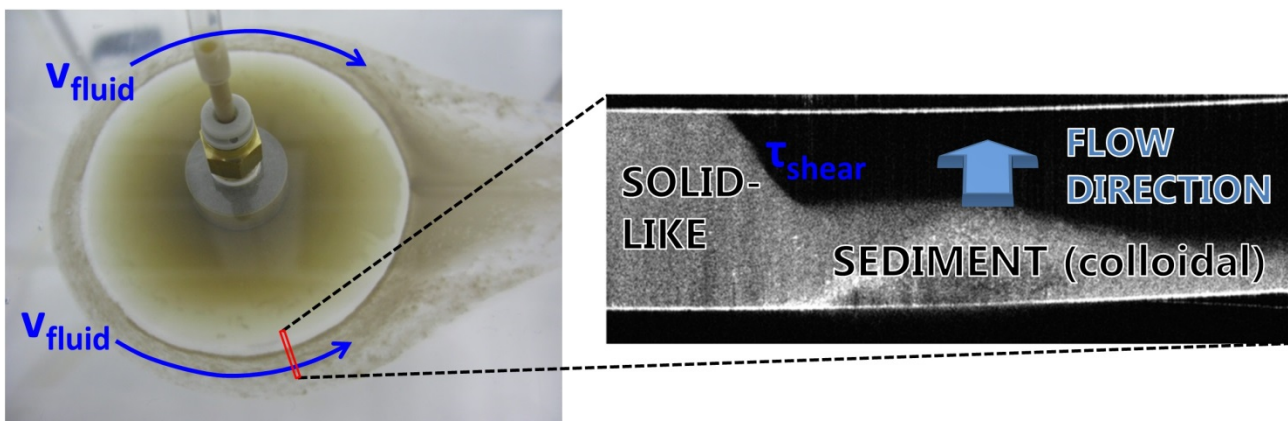


Figure 1. On the left: Overhead photograph of an artificial fracture test. The expanding solid-like phase can be clearly identified as the white-rimmed circular zone slightly to the left of center in the picture. The colloidal (sedimenting) phase is also visible outside of the solid-like phase as a light brown-colored zone that is arranged along the water flow path. On the right: Optical Coherence Tomography (OCT) image of the region marked with red color in the photograph. The OCT image is

a side-view of the interfacial zone from which the sharpness of the solid-liquid interface can be clearly seen.

OCT imaging was also performed in the presence of imposed flow through the artificial fracture system. At volumetric flow rates ranging between 1 - 10 ml/min only small perturbations could be observed to occur in or around the sedimented zone, but overall, the sediment appears to remain structurally intact. Even at flow rates of 200 mL/min the sedimented zone remains mostly intact, although large flocs can be seen to move over the sedimented zone at this flow rate. It is likely that the strongly deposited sediment originates from colloidal material which is initially generated at the gel/sol interface and which later aggregates, downstream of the source, leading to the formation of the sedimented zone.

Based on rheological data as well as other studies (Schatz, et al., 2012) we have determined that for Na clay and 50/50 mixtures of Na and Ca clay, the solids content near the outer perimeter of the inner, rigid body lies between 2 - 4 vol %. In this range the clay suspensions exhibit a distinct jump from predominantly viscous character to predominantly gel-like character (see Figure 2a). By contrast, Ca clay displays no gel-like character, even at 4 vol% (Fig. 2b). Furthermore, at high electrolyte concentrations (170 mM NaCl) the gel-like, elastic response for any clay is significantly reduced or disappears entirely (Fig. 2b). The reason for the lower storage moduli in these cases is most likely sedimentation due to flocculation, even if the samples appear to be non-flowing and solid-like.

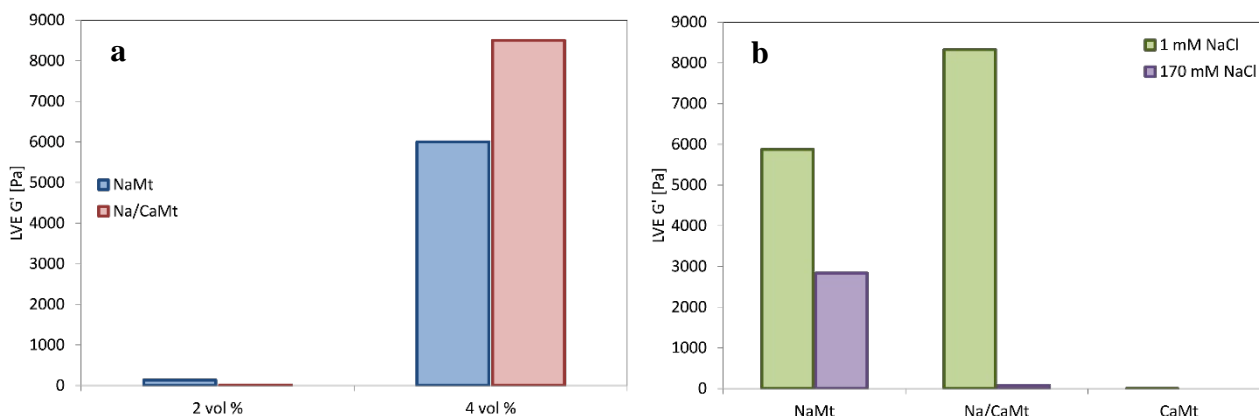


Figure 2. The average elastic modulus (G') of montmorillonite suspensions in the linear viscoelastic region (LVE). a) Comparison of solids contents at 1 mM NaCl. b) Effect of electrolyte concentration.

The shear forces experienced by the outer rim of the expanding gel-like phase were compared to experimentally determined yield stresses of montmorillonite suspensions comparable in composition to the expanding gel-like phase (Eriksson & Schatz, 2015). It was found that the shear stress on the outer rim (at realistic groundwater flow velocities) is much lower than the yield stress of the gel-like expanding phase and therefore it was considered highly unlikely that mechanical shear can perturb the gel-like phase in any way, including detaching particles from the interface. This conclusion assumes that the outer rim interface is relatively smooth, and that a low viscosity liquid (i.e. water) is exerting the shear stress. Based on OCT imaging (see Fig. 1) both requirements seem to be met, at least in artificial fracture tests. However, erosive mass loss does occur at some conditions, and the detachment mechanism, if not due to mechanical shear, must be due to some chemical process. In this case it is most likely the swelling process itself that leads to particle detachment. From a chemical, and somewhat simplified perspective, detachment may occur when the driving force for water uptake (of osmotic nature) overcomes the attractive forces between the clay platelets. In such a situation, the clay platelets are driven further and further apart until the

attraction between them has become so weak that they can be picked up by the water flowing around the rim or they simply diffuse away (if there is no water flow). Hence, the particles that are detached and transported away are very small (single platelets or aggregates consisting of a few platelets), because larger particles would sediment. Of course, some of these particles will at some point collide with other particles to form larger aggregates that sediment (c.f. Fig. 1), while others escape further downstream. However, it is uncertain how far they could travel since their long-term stability is unknown.

REFERENCES

- Eriksson, R., & Schatz, T. (2015). Rheological properties of clay material at the solid/solution interface formed under quasi-free swelling conditions. *Applied Clay Science*, 108, 12-18. doi:10.1016/j.clay.2015.02.018
- Schatz, T., Kanerva, N., Martikainen, J., Sane, P., Olin, M. S., & Koskinen, K. (2012). *Buffer erosion in dilute groundwater*. Olkiluoto: Posiva Oy.

SORPTION BEHAVIOR OF Np(V) ONTO CLAYS FROM RUSSIAN AND INDIAN DEPOSITS

**A.Yu. Romanchuk¹, I.E. Vlasova¹, P.K. Verma², V.V. Krupskaya^{1,3}, V.G. Petrov¹,
P.K. Mohapatra², S.N. Kalmykov¹**

¹*Lomonosov Moscow State University, romanchuk.anna@gmail.com*

²*Bhabha Atomic Research Centre, Mumbai, India*

³*Institute of Geology of Ore Deposits, Petrography, Mineralogy and Geochemistry Russian Academy of Science, Moscow, Russia*

Bentonite was found to be a promising candidate for backfill material for nuclear waste repository due to its favorable chemical and physical properties under deep geological conditions with efficient radionuclide retention capacity. The sorption onto clay minerals plays an important role in immobilization/retention of radionuclides. The long term safety assessment of the future repository and the model of migration of radionuclides in the geosphere require a thorough knowledge of the sorption processes of actinides in the presence of different clay minerals under various physical and chemical conditions. At the same time natural clays often contain different admixture (calcite, iron and titanium oxide and others) that can influence on sorption process.

In this work sorption behavior of Np(V) onto suspended bentonite samples of different origin under varying experimental conditions of pH, time and ionic strength was studied. Various techniques, e.g. XRD, XRF, BET absorption, Mossbauer etc. were used to characterize clays. Efforts have also been made to identify the role of different minerals in the composite bentonite which are responsible for Np(V) sorption. Thermodynamic modeling and speciation calculations for different species have been done for better understanding of experimental results.

Clay samples from Khakassia (Russia), Rajasthan and Kutch (India) deposits were studied. Elemental composition and surface area of clays sample present in Table 1. Rajasthan and Kutch clays demonstrate higher content of iron and titanium. At the same time using XRD technique it was found that the bentonite clay from the Kutch deposit contains the greatest amount of montmorillonite (90%) and a rather low amount of non-clay minerals - quartz, goethite, calcite, anatase. Bentonite from Khakassia deposit contains montmorillonite in the sodium form (66%) and rather high amount of kaolinite (5.5%) and non-clay impurities like quartz, feldspar, and calcite (3%). Natural clay from Rajasthan deposit has different composition and contains smectite and mixed-layered illite-smectite (62%), and kaolinite and mixed-layered kaolinite-smectite (16%). the following non-clay minerals were defined (in descending order of content): dolomite, calcite, brucite, quartz, anatase, goethite, gypsum, hematite. XRD also show that montmorillonite in Khakassia sample present in Na-form while in Kutch sample in Ca-form.

Table1. XRF data and surface area for studied clays samples

Sample	Composition, %											Surface area, m ² /g
	LOI	Na ₂ O	MgO	Al ₂ O ₃	SiO ₂	K ₂ O	CaO	TiO ₂	MnO	Fe ₂ O ₃	P ₂ O ₅	
Rajasthan clay	20,06	1,15	4,64	16,28	35,12	0,30	6,67	3,09	0,16	12,27	0,11	50
Kutch clay	21,43	0,72	2,02	12,33	42,52	0,11	2,77	1,42	0,19	15,58	0,27	115
Khakassia clay	12,74	2,98	2,48	15,19	58,36	0,97	3,05	0,63	0,09	3,42	0,11	15

Iron speciation was found combining results from XRD and Mössbauer spectroscopy. Clay samples from Indian deposits contain only Fe(III), while sample from Khakassia deposit – Fe(II) and Fe(III). Part of Fe(III) from Kutch and Rajasthan clays demonstrate magnetic properties that confirm presence of iron oxide/hydroxide phases. At the same time both samples have Fe(III) which does not show magnetic ordering even at 77K. This iron can be structural iron in clay minerals or presents as iron oxide nanoparticles (less 10 nm in size). In Khakassia clay all iron do not demonstrate magnetic properties. We assume that all this iron is structural iron in bentonite.

Np(V) sorption on different samples depending on pH, time and ionic strength was established. It was found that steady-state equilibrium in all systems is reached in 1 day of equilibration. Figure 1 shows pH-dependence of Np(V) sorption onto studied clays at 0.01 ionic strength. Khakassia clay demonstrates a lower sorption affinity to Np(V). It was found that ionic strength does not influence on Np(V) sorption onto Khakassia and Rajasthan clays. From that we proposed that surface complexation is the dominant mechanism of neptunium sorption. Sorption of Np(V) on Kutch clay increases with increasing of ionic strength. Such untypical behavior was explained by modification of Kutch clay from Ca-form to Na-form during its equilibration in 1M NaClO₄ solution. This conclusion was also approved by XRD.

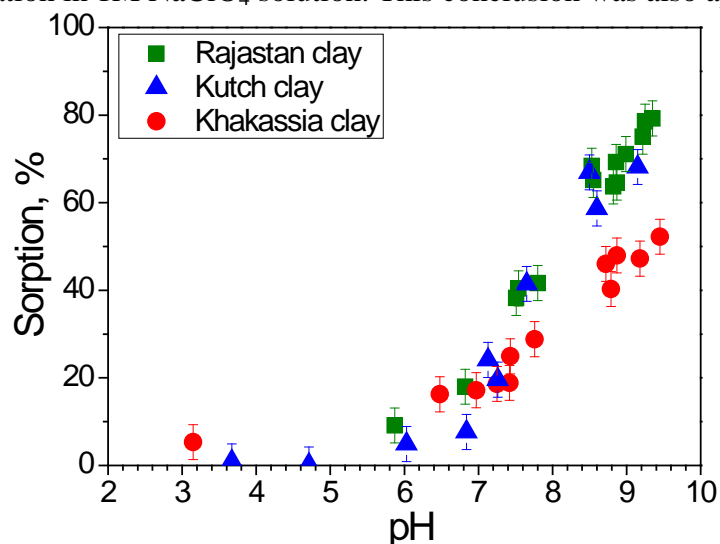


Figure 1. pH-dependence of Np(V) sorption onto clays ([solid phase] = 0.5 g/L, I = 0.01 NaClO₄, [Np(V)] = 4·10⁻¹⁴ M)

Alpha-track analysis was used for determination of local distribution of neptunium on clay. After sorption solid phase was separated by centrifugation on “light” fraction which predominantly contain clay minerals and heavier “dark” fraction. Using SEM it was found that “dark” fraction has heterogeneous composition. There are iron oxide, titania, quartz and other. It was estimated qualitatively that correlation of alpha-activity values between “light” and “dark” fractions differs in three studied bentonite samples. While alpha-activity of Khakassia bentonite is equal in both fractions, Rajasthan “dark” fraction, rich in Fe-containing minerals, demonstrated lower alpha-activity than “light” clayey fraction (figure 2). On the contrary, Kutch “dark” fraction is characterized by higher Np sorption than “light” clayey fraction (figure3). Therefore for Kutch and Rajasthan samples it is seen that sorption on some particles from “dark” fraction is significant and should be accounted in thermodynamically modeling.

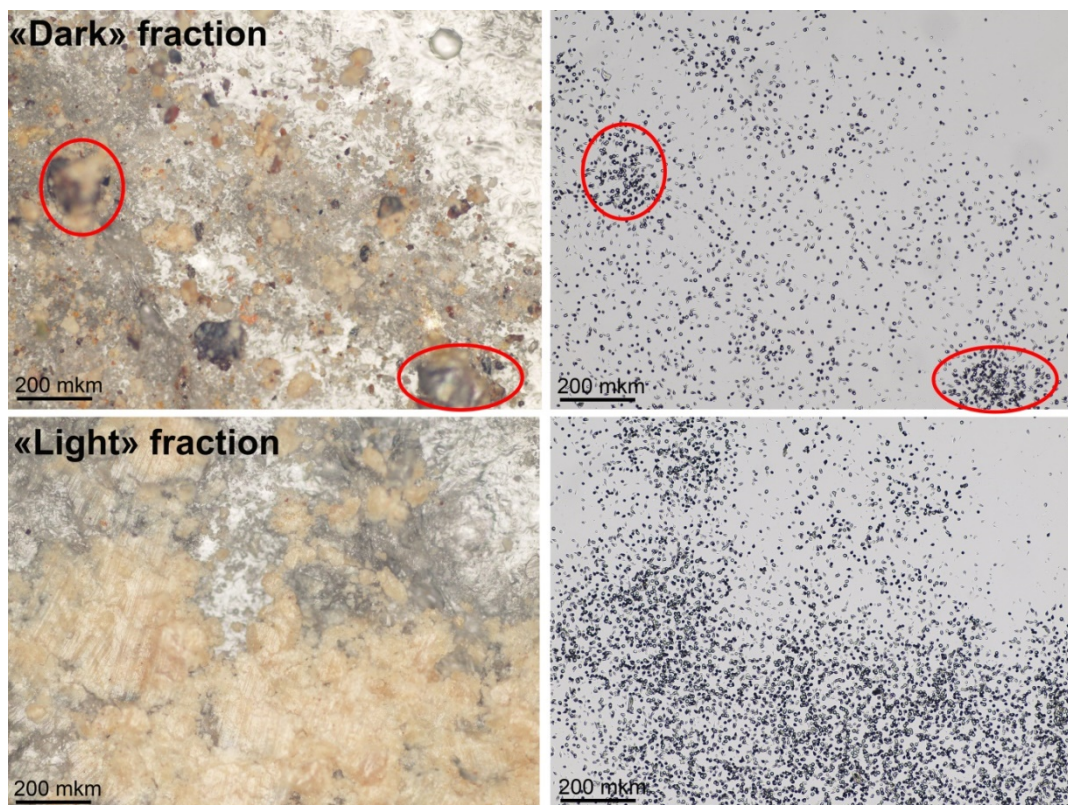


Figure 2. Optical microscope images and corresponding α -track analysis images for Np(V) sorbed onto Rajasthan clay.

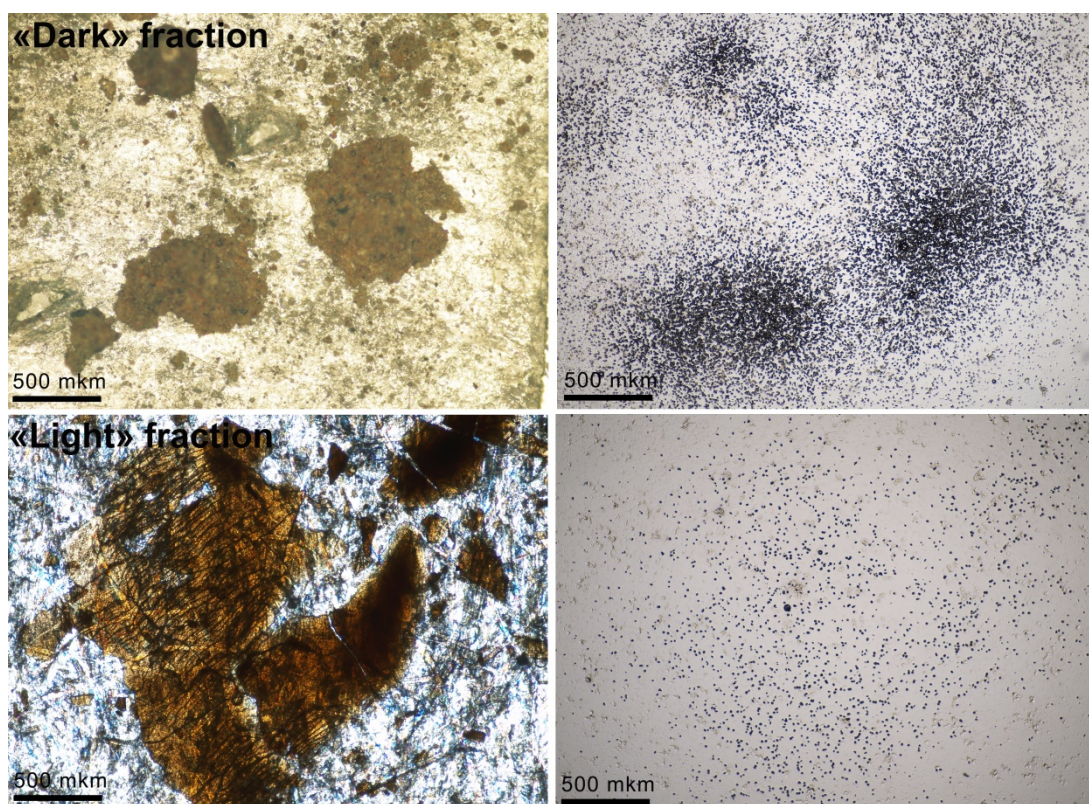


Figure 3. Optical microscope images and corresponding α -track analysis images for Np(V) sorbed onto Kutch clay.

Redox potential in clay suspension was measured (figure 4). It was found that for all three samples redox condition are quite similar. Non influence of Fe(II) from Khakasia clay on redox potential and neptunium valence state was observed. Experimental data of Np(V) sorption onto studied bentonite samples were simulated using PHREEQC software and available in literature equilibrium constants.

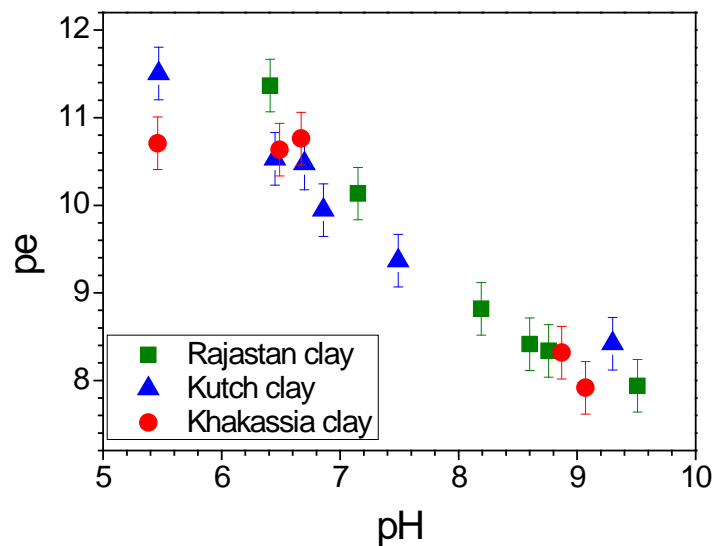


Figure 4. Redox potential in clay suspensions.

This work was supported by the Russian Science Foundation (project 16-13-00049).

STUDY OF RADIONUCLIDES MIGRATION THROUGH CRUSHED GRANITE IN PRESENCE OF BENTONITE COLLOIDS

Kateřina Kolomá (katerina.koloma@ujv.cz) and Radek Āervinka

ÚJV Řeř, a. s., Fuel Cycle Chemistry and Waste Management Division, Fuel Cycle Chemistry Department, Hlavní 130, Řeř, 250 68 Husinec, Czech Republic

The presented work is focused on the study of radionuclides transport through granitic rock in presence of bentonite colloids. The bentonite colloids are formed in engineered barrier system of deep geological repository for radioactive waste and may have direct impact on its safety. The main aims of experiments were to study the mobility of colloid particles in granitic matrix, reversibility of radionuclides sorption on bentonite colloids and the influence of liquid phase composition and colloid particles presence on the radionuclides transport in granitic rock. The performed experiments with crushed granite represent system of disturbed granitic rock with fissure network and cationic sorbing tracers.

The radionuclides migration in presence of bentonite colloids was studied by dynamic column experiments (see Fig. 1) with continues inlet of liquid phase (Videnská at al., 2013). The dynamic experiments were conducted with several tracers: radionulides $^{85}\text{SrCl}_2$ and $^{137}\text{CsCl}$, bentonite colloids, the radiocolloids ^{85}Sr -colloids and ^{137}Cs -radiocolloids. The transport of each tracer was described by breakthrough curve and transport parameters R (retardation coefficient) and K_d (distribution coefficient), the different behaviour of tracers as well as the influence of bentonite colloids on radionuclides migration was evident from comparison of breakthrough curves and transport parameters.



Fig. 1: The dynamic column experiment.

The results of dynamic experiments were evaluated in several aspects. Firstly, we focused on study of the influence of liquid phase composition on radionuclides migration. The liquid phase properties (e.g. ionic strength, composition) are one of the most important parameters, influencing the radionuclides transport. For system simplification, all migration experiments with radionuclides, colloids and radiocolloids were performed in deionised water. However radionuclide behaviour in deionised water and groundwater may differ from each other. For this reason the transport of radionuclides in deionised water and synthetic granitic water (SGW) was studied and compared. The results showed the completely different behaviour of radionuclides in deionised water and in SGW. Migration of radionuclides through granite in SGW was significantly faster than migration in deionised water. The rapid transport in SGW was caused by the competition effect of the cations in SGW, which occupied sorption sites in granite structure and limited radionuclide sorption (Kütahyalı at al., 2012; Wallace et al., 2012).

Secondly, we studied the radionuclides migration in presence of bentonite colloids. The experiment was conducted with radiocolloid suspension, so at the beginning of the experiment, the radionuclide was sorbed on the bentonite colloids and this complex entered into column with granite. However the sorption potential of granite material was higher than the forces of interaction between radionuclides and bentonite colloids, and the radiocolloid complex was partitioned in the crushed granite. The colloid particles free of radionuclide passed through crushed granite fast, immediately after injection of radiocolloid and the radionuclide was sorbed on granite. From breakthrough curves is evident, that radionuclide passed through granitic rock faster in presence of bentonite colloids than without presence of bentonite colloids. The colloid particles probably carried radionuclide further into the column and after that the radiocolloid complex broke, radionuclide was sorbed on granite and colloid particles left the column (Albarran et al., 2011). For illustration purpose the resulting breakthrough curves of strontium are displayed in Fig. 2.

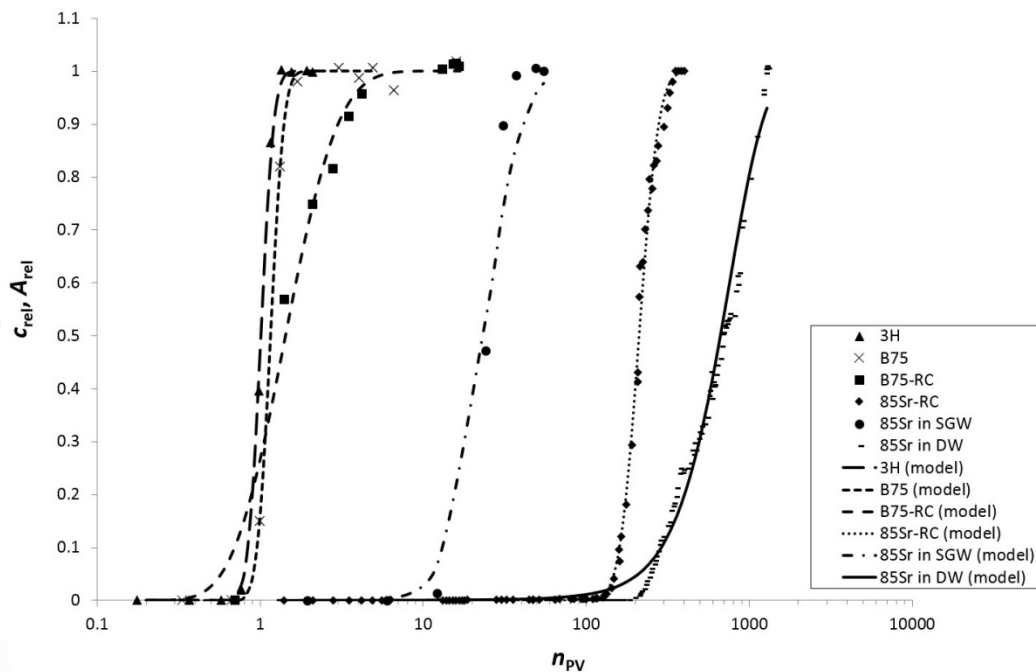


Fig. 2: The breakthrough curves of ^{85}Sr , the bentonite colloids and radiocolloids used in dynamic experiments.

Finally, we focused on reversibility of radionuclide sorption on the bentonite colloids. The fully reversible sorption on clay colloids was observed in case of strontium. Immediately after enter into the column, the strontium was completely desorbed from clay colloids and was retained in granitic rock. In case of cesium, major part (98 %) was sorbed on the granite and minor part (about 2 %) left the column together with clay colloids (see Fig. 3). The different behaviour of cesium and strontium transport is caused by different sorption mechanism of radionuclides on clay colloids. Strontium was sorbed by ion-exchange on the planar sites in bentonite interlayers. This bond was weak and reversible, so the all strontium was desorbed from bentonite colloids and was retained in granitic rock. On the other hand the part of cesium (about 2 % of cesium) was sorbed on frayed edge sites (FES) at bentonite structure by strong, irreversible bond and major part of cesium (about 98 %) was reversible sorbed on the planar sites in bentonite intelayers (Missana et al., 2004).

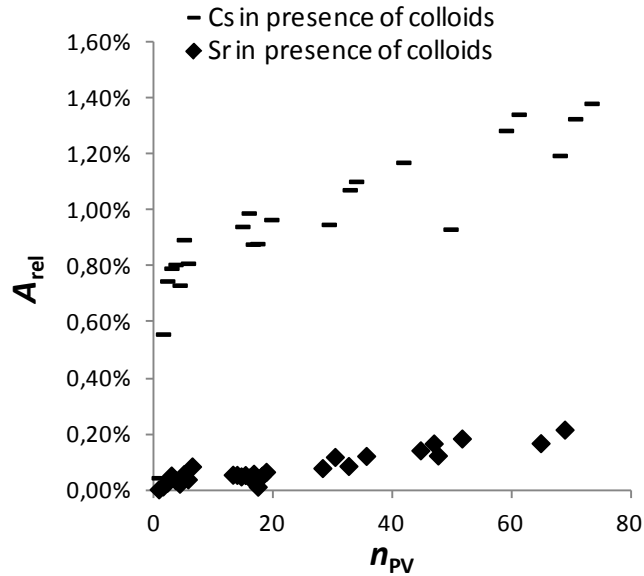


Fig. 3: The experimental breakthrough curves of Cs and Sr at the beginning of dynamic experiments.

The laboratory dynamic experiments revealed the significantly influence of bentonite colloids on the radionuclide migration in granitic rock. The results showed that radionuclide transport was faster in presence of bentonite colloids, the colloids particles acted as a carrier of radionuclide in the rock matrix. The sorption of radionuclides on bentonite colloids was fully or partially reversible. The transport of radionuclide in granite was therefore influenced by mechanism of radionuclide sorption on bentonite colloids and also by composition of liquid phase.

References:

- Albarran N., Missana T., García-Gutiérrez M., Alonso U., Mingarro M. (2011): Strontium migration in a crystalline medium: effects of the presence of bentonite colloids. *Journal of Contaminant Hydrology*. 122, 76-85
- Kütahyalı C., Çeinkaya B., Bahadır Acar M., Işık N. O., Cireli İ. (2012): Investigation of strontium sorption onto Kula volcanic using Central Composite Design. *Journal of Hazardous Materials*. 201-202, 115-124.
- Missana T., García-Gutiérrez M., Alonso U. (2004): Kinetics and irreversibility of cesium and uranium sorption onto bentonite colloids in a deep granitic environment. *Applied Clay Science*. 26, 137-150.
- Videnská K., Palágyi Š., Štamberg K., Vodičková H., Havlová V. (2013): Effect of grain size on the sorption and desorption of SeO_4^{2-} and SeO_3^{2-} in columns of crushed granite and fracture infill from granitic water under dynamic conditions. *Journal of Radioanalytical and Nuclear Chemistry*. 298, 547-554.
- Wallace S. H., Shaw S., Morris K., Small J. S., Fuller A. J., Burke I. T. (2012): Effect of groundwater pH and ionic strength on strontium sorption in aquifer sediments: Implications for ^{90}Sr mobility at contaminated nuclear sites. *Applied Geochemistry*. 27, 1482-1491.

Effect of clay nanoparticle mobility, desorption and redox kinetics on radionuclide mobility: Observations made on the field scale

T. Schäfer (thorsten.schaefer@kit.edu), F. Quinto, M. Lagos, F.M. Huber, S. Heck, Karlsruhe Institute of Technology (KIT), Institute for Nuclear Waste Disposal (INE), P.O. Box 3640, D-76021 Karlsruhe, Germany.

A. Martin, I. Blechschmidt, NAGRA, Wettingen, Switzerland
Bill Lanyon, Fracture Systems Ltd., St. Ives, UK

Transport of contaminants in crystalline environments might occur through dissolved species or attached to colloidal or nano-particulate phases being mobile in water conducting features of the host rock. The importance of colloidal phases has been demonstrated in a number of laboratory investigations [1, 2] or field studies [3-5]. It could be already demonstrated that the recovery of colloids like latex microspheres frequently used as reference material or bentonite derived clay colloids is clearly depending on the flow velocity established in the tests [6] and sorption/desorption kinetics are involved in the transport process [7]. Almost quantitative colloid recovery was observed under rather fast flow conditions [5] or respectively low residence times with decreasing recovery for longer residence times or shorter pathways. The influence of surface roughness and fracture geometry on the colloid retention was investigated by CFD models implementing computer tomography (μ CT) data [8] or measuring the mineral specific surface roughness by vertical scanning interferometry and its effect on colloid attachment probabilities using atomic force microscopy and its colloid probe technique [9, 10]. Furthermore, it could be observed that the non-colloidal Np(V) and U(VI) are mobile under the short residence times [11], which can be explained by the rather slow reduction kinetics observed in the laboratory [12].

To overcome the criticism of transferability of this data to the near-natural or post-closure situation of a deep-geological repository a twofold approach was taken. On one hand side underground research facilities, more specifically an experiment, the so-called Colloid Formation and Migration (CFM) project at the Grimsel Test Site (GTS, Switzerland; <http://www.grimsel.com/gts-phase-vi/cfm-section/cfm-introduction>) was designed to establish long residence times in a shear zone without losing the injected tracer in the 3D flow field. On the other hand side the high sensitivity of accelerator mass spectrometry (AMS) [13] was used to investigate the mobility of fall-out actinides in the Aar massif down to the GTS level.

In this presentation we will discuss the mobility of clay nanoparticles as detected by e.g. laser-induced breakdown detection (LIBD) as a function of fracture surface roughness and groundwater chemistry. In order to increase our sensitivity for the clay nanoparticles we used beside natural bentonite derived colloids (e.g. Febex, MX-80) also smectites synthesized via a hydrothermal route having transition metals (Ni, Zn) structural (irreversible) incorporated in the octahedral layer [14, 15]. The clay colloid injection suspension for the field experiments as well as for the laboratory batch-type studies contained approx. 100 mg/L clay colloids a number of actinides as $^{233}\text{U(VI)}$, $^{237}\text{Np(V)}$, $^{242}\text{Pu(IV)}$ and $^{243}\text{Am(III)}$. All experiments performed so far in the field or in the laboratory show radionuclide desorption kinetics from the clay nanoparticles. The desorption or redox kinetics were monitored over a duration of up to 426 days using natural fracture filling material as a concurrence ligand and monitoring the colloid attachment via detection of Al, Si, Ni and Zn as smectite structural elements [16]. For trivalent actinides clay colloid desorption rates in the range of 1.2 - 3.7E-3 per hour for batch-type studies [16] and orders of magnitude higher desorption rates of 0.91-0.98 per hour for column experiments with crushed granite [17] could be determined. These studies having focused on the trivalent actinides/lanthanides clay colloid interaction indicate full reversibility

and an establishment of a sorption equilibrium [17, 18], whereas for the tetravalent actinides much slower desorption kinetics and no equilibrium could be found. These results are compared with field data of migration experiments performed within the CFM project at the Grimsel Test Site (GTS, Switzerland) using the same radionuclides and clay colloidal phases varying the fracture residence time by flow rate adjustment.

Furthermore, the long-term actinide mobility on the formation scale has been addressed by AMS and also resonance ionization mass spectrometry (RIMS) measurements of (a) samples collected several months into the tailing of the breakthrough curves not any longer detectable by HR (high resolution) -ICP-MS and (b) background samples of different GTS ground waters. Focusing on the mobility of the fallout radionuclides [19] in background samples of the Grimsel Test Site by the analysis of a small sample set taken so far it could be shown that fallout ^{236}U can be detected, whereas fallout Pu could not be detected indicating a much lower mobility under the given conditions. These first results presented here using fall-out radionuclides give valuable information of actinide mobility on the formation scale over decades. The AMS analysis of tailing samples shows that all injected radionuclides can be detected over several months in the tailing of the breakthrough curve. A clear differentiation of (a) a detachment of injected colloids and transport of this colloid-associated radionuclides or (b) a desorption of radionuclides from fracture surface irreversible attached colloids and transport of the desorbed radionuclides as solute species cannot be conclusively given at this time. Here, new experiments are foreseen within the next CFM project phase to clarify this open question. However, beside the unfavorable conditions for colloid attachment established at the Grimsel Test Site (low ionic strength and high pH) in all the experiments going to longer residence times a colloid retention could be observed.

Having this knowledge about forward and backward rate constants implemented in transport models gives the opportunity to predict more reliably the long-term evolution of the system under investigation [20, 21].

Acknowledgements

The work has received partial funding by the Federal Ministry of Economics and Technology (BMWi) under the joint KIT-INE, GRS research project “KOLLORADO-e” (02E11203B) and the European 7th Framework Programme (FP7/2007- 2011) under grant agreement no. 295487 (BELBaR Project). Furthermore, the authors would like to acknowledge the support of the CFM Project partners and the support of the local Grimsel Test Site/NAGRA staff.

References

1. Gamerding, A. P.; Kaplan, D. I., Colloid transport and deposition in water-saturated yucca mountain tuff as determined by ionic strength. *Environ. Sci. Technol.* **2001**, *35*, (16), 3326-3331.
2. Vilks, P.; Miller, N. H.; Vorauer, A., Laboratory bentonite colloid migration experiments to support the Aspo Colloid Project. *Physics and Chemistry of the Earth* **2008**, *33*, (14-16), 1035-1041.
3. Vilks, P.; Frost, L. H.; Bachinski, D. B., Field-Scale colloid migration experiments in a granite fracture. *J. Contam. Hydrol.* **1997**, *26*, (1-4), 203-214.
4. Möri, A.; Geckeis, H.; Fierz, T.; Eikenberg, J.; Degueldre, C.; Hauser, W.; Geyer, F. W.; Schäfer, T., Grimsel Test Site - Investigation Phase V “The CRR final project report series I: Description of the Field Phase - Methodologies and Raw Data” **2004**, *03-01*, (Nagra Technical Report).
5. Geckeis, H.; Schäfer, T.; Hauser, W.; Rabung, T.; Missana, T.; Degueldre, C.; Möri, A.; Eikenberg, J.; Fierz, T.; Alexander, W. R., Results of the Colloid and Radionuclide Retention experiment (CRR) at the Grimsel Test Site (GTS), Switzerland -Impact of reaction kinetics and speciation on radionuclide migration-. *Radiochim. Acta* **2004**, *92*, (9-11), 765-774.
6. Schäfer, T.; Huber, F.; Seher, H.; Missana, T.; Alonso, U.; Kumke, M.; Eidner, S.; Claret, F.; Enzmann, F., Nanoparticles and their influence on radionuclide mobility in deep geological formations. *Appl. Geochem.* **2012**, *27*, (2), 390-403.

7. Missana, T.; Garcia-Gutierrez, M.; Alonso, U., Kinetics and irreversibility of cesium and uranium sorption onto bentonite colloids in a deep granitic environment. *Appl. Clay Sci.* **2004**, *26*, (1-4), 137-150.
8. Huber, F.; Enzmann, F.; Wenka, A.; Bouby, M.; Dentz, M.; Schäfer, T., Natural micro-scale heterogeneity induced solute and nanoparticle retardation in fractured crystalline rock. *J. Contam. Hydrol.* **2012**, *133*, 40-52.
9. Darbha, G. K.; Fischer, C.; Luetzenkirchen, J.; Schäfer, T., Site-Specific Retention of Colloids at Rough Rock Surfaces. *Environ. Sci. Technol.* **2012**, *46*, (17), 9378-9387.
10. Darbha, G. K.; Fischer, C.; Michler, A.; Luetzenkirchen, J.; Schäfer, T.; Heberling, F.; Schild, D., Deposition of Latex Colloids at Rough Mineral Surfaces: An Analogue Study Using Nanopatterned Surfaces. *Langmuir* **2012**, *28*, (16), 6606-6617.
11. Möri, A.; Alexander, W. R.; Geckeis, H.; Hauser, W.; Schäfer, T.; Eikenberg, J.; Fierz, T.; Degueldre, C.; Missana, T., The colloid and radionuclide retardation experiment at the Grimsel Test Site: influence of bentonite colloids on radionuclide migration in a fractured rock. *Colloids Surf. A* **2003**, *217*, (1-3), 33-47.
12. Huber, F.; Kunze, P.; Geckeis, H.; Schäfer, T., Sorption reversibility kinetics in the ternary system radionuclide–bentonite colloids/nanoparticles–granite fracture filling material. *Appl. Geochem.* **2011**, *26*, (12), 2226-2237.
13. Vockenhuber, C.; Ahmad, I.; Golser, R.; Kutschera, W.; Liechtenstein, V.; Priller, A.; Steier, P.; Winkler, S., Accelerator mass spectrometry of heavy long-lived radionuclides. *Int. J. Mass Spectrom.* **2003**, *223*, (1-3), 713-732.
14. Reinholdt, M.; Brendlé, J.; Tuilier, M.-H.; Kaliaguine, S.; Ambroise, E., Hydrothermal Synthesis and Characterization of Ni-Al Montmorillonite-Like Phyllosilicates. *Nanomaterials* **2013**, *3*, (1), 48-69.
15. Reinholdt, M.; Mieke-Brendle, J.; Delmotte, L.; Tuilier, M. H.; le Dred, R.; Cortes, R.; Flank, A. M., Fluorine route synthesis of montmorillonites containing Mg or Zn and characterization by XRD, thermal analysis, MAS NMR, and EXAFS spectroscopy. *Eur. J. Inorg. Chem.* **2001**, (11), 2831-2841.
16. Huber, F. M.; Heck, S.; Truche, L.; Bouby, M.; Brendle, J.; Hoess, P.; Schafer, T., Radionuclide desorption kinetics on synthetic Zn/Ni-labeled montmorillonite nanoparticles. *Geochim. Cosmochim. Acta* **2015**, *148*, 426-441.
17. Dittrich, T. M.; Boukhalfa, H.; Ware, S. D.; Reimus, P. W., Laboratory investigation of the role of desorption kinetics on americium transport associated with bentonite colloids. *Journal of Environmental Radioactivity* **2015**, *148*, 170-182.
18. Bouby, M.; Geckeis, H.; Lützenkirchen, J.; Mihai, S.; Schäfer, T., Interaction of bentonite colloids with Cs, Eu, Th and U in presence of humic acid: A flow field-flow fractionation study. *Geochim. Cosmochim. Acta* **2011**, *75*, (13), 3866-3880.
19. Quinto, F.; Golser, R.; Lagos, M.; Plaschke, M.; Schäfer, T.; Steier, P.; Geckeis, H., Accelerator Mass Spectrometry of Actinides in Ground- and Seawater: An Innovative Method Allowing for the Simultaneous Analysis of U, Np, Pu, Am, and Cm Isotopes below ppq Levels. *Anal. Chem.* **2015**, *87*, (11), 5766-5773.
20. Dittrich, T. M.; Reimus, P. W., Reactive transport of uranium in fractured crystalline rock: Upscaling in time and distance. *Journal of Environmental Management* **2016**, *165*, 124-32.
21. Reiche, T.; Noseck, U.; Schäfer, T., Migration of Contaminants in Fractured-Porous Media in the Presence of Colloids: Effects of Kinetic Interactions. *Transport in Porous Media* **2015**, 1-28.

RADIONUCLIDE TRANSPORT IN GRANITE FRACTURES IN THE PRESENCE OF BENTONITE COLLOIDS: SUMMARY OF THE STUDIES CARRIED OUT AT CIEMAT

Tiziana Missana, Miguel García-Gutiérrez, Ursula Alonso, Manuel Mingarro

CIEMAT, Department of Environment, Avenida Complutense, 40- 28040 MADRID (Spain).

E-mail: tiziana.missana@ciemat.es

Compacted bentonite is envisaged as engineered barrier in high level radioactive waste repositories (HLRWR), because it is able to prevent the water influx to the waste and to delay radionuclide transport towards the geosphere, providing high sorption capability for most radionuclides.

The possible mechanisms of bentonite erosion and clay colloids formation are the main research subjects in the BELBAR Project. Erosion causing an extensive mass loss would, in fact, compromise the barrier functionality at the *long-term*; additionally clay colloids dispersed from the barrier could act as radionuclide carriers in groundwater. To establish under what conditions the presence of colloids can favour radionuclide migration is a crucial task for the performance assessment (PA) of HLRW repositories.

From the well-known “*colloid ladder*” several conditions must be fulfilled to consider the presence of colloids as a concern. Basically, they must exist, be stable and mobile and to adsorb radionuclides significantly and irreversibly. Therefore the studies of radionuclide transport in the presence of clay colloids must cover different aspects to be treated in combination, from physico-chemical aspects related to colloid formation and their stability/mobility and those related to radionuclide adsorption. In both cases, the (ir-) reversibility of the critical processes (colloid aggregation or filtration and radionuclide sorption) is a fundamental aspect to be analysed.

In CIEMAT, during the last ten years, several laboratory experiments with bentonite colloid (and radionuclides) were carried out, trying to elucidate the main important parameters affecting their transport in crystalline rock fractures. Furthermore, the mobility of colloids was also studied under natural realistic conditions at the Grimsel Test Site (GTS), in the Febex tunnel. In parallel, mechanistic sorption studies of different types of radionuclides on bentonite colloids were conducted.

The objective of this work, far from being exhaustive, is to summarize the main conclusions, obtained over this period, on the analysis of the radionuclide migration processes in crystalline rocks when bentonite colloids are present.

The chemical conditions span from those of the GTS (dilute and alkaline waters) to those of Äspö (significantly more saline). The chemistry of the groundwater/clay system plays an important role on the erosion of the bentonite, on the stability and mobility of generated colloids and also on the adsorption of the contaminant at the colloid surface. On the other hand, water flow and flow paths are decisive on colloid transport. Indeed, hydrodynamic and chemistry are always strictly related. Filtration of bentonite colloids in crystalline fractures was always observed below a threshold limit of the water flow rate (or residence time) (Albarran et al. 2013). This threshold is somewhat colloid and groundwater chemistry dependent.

Figure 1 draws an example of this important point, showing the bentonite colloid recovery under different experimental conditions.

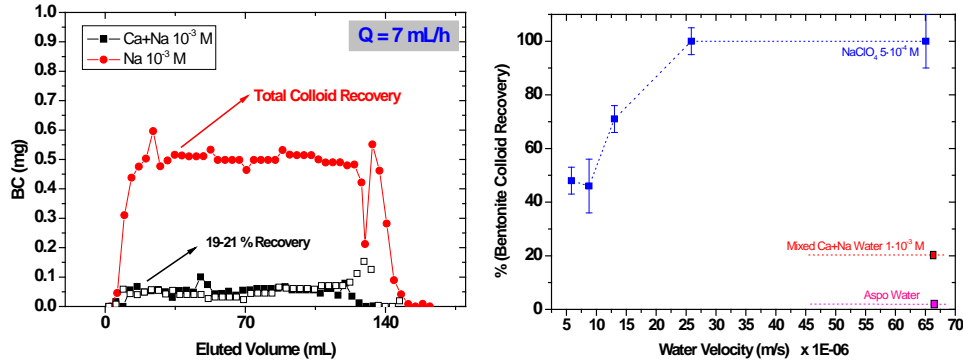


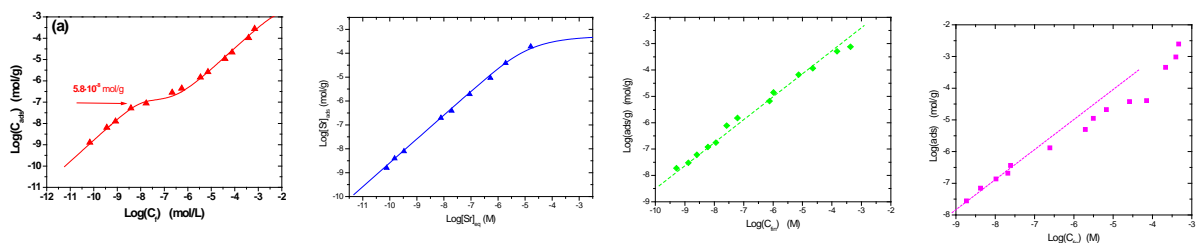
Figure 1: Comparison of bentonite colloid recovery under different chemical conditions.

The left part of Figure 1 shows the elution curves of bentonite colloids at the same flow rate (approx. $6 \cdot 10^{-6}$ m/s) and solution ionic strength. In one case (black points), $5 \cdot 10^{-4}$ M of Ca was present in solution. Such a relatively small difference caused a large difference on the colloid elution behavior. The elution in the Na system was 100%, but only 20 % in the Ca-Na electrolyte. In the left part, it can be seen that performing the experiment in Äspö water, the recovery decreased further to values less than 5%. Furthermore, the recovery is strictly dependent on the water flow rate (even in the pure Na-electrolyte) and lower recoveries are then expected under repository conditions. High filtration of colloids in the fractures, will indeed affect the transport of adsorbed radionuclides. The question is if the colloid retention is or not reversible. Clear hysteresis has been seen in the disaggregation of colloids upon their aggregation but experimental evidences exist that colloids can be removed from the fracture increasing the water flow to very high values.

It is important remarking that the mobile fraction of bentonite colloids always moved unretarded with respect to the water. The fate of the radionuclides will be dependent on the clay/radionuclide interactions especially the reversibility of the adsorption process.

At CIEMAT, the sorption of different types of radionuclides (Eu, Pu, Sr, U, Cs, Cd, etc...) on bentonite was studied. Different sorption mechanisms are dominant for each radionuclide also according to the specific chemical conditions. Figure 2 shows an example of sorption isotherms for four different radionuclides, between those analyzed, in which the main sorption mechanism is indicated and if sorption is linear or not.

The reversibility of the sorption process was tested with desorption tests. In most of the cases investigated, the sorption K_d were similar to desorption ones, basically indicating sorption reversibility.



Cs: Cation exchange; Non linear.

Sr: Cation exchange and inner sphere surface complexation; Linear.

Eu (U): Inner sphere surface complexation and cation exchange; Linear.

Cd: Inner and outer sphere surface complexation and cation exchange; Linear.

Figure 2: Examples of sorption isotherms of different radionuclides on bentonite colloids. The sorption mechanisms are indicated as well as if their sorption is linear or not.

Table 1: Comparison of transport tests performed with different radionuclides.

Element	Initially adsorbed on colloids	Transported “unretarded” with BC
Sr	> 80%	< 2 %
Eu	> 80%	< 7 %
U	~30 %	<1 %
Cs	> 80%	0.15 %

Only in the case of Cs, an irreversible retention mechanism was clearly observed: i.e. the incorporation in the frayed edge sites of the illite/smectite mixed layer (Missana et al., 2004). Cs was also the unique case in which sorption was clearly nonlinear.

In order to study the radionuclide transport in the presence of colloids, and to evaluate the sorption reversibility under dynamic conditions, experiments were designed to favor high recovery of the particles i.e. using high enough water flow.

Table 1 shows a comparison of tests performed with different radionuclides under Grimsel Water conditions. In all the cases, sorption onto the bentonite particle was medium-high, but the fraction of radionuclide that was actually transported without retardation, along with the colloids, was much lower than the initially adsorbed on them. These results indicate that sorption on colloids is at least partially reversible (Missana et al., 2008). Desorption from the colloids is a very important factor limiting the role of colloids in radionuclide transport.

Nevertheless, the radionuclide breakthrough curves in the presence of bentonite colloids presented, in certain cases, substantial differences from those in which colloids were not present (Albarra et al., 2011). Figure 3 shows the comparison of Cs transport experiments in granite fractures under Grimsel or Äspö conditions, using similar water flow rates. 100 ppm of bentonite colloids in which Cs ($[Cs]=1 \cdot 10^{-7}$ M) was previously adsorbed (80 % in the Grimsel case and 20 % in the Äspö case) and suspended in synthetic waters representative of the two different cases. The eluted water was analysed to measure Cs activity and the presence of bentonite colloids by photon correlation spectrometry (PCS) in the same samples and to obtain simultaneously colloid and Cs breakthrough curves. The breakthrough curve of Cs, without colloids, presented a single peak with a retardation factor (R_f) of ~200 in the Grimsel case and of ~170 in the Äspö case.

In the Grimsel case, Cs transport was significantly different in the presence or absence of colloids, whereas the Cs breakthrough curves were very similar in the Äspö case. In the presence of bentonite colloids, in the Grimsel case, the breakthrough curve clearly showed a small Cs peak in a position very similar to that of the conservative tracer (HTO), with an R_f of 0.8, coincident with the colloid breakthrough peak measured by PCS.

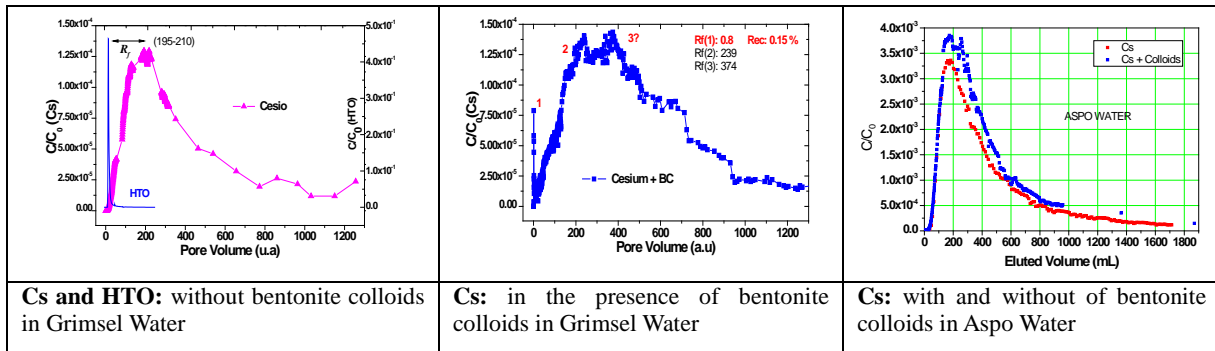


Figure 3: Examples of transport experiments in fracture with Cs with and without bentonite colloids.

The quantity of Cs recovered after this peak was only the 0.15 % of the injected. Other two peaks were observed in the breakthrough curve with R_f of 200 and 370 approximately. In the Äspö case, no elution of colloids was seen at all, which was no surprising considering that they aggregate fast, under the Äspö water conditions, and can be completely retained in the fracture. Cs, however, eluted. The “split” of the main Cs peak in two peaks with R_f of approximately 170 and 270 was also clearly observed. The appearance of new peaks with retardation factors higher than those showed in the same system without colloids, is most probably due to the modification of the sorption properties of the fracture surface caused by bentonite colloid deposition (Albarran et al., 2013).

Filtration of bentonite colloids (above all at low water flow rates) and their deposition modifies the sorption properties of the granite fracture surface. In most of the cases, the presence of bentonite colloids did not significantly enhance radionuclide transport in the medium, but rather produced a slight increase in the overall retardation in the fracture. Only in the case of very highly sorbing radionuclides like Eu, for which elution was not expected, small elution (less than 7% of the initially adsorbed) was observed and clearly attributable to the presence of the mobile colloidal particles.

REFERENCES

- Albarran N., T. Missana, M. Garcia-Gutiérrez, U. Alonso, M. Mingarro. Strontium migration in a crystalline medium: effects of the presence of bentonite colloids. *Journal of Contaminant Hydrology*, 122 (1-4) 76-85 (2011)
- Missana T., U. Alonso, M. García-Gutiérrez, M. Mingarro. Role of bentonite colloids on the migration of Eu and Pu in a granite fracture. *Applied Geochemistry*, 23, 1484-1497 (2008).
- Albarran N., T. Missana, U. Alonso, M. García-Gutiérrez, T. López. Analysis of latex, gold and smectite colloid transport and retention in artificial fractures in crystalline rocks, *Colloids and Surfaces A: Physicochemical and Engineering Aspects* 435, 115-126 (2013).
- Missana T., M.G.Gutiérrez, Ú. Alonso. Kinetics and irreversibility of cesium and uranium sorption onto bentonite colloids in a deep granitic environment. *Applied Clay Science*, 26 (1-4), 137-150 (2004).

MODELLING BENTONITE EROSION

Ivars Neretnieks, Luis Moreno, Longcheng Liu
Department of Chemical Engineering and Technology
Royal Institute of Technology, KTH
Stockholm, Sweden
niquel@kth.se

Summary

Within the BELBaR project we have further developed our model (1) for bentonite expansion and erosion in fractures with seeping water. The expanding clay is recognized to behave as a Bingham fluid/body, which expands but is not deformed up to the rim where colloid particles are released to the seeping water. The resolution of flow velocity and smectite concentration in the very thin rim zone has been considerably improved by introduction of a two-region model (2). The model was used to predict experimental data of expansion and erosion in an artificial fracture (3, 5). The experimental results also showed that floc formation increased erosion in sub-vertical fractures. The model was then further extended to also account for floc formation in the rim zone, which considerably changes the rate of erosion. The model was successfully validated by simulating a series of experiments in which smectite expands into a narrow slot with stagnant or seeping water and with different salinities. Flocculation can sediment, which increases erosion in sloping and vertical fractures. This loss can be larger than that to the seeping water. An extension of the model to set up an upper bound for the erosion by gravity is proposed.

The two-region model (2)

In previous work it was found that even large computers using sophisticated finite element methods could not resolve the details of the very sharp front in the rim-region of the expanding gel. A two-region model, which avoids some problems in earlier work, was developed and tested. The model divides the region of the expanding clay in the fracture in one, the expanding-region where the clay behaves like a Bingham fluid/body that cannot flow but can expand by the repulsive forces between the smectite particles and another, the rim-region surrounding the former where the gel/sol, although highly viscous near the rim-border, can flow and carry away the smectite particles that diffuse into this region. This two-region model gives results that are more accurate than those obtained earlier by the fully coupled model because a special technique that gives much higher resolution in the region where the erosion loss occurs was developed and implemented.

Extension and validation of the two-region model (3)

The two-region model predicted the expansion of the gel into the horizontal artificial fracture (5) well when there was no water flow to carry away the sol. However, when water flowed in the fracture, the predictions were very poor. This was found to be caused by rapid floc formation at the rim of the expanding clay gel. Including rapid floc formation and flow of the floc suspension, which does not exhibit the viscosity increase as a smectite sol does, gave very good agreement between modelled and experimental results. These comparisons are shown in Figure 1, where water velocities in the experiments ranged from 5.6×10^{-6} to 2×10^{-4} m/s and salt concentration ranged from 0 up to 170 mM NaCl.

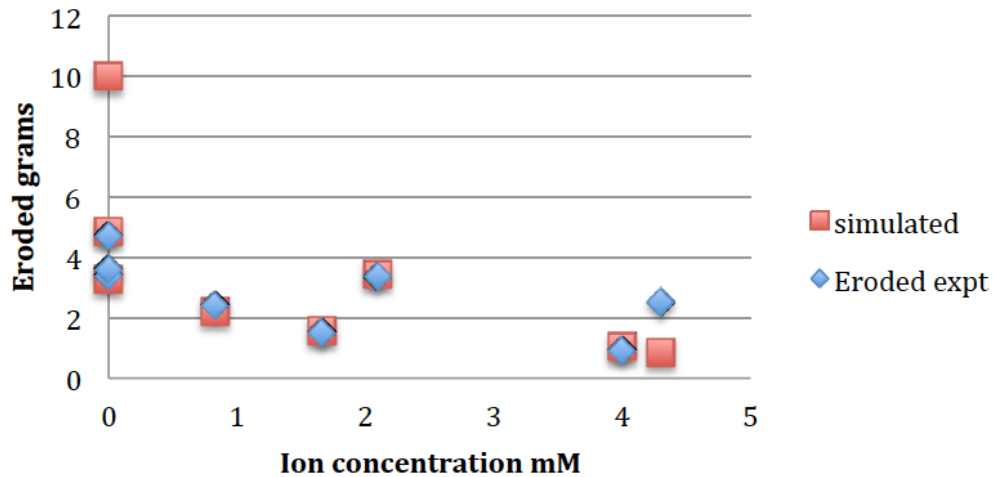


Figure 1. Comparison between predicted and experimental erosion rate with the two-region model extended to account for floc formation (3)

The experiments also showed that when the fracture was turned to be vertical, the flocs that detached themselves from the expanded gel rapidly sedimented. The loss of smectite by sedimentation was as large as or larger than that caused by the flowing water.

Modelling floc sedimentation rates (4)

Figure 2 shows an example of release and sedimentation of flocs



Figure 2. Close-up picture of sedimenting agglomerates in de-ionised water. The cylindrical region is 2 cm in diameter. Figure 59 in (5).

It was seen in this and other similar pictures that streams of small particles are released from the gel surface and sediment downward. The somewhat larger particles fall more rapidly, which catch up with and join smaller slower particles and form larger particles. When the particles grow to sizes comparable to or larger than the fracture aperture, wall friction slows

down the sedimentation of flat flocs. The large floc sheets move slowly downward. From the lower part of these flocs, small particles are again released as seen in the figure.

The sedimentation rate of the flocs, smaller than the fracture aperture, is described by Stokes’ law for spheres. The sedimentation rate of the larger agglomerates that touch the wall is modelled as an “agglomerate fluid”, AF, that moves downward in the slightly less dense water. Using this approach, the rate of downward flux of smectite can be determined. The upper limit of the sedimentation flux is predicted to result when the small particles have agglomerated to touch the walls. The flux will then be proportional to the fracture aperture squared and the rate of loss per width of source will then be proportional to the fracture aperture to the third power.

The width of the expanded gel from the source into the fracture will depend on the balance of the rate of sol loss from the rim and the rate of gel loss from the source. The rate of expansion was found to be well predicted by our dynamic gel expansion model, as mentioned earlier. This combined with the sedimentation model is used to arrive at a steady state loss and a steady state width of the expanded gel in the fracture, as illustrated in Figure 3.

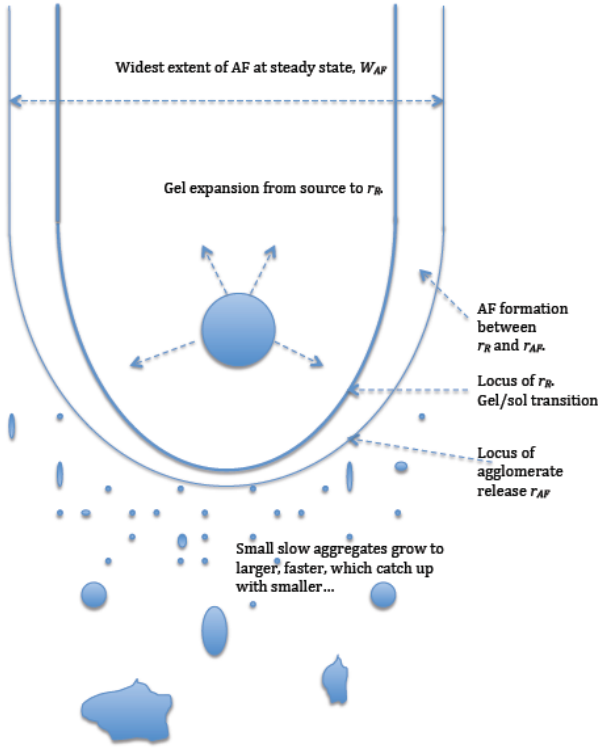


Figure 3. Concept of loss of smectite by sedimentation balanced by expansion of gel from the source.

Figure 4 shows how the steady state expansion and loss can be determined by combination of the two-region model and the sedimentation model, exemplified for a source (deposition hole) with 1 m radius intersected by a 0.1 mm aperture semi-vertical fracture. The figure shows how the loss from the deposition hole decreases as the radius of the expanded gel increases, the curve, and how the loss from the expanded gel increases with the radius of the expanded gel, the straight line. When these are equal the gel expansion reaches a steady state and the rate of loss becomes constant.

We suggest that this approach can be used to estimate an upper bound of smectite loss from a deposition hole by flocculation and sedimentation because new flocs cannot be released and carried away unless those previously generated have moved away.

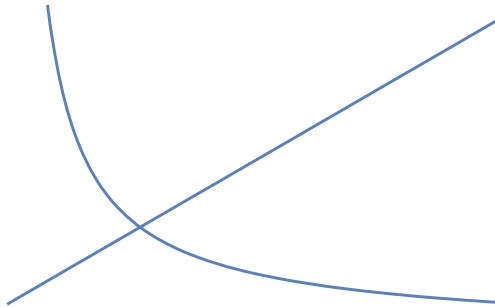


Figure 4. Rate of loss from deposition hole N_{PSS} (curved line) and rate of loss by sedimentation N_{smec} (straight line) as function of the radius to the rim

It is essential that these model predictions be validated by additional experiments.

References

1. Neretnieks, I., Liu, L., Moreno, L., 2009. Mechanisms and Models for Bentonite Erosion. Swedish Nuclear Fuel and Waste management Co., Technical report, SKB TR-09-35
2. Neretnieks, I., Moreno, L., Liu, L., (2015), Bentonite expansion and erosion- Development of a two-region model, Report submitted to BELBaR project
3. Neretnieks, I., Moreno, L., Liu, L., (2015), Evaluation of some erosion experiments by the two-region model, Report submitted to BELBaR project
4. Neretnieks I., (2015), Release and sedimentation of smectite agglomerates from bentonite gel/sol, Report submitted to BELBaR project
5. Schatz, T., Kanerva, N., Martikainen, J., Sane, P., Olin, M., Seppälä, A and Koskinen, K., (2012,) Buffer Erosion in Dilute Groundwater. Posiva Report 2012-44.

Acknowledgements

The research leading to these results has received funding from the European Atomic Energy Community's Seventh Framework Programme (FP7/2007-2011) under grant agreement n° 295487

A LARGE DEFORMATION MODEL WITH STRONG CHEMICAL-MECHANICAL COUPLING FOR BENTONITE TO ASSESS THE BENTONITE BUFFER BEHAVIOUR IN SPENT NUCLEAR FUEL DISPOSAL CONDITIONS

Veli-Matti Pulkkanen (veli-matti.pulkkanen@vtt.fi), Markus Olin, VTT Technical Research Centre of Finland Ltd, P.O. Box 1000, FI-02044 VTT, Finland

Introduction

Bentonite is a peculiar material, since it forms force withstanding structures from high to very low densities. The stability of the structures is controlled by the chemical environment and the applied force. From material scientific perspective, the stable structure acts as a solid which can flow plastically (or visco-elasto-plastically) if the forces acting on it are sufficiently large. To describe the behaviour of such chemically active solid mathematically, a model combining continuum mechanics and thermodynamics is needed. The commonly used soil scientific modelling approaches lack the ability to account for the chemical interactions properly. In these models, also the large deformations that the bentonite mostly undergoes in practical applications are often simply neglected and the small deformation theory is utilized. Thus a significant source of error is introduced in the simulations. In the work here, a large deformation model with a strong chemical-mechanical coupling is developed to describe the bentonite behaviour. The specific aim is to model the solid bentonite swelling in dilute waters until the structure breaks down to form colloids.

Modelling approach

The continuum mechanical and thermodynamic model for bentonite bases on the division of water in bentonite to 1) the structurally bound water that makes the bentonite structure swell (the bentonite volume increases by the volume of the bound water in swelling) and 2) free water that can partly or fully occupy the rest of the pore space (the “free” porosity). The bound water is characterised by the amount of it and by the equilibrium water vapour partial pressure. A strong coupling between the bound water and the mechanical stress-strain state has been rigorously and lengthily derived from the basic principles of continuum thermodynamics. The chemical imbalance (or balance) between the bound and free waters drives the water movement from the free pores to the bound water (swelling) or vice versa. By the strongly coupled model, the chemical state of the bound water depends on not only the equilibrium vapour pressure, but also the stress-strain state of the material. The salinity decides the chemical activity of the free water. As a result of the mathematical formulation of these, lowering salinity in bentonite free porosity makes the amount of bound water to increase and the bentonite to swell. The swelling stops when the chemical swelling tendency is in balance with the stress state. The above model is formulated in a large deformation setting making it suitable for practical simulations (small deformation models are suitable for strains less than approximately 1%).

Main findings

In the context of dilute water erosion of bentonite, the model suggests swelling of fully saturated bentonite, if it is in contact with water and a boundary of the bentonite body can move freely. The model also indicates swelling of bentonite if the salinity of the pore water decreases. Both of the phenomena are important when analysing the swelling of bentonite in the artificial fracture erosion experiments.

Main applications and implications

The basic frame of the model is applicable to mathematically describe the chemical-mechanical coupling of bentonite when the material is in solid form: the bentonite can be either partially or fully saturated at high or low densities. The parametrization of the model to these conditions, however, requires a significant amount of experimental work. Especially, the exact mechanical constitutive relations can be formulated only using material and condition specific data.

HYDRATION AND SWELLING BEHAVIOUR OF FEBEX BENTONITE OBSERVED BY ENVIRONMENTAL SCANNING ELECTRON MICROSCOPY

Frank Friedrich (frank.friedrich@kit.edu), Dieter Schild, Thorsten Schäfer, Institute for Nuclear Waste Disposal (INE), Karlsruhe Institute of Technology, Peter G. Weidler, Institute for Functional Surfaces (IFG), Karlsruhe Institute of Technology, D-76344 Eggenstein-Leopoldshafen, Germany

1. Introduction – Significance for BELBaR

In erosion experiments within the BELBaR project not only the formation of colloidal particles is observed, but also a strong swelling of the compacted bentonites occurs during the hydration process. This swelling behaviour of bentonites is strongly affected by their interlayer chemistry and therefore the water adsorption, a complex process related to their structural and physical-chemical properties (Bergaya *et al.* 2006). And the structure of smectites is characterized by isomorphous ion replacements, which cause a deficit of positive charge in their octahedral and sometimes tetrahedral sheets. This deficit is balanced by interlayer cations like Na^+ , K^+ , or Mg^{2+} and Ca^{2+} . This means, that these interlayer cations are accessible for water molecules in an aqueous environment. There the water molecules are arranged in a partly ordered structure forming one or two water layers around the interlayer cations, leading to an increased interlayer space. Hence, these interlayer cations play an important role in the smectite-water interaction. Not only the interlayer spacing of the clay mineral depends on the kind of cation, but also the amount of adsorbed water. Thus leading to a strongly increased particle volume and finally resulting in a complete delamination of the aggregates, forming colloidal suspensions or voluminous clay gels (Lagaly *et al.* 1997).

Environmental scanning electron microscopy (ESEM) reveals the unique possibility to investigate sensitive and even wet materials (e.g. Donald 1998, Stokes 2008). Due to its ability to adjust the relative humidity around the sample very precisely, it is an excellent tool for the investigation of the swelling behavior of clays (e.g. Carrier *et al.* 2013, Friedrich *et al.* 2015, Montes-H *et al.* 2003). Thus our focus was set on the in-situ electron microscopic quantification of the swelling of different cation exchanged bentonite samples, which than was compared to the raw material.

2. Material and Method Description

Material. In our study the Spanish Febex bentonite from Almeria was used. This raw bentonite is very rich in montmorillonitic clay minerals (> 90 %), with minor amounts of quartz, feldspars and cristobalite. For the hydration experiments the fraction < 2 μm of the untreated bentonite was used. Therefore, 20 g of the clay were purified according to the procedure established by Tributh and Lagaly (1986). Li-, Na-, and Sr-exchanged samples were produced by adding 250 mL of 1 M metal chloride solutions to 2 g of the bentonite fraction < 2 μm . To achieve a layer charge reduced smectite, the Li-exchanged sample was heated to 300 °C. At this temperature the Li^+ cations migrate from the interlayer space into the smectite framework and remarkably reduce its layer charge (e.g. Hofmann and Klemen 1950).

Environmental scanning electron microscopy (ESEM). All microscopic measurements were carried out in a FEI Quanta 650 field emission gun environmental scanning electron microscope (FEG-ESEM), which was equipped with a gaseous secondary electron detector (GSED). The microscope was operated at 20 kV in wet-mode under varying water vapor pressures between 130 and 870 Pa and at a fixed working distance of 9.5 mm. To control the sample temperature during the hydration experiments a water cooled peltier cooling stage was used.

With this instrumentation it is possible to create a defined relative humidity around the specimen by varying water vapor pressure in the microscope chamber and temperature of the peltier stage (= specimen temperature). For example, if the temperature is set to 5 °C and water vapor pressure is set to 499 Pa, according to the phase diagram of water a relative humidity (RH) of 55% results around the specimen.

For swelling isotherm measurements small amounts of clay powder were poured on the stainless steel sample holder and stage temperature and chamber pressure were set to 5 °C and 130 Pa, respectively. According to these parameters the relative humidity around the sample was 15 %.

The isotherms then were measured by increasing the water vapor pressure in five steps from 130 Pa to 862 Pa, which correspond to relative humidities of 15, 35, 55, 75, 85, and 95 % RH respectively. At each step of pressure an image was taken after an equilibration time of 15 minutes. The last step of the hydration cycle at 862 Pa (95 % RH) also was used as the first step of the dehydration cycle. Then the chamber pressure was decreased via the same five steps as in the hydration cycle until the starting conditions were achieved (130 Pa, 15 % RH). The sample temperature was always kept constant at 5 °C.

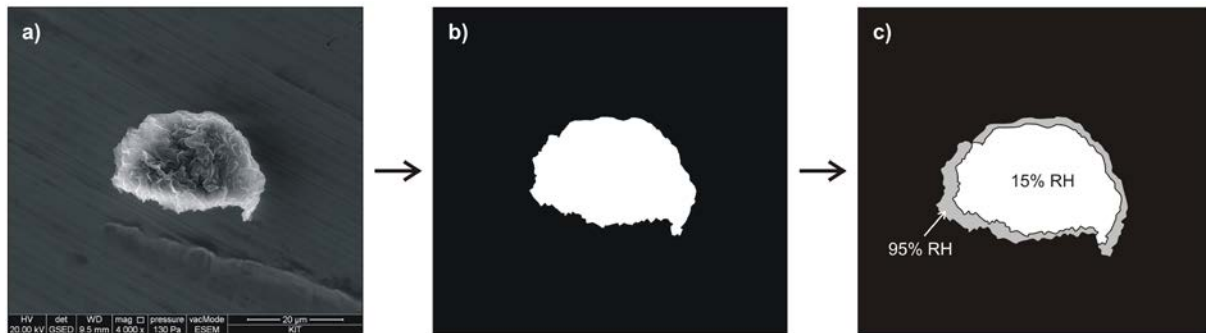


Figure 1. Digital image analysis of the clay images. a) ESEM image, b) binary image of the selected aggregate, obtained from the image analysis done with the ImageJ software (15 % RH), c) overlap of two binary images at 15 % and 95 % RH showing the increased aggregate area.

For digital image analysis the open source software *ImageJ* was used (Rasband 2015). Bentonite aggregates with diameters between 30 and 50 μm were selected for area measurements. The selected ESEM-images were converted to 8-bit and covered 1024 x 943 pixels. The area of interest (AOI) was isolated by applying a grey level threshold (Figure 1). Therefore, *ImageJ* considered a grey level range of 0-255 for all area measurements. Then the increase in area was calculated from the following equation:

$$\text{Swelling (\%)} = ((A_h - A_0) / A_0) \times 100 \quad (1)$$

Where A_h represents the area (μm²) of the hydrated sample and A_0 represents the initial area (μm²) of the dry sample at 5 °C and 15 % RH. The data are displayed as areal expansion (swelling %) versus relative humidity at a fixed temperature and therefore can be indicated as isotherms.

3. Results

A water adsorption isotherm of Na-Febex at 5 °C is displayed in Figure 2a. The swelling rates are very low at the beginning of the experiment. Not till relative humidities of 55 % the changes in particle morphology are clearly visible. The swelling finally increases exponentially at high humidities above 75 %. The dehydration path proceeds at slightly higher swelling percentages with decreasing relative humidities. In gas adsorption (BET-) measurements of smectites similar types of hysteresis are observed. There, this kind of

hysteresis loop is called type H3, and is typical for plate-like particles giving rise to slit shaped pores (e.g. Sing *et al.* 1985).

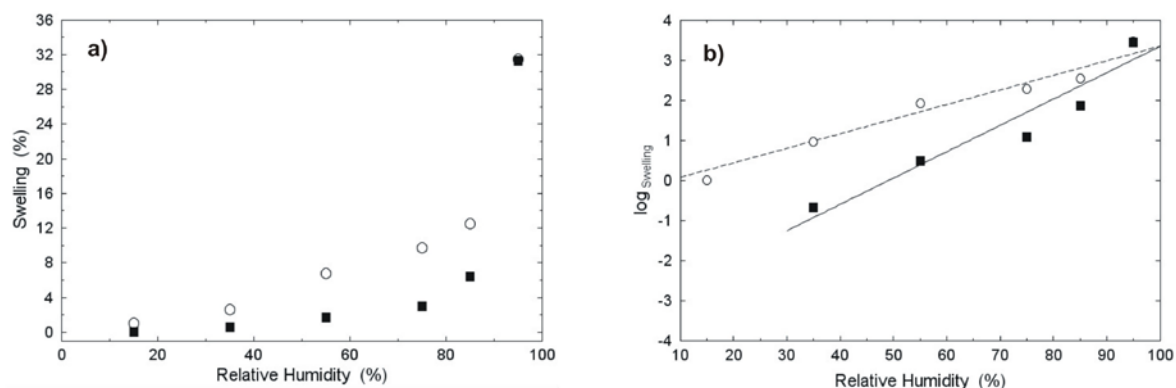


Figure 2. a) Measured isotherms of Na-Febex bentonite at 5 °C. Black squares: hydration path, white circles: dehydration path. b) Logarithmic plot of swelling vs. relative humidity representing a first order reaction of the hydration process with hindered dehydration.

A logarithmic representation of the swelling data is shown in Figure 2b. The measured data were fitted with a linear function. The slope of the hydration path (0.061 ± 0.01 , $R^2 = 0.914$) is larger than the one determined for the dehydration (0.036 ± 0.004 , $R^2 = 0.967$). Thus, hydration and dehydration can be assigned to a first order reaction, where the water availability is the driving force. Furthermore, the hydration exhibits a more pronounced dependency on the value of the relative humidity, than on the reverse action.

Hydration experiments with various cation exchanged bentonite samples (Figure 3) did not yield as many differences as reported by earlier studies (e.g. Keren and Shainberg 1975).

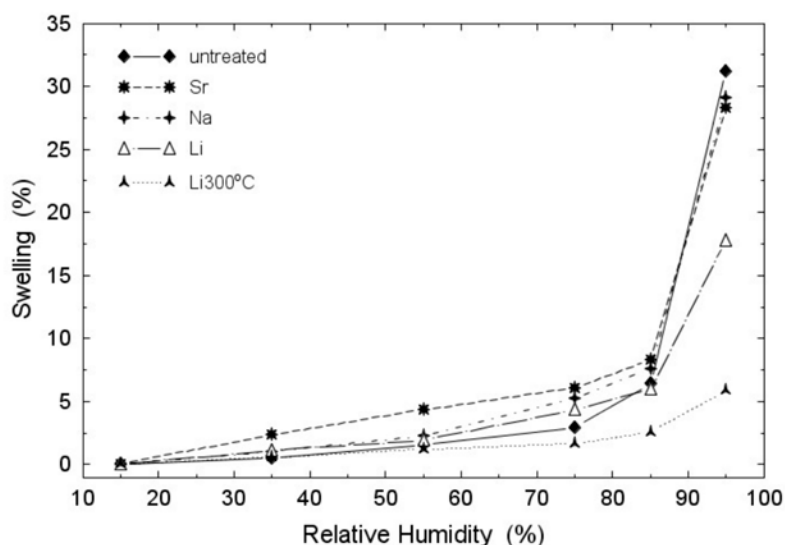


Figure 3. Comparison of the water adsorption isotherms of Na-, Li-, Li300- and Sr-exchanged bentonite vs. the untreated raw-material.

Untreated, Na- and Sr-exchanged samples swell to a similar maximum (max. swelling 29 and 28 %), while the swelling of Li-exchanged bentonite was slightly lower (max. swelling 18 %). Apart from that, the shapes of the hydration paths are very similar. In the layer charge reduced Li-sample (Li300) the migration of water molecules into the interlayer is hindered, thus it swelled only to 6 %. This behavior may have two reasons: First, the heat treatment leads to the migration of the lithium cations into the ditrigonal cavities of tetrahedral sheet, resulting in both a reduction of layer charge and the amount of interlayer cations. Secondly, this causes a collapse of the interlayer sheet to an illite-like d-spacing (e.g. Pálková *et al.* 2003).

The behavior of the untreated sample was similar to that of the Na- and Sr-samples with a slightly higher maximum swelling (31 %), which is related to a mixed cation occupancy of its interlayers (Na, Ca). Beyond that, the Sr-saturated bentonite showed a significantly higher swelling already at low relative humidities compared to the other samples. This can be assigned to the much higher hydration energy of divalent cations like Strontium ($\Delta H_h^\circ = -1415$ kJ/mol) compared to alkali metals like Lithium or Sodium ($\Delta H_h^\circ = -499$ and -390 kJ/mol). Bol *et al.* (1970) suggested, that divalent cations form two clear-cut hydration shells. This increases the hydration force within the clay interlayers, and results in large water spheres around the cation. Nevertheless, the effect of the kind of interlayer cation on the swelling behavior of the clay aggregates was not as pronounced as it was discussed by earlier studies (e.g. Keren and Shainberg 1975).

4. Conclusions

Environmental scanning electron microscopy coupled with digital image analysis is a powerful method for the in-situ observation and measurement of the swelling behavior of Febex bentonite in the range between 14 % and 95 % relative humidity. Generally, in this study it was not expected to receive completely new findings on the hydration behavior of smectites, but the behavior of Febex-bentonite has not been investigated yet. This material is very frequently used in many studies, and it turned out that its hydration behavior is a very important question. Thus the ESEM observation of its swelling behavior, which obviously is different to other bentonites like MX80, is a new finding. The hydration isotherms of various cation exchanged Febex samples have an exponential form with strongly increasing swelling at high relative humidities. Although discussed by many authors the effect of kind and charge of interlayer cation seems to be not very strong in this bentonite.

References

- Bergaya F., Theng B.K.G., Lagaly G. (2006) *Handbook of Clay Science*. Elsevier, Amsterdam.
- Bol W., Gerrits G.J.A., van Panthaleon van Eck C.L. (1970) *J. Appl. Crystallogr.*, **3**, 486.
- Carrier B., Wang L., Vandamme M., et al. (2013). *Langmuir*, **29**, 12823.
- Donald A.M. (1998) *Curr. Opin. Colloid In.*, **3**, 143–147.
- Friedrich F., Schild D., Weidler P.G. Schäfer T. (2015) Hydration of Febex-Bentonite observed by Environmental Scanning Electron Microscopy (ESEM). *CMS Workshop Lecture Series, Vol. 19*.
- Hofmann U. and Klemen R. (1950) *Z. Anorg. Allg. Chem.*, **262**, 95.
- Keren R., and Shainberg I. (1975) *Clays Clay Min.*, **23**, 193.
- Lagaly G., Schulz O., and Zimehl R. (1997) *Dispersionen und Emulsionen*. Steinkopff, Darmstadt.
- Montes-H G., Duplay J., Martinez L., et al. (2003). *Appl. Clay Sci.*, **22**, 279.
- Pálková H., Madejová J., Righi D. (2003) *Clays Clay Min.*, **51**, 133.
- Rasband W. (2015) ImageJ 1.48v. National Institutes of Health, USA. <http://imagej.nih.gov/ij>.
- Sing K.S.W., Everett D.H., et al. (1985). *Pure Appl. Chem.*, **57**, 603.
- Stokes D. (2008) *Principles and practice of variable pressure/environmental scanning electron microscopy (VP-ESEM)*. Wiley & Sons, Chichester.
- Tributh H. and Lagaly G. (1986) *GIT Fachzeitschrift für das Laboratorium*, **30**, 524.

DETERMINATION OF SPECIFIC SURFACE AREA OF CLAY MINERALS BY EGME METHOD

Lukáš Brázda (lukas.brazda@ujv.cz), Radek Červinka, ÚJV Řež, a. s., Fuel Cycle Chemistry Department, Hlavní 130, Řež, 250 68 Husinec, Czech Republic

The specific surface area (SSA) of a material is an important factor that influences its properties and behavior. A determination process of the specific surface area is provided usually by adsorption of molecules on the sample surface. There are two general approaches for indirect determination of specific surface area of clay minerals:

- 1) adsorption of simple molecules of non-polar gas (e.g. N_2 , Kr) – BET (Brunauer et al., 1938);
- 2) adsorption of polar liquids – e.g. EGME (Carter et al. 1965) or methylene blue (Hang and Brindley, 1970).

The determination of specific surface area by evaluation of BET isotherms is widely used laboratory method, but for clay minerals the outgoing results are very often highly underestimated (as can be seen later in Tab. 1). A reason can be found in the fact that for gas molecules only external surface is accessible. However, layered clay minerals have large internal surface as well, which is accessible for polar liquids.

The EGME method is based on wetting of clay samples with ethylenglycol monoethylether (CAS 110-80-5). Samples are equilibrated in a desiccator with $CaCl_2$ -EGME solvate. An excess of EGME solution is removed by evacuation. When the equilibrium between EGME vapors and EGME adsorbed on the sample is reached the sample surface is covered with monolayer of EGME molecules. The amount of adsorbed EGME is determined from the sample weight changes. It is known from theoretical calculations that 1 m^2 of the monomolecular layer weights about 0,286 mg of EGME. Therefore, from the amount of adsorbed EGME on the sample the specific surface area (overall inner and outer) of the tested clay can be calculated.

The aim of this work was to adopt EGME method in our laboratory as routine for determination of specific surface area of clay minerals and to confirm known correlations among specific surface area and other geochemical clay properties such as cation exchange capacity (CEC), type of cation in the interlayer or smectite content.

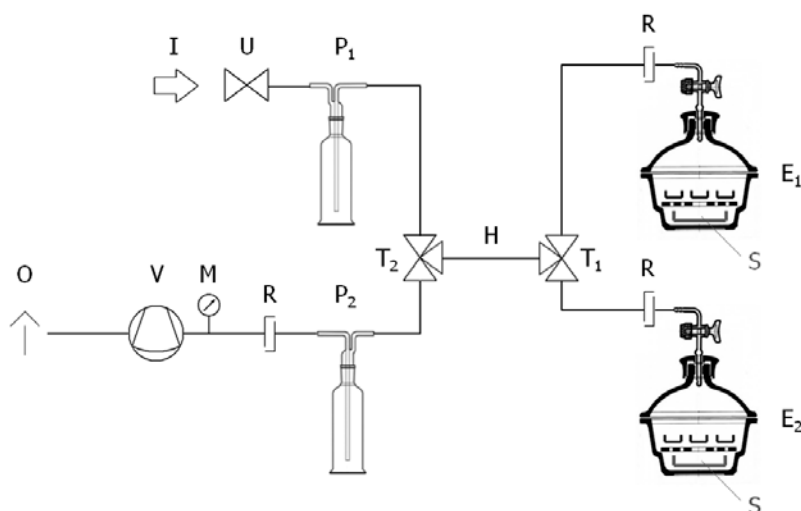


Fig. 1: Scheme of the apparatus for sample surface area measurements

Schematic drawing of used apparatus for measuring of clay sample surface area can be seen in Fig. 1. The described apparatus and experimental routine is based on several literature resources, e. g. Carter et al., 1986; Cerato and Luttenegger, 2002; van Reeuwijk, 2002.

In the first step powdered clay samples on Petri dishes were dried at 105°C to constant weight. It is favorable if the dishes can be covered with lid during all measurements to avoid adsorption of humidity. In next step, the EGME solution was added to the samples and the Petri dishes were immediately closed in the desiccator (E) with CaCl₂-EGME solvate (S) at the bottom. In our experiments 1.8–2.0 ml of the EGME solution was enough to form a clay slurry. Two desiccators can be connected to the apparatus at the same time; each desiccator carrying six Petri dishes with clay samples (may vary on size of the dishes as well as desiccators). Thanks to the hose coupling (R) and three-way stopcock T₁ each desiccator can be easily disconnected independently on the rest of the apparatus.

The desiccators were connected through the EGME vapor trap (P – a gas washing flask filled with CaCl₂ granules) to a vacuum pump (V). The vacuum pump should be able to produce vacuum about 0.05 bar which is measured with manometer (M). Water-jet pump worked fine for this purpose. The vacuum was applied for 20–30 minutes, than the stopcocks on desiccators were closed. The evacuation was usually repeated twice a day. It was not worth weighing the samples with EGME before the visible excess of EGME was evaporated (the samples started to look dry). This took usually about two, three days. Before weighting the samples, the vacuum in desiccators had to be released. It was necessary to make delay between applying vacuum and weighing the samples so that EGME equilibrium in the desiccators can be reached (at least 4 hours, better till next day). To release vacuum, an air inlet (I) branch was connected using three-way stopcock T₂. If not in use, the air inlet branch was closed with stopcock (U). After opening the stopcock, air enters another gas washing flask filled with CaCl₂ granules to eliminate air humidity. P₂O₅ can be used instead of CaCl₂ as well. In next step stopcock of the desiccator was opened carefully not to dust powdered clay samples. When the vacuum was released, desiccators were unplugged from the rest of the apparatus and taken easily to an analytical balance. After weighing of the Petri dishes with clay samples, the desiccators were connected with hose coupling back to the apparatus, the three-way stopcock T₂ was switched to the vacuum pump branch and the vacuum is applied. The measurement was stopped when two consecutive weightings deviated in less than 1 mg. Average values of the two latest weightings were taken. The specific surface area in m²/g was calculated as

$$SSA = \frac{m_E}{m_D \cdot 0,000286}$$

where m_E is weight of adsorbed EGME and m_D is weight of dried clay sample, both in grams.

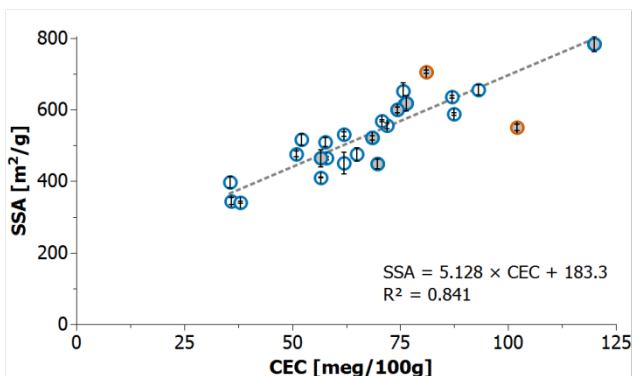


Fig. 2: Relationship between specific surface area and cation exchange capacity

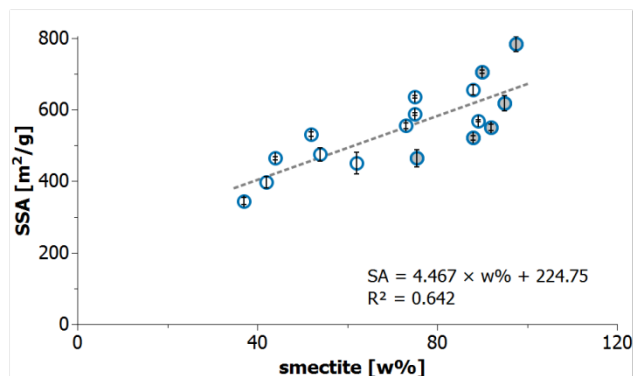


Fig. 3: Relationship between specific surface area and smectite content (in weight %)

To verify the correct function of the apparatus and the method itself 28 different clay samples were taken for experiments. In the desiccator surface areas of two clays were measured at the same time, each on three Petri dishes. If determined specific surface area is plotted as a function of the clay cation exchange capacity, clear linear dependency can be seen (Fig. 2). Two outlying orange-lined points (FEBEX and Volclay) are not included in the regression. Points with gray background represent average values from two measurements. When the modified homoionic bentonites are omitted, the equation of regression is similar, but the correlation coefficient is much better ($R^2 = 0,923$). Specific surface area can be plotted as a function of smectite content as well (see Fig. 3; homoionic clays are excluded from the chart). A linear dependency can be seen again, even though it is not so sharp.

To check reproducibility of the method, some clays were measured twice. As can be seen on examples in Tab. 1, the match of both measurements is quite good.

Tab. 1: Examples of determined SSA-EGME in comparison with BET data, if available

Clay	CEC [meq/100g]	SSA-EGME [m ² /g]	SSA-BET [m ² /g]	Note
SAz-1	*120	768 ± 37 799 ± 10	*97,4	*) Clay Minerals Society
SWy-2	*76,4	635 ± 19 601 ± 20	*31,8	*) Clay Minerals Society
Volclay KWK20-80	81	710 ± 11 703 ± 13	97	
FEBEX	°102	544 ± 4 558 ± 8	°56,4	°) Fernández et al., 2004
BaM_2014	68,6	516 ± 3 527 ± 4		
BM	62,0	531 ± 6	123	
RO-M	58,0	464 ± 5	71	
SPA 04	87,5	588 ± 4	56,7	
SPA 050	93,1	656 ± 14	76,4	
SPA 051	64,9	475 ± 19	50	

As mentioned earlier, among tested clays two sets of homoionic clays/bentonites were measured. From the results summarized in Tab. 2 an influence of the dominant cation in the clay interlayers on both CEC and specific surface area is apparent. This behavior is connected with the surface charge density of the clay mineral and the nature of the exchangeable cation and its corresponding enthalpy of hydration (K^+ -321; Na^+ -405; Ca^{2+} -1592; Mg^{2+} -1922 kJ/mol).

Tab. 2: Bentonites B75_2010 and BaM_2014 and their homoionic modifications

	CEC [meq/100g]	SSA [m ² /g]		CEC [meq/100g]	SSA [m ² /g]
B75_2010	56,6	464 ± 24	BaM_2014	68,6	521 ± 6
B75_Mg ²⁺	57,7	509 ± 12	BaM_Mg ²⁺	76,1	615 ± 12
B75_Ca ²⁺	52,1	517 ± 16	BaM_Ca ²⁺	75,7	652 ± 23
B75_Na ⁺	51,0	476 ± 8	BaM_Na ⁺	74,3	600 ± 8
B75_K ⁺	38,0	341 ± 3	BaM_K ⁺	69,8	448 ± 13

It was shown that the EGME method is efficient laboratory method how to determine total surface area of the clay minerals (in comparison with BET method by which only external clay surface can be determined). The method does not need sophisticated laboratory equipment and can be relatively easily introduced in a laboratory routine.

Acknowledgment

This contribution is the result of Radioactive Waste Repository Authority project „Research and development of the DGR disposal canister”.

References

- Brunauer, S., Emmett, P. H., Teller, E. (1938): Adsorption of gases in multi-molecular layers. *J. Am. Chem. Soc.* 60, 309–319.
- Carter, D. L., Heilman, M. D., Gonzalez, C. L. (1965): Ethylene glycol mono-ethyl ether for determining surface area of silicate minerals. *Soil Science* 100, 356–360.
- Carter, D. L., Mortland, M. M., Kemper, W. D. (1986): Specific Surface. *Methods of Soil Analysis, Part 1. Physical and Mineralogical Methods*, 2nd ed.; American Society of Agronomy–Soil Science Society of America: Madison, USA, Chapter 16, 413–423.
- Cerato, A. B., Lutenecker, A. J. (2002): Determination of Surface Area of Fine-Grained Soils by the Ethylene Glycol Monoethyl Ether. *Geotechnical Testing Journal* 25 (3), 1–7.
- Clay Minerals Society, 2016-01-07, retrieve from <http://www.clays.org/SOURCE/CLAYS/SCdata.html>
- Fernández A. M., Baeyens B., Bradbury M., Rivas P. (2004): Analysis of the porewater chemical composition of a Spanish compacted bentonite used in an engineered barrier, *Physics and Chemistry of the Earth* 29, 105–118.
- Hang, P. T., Brindley, G. W. (1970): Methylene blue adsorption by clay minerals: determination of surface areas and cation exchange capacities (clay organic studies XVIII). *Clays Clay Miner.* 18, 203–212.
- van Reeuwijk, L. P. (2002): Specific surface area. *Procedures for soil analysis (6th ed.)*, International Soil Reference and Information Center, Wageningen, Holland, 17-1–17-3.

COMPARISON OF EROSION BEHAVIOR OF DIFFERENT CLAYS

Ursula Alonso (ursula.alonso@ciemat.es), Tiziana Missana, Ana María Fernández, Miguel García-Gutiérrez. CIEMAT, Avda. Complutense 40, 28040 Madrid SPAIN.

Safety analyses of nuclear waste repositories deemed necessary to clarify if bentonite backfill barrier can be eroded, under what conditions and to what extent, because erosion may compromise its performance and eroded colloids may contribute to radionuclide transport. Within EC-BELBaR project, experimental and modelling efforts were dedicated to this purpose, and main physico-chemical factors playing a role on erosion have been identified.

The aim of the work here presented was to assess the relevance of the inherent physico-chemical properties of clay minerals on erosion. More than 15 different natural clays, mainly bentonites from different sources, were selected. A wide range of compositions, properties and structural and chemical characteristics were covered. Selected clays mainly fall within the group of smectites and included montmorillonites, saponites, beidellite and nontronite. The erosion behaviour of kaolinite and illite was also analysed.

A complete geochemical and mineralogical characterisation was carried out, by different techniques, to evaluate major and minor minerals, clays content, cation exchange capacity, major cations, water content, pore water chemistry, charge distribution and unit cell formula of the different selected clays [1].

The selected clay minerals have different smectite content and structural properties (di- or tri-octahedral) and can be initially divided according to their main exchangeable cation: (1) Na-clays: Wyoming MX-80 bentonite (USA) [2], MSU Russian bentonite from the Khakassia deposit [3], B75 a Na activated bentonite from Czech Rokle deposit [4], Sabenil S65 Czech Na-activated bentonite produced by KERAMOST Plc. Ypresian YC-D40 Doel and YC-K38 Kallo clays, with lower smectite content (40-50%) [5] were also studied. (2) Ca-Mg clays: FEBEX bentonite from Spain [6] and IBECO bentonite from Mylos island in Greece [7-8]. (3) Ca clay: SAz-1 clay from Arizona, provided by the Clay Mineral Society (CMS, USA) (4) Fe clay: Nontronite Nau-1 from the Uley Graphite Mine (South Australia) [9], (5) Beidellite SBId-1 from Idaho (USA) and (6) Saponites: MCA from Cerro del Aguila (Spain) [10] and B64 from Germany [11].

Other relevant clay minerals, out of the smectite group, were the natural illite du Puy [12] from France and the kaolinite KGa-1-b from the Clay Mineral Society (CMS, USA).

The experimental set-up used to quantify colloid erosion from compacted and confined bentonite is described in [13]. Approximately 4 g of compacted raw bentonite at 1.65 g/cm³ are placed in a stainless steel cylinder that is sandwiched between two sintered stainless-steel filters (20 mm diameter, 3 mm thick and 100 µm porous size). The cell is closed and confined by two open Delrin grids, allowing the colloid transport at both filter surfaces. The cell is immersed in 200 mL of deionised water, to account for the most favourable conditions for colloid erosion (high compaction density, low ionic strength and absence of bivalent cations) [13-15]. All experiments were carried out at room temperature and in an anoxic glove box.

The bentonite colloid generation is analysed by periodically sampling about 2 mL of the aqueous phase. Photon Correlation Spectrometry (PCS) technique was selected to evaluate the colloid size distribution and colloid concentration. PCS analyses were carried out with a Malvern 4700 system equipped with a Spectra-Physics 4W argon laser ($\lambda = 514$ nm) and the photomultiplier located at a scattering angle of 90° and the signal transmitted to a Malvern 7032 Multi-8 auto-correlator.

The electrolyte in contact to the different compacted clays was analysed, as a function of time, to measure the concentration of eroded particles that were mobilized to the liquid phase. The

initial electrolyte is deionized water and the system is closed: in contact with the different raw clays (4 g) the composition of the initial water (200 mL) evolves, soluble salts/minerals will dissolve and cation exchange processes will take place. This is an important point as the chemical conditions are critical for erosion.-Therefore, conductivity and pH were periodically measured, and the equilibrium water was analysed at the end of the experiment.

Figure 1 presents the eroded masses eluted from the different bentonites compacted at 1.65 g/cm^3 , from which higher erosion was measured. It can be appreciated that, after the hydration period, clay particles are released and eroded mass eluted in the liquid phase, initially increases linearly with time. After about 100 days equilibrium was achieved in all studies cases, as described in [13-15].

Higher erosion was always measured at higher compaction densities, and the higher erosion, under our experimental conditions, was obtained from Na-exchanged FEBEX bentonite [14].

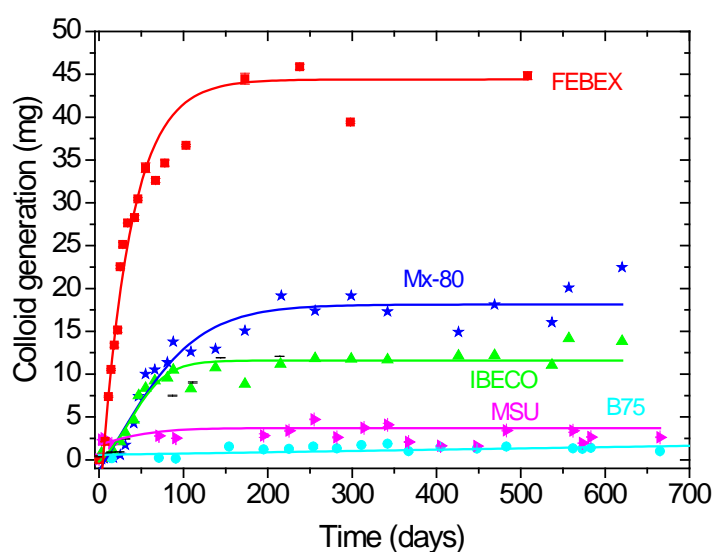


Figure 1. Eroded mass released, as a function of time, from different raw bentonites compacted at 1.65 g/cm^3 in deionised water in a confined and closed system.

Table 1 summarizes the maximum colloidal masses eroded and released from all studies compacted clays compacted at 1.65 g/cm^3 . Values are referred to the area available for colloid transport (in this case 3.54 cm^2). The main diameter of the eroded particles, measured by PCS is also indicated. It is remarkable that when appreciable erosion was measured, the average diameter of the eroded particles was around 300-500 nm, values that are by definition, in the colloid range ($< 1 \mu\text{m}$).

The clay in our experiments is compacted, but confined, so that free swelling is not allowed. By analysing the liquid phase, we measure only the fraction colloids eroded from the clay and eluted to the liquid phase. In comparison to other experiments in which free swelling is allowed, we consider as mass loss only the fraction of colloids eluted in the liquid phase.

Amongst the natural clays, the ones showing higher erosion are all within the group of Na or Na-Ca-Mg montmorillonites (Figure 1). The erosion from Ca-montmorillonites (SAz1) or Fe-nontronite (Nau-1) was very limited. It is also noteworthy that non appreciable erosion was neither measured, or values were under detection limit, from any of the other selected smectites (Beidellite SBId-1 or MCA and B64 saponites). The non - smectitic clays (illite and kaolinite) did not generate colloids as well. The pH and conductivity of the equilibrium water are also included, since the equilibrium chemical conditions can explain small differences found for similar clays.

Table 1. Maximum masses eroded and mobilized to the liquid phase from clay minerals compacted at 1.65 g/cm^3 , in a confined and closed system. Initial water was deionized. pH and conductivity at equilibrium and average particle diameter are also included.

Clay	Type	Colloid/S (Kg/m ²)	Mean size (nm)	pH	Conductivity ($\mu\text{S/cm}$)
FEBEX	Ca-Mg montmorillonite	$(1.2 \pm 0.5) \cdot 10^{-1}$	340 ± 24	7.9	190
Mx-80	Na- montmorillonite	$(5.2 \pm 0.5) \cdot 10^{-2}$	290 ± 30	8.9	370
Ibeco	Ca-Mg montmorillonite	$(3.4 \pm 0.5) \cdot 10^{-2}$	370 ± 50	9.3	290
MSU	Na- montmorillonite	$(1.13 \pm 0.2) \cdot 10^{-2}$	330 ± 140	9.9	685
B75	Na- montmorillonite	$(5.4 \pm 0.5) \cdot 10^{-3}$	$> 1 \mu\text{m}$	9.3	395
Sabenil S65	Na-montmorillonite	$(2.9 \pm 0.5) \cdot 10^{-3}$	$\cong 1 \mu\text{m}$	9.6	270
Kallo-38	Na- montmorillonite	$(1.5 \pm 0.5) \cdot 10^{-3}$	600 ± 200	7.6	250
Doel-40	Na- montmorillonite	$(1.4 \pm 0.5) \cdot 10^{-3}$	400 ± 50	8.8	260
Nau-1	Fe- nontronite	$(1.13 \pm 0.5) \cdot 10^{-3}$	$> 1 \mu\text{m}$	6.4	200
Saz-1	Ca-montmorillonite	$< 8 \cdot 10^{-4}$	n/a	7.6	250
SB-Id	Beidellite	$< 8 \cdot 10^{-4}$	n/a	7.3	125
MCA	Saponite	$< 8 \cdot 10^{-4}$	n/a	7.8	80
B64	Saponite	$< 8 \cdot 10^{-4}$	n/a	7.6	90
Illi Du Puy	Illite	$< 8 \cdot 10^{-4}$	n/a	8.8	70
KGa-1b	Kaolinite	$< 8 \cdot 10^{-4}$	n/a	6.7	85

The obtained erosion values are in agreement with the fact that higher generation was observed from homoionic Na-bentonite than from raw or Ca - homoionic clay [14], but the erosion behaviour seems to be not only related to the main exchangeable cation.

Figure 2 presents the obtained eroded masses as a function of the clay smectite content. Only clays showing appreciable erosion were included.

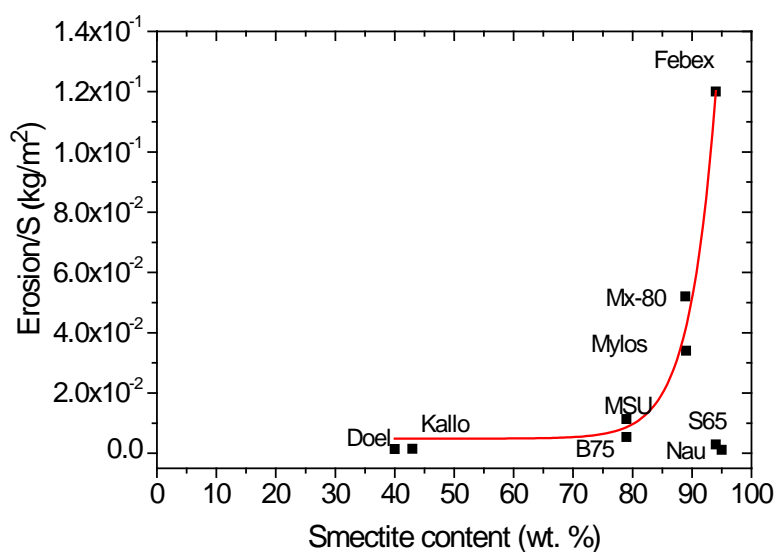


Figure 2. Eroded mass eluted in deionised water from different raw bentonites compacted at 1.65 g/cm^3 in a confined and closed system, as a function of clay smectite content.

For the eroding clays, erosion behaviour seems to be more or less related to the clay smectite content (higher in the FEBEX case), rather than only to the exchangeable Na (higher in MX-80, MSU, B75 or S65 clays) and lower erosion was observed from the Na-bentonites with lower smectite content (Doel-40 and Kallo-38 Ypresian clays). In this eroding group, the behaviour of S65 Czech bentonite is remarkable; despite being Na- clay with high smectite content did not showed appreciable erosion. It is possible that its higher Fe-oxide content may be playing a role, inhibiting colloid erosion. Indeed is being analysed that the presence of certain minerals and oxides affects bentonite colloid stability [15-16] and may also affect the erosion.

The group of montmorillonites that did not showed appreciable erosion (beidellite, saponites and nontronite) is also remarkable. In principle, those clays have relatively high smectite content but no erosion was measured. Looking to the structural characterization of these clays [1], it is noticeable that in all cases their surface charge is mainly located in the tetrahedral sheet (>50%). This favours interparticle aggregation. Therefore, not only the main exchangeable cation and the smectite content are playing a role, but the charge distribution (octahedral/tetrahedral) is an additional parameter to be considered in evaluating erosion data.

The maximum masses determined (0.1 Kg/m^2) seems to be related to the main exchangeable cations, to the smectite content, but also to the charge distribution. Limited erosion was measured from Ca or Fe-bentonites, from nontronite, beidellite or saponite and none from illite or kaolinite.

The research leading to these results received funding from EU 7th Framework Programme (FP7/2007-2011) under the grant agreement N° 295487 (BELBAR, Bentonite Erosion: effects on the Long term performance of the engineered Barrier and Radionuclide Transport).

- [1] Fernández, A.M., Alonso, U, and Missana, T. *This volume*.
- [2] Müller-Vonmoss, M. and Kahr, G., 1983. NTB 83-13, Nagra, Wettingen, Switzerland.
- [3] Sabodina, M.N., Kalmykov, S.N., A., A.e.K., V., Z.E. and A., S.Y., 2006.. Radiochemistry, 48(5): 488 – 492.
- [4] Konta, J., 1986. Clays and Clay Minerals, 34(3): 257-265.
- [5] Marcke, P.V. and Laenen, B., 2005. NIROND TR.2005-01 Report (Belgium).
- [6] Huertas, F. et al., 2000. EC Final REPORT EUR 19147, EC Final REPORT EUR 19147.
- [7] Koch, D., 2002. Applied Clay Science, 21(1-2): 1-11.
- [8] Koch, D., 2008. Science & Technology Series, 334: 23-30.
- [9] Keeling, J.L., Raven, M.D. and Gates, W.P., 2000. Clays & Clay Minerals, 48(5) 537-548.
- [10] Pusch, R., Karnland, O. and Sanden, T., 1996. ENRESA Report 02/96, (Spain).
- [11] Kaufhold, (*personal communication*).
- [12] Gabis, V., 1958. Bull. Soc. Franc. Minéral. Cristallog., 81: 183-185. S.
- [13] Alonso, U., Missana, T. and Garcia-Gutierrez, M., 2007. Scientific Basis for Nuclear Waste Management XXX. Materials Research Society Symposium Proceedings, pp. 605-610.
- [14] Missana, T., Alonso, U., Albarran, N., Garcia-Gutierrez, M. and Cormenzana, J.-L., 2011. Physics and Chemistry of the Earth, 36(17-18): 1607-1615
- [15] Albarran, N. et al., 2014. Size distribution analysis of colloid generated from compacted bentonite in low ionic strength aqueous solutions. Applied Clay Science, 95: 284–293.
- [16] Mayordomo, N., Alonso, U., Missana, T., Benedicto, A. and García-Gutiérrez, M., 2014. Scientific Basis For Nuclear Waste Management XXXVII. Mat. Res. Symp. Proc., pp. 131-138.
- [17] Mayordomo, N., Alonso, U. and Missana, T., In prep. Heteroaggregation of alumina nanoparticles with smectite.

THE ELECTROPHORETIC MOBILITY OF MONTMORILLONITE. ZETA POTENTIAL AND SURFACE CONDUCTIVITY EFFECTS.

Philippe Leroy (p.leroy@brgm.fr), Christophe Tournassat, French Geological Survey, Orléans, France, Olivier Bernard, CNRS, Paris, France.

The zeta potential is the electrical potential at the shear plane when water flows along the surface of charged particle. This electrical potential results from the ions distribution in the electrical double layer (EDL) surrounding the particle to compensate its surface charge. The knowledge of the zeta potential has many applications in the colloid and interface science, for instance, it can be used as an experimental data to calibrate the parameters (equilibrium sorption constants, capacitances) of an electrostatic surface complexation model (Hunter, 1981, Leroy and Revil, 2004) or to estimate the electrostatic forces between two charged particles in water and hence their stability, aggregation, and attachment behavior (Lyklema, 1991, Bouhaik *et al.*, 2013). Clay particles and especially montmorillonite are characterized by their large specific surface area, negative surface charge, and very low permeability which make them useful materials for the storage of domestic and industrial wastes including radioactive wastes (Tournassat *et al.*, 2011). The surface, transport, and mechanical properties of montmorillonite are dominated by the electrochemical properties of the EDL surrounding the basal planes of the particles. For instance, the sorption and swelling properties of montmorillonite is dependent on the ions distribution in the EDL (Goncalves *et al.*, 2007). Nevertheless, it is not possible to directly measure the electrochemical properties of montmorillonite due to their microscopic origin and hence the electrochemical properties of montmorillonite are dependent on the model chosen to interpret the electrokinetic experiments. Furthermore, during electrophoretic mobility measurements, Na-montmorillonite particles develop a very high surface electrical conductivity that decreases their velocity under the applied field and considerably complicates the interpretation of electrophoretic mobility measurements into zeta potentials. The Smoluchowski equation neglects the effect of surface conductivity onto electrophoretic mobility and its use may lead to apparent zeta potentials of considerably lower magnitude than the corrected zeta potentials. The use of low apparent zeta potential may lead to approximate parameters of the surface complexation model and underestimated swelling pressure of Na-montmorillonite in water.

We propose a new electrophoretic mobility model to interpret the electrophoretic mobility measurements of the basal planes of Na-montmorillonite dispersions in a NaCl aqueous solution (Leroy *et al.*, 2015) (Fig. 1). The electrophoretic mobility model is combined with a triple layer model (TLM) of the Na-montmorillonite/water interface (surface, Stern and diffuse layer; Fig. 2) constrained by the results of recent molecular dynamics simulations (Bourg and Sposito, 2011) and with a surface conductivity model of the Stern and diffuse layer of the clay/water interface. The montmorillonite aggregate was assumed to contain diffuse layer water and very elongated and charged particles surrounded by their Stern layer. The Poisson-Boltzmann equation was solved numerically to compute the electrical potentials profiles in the diffuse layer between two particles and outside the aggregate. The surface charge density was fixed to $Q_0 = -0.15 \text{ C m}^{-2}$ according to CEC measurements and four parameters were adjusted by matching the predicted to the measured electrophoretic mobility (Fig. 1). The capacitance C_2 between the Stern plane (“ β -plane”) and the beginning of the diffuse layer (“ d -plane”) and the equilibrium sorption constant of Na^+ at the Stern layer were adjusted to match the electrophoretic mobility measured at high salinity (1 M NaCl) where surface conductivity effect on electrophoretic mobility can be neglected.

The remaining parameters are the size of the Na-montmorillonite aggregate and the number of stacked TOT layers per particle. The predicted zeta potential was assumed to be located at the beginning of the diffuse layer, in the “d-plane”. Once the two TLM parameters were adjusted, the TLM was used to compute the corrected zeta potential as a function of NaCl concentration (10^{-5} to 1 M NaCl, pH=7).

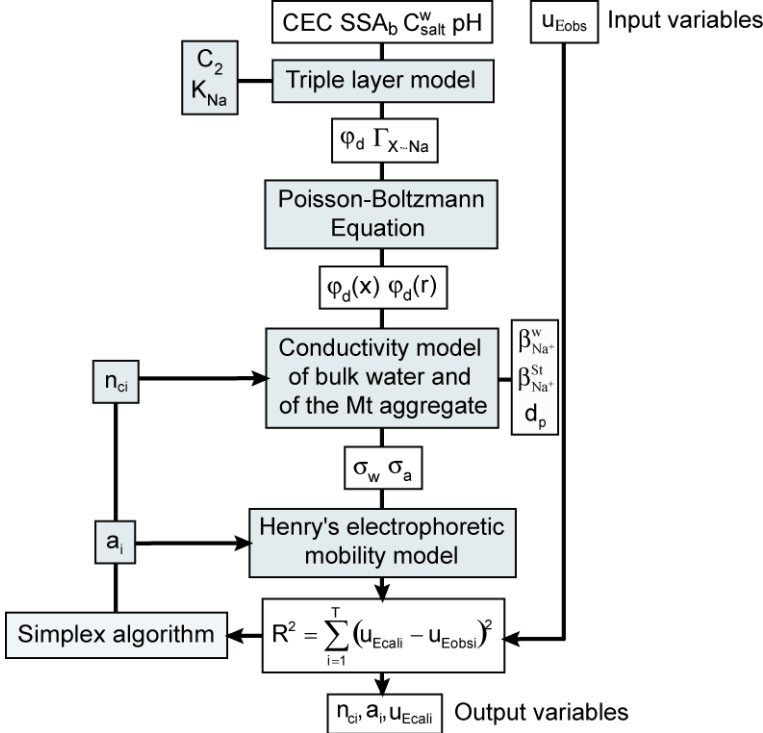


Fig. 1. Modeling strategy to determine the number of TOT layers per particle n_c and the mean radius a of the Na^+ -Mt aggregates according to CEC, specific surface areas, chemical composition of bulk water, and electrophoretic mobility measurements.

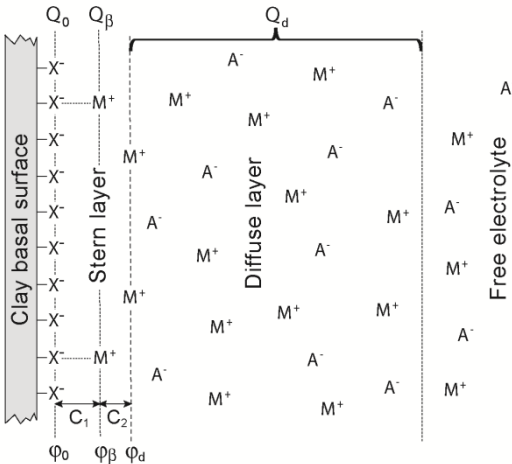


Fig. 2. Triple-layer model in the case of a Mt basal surface in contact with a 1:1 electrolyte. M^+ are metal cations (e.g., Na^+ or K^+ ions) and A^- are anions (e.g., Cl^-). The parameters φ and Q are the electrical potential and surface charge density, respectively. The parameters of our TLM are the equilibrium constant of counterion adsorption at the Stern layer K_M and the capacitance C_2 .

Apparent zeta potentials are showed at Fig. 3 to compare TLM-predicted to measured apparent zeta potentials. We observe that surface conductivity effect is increasingly important as salinity decreases. The predicted zeta potential is considerably higher in magnitude than the apparent one, showing the strong effect of surface conductivity of Na-montmorillonite particles on their mobility in water under the electric field and the large underestimation of the corrected zeta potential by the use of the Smoluchowski equation. The corrected zeta potential values were also in agreement with the values reported by Ramusson *et al.* (Rasmusson *et al.*, 1997) for Na-montmorillonite in a NaCl solution (pH=10.2). Our model was also able to reproduce perfectly the measured electrophoretic mobility (Fig. 4). Furthermore, our electrophoretic mobility model also predicted a decrease of the size of the micrometric and very porous Na-montmorillonite aggregate with salinity in dilute aqueous solutions (10^{-5} to 10^{-2} mol L $^{-1}$ NaCl) because of the compression of the diffuse layer inside the aggregate, and an increase of the size and density of the aggregate with salinity at salinities superior to the critical coagulation concentration (10^{-1} to 1 mol L $^{-1}$ NaCl).

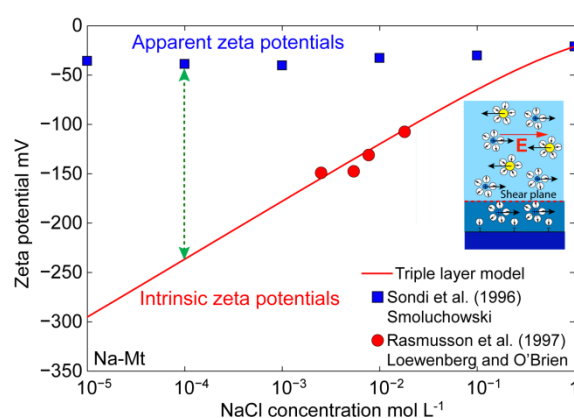


Fig. 3. Zeta potentials of Na $^{+}$ -Mt dispersions calculated as a function of NaCl concentration. Line: “intrinsic” zeta potentials predicted with the TLM. Symbols: “apparent” zeta potentials calculated with the Smoluchowski equation applied to the electrophoretic mobility measurements from Sondi *et al.* (Sondi *et al.*, 1996) (filled squares, pH = 6.5) and average zeta potentials reported by Rasmusson *et al.* (Rasmusson *et al.*, 1997), based on the interpretation of electroacoustic and dielectric dispersion measurements (filled circles, pH = 10.2).

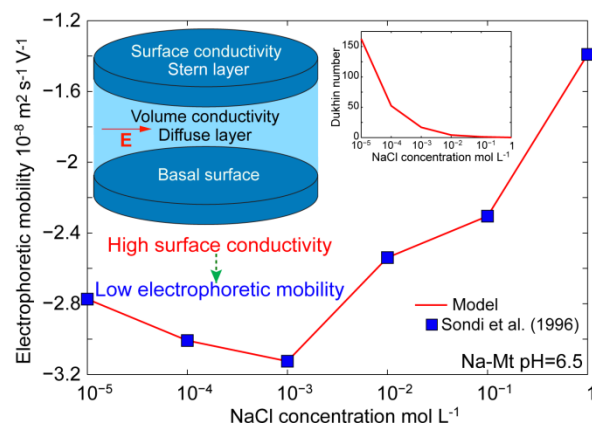


Fig. 4. Electrophoretic mobility of Na $^{+}$ -Mt dispersions as a function of NaCl concentration. Line: electrophoretic mobilities predicted with the model. Symbols: measured electrophoretic

mobilities from Sondi et al (Sondi *et al.*, 1996). The Dukhin number is the ratio of the internal conductivity of the Mt aggregate to the water conductivity.

Our results may have strong implications for calculating, according to electrophoretic mobility measurements, the sorption, attachment properties, stability, and the swelling pressure of montmorillonite dispersions (by using DLVO or extended DLVO theory). In addition, our combined surface complexation, conductivity and electrophoretic mobility models successfully reproduced the measured low electrophoretic mobilities of Na-montmorillonite dispersions, confirming the assumptions that the very high montmorillonite conductivity is responsible for its low electrophoretic mobility and that the zeta potential of the basal surface of montmorillonite is located at the beginning of the diffuse layer. In the future, our approach could be used to better predict the electrostatic interactions at the surface of the montmorillonite basal surface as a function of the chemical composition of the surrounding water. In addition, our surface complexation and transport models can be used to better understand ionic diffusion in clays and the electrochemical interactions between clays and other colloids like nanoparticles or biocolloids during their transport. It could also be used to improve the interpretation of resistivity and low-frequency complex conductivity measurements on clays.

References

- Bouhaik, I.S., Leroy, P., Ollivier, P., Azaroual, M. & Mercury, L., 2013. Influence of surface conductivity on the apparent zeta potential of TiO₂ nanoparticles: Application to the modeling of their aggregation kinetics, *Journal of Colloid and Interface Science*, 406, 75-85.
- Bourg, I.C. & Sposito, G., 2011. Molecular dynamics simulations of the electrical double layer on smectite surfaces contacting concentrated mixed electrolyte (NaCl-CaCl₂) solutions, *Journal of Colloid and Interface Science*, 360, 701-715.
- Goncalves, J., Rousseau-Gueutin, P. & Revil, A., 2007. Introducing interacting diffuse layers in TLM calculations: A reappraisal of the influence of the pore size on the swelling pressure and the osmotic efficiency of compacted bentonites, *Journal of Colloid and Interface Science*, 316, 92-99.
- Hunter, R.J., 1981. *Zeta Potential in Colloid Science: Principles and Applications*, 386pp., Academic Press, New York.
- Leroy, P. & Revil, A., 2004. A triple-layer model of the surface electrochemical properties of clay minerals, *Journal of Colloid and Interface Science*, 371-380.
- Leroy, P., Tournassat, C., Bernard, O., Devau, N. & Azaroual, M., 2015. The electrophoretic mobility of montmorillonite. Zeta potential and surface conductivity effects, *Journal of Colloid and Interface Science*, 451, 21-39.
- Lyklema, J., 1991. *Fundamentals of interface and colloid science. Volume I: fundamentals*, 736pp., Academic Press, London.
- Rasmusson, M., Rowlands, W., O'Brien, R.W. & Hunter, R.J., 1997. The dynamic mobility and dielectric response of sodium bentonite, *Journal of Colloid and Interface Science*, 189, 92-100.
- Sondi, I., Biscan, J. & Pravidic, V., 1996. Electrokinetics of pure clay minerals revisited, *Journal of Colloid and Interface Science*, 178, 514-522.
- Tournassat, C., Bizi, M., Braibant, G. & Cruzet, C., 2011. Influence of montmorillonite tactoid size on Na-Ca cation exchange reactions, *Journal of Colloid and Interface Science*, 364, 443-454.

COMPARISON OF THE STABILITY BEHAVIOR OF COLLOIDS OBTAINED FROM DIFFERENT RAW BENTONITES AND CLAYEY MATERIALS OF INTEREST IN THE FRAME OF HIGH-LEVEL WASTE REPOSITORIES

Tiziana Missana, Ursula Alonso, Anamaria Fernandez, Trinidad López

CIEMAT, Department of Environment, Avenida Complutense, 40- 28040 MADRID (Spain).
E-mail: tiziana.missana@ciemat.es

In the BELBAR Project, the possible erosion of the bentonite barrier of a high-level waste repository (HLWR), leading to the generation of bentonite colloids is being investigated.

Both the erodibility of the clay barrier and colloid transport in groundwater are strictly related to the water chemistry, and their stability behavior. The analysis of the chemical conditions that make stable or unstable a colloidal system is important because the conditions that favor colloid stability are also expected to favor colloid transport and erosion processes. Nevertheless, the intrinsic physico-chemical properties of the clay may play a role in colloid formation, dispersion, stability and, in the end, on the erodibility of the bentonite barrier. In erosion experiments (Deliverable 2.12) certain differences were observed on the erosion behavior of different bentonites under the same chemical environment. Thus, the main objective of this work is to analyze different bentonites (and some other clay mineral) to understand what are the main properties favoring or hindering colloid dispersion and stability.

Five raw bentonites were selected for this work. Apart from the smectite (as main component of the bentonite) and its properties, other elements may affect the overall behavior of the clay barrier, for example the presence of other minerals.

The bentonite selected for this study are: FEBEX bentonite from Spain (Huertas et al., 2000); IBECO bentonite from Mylos island in Greece (Koch, 2008); Wyoming MX-80 bentonite from USA (Müller-Vonmoss and Kahr, 1983); Czech Rokle bentonite Na-activated (B75, Konta, 1986) and a Russian bentonite from the Khakassia deposit (MSU, Sabodina et al., 2006). The data were compared with a commercial pure Na-montmorillonite (NANOCOR).

Colloids were extracted from the different raw clays by dispersing them (1 g/L) in deionized water (DW) and collecting the supernatant after centrifuging at approximately 600·g. The quantity of colloids generated in each case was measured by gravimetry. Under these experimental conditions, with a relatively low solid to liquid ratio, a large difference between the salinity of the initial suspensions is not expected. However, the initial conductivity was measured and the water in equilibrium with the solid phase was analyzed to account for the possible presence of ions leached directly from the clays.

The size of colloids was measured initially and upon progressive additions of Na⁺ or Ca²⁺ to check their stability and the concentration of monovalent or divalent cation needed to start coagulation process. In parallel, the zeta potential of the particles was also determined.

The size of colloids was measured by Photon Correlation Spectrometry with a Malvern NanoS apparatus with He-Ne laser and at a measurement angle of 173°. Zeta potentials were determined with a Zetamaster Malvern system equipped with a Spectra-Physics 2mW He-Ne laser ($\lambda = 633 \text{ nm}$).

The quantity of colloids initially generated is summarized in Table 1; this value provides the first indication of the capability of all the clays to disperse colloidal particles under favorable chemical conditions (DW).

Table 1. Summary of main data obtained from the stability experiments with the different clays.

BENTONITE	Concentration of particles by gravimetry (mg/L)	Initial Size in DA	Initial Conductivity (μScm^{-1}) / and pH	Onset coagulation (Na, mM)	Onset coagulation (Ca, mM)
FEDEX	166±20	351±2	25.2 / 8.77	7-10	0.2-0.3
MX-80	178±10	336±2	28.5 / 8.75	5-7	0.2-0.3
IBECO	157±10	367±2	56.8 / 9.47	2-3	0.1
B75	120±10	378±9	51.2 / 8.09	0.5-1	0.05
MSU	260±10	304±9	73.3 / 9.56	2-3	0.2
NANOCOR®	720±30	306±1	41.0 / 7.82	10-15	0.3

For the selected bentonites, which are Na or Ca-Mg bentonites (with at least 20% of Na in the exchange complex), the concentration of generated colloids correlated quite well with the quantity of Na in the exchange complex, as can be observed in Figure 1a, which presents both the measured data and the ones normalized to the actual smectite content of each bentonite. Interesting, even the initial colloid size was similar for all the bentonite considered (between 300 and 400 nm), a good correlation with the Na content could be found (Figure 1b). The particle size is smaller for higher Na content. The small deviation for S65 can be explained considering that most of its charge is located in the tetrahedral layer (72%). In general, those clays having the charge located in the tetrahedral layer forms larger colloids because, in fact, this may favor inter-particle aggregation: larger particles sediment easier being less stable than others even in DW. This analysis is being extended to other smectites (Missana et al 2016).

After the characterization of the colloids as dispersed from the raw clays, stability tests were carried out. Small progressive additions of Na^+ or Ca^{2+} were performed and the variations of mean colloid size and electrophoretic potential measured. In this way, the concentration of monovalent or divalent cation needed to start coagulation process in each clay could be determined with precision.

Figure 2 shows the zetapotential measured at different concentrations of Na or Ca for the different clays. The Na increase produced a slow decrease in the negative value of the zeta-potential up to a plateau value around -40 mV for most of the clays. The behavior observed, upon the very first additions, is not exactly the same for all the clays and might be related to Na-Ca exchange processes. In fact, almost all the clays suspended in DW released small quantities of Na, Ca or Mg due to dissolution of soluble salt /impurities.

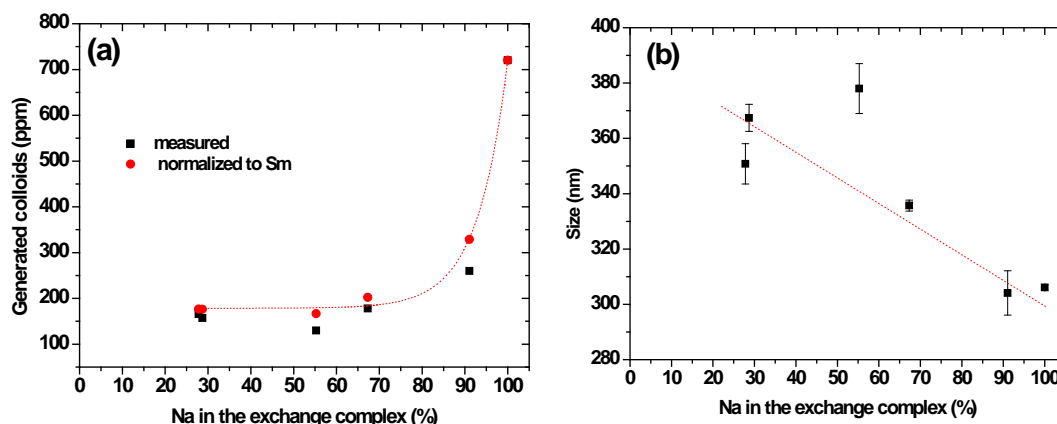


Figure 1. a) Dependence on colloid generation and b) initial colloid size on the Na content in the exchange complex of the different bentonites.

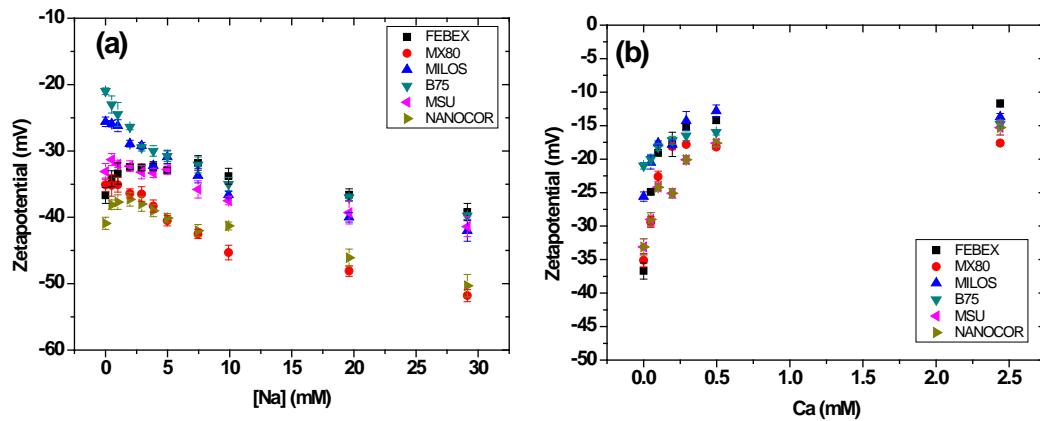


Figure 2: Zetapotential measured at different concentrations of a) Na or b) Ca for the different clays.

The clay presenting more negative zetapotentials (around -50 mV) are MX-80 and Nanocor. The addition of Ca, on the other hand, produces a pronounced and rapid decrease in the negative zetapotential value with respect to the initial untreated sample. This variation is similar in all the cases, but less sharp for the clays having predominantly Na in the exchange complex. The value at the plateau for all the samples after Ca addition is around -15 mV.

Figure 3 shows the size of the clay colloids after the additions of Na (in the right part the magnification for low concentrations). The increase of Na concentration, clearly produces clay colloid aggregation in all the cases, even if most of the clays present particles in the colloidal size range (<1 μm) even after the addition of 20-30 mM of Na. The onset of aggregation occurs at the lowest Na concentrations in the case of B75. Again, the location of the charge has a clear effect on particle aggregation.

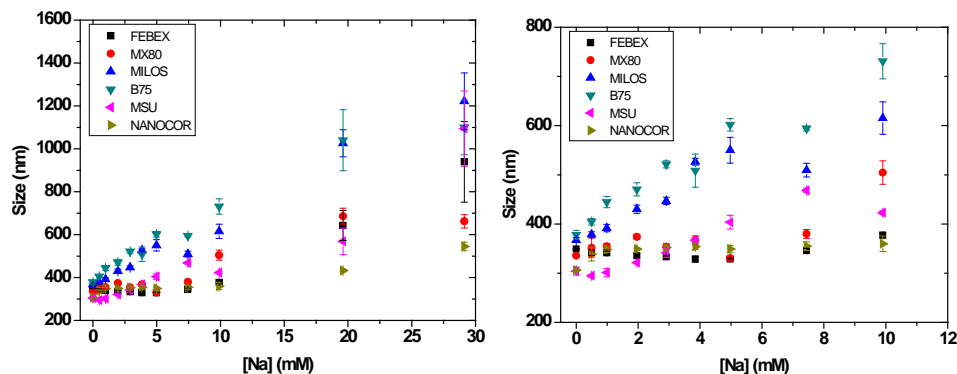


Figure 3: Size of the clay colloids after the additions of Na (complete measurements in the left part and amplification at low Na concentrations in the right).

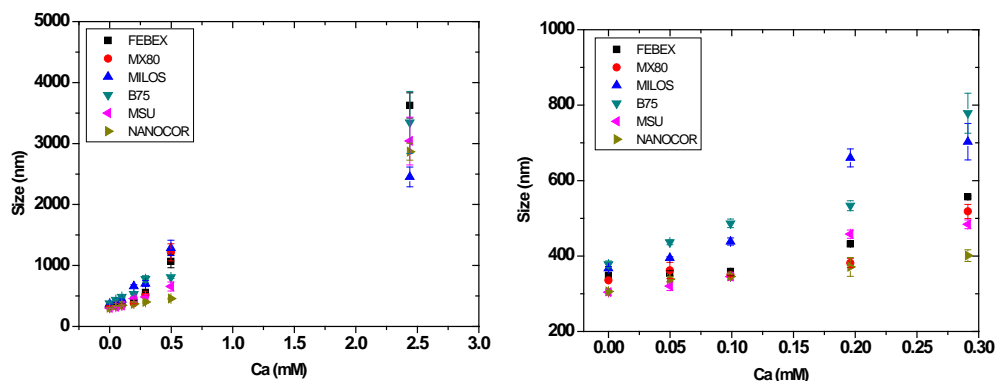


Figure 4: Size of the clay colloids after the additions of Ca (complete measurements in the left part and amplification at low Ca concentrations in the right).

Figure 4 shows the size of the clay colloids after the additions of different Ca concentration (in the right part the magnification for low concentrations). The aggregation behavior is similar for all the selected clays and the onset of coagulation is around 0.1 - 0.3 mM (more than one order of magnitude lower for Ca than Na is needed for aggregating the particles). For Ca concentration larger than 0.5 mM most of the clay particles have aggregated to give size larger than 1 μm . Again, the lowest Ca concentration for triggering coagulation is found for B65.

Parallel studies clearly evidenced the importance on the presence of trace minerals in the bentonite. The interaction of smectite with mineral like kaolinite or Al_2O_3 produces the aggregation of particles that, alone under the same chemical conditions would be stable; this means that the presence of certain minerals not only would inhibits clay colloid generation “by dilution” of the smectite, but also might affect the properties of the bentonite itself making the system more unstable.

References

- Fernandez, A.M. Mineralogical, geochemical and pore water characterization of different bentonites. CIEMAT Report June 2013, 40 pp. Madrid (Spain), (2013).
- Gabis, V. Etude préliminaire des argiles oligocènes du Puyen-Velay (Haute-Loire). Bull. Soc. Franç. Minéral. Cristallog. 81, 183–185 (1958).
- Huertas, F. et al. Full scale engineered barriers experiment for a deep geological repository for high-level radioactive waste in crystalline host rock, EUR 19147, (2000).
- Koch, D., European Bentonites as alternatives to MX-80, Science & Technology Series 334 23-30 (2008).
- Konta, J. Textural variation and composition of bentonite derived from basaltic ash. Clays and Clay Minerals 34 257-265 (1986).
- Missana T., Alonso U., Fernandez A.M. (2016) Stability behavior of natural clays: the importance of physico-chemical characteristics of the clay. In preparation.
- Müller-Vonmoss, M, Kahr, G. Mineralogische Untersuchungen von Wyoming Bentonite MX-80 und Montigel. NTB 83-13, Nagra, Wettingen, Switzerland, (1983).
- Sabodina, M.N, et al. Behavior of Cs, Np(V), Pu(IV), and U(VI) in Pore Water of Bentonite, Radiochemistry 48 488 (2006).

SWELLING OF CA/NA MONTMORILLONITE AT DIFFERENT TEMPERATURES, PHYSICAL INSIGHTS WITH THE PRIMITIVE MODEL

Axel Thuresson (axel.thuresson@teokem.lu.se), Bo Jönsson, Division of Theoretical Chemistry, Department of Chemistry, Lund University, Sweden and Ola Karnland, Clay Technology AB, IDEON Research Center, S-223 70 Lund, Sweden

Several countries plan to deposit spent nuclear fuel for long-term storage in deep geological repositories with bentonite clay as a barrier material.^{1,2} The success for such containment depends of course on the clay structure and its stability under varying conditions.^{1,3,4,5} In this context stable means that the clay should be able to sustain considerable changes in the surrounding ground water including salinities of glacial melt water as well as seawater, while still being an effective hydraulic barrier. Another factor of concern is the heat production by the nuclear waste leading initially to a temperature increase. We show, experimentally and theoretically, that the swelling of both natural and refined clays have an anomalous temperature behavior depending on the valency of the counterion. In an aqueous clay dispersion dominated by monovalent counterions, the swelling pressure (Π) increases with temperature as could be expected from entropic arguments. In a clay with predominantly divalent counterions the opposite behavior is found. The explanation is due to the fact that ion-ion correlations increase with temperature. Hence, ion-ion correlations are important at strong electrostatic coupling. In an aqueous solution it means that the dielectric permittivity, ϵ_r , decreases with increased temperature, T , and thereby the product $\epsilon_r T$ also decreases. Thus, the net effect is an increased coupling.

The interaction between charged particles has successfully been described within the dielectric continuum model using the Poisson-Boltzmann (PB) equation. This so-called DLVO theory^{6,7} has been extensively applied to charged aqueous colloidal suspensions containing monovalent salt. The number and the diversity of applications, where the PB equation has been successfully applied is so large, that we are led to the conclusion that both the primitive model and the mean field approach are legitimate approximations. The numerically most striking examples of the accuracy of the PB equation have come from direct force measurements using a surface force apparatus.^{8,9} Surprisingly enough, the theory fails completely when divalent counterions are present. The origin of the breakdown of the mean field approach is due to the exclusion of ionic correlations, which are important when multivalent ions are present. The electrostatic correlations contribute to an attractive component to the osmotic pressure, which will eventually make the net osmotic pressure negative. In order to describe these correlations quantitatively one generally needs to perform Monte Carlo (MC) simulations or solve integral equations. It has been shown that the tactoid formation in Ca-montmorillonite can be qualitatively understood due to the ion-ion correlations if the primitive model (PM) is solved exactly.¹⁰

In this study we focus on montmorillonite clays from two different sources (i) MX80, a natural Wyoming bentonite, where the counterions are predominantly monovalent Na^+ ions, and (ii) WB, which originates from a natural source in Wadi Bashira in Iraq with predominantly divalent calcium counterions¹¹. Both of these clays have been used as as is, but we have also

purified MX80 and performed ion exchange in order to obtain pure calcium MX80 (Ca-MX80) - the cleaning procedure has been described elsewhere.¹¹

A simple experiment illustrating the forces acting in a dispersion is to put one gram of clay into semipermeable membrane pockets. Thereafter, the pockets are placed into beakers with Milli-Q water at different temperatures and the swelling (weight) is monitored on a daily basis. Fig. 1 shows the difference in swelling at $T=60$ and 25 °C for sodium dominated MX80, Ca-MX80, and calcium dominated WB clays. MX80 shows the expected increase in swelling with temperature, while the WB clay and Ca-MX80 exhibit the opposite behavior which is in contradiction with mean field predictions. The PB equation has a closed solution for the salt-free double layer and it is straightforward to show that $\partial\Pi/\partial T > 0$ for both mono- and divalent counterions. This is, however not the case if ion correlations are included as we will demonstrate below. The reduced swelling in the presence of divalent counterions upon a temperature increase has three components: (i) the clay forms larger tactoids, (ii) the repulsion between the free platelets (those which do not form tactoids) is reduced, and (iii) the water layer between the platelets in a tactoid decreases.

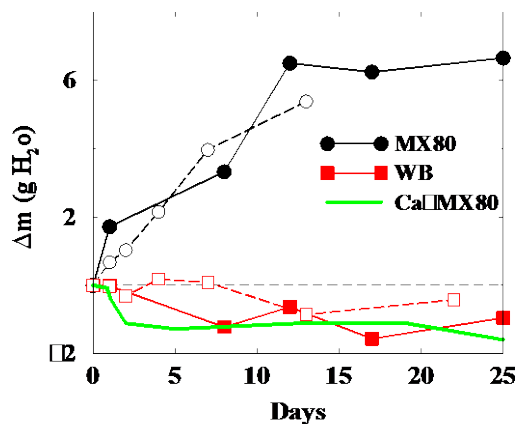


Fig. 1. The difference in swelling in pure water at $T=60$ and 25 °C. The dialysis bags are sealed with either clips (solid lines) or knots (dashed lines). MX80 is Sodium dominated but it also contains Calcium as well, and vice versa for WB. The thick green lines without symbols show the deviance in swelling for refined and calcium enriched MX80.

It is also possible to directly measure the force in a cylindrical test cell equipped with a force transducer.¹² In this experiments, clay powder was compacted directly in the cells. Thereafter the cell was adjusted according to height and put into contact with water via sintered filters, and allowed to equilibrate at room temperature. The test cell was placed inside an incubator where the temperature can be varied between 5 and 50 °C. Fig. 2 shows, with a surprising clarity, the difference between a clay dominated by monovalent counterions (MX80; upper left graph) and the clays dominated by divalent counterions (WB; upper right graph and Ca-MX80; lower left graph). Thus, the interpretation of the free swelling results (Fig. 1) is confirmed by direct force measurements.

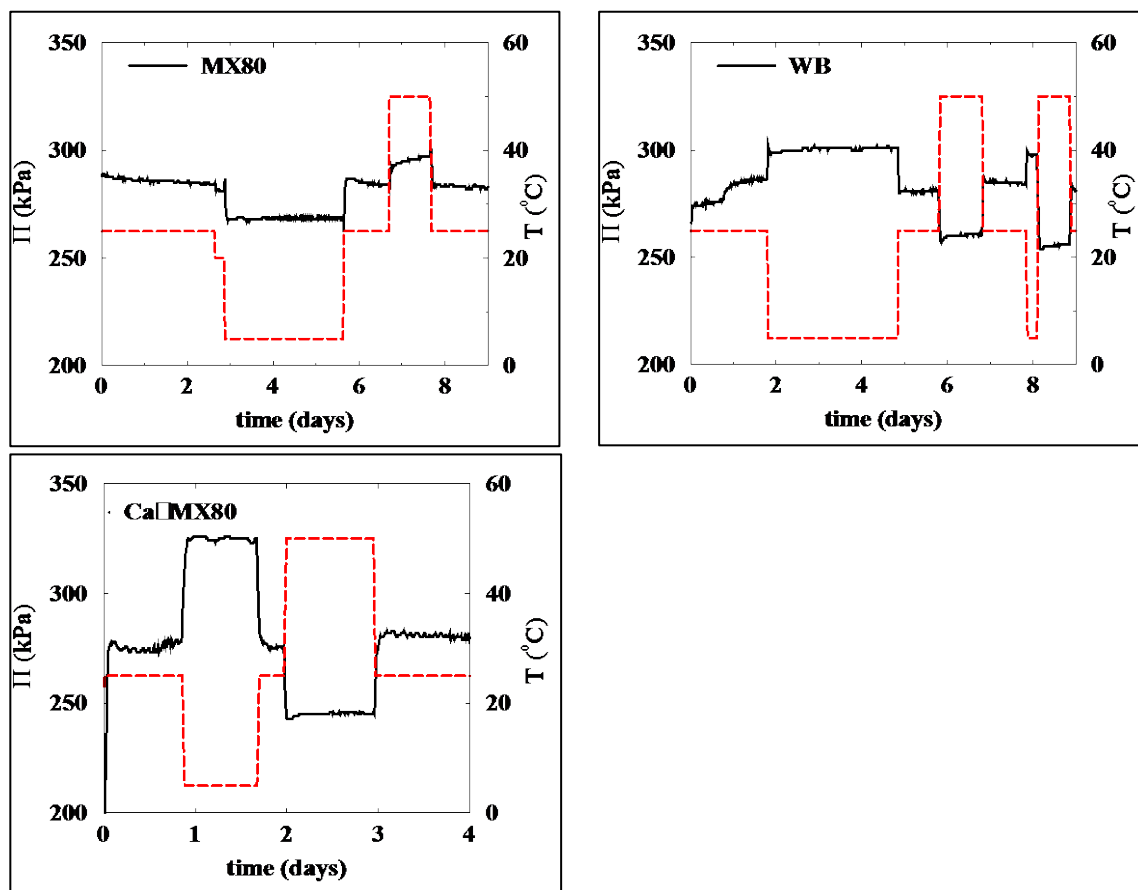


Fig. 2. Monitoring the pressure in the cell while varying the temperature between 5 and 50 °C. Upper left figure shows Na⁺ rich MX80 clay, whereas upper right shows the Ca²⁺ rich WB clay, and lower right figure the purified Ca-MX80. The red lines show the temperature variation and black lines the resulting pressure.

A common model for montmorillonite swelling^{13,14} is to treat it as two planar negatively charged surfaces neutralized by sodium and/or calcium counterions.¹⁵

We have performed MC simulation (the model is described in reference 15) and calculated the osmotic pressure at four different temperatures, 5, 25, 50 and 75 °C. The corresponding dielectric permittivity's of water are 85.76, 78.30, 69.91 and 62.43, respectively.¹⁶ Fig. 3 shows the simulated pressures for both monovalent and divalent counterions. For clarity, we present the pressure difference, $\Delta\Pi_T = \Pi_T - \Pi_{T=5\text{ }^\circ\text{C}}$. The MC simulations show the same trends as was observed experimentally. That is, with monovalent counterions the pressure increases with temperature, while with divalent ions, it decreases. It would be tempting to make more quantitative comparisons between the simulated results in Fig. 3 and the experimental ones presented in Fig. 2. It could be possible for the monovalent case as we, presumably, have a fully exfoliated system. In the divalent case, we have a mixture of tactoids and freely moving platelets whose structural details are unknown. We note, however, that the pressure changes in both theory and experiments are in the range of 100 kPa.

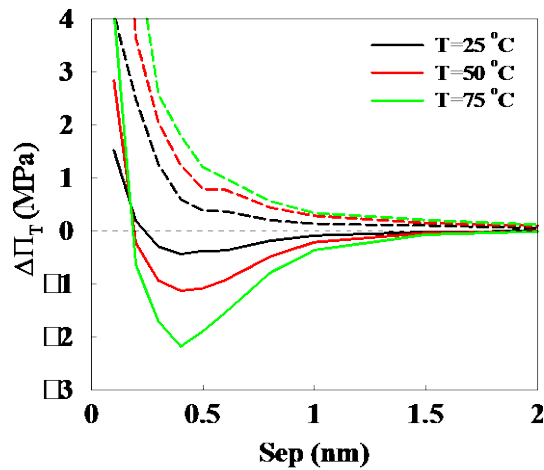


Fig. 3. The difference in simulated osmotic pressure taking $T=5\text{ }^{\circ}\text{C}$ as our reference system, $\Delta\Pi_T = \Pi_T - \Pi_{T=5\text{ }^{\circ}\text{C}}$. Solid curves are for divalent and dashed curves for monovalent counterions.

To understand the fundamental behavior of clay under the different conditions in the deposits of spent nuclear fuel, it is crucial to evaluate the barrier properties. In this study we have focused on the temperature response of the clay. We conclude that the swelling of both natural and refined clays have an anomalous temperature behavior which depends on the valency of the counterion. We have also showed that (i) the increase in swelling pressure with increasing temperature for monovalent counterions can be understood from entropic reasons, and (ii) the decrease in swelling pressure with increasing temperature for divalent counterions can be understood from ionic correlations that are important multivalent ions are present. The key point is that the product $\epsilon_r T$ decreases as the temperature increases in aqueous solutions, hence, the net effect is an increased coupling.

- ¹ H. Komine and N. Ogata, *Can. Geotech. J.* **40**, 460 (2003).
- ² O. Buzzi, M. Boulon, F. Deleruyelle, and F. Besnus, *Rock Mech Rock Eng.* **41**, 343 (2008).
- ³ R. Pusch, *Clay Minerals* **27**, 353 (1992).
- ⁴ R. Pusch, SKB Technical Report TR-01-08, 1 (2001).
- ⁵ O. Karnland, S. Olsson, U. Nilsson, and P. Sellin, SKB Technical Report TR-06-30, 1 (2006).
- ⁶ B. V. Derjaguin, L. Landau, *Acta Phys. Chim. URSS* **14**, 633 (1941).
- ⁷ E. J. W. Verwey, J. Th. G. Overbeek, *Theory of the Stability of Lyophobic Colloids.* (Elsevier, Amsterdam, 1948).
- ⁸ R. M. Pashley, *J. Coll. Interface Sci.* **83**, 531 (1981).
- ⁹ J. N. Israelachvili, G. E. Adams, *J. Chem. Soc. Faraday Trans. I* **74**, 975 (1978).
- ¹⁰ L. Guldbrand, B. Jönsson, H. Wennerström, P. Linse, *J. Chem. Phys.* **1984**, **80**, 2221–2228.
- ¹¹ M. Segad, *J. Applied Crystallography*, **46** (5), 2013.
- ¹² M. Birgersson, O. Karnland, U. Nilsson SKB Technical Report TR-10-40, 1 (2010).
- ¹³ K. Norrish and J. P. Quirke, *Nature* **18**, 120 (1954).
- ¹⁴ O. Karnland, SKB Technical Report TR-97-31, 1 (1997).
- ¹⁵ M. Segad, B. Jönsson, T. Åkesson, B. Cabane, *Langmuir* **2010**, **26** (8), 5782-5790
- ¹⁶ R. C. Weast, *Handbook of Chemistry and Physics*, 1969

BEHAVIOUR OF THE PHASE INTERFACE OF COLLOIDAL SYSTEMS AT HIGH TEMPERATURES IN NEW EXPERIMENTS OF JOSEF MOCK-UP TYPE

General information:

The safety of a deep geological repository of nuclear waste is a highly topical issue. The Czech Republic currently promotes the concept of vertical storage of containers with spent nuclear fuel with a bentonite sealing barrier between the container and the surrounding rock. Disposal wells will be situated in a tectonically stable and intact medium of granitoid rocks. The issues related to the disposal of radioactive materials have been studied for many years using laboratory experiments, in-situ experiments and numerical modelling.

The in-situ environment of the experiments is partially defined by a system of discontinuities of various orders (regional faults, local faults, cracks, fissures, micro fractures) occurring both in the rock and in the bentonite. Colloidal systems are the main transport medium, particularly in fissure systems and other microstructures.

Presentation:

The Centre of Experimental Geotechnics (CEG) of the Faculty of Civil Engineering CTU in Prague is preparing a new experiment of the Mock-up type, called the “hot” Mock-up. The experiment will be represented by two physical models situated in the Josef Underground Laboratory. The construction of the models consists of a heater (simulating a container with spent fuel), a barrier, lower and upper concrete layers with a low pH, all situated in a rock continuum (granodiorite or tonalite).

More detailed specifications:

In both models, the technology of dynamically compacted bentonite pellets with different granulometry will be used for the construction of the bentonite sealing layer, but bentonite with a different chemical composition will be selected for each model. In the first case, Ca-Mg bentonite from the Černý Vrch site (labelled B75) will be used, while in the second case it is Na bentonite (labelled MX-80). Both models will be saturated with natural water from the Josef Gallery so that the bentonite barrier is fully saturated in the shortest time possible. Immediately after their launch, both models will be heated by heaters to a temperature of 150-200 °C (heater-bentonite contact). According to the established procedure, the temperature will be reduced during the experiment. One of the objectives is to verify the behaviour of the bentonite sealing layer at temperatures above 100 °C. The models will be instrumented for a continuous monitoring of changes in significant parameters, core drilling will serve for continuous sampling of specimens for the monitoring of the saturation pattern, changes in the geotechnical, geochemical and mineralogical parameters and the course of the bentonite barrier homogenisation.

Possibilities for cooperation:

In the geochemical part, the study into colloids, their chemistry and potential changes in their chemistry, migration abilities, transport potential and sorption capacity of respective colloids,

their interactions with the surrounding rock and bentonite (erosion and alteration abilities) certainly represent a big challenge. The presence of microorganisms and their functions, study into the evolution of vapours and their interaction with the other phases, all within a system with high kinetics due to its setting in a significantly endothermic environment, will undoubtedly result in the formulation of important findings.

The design and preparation of the experiment are within the responsibility of the Centre of Experimental Geotechnics (CEG) of the Faculty of Civil Engineering CTU in Prague, which is in charge of the geotechnical part of research. Experts from the Department of Hydrogeology and Environmental Geology of the Faculty of Natural Science, MU in Brno are responsible for the geochemical part of research. CEG offers participation in this “hot” Mock-up project to other research establishments. CEG will hold a workshop in the URC Josef Regional Underground Research Centre in spring 2016 where all interested in the above research will be invited.

Jaroslav Pacovský, pacovsky@fsv.cvut.cz, Michal Roll, michal.roll@fsv.cvut.cz, Centre of Experimental Geotechnics, Faculty of Civil Engineering, Czech Technical University in Prague, Czech Republic

Tomáš Kuchovský, tomas@sci.muni.cz, Masaryk University, Faculty of Science, Brno, Czech Republic

EFFECTS OF BENTONITE COLLOIDS ON THE RADIONUCLIDE MIGRATION IN GRANITIC ROCK

Pirkko Hölttä (pirkko.holtt@helsinki.fi), Outi Elo, Valtteri Suorsa, Elina Honkaniemi and Suvi Niemiaho. University of Helsinki, Department of Chemistry, Laboratory of Radiochemistry, Finland.

Introduction

In Finland, the repository for spent nuclear fuel (SNF) will be excavated at a depth of about 500 meters in the fractured crystalline bedrock in Olkiluoto at Eurajoki implemented by Posiva Oy. The bentonite erosion resulting in the formation of colloids may have a direct impact on the overall performance of the bentonite buffer used in the Engineered Barrier System (EBS). The potential relevance of colloids for radionuclide transport is highly dependent on the colloid formation, the stability and mobility of colloids in different chemical environments and their interaction with radionuclides [1]. Radionuclides diffused and retarded in the buffer could be released directly into the groundwater flow attached with generated colloids. If colloids are sufficiently stable and mobile, irreversible sorption on colloids may increase radionuclide transport. Determination of parameters required to get information of the colloid mobility, amount of the radionuclide sorption and the chemical nature of the bond between radionuclide and mineral surface. In this work radionuclide sorption on bentonite colloids and clay suspension, colloid mobility and the effect of colloids on radionuclide migration were studied.

Experimental

The materials were MX-80 Volclay type bentonite (76 % montmorillonite), Nanocor PGN Montmorillonite (98 %) and colloid dispersion solutions separated ultrasonically from bentonite powder. Solutions of different ionic strength and pH used in the experiments were low salinity granitic Allard ($I = 4.2 \cdot 10^{-3}$ M) and saline OLSO ($I = 0.517$ M) reference groundwater, diluted OLSO, NaCl and CaCl₂ electrolytes. OLSO simulated the current saline groundwater in Olkiluoto in oxic conditions. The stability of colloids was determined by analysing colloid size distribution, concentration and zeta potential applying the photon correlation spectroscopy (PCS) method (Malvern Zetasizer Nano ZS). Colloid concentration was estimated using a standard series made from bentonite colloids and a count rate obtained PCS measurements or by analyzing the aluminum content of montmorillonite using ICP-MS.

The interaction of the radionuclides (Sr-85 and Eu-152) with bentonite colloids and suspension was investigated as a function of ionic strength (1 – 100 mM) and pH (3 to 11). The sorption parameters were determined by conducting batch experiments in a clove box under CO₂ free conditions. In the sorption experiments, mineral or colloid suspension was added to the solution spiked with a tracer, 4.7 mL aliquot were taken after 2 h, 1, 2 and 7 days and solid colloid fraction was separated by ultracentrifugation (90000 rpm/60 min). Sorption was quantified by the determination of the distribution ratio of radionuclide activity between solid and liquid phase. The solid liquid–ratio was studied to obtain an optimum mineral concentration needed to conduct batch experiments. Desorption experiments were done to investigate the reversibility of europium sorption reaction on colloids and montmorillonite. The Zeta potential of the system was determined as a function of pH with and without a studied radionuclide in order to provide information about the adsorption mechanisms.

The colloid mobility and radionuclide-colloid migration was studied in the crushed rock, drill core and rock fracture columns. The crushed rock columns were made of intact, fine-grained granite and strongly and homogeneously altered tonalite. The column diameter was 1.5 cm and length 15 cm or 30 cm. Drill core columns were constructed from Kuru gray granite cores which were placed inside a tube to form a flow channel ($L = 68.5$ cm, $w = 4.4$ cm) representing an artificial fracture formed by the 0.5 mm gap between the core and the tube [2]. The rock fracture column from Olkiluoto tonalite drill core was artificially fractured along the natural fracture. The fracture width in the column was about 3.5 cm, the column length 6.8 cm and the fracture aperture 100 μm . In the experiments, colloid solution (3 g/L) was injected into the water flow as a short pulse. The experiments were performed in the low salinity Allard reference groundwater, in which the colloids are assumed to be stable and mobile.

Results

Strontium and europium adsorption onto the bentonite colloids and montmorillonite was highly pH dependent, adsorption increasing with increasing pH. K_d -values of Sr-85 for MX-80 bentonite colloids in diluted OLSO and in Allard reference groundwater are shown in Fig. 1. K_d -values of Eu-152 for MX-80 bentonite and Nanocor PGN Montmorillonite colloids in Allard reference groundwater are shown in Fig. 2. Radionuclide adsorption was also dependent on water salinity shown in Fig. 1 (left), adsorption decreasing with increasing ionic strength owing to particle aggregation and lower specific surface area.

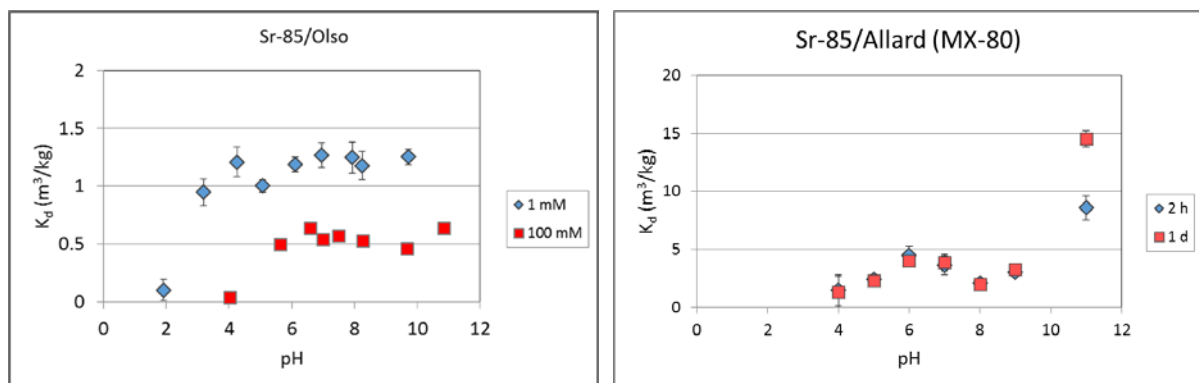


Figure 1. K_d -values of Sr-85 for MX-80 bentonite colloids in diluted OLSO (left) and in Allard (right) reference water.

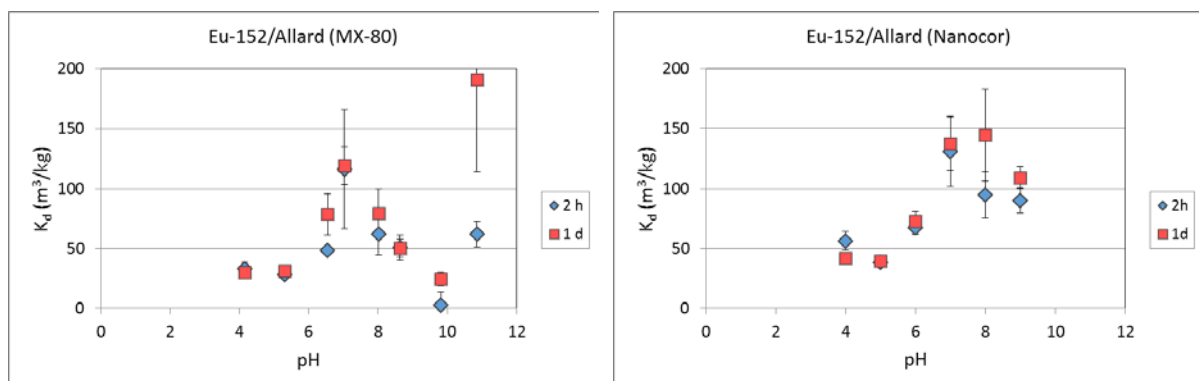


Figure 2. K_d -values of Eu-152 for MX-80 bentonite (left) and Nanocor PGN Montmorillonite (right) colloids in Allard reference water.

In desorption experiments at constant pH 8, almost 60 % of Eu-152 was removed from the Nanocor PGN Montmorillonite colloid solution and suspension after two weeks when the solution was changed every second day. After one month and the change one a week, slightly higher desorption was obtained.

Zeta potential of Nanocor colloid solution and mineral suspension in Allard reference water as a function of pH at the presence and absence of Sr-85 and Eu-152 are shown in Fig. 3. Zeta potential of montmorillonite or colloid dispersion determined as a function of pH was negative from the beginning and decreased with increasing pH due to deprotonation and that the mineral surfaces were negatively charged across the pH range. Zeta potential was less negative with europium suggesting europium adsorption mechanism appeared not to be purely electrostatic but also via inner-sphere complex due to the aluminol sites present on clay minerals. In the case of strontium, no change in the Zeta potential curve was found meaning the sorption is based on electrostatic ion-ion interactions.

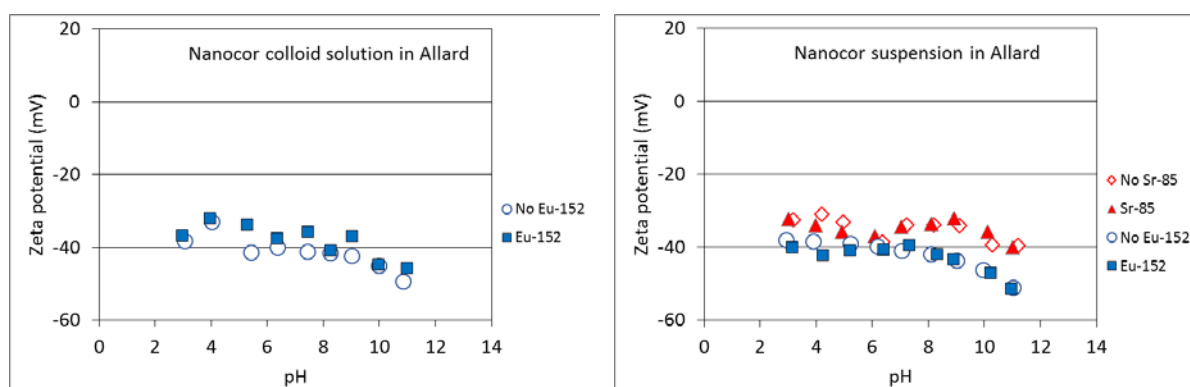


Figure 3. Zeta potential of Nanocor colloid solution (left) and suspension (right) in Allard reference water as a function of pH at the presence and absence of Sr-85 and Eu-152.

Migration of colloids was affected by the rock alteration, the type and length of column, water flow rate and colloid size. The recovery of bentonite colloids shown in Fig. 4 in these experiments was low, the lowest recoveries were found in crushed rock columns (< 4 %). The highest recoveries were found in the drill core (30 %) and rock fracture columns (60 %). Slowing down the water flow rate, the recovery was decreased. However, the flowrates in these experiments were orders of magnitudes faster than the groundwater flow. The colloid recovery was determined also from the Np-237 migration experiments, where colloid solution was pumped continuously into the water flow. The recovery of colloids in the crushed rock column was 20 % and in the drill core column 30 - 40 %.

The effect of bentonite colloids on Sr-85 and Eu-152 transport was studied in the column experiments. The retardation factor was estimated from the breakthrough curves of the conservative tracer and the radionuclide when the same experimental conditions have been used. However, the retardation factor was an approximation, because in the course of column experiment equilibrium between sorbed and dissolved species may not have been attained. In the all columns particularly Eu-152 was strongly retarded but also Sr-85 was retarded without colloids. In the presence of bentonite colloids, the slow elution of Sr-85 was obtained. In the Olkiluoto rock fracture column, the retardation factor, R_f of 56 was estimated without the

presence of colloids at water flow rate of 10 $\mu\text{l}/\text{min}$. In the presence of colloids, R_f of 7.1 was estimated. No breakthrough of Eu-152 activity was detected during two week experiment with or without the addition of bentonite colloids. In these experiments, colloid solution (3 g/l) was injected into the water flow as a short pulse resulting in very low colloid concentration available.

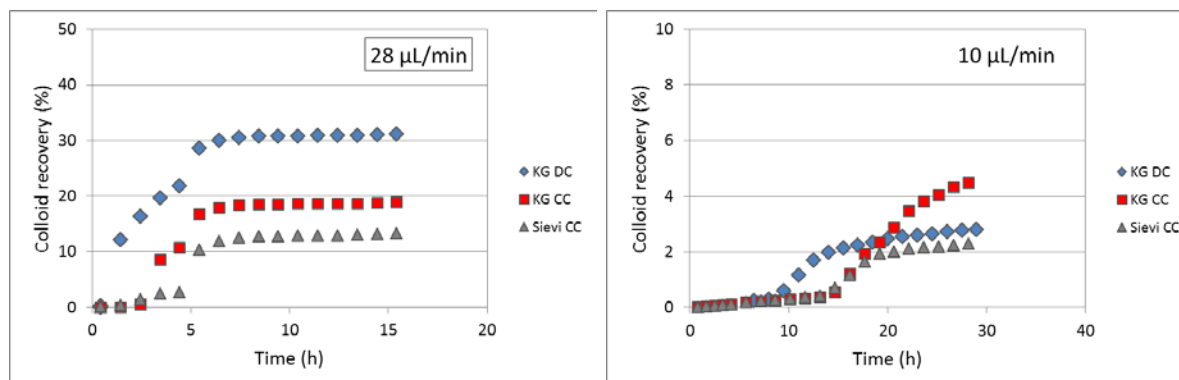


Figure 4. Colloid recovery in Kuru grey granite drill core column (28 cm) (blue), crushed rock columns (15 cm): Kuru grey (red) and Sievi altered tonalite (grey), flow rate 28 $\mu\text{l}/\text{min}$ (left) and 10 $\mu\text{l}/\text{min}$ (right), average particle size 230 nm.

Conclusions

pH had a great influence on the chemical form of the radionuclides (Eu-152) and thus on their sorption onto colloids. Eu speciation calculations are needed to explain its sorption behavior. Desorption experiments showed reversible europium sorption on bentonite colloids and mineral surfaces. However, fully reversible sorption was not obtained. Zeta potential was less negative with europium only in colloid solutions suggesting also outer-sphere or inner-sphere complex due to the aluminol sites present on clay minerals. No change in the Zeta potential curve with strontium suggest electrostatic ion-ion interactions. Colloid mobility and radionuclide-colloid migration experiments performed in a small laboratory scale, showed that colloids had an effect on radionuclide transport. Mobility of colloids was affected by the water flow rate, colloid size, column material and type. The main uncertainties remain still in the quantification of colloids under realistic repository conditions and how mobile colloids are. Thus, the assumption of the low contribution of colloids as radionuclide carriers could not be validated properly.

The research leading to these results has received funding from the European Atomic Energy Community's Seventh Framework Programme (FP7/2007-2011) under grant agreement n^o 295487. Research has received funding also from Finnish Research Programme on Nuclear Waste Management financed by The State Nuclear Waste Management Fund.

[1] Schäfer, T., Hüber, F., Seher, H., Missana, T., Alonso, U., Kumke, M., Eidner, S., Claret, F. and Enzmann, F. (2012) *Appl. Geochem.*, 27(2), 390-403.

[2] Hölttä, P., Poteri, A., Siitari-Kauppi, M. and Huittinen, N. (2008). *Phys. Chem. Earth* 33, 983–990.

GEOMICROBIOLOGICAL ASPECTS OF CLAY COLLOIDS – CULTURABLE MICROORGANISMS

Jiri Mikes (mikes@teramed.cz) TERAMED, s.r.o. Czech Rep. and Pavel Spacek, CHEMCOMEX Praha a.s. Czech Rep.

Paragraph 1: Why is this abstract important?

Microbiological aspects of many engineering applications (civil engineering, geotechnics, mining) seem to be somewhat sidelined. There are some explanations for this situation, for instance special methods, analysis, and need for biological background. However, last outputs in many human activities are showing that it is not only remarkable to use an interdisciplinary approach but it may be a source of many valuable findings for the practical usage. This contribution makes an effort to present what is the main benefit of novel microbiological methods in clay colloids studies, mainly methods based on new cultivation microbiology and serving for the characterisation of the whole microbial community from phylogenetical, quantitative, however, first of all from functional and physiological point of view. Only such an approach enables to predict a set of possible risks and/or opportunities which may change many decisions significantly. Basically much more important description provides the interpretation which focuses on the particular bioprocess, their results in the system (clay colloids) and in biological agents.

Clay (bentonite, Montmorillonite) offer unique system for new research strategies focusing on more complex view, what may happen when microorganism are present in metabolic active state. Their extracellular products have been supposed for substantial impact on material rheology, other transport processes, and new sorption sites for all biological and chemical agents. This study and its result try to create a bridge between non-biological disciplines for better understanding of all processes (Rättö, 2012).

Paragraph 2: What is novel approach; what was done?

All natural processes are coupled with set of specific conditions significantly. Many experimental results may be affected by the approach which has been selected for purposes of a study. In this work, there was a strong impact on:

- the experimental set-up close to the natural (original) conditions
- intact sampling approach
- special experimental infrastructure (large-scale anaerobic chambers)

Methods used in this work deal with microorganisms and their abilities to change their environment (metabolic transformation of chemical compounds being a natural of the clay environment, the amendment of the environment by extracellular compounds produced by microorganisms). Origin samples of Montmorillonite (KERAMOST a.s.) have been analysed

due to their microbiological inhabitation by set of cultivation methods respecting the fact that the most of these microorganisms have lithotrophic/mixotrophic metabolic feature. There is a significant constraint in the offer of cultivation media. In order to minimize false positive/negative results, all cultivation have been carried out on agar-like plates, where instead of agar, inorganic solidifying agent was used. Isolated microbial consortia of Montmorillonite samples were compared to origin microbial consortia due to physiological state characterisation, metabolic rate estimation, and finally, survival mechanisms. In the second part, Montmorillonite samples were inoculated by sulphate reducing bacteria (SRB). In this system, their ability to live under such conditions was observed for further studies, especially from the view of mass transport and corrosion effects.

Paragraph 3: What are main findings?

Description of microbial inhabitation in Montmorillonite

In commercial Montmorillonite (KERAMOST a.s.), the number of all culturable microorganisms was detected by cultivation methods based on most probable number (MPN) quantification. As solidifier in agar-like media, a hydrogel derived from (hydroxyethyl)methacrylate was used. This approach enables to focus on more realistic conditions similar to mainly oligotrophic feature of clay environment. The basic experimental set-up led to distinguishing of aerobic and anaerobic microorganisms that are lithotrophic autotrophs. In the sample of Montmorillonite, 10^6 cfu/g aerobic and 10^3 cfu/g anaerobic microorganisms, capable of growing on the plate, was estimated. Stroes-Gascoyne et al. (2010) focused on aerobic and anaerobic heterotrophs in the commercial Wyoming MX-80.

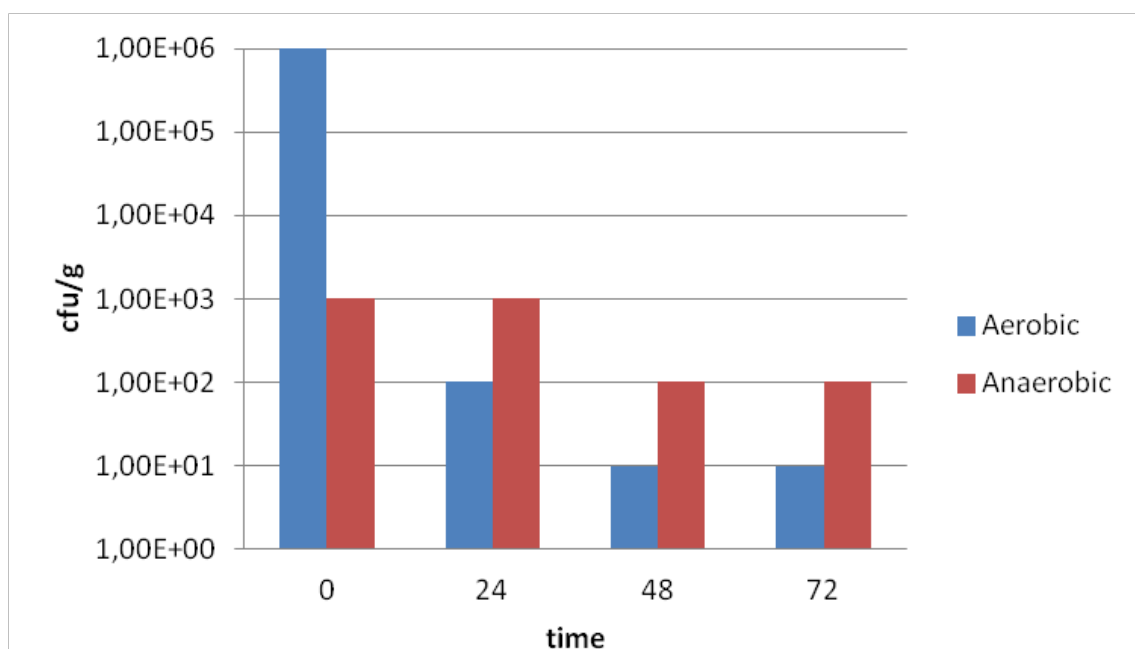


Fig. 1 Analysis of aerobic and anaerobic microorganisms

The number of bacteria living in such sample was 10^5 cfu/g and 10^2 cfu/g respectively. In the picture 1, a comparative study of the ability to survive the change of aerobic and/or anaerobic

atmosphere was carried out in order to get basic information of the strain vulnerability to oxygen exposition.

Masurat et al. (2010) isolated *Desulfovibrio africanus* from Wyoming bentonite MX-80 using medium selective for SRBs. The strain could grow near to 40°C and in high salinity range (up to 4 %). The most frequented strain isolated from the anaerobic consortium was very similar to *Desulfovibrio* in its cultivation patterns on SRB agar. It remained viable in Montmorillonite after 24 h of high temperature exposition (100°C).

More detailed characterisation of these microorganisms (physiology, metabolic features)

The usually available LIVE/DEAD BacLight kit is still more widespread in many microbiological applications. There is confusion over viability state of microorganisms. Viability staining or vital staining techniques are used to distinguish live from dead bacteria. These staining, first established on planktonic bacteria, may have serious shortcomings when applied to multispecies biofilms. Results of staining techniques should be compared with appropriate microbiological data (Netuschil, 2014). In this study, a compromising solution has been chosen. All biofilm growth form has been carefully released from the solid particle surface by ultrasound detachment. Prepared microbial suspension was processed by LIVE/DEAD protocols immediately. There are some very remarkable results which strengthen the statement about surprisingly high endurance of anaerobic microorganisms associated with Montmorillonite clay. A comparison illustration of above mentioned fact is well depicted in the figure 2.

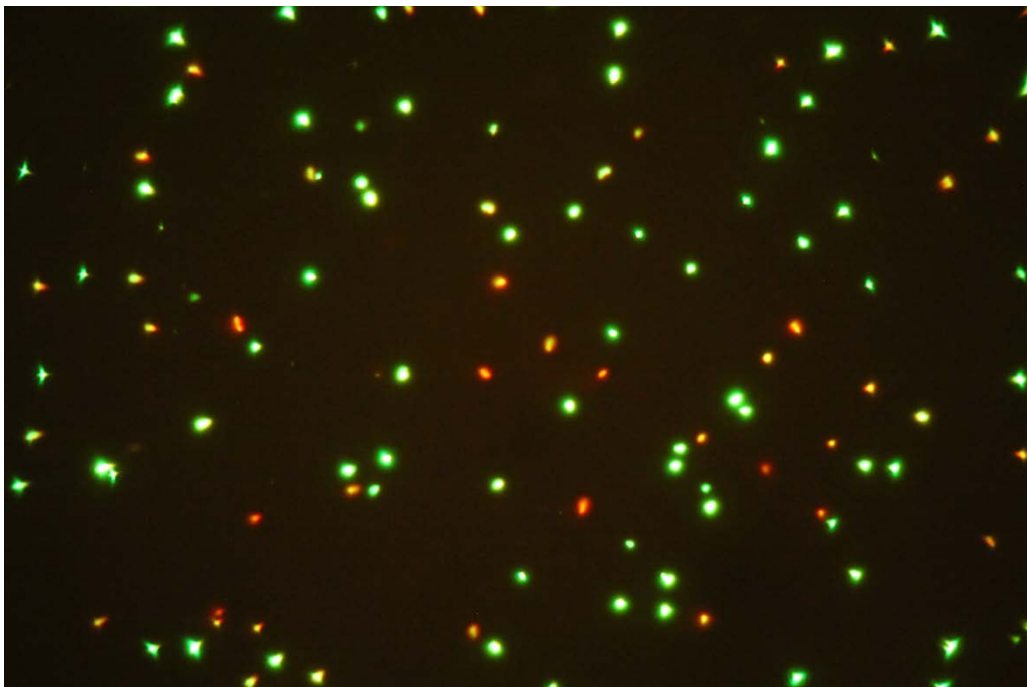


Fig. 2 Live (green) and dead (red) anaerobic cells after 72 hours under aerobic conditions

A result of this staining technique was compared with the cultivation data obtain simultaneously. With the regard to the standard error of all cultivation fact, there is significant evidence about correlation of both methodical approaches.

Description of the changes which have been done by these microorganisms (extracellular compounds production)

Extraction procedures were done according to the approach employed by Chung (2001). Under anaerobic conditions, biofilm created on clay surface was analysed for exopolymeric compound content and then compared to exopolymeric content in planktonic population. After 6 days of anaerobic cultivation, the content of exopolymeric compound (expressed as total saccharides) increased on clay particles from the origin 10 mg/g to 56 mg/g. In the case of planktonic cells, extracellular layers created on the cell surface increased from 2.6 mg/g to 12.5 mg/g biomass. This finding represents significant increase of organic content in the environment which is poor in organic compounds. Extracellular compounds are suspected from serious impact on corrosion processes.

Simulation of SRB colonisation

Capabilities of the microorganisms to attach the surface was found slightly lower when compared to the biofilm count of 1.5×10^{10} cfu/g of bentonite clay as described by Vadakel (2001) and Rajagopal (2013). Vadakel (2001) also reported a rapid decline of planktonic cells during the subsequent days of incubation, which was not observed. After 6 days of experimental cultivation, 108 cfu/g of Montmorillonite clay was found.

Paragraph 4: What are main applications and implications?

- new inside for MIC
- new findings in surface colonisation
- microorganisms as a carriers of colloid-metal complexes
- simulation of microbial behaviour under anaerobic conditions
- impact on the kind of experimental design, intact sampling, and research infrastructure

References

- Chung JY, Wilkie I, Boyce JD, Townsend KM, Frost AJ, Ghoddsi M, et al. (2001) Role of capsule in the pathogenesis of fowl cholera caused by *Pasteurella multocida* serogroup A. *Infect Immun.*;69:2487–2492.
- Masurat, P., Eriksson, S., Pedersen, K. (2010a). Evidence of indigenous sulphatereducing bacteria in commercial Wyoming bentonite MX-80. *Applied Clay Science* 47: 51–57
- Netuschil, L., Auschill, T., Sculean, A. and Arweiler, N. (2014). Confusion over live/dead stainings for the detection of vital microorganisms in oral biofilms - which stain is suitable?. *BMC Oral Health*, 14(1), p.2.
- Oulkadi, D., Balland-Bolou-Bi, C., Billard, P., Kitzinger, G., Parrello, D., Mustin, C. and Banon, S. (2014). Interactions of three soil bacteria species with phyllosilicate surfaces in hybrid silica gels. *FEMS Microbiol Lett*, 354(1), pp.37-45.
- Rajagopal, R. (2013). Biofilm formation of *Pasteurella multocida* on bentonite clay. *Iran J Microbiol.*, 5(2), pp.120-125.
- Rättö, M. and Itävaara, M. (2012). Microbial activity in bentonite buffers. *VTT TECHNOLOGY* 20.
- Stroes-Gascoyne, S., Hamon, C.J., Maak, P., Ruissell, S. (2010). The effects of physical properties of highly compacter smectic clay (bentonite) on the culturability of indigenous microorganisms. *Applied Clay Science* 47: 155–162.
- Vadakel L. (2001) Growth kinetics and outer membrane protein profiles of biofilm and free cells of *Pasteurella multocida* serotype A: 1; Bangalore, India: University of Agricultural Sciences; M. V. Sc. Thesis.

Acknowledgement: This study was carried out in close cooperation with Centre of Experimental Geotechnics, Czech Technical University in Prague.

GENERATION AND STABILITY OF BENTONITE COLLOIDS

Valtteri Suorsa (valtteri.suorsa@helsinki.fi), Pirkko Hölttä, University of Helsinki, Department of Chemistry, Laboratory of Radiochemistry, Finland.

Introduction

In Finland, the repository for spent nuclear fuel (SNF) will be excavated at a depth of about 500 meters in the fractured crystalline bedrock in Olkiluoto at Eurajoki implemented by Posiva Oy. The spent uranium fuel placed in the final disposal tunnels in copper iron canisters will be surrounded with bentonite clay, which is assumed to be a potential source of colloids due to bentonite erosion. Colloids may affect the migration of radionuclides and the colloid-facilitated transport may be significant to the long-term performance of a spent nuclear fuel repository. The potential relevance of colloids for radionuclide transport is highly dependent on the release and stability of colloids in different chemical environments and their interaction with radionuclides. [1] As the bentonite barriers are a critical part of SNF disposal concept, investigation of the processes that control bentonite erosion, clay colloid generation and stability under different chemical conditions is essential to ensure safety. The objective of this work was to determine the bentonite erosion and stability of colloids generated from bentonite clay, which mainly consists of montmorillonite.

Experimental

The bentonite materials investigated in the experiments were MX-80 Volclay powdered bentonite (76 % montmorillonite) or bentonite pellets and Nanocor PGN Montmorillonite powder (98 %). In batch type experiments, 1 g of bentonite powder or two pellets were placed in a sample tube where 50 mL of solution was added. The reference groundwater used was low salinity granitic Allard ($I = 4.2 \text{ mM}$) and OLSO ($I = 0.517 \text{ M}$), which simulates the current saline groundwater at the Finnish repository site in Olkiluoto in oxic conditions. Diluted OLSO, NaCl and CaCl_2 electrolyte solutions ($I = 0.1 \text{ mM} - 0.1 \text{ M}$) were used to determine the stability of colloids as a function of ionic strength. The samples were stored for the sampling with and without agitation and the colloidal particle fraction was separated by centrifugation. The colloid generation and stability were followed as a function of time by analysing particle size distribution applying the photon correlation spectroscopy (PCS) method and Zeta potential applying the dynamic electrophoretic mobility (Malvern Zetasizer Nano ZS). Colloid concentration was estimated using a standard series made from bentonite colloids and a count rate obtained PCS measurements or by analyzing the aluminum content of montmorillonite using ICP-MS.

Results

The formation and stability of bentonite colloids in diluted OLSO reference groundwater and electrolyte solutions have been followed as a function of ionic strength in a long-term experiment. The size of the bentonite colloids increased strongly as the ionic strength of the solution was increased. In dilute solutions (0.001–0.01 M), the mean particle diameter was less than 500 nm and the colloid size distribution has been rather constant during the following time. In saline solutions, the mean particle size distribution is wide, from nanometers to thousands of nanometers. Small particle sizes indicated that reversible flocculation or irreversible coagulation had taken place. In the presence of divalent calcium

cations, the bentonite colloids were larger and less stable than when there were only monovalent cations present. Mean Zeta potentials of colloids generated from bentonite powder in diluted OLSO reference groundwater are presented as a function of time in Figure 1. The colloidal dispersion has remained stable in low salinity solutions so far for over four years. In a stable dispersion, all suspended particles have a large negative or positive zeta potential and they tend to repel each other. The colloidal system is least stable near the isoelectric point where zeta potential is near zero and there is no force to prevent the particles from aggregating. The cumulative particle concentration is presented in Figure 2. Noticeable colloid generation occurred only in the most diluted (1 and 5 mM) solutions and the colloid concentration reached the level where no more colloids were released.

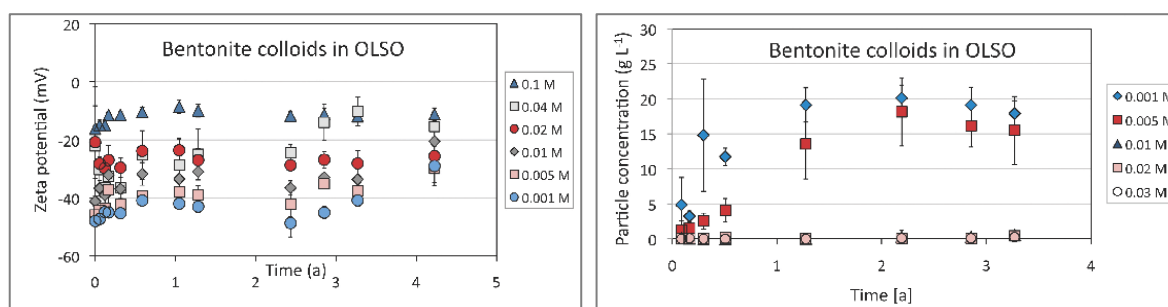


Fig. 1 (left). Mean Zeta potential of colloids generated from bentonite powder in diluted OLSO reference groundwater.

Fig. 2 (right). The cumulative particle concentration of colloids generated from bentonite powder in diluted OLSO reference groundwater.

The bentonite generation was significantly increased with the slow agitation. A thin layer between bentonite suspension and colloidal fraction was formed as a result of bentonite erosion via gel phase. The stability and therefore the concentration of bentonite colloids depended strongly on the ionic strength of the medium and the valence of the cation. Colloids were smaller and more stable in monovalent (Na^+) than in divalent (Ca^{2+}) dominated solutions. The formation of bentonite colloids from Nanocor powder in different water solutions is presented in Figure 3. The clear difference can be seen between the solutions. The liquid phase is clear in saline OLSO, while in other more diluted solutions it is muddy because of the formatted colloids. The particle concentrations measured with the photon correlation spectroscopy in different solutions are presented in Figure 4.

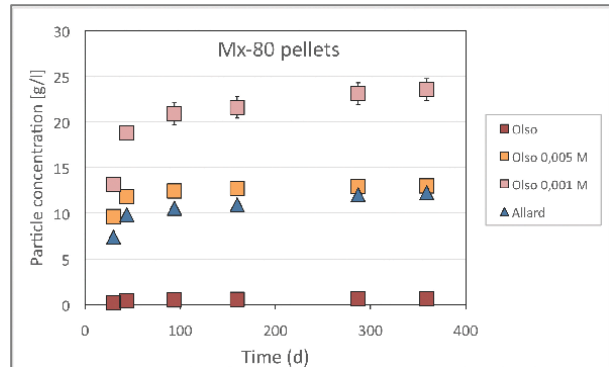


Fig. 3 (left). Formation of bentonite colloids in different water solutions. Allard, OLSO, OLSO 5 mM, OLSO 1 mM, NaCl & CaCl₂ 1 mM, respectively.

Fig. 4 (right). Mean particle concentration of formed from MX-80 bentonite pellets.

The number mean values for the colloid particle sizes in different solutions are presented in Figure 5. In low salinity solutions, high negative Zeta potential values, lower than -20 mV, indicated the existence of stable colloid dispersion. The Zeta potentials for different solutions are presented in Figure 6. In more saline solutions, Zeta potential values were near zero indicating particle aggregation and instable colloids.

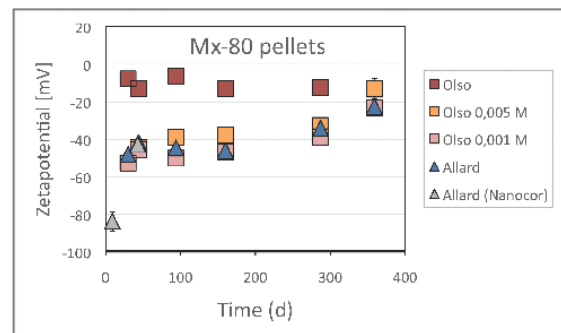
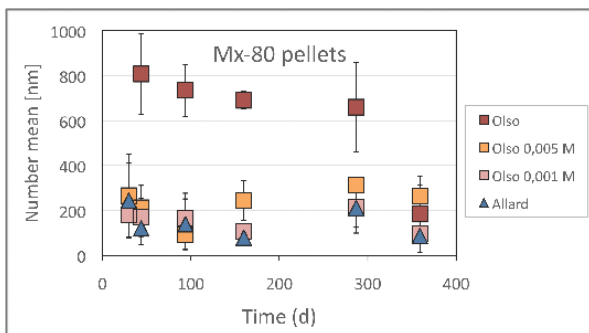


Figure 5 (left). The mean particle size of colloids formed from MX-80 bentonite pellets and Nanocor PGN powder.

Figure 6 (right). Mean Zeta potentials of colloids formed from MX-80 bentonite pellets and Nanocor PGN powder.

The effect of ionic strength can be clearly seen from Figure 7. As the ionic strength of solution increases, the Zeta potential of the bentonite colloids rises towards zero, although staying still quite far in the negative side because of the dilute solutions.

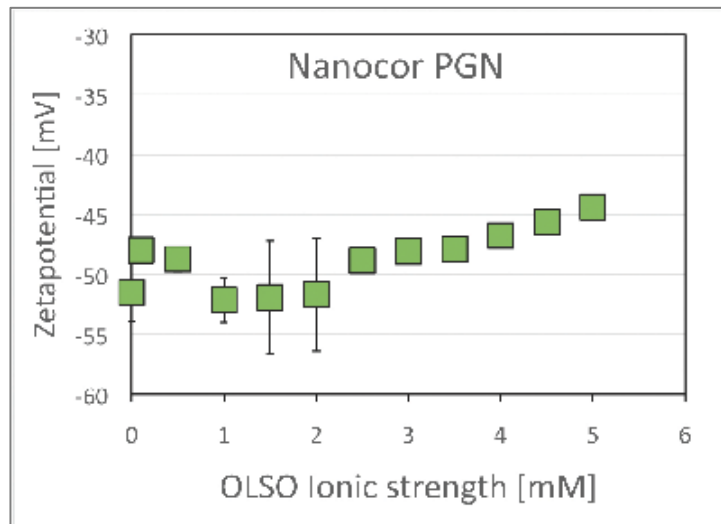


Figure 7 (right). Mean Zeta potentials of colloids formed from Nanocor powder in the different dilutions of OLSO.

Conclusion

The experiments show a clear difference between saline OLSO and the more diluted solutions. The colloids were stable in diluted solutions but not in saline OLSO. The colloids release was noticeable in the diluted solutions at the beginning of the experiments but decreased clearly after a couple of measurements. The colloid dispersion has remained stable in low salinity water solutions for over four years. The main uncertainties remain in the quantification of colloids under realistic repository conditions and how stable and mobile colloids are. However, this knowledge and understanding about bentonite erosion in colloidal form can be utilized in the estimation of performance of the bentonite barrier. At saline conditions, like at Finnish repository site in Olkiluoto, the colloids are unstable and therefore do not affect the radionuclide transport. The possible post-glacial diluting of the groundwater may still have taken into account.

[1] Schäfer T, Huber F, Seher H, Missana T, Alonso U, Kumke M, Eidner S, Claret F and Enzmann F (2012). Nanoparticles and their influence on radionuclide mobility in deep geological formations. *Appl. Geochem.*, 27(2), 390-403.

The research leading to these results has received funding from the European Atomic Energy Community's Seventh Framework Programme (FP7/2007-2011) under grant agreement n° 295487. Finnish Research Programme on Nuclear Waste Management and funding from the State Nuclear Waste Management Fund is also acknowledged.

The effect of aperture variability and accessory minerals on the erosion of MX80 form a fracture intersecting a deposition hole.

Christopher Reid, Rebecca Lunn, Grainne El Mountassir and Alessandro Tarantino.

Department of Civil and Environmental Engineering, University of Strathclyde, Glasgow.

This research was undertaken with a view to examining the mechanism through which MX80 bentonite buffer extrudes into and erodes from a rock fracture intersecting a deposition hole. Previous researchers have examined the mechanism for, and rates of bentonite erosion, using purified montmorillonite in planar fractures (Schatz et al 2013). Here, we explore the effects of using *as delivered* MX-80 bentonite i.e. including accessory minerals and a naturally variable aperture designed to mimic a rock fracture, constructed by taking a cast of a natural fracture present in a core of microgranite. The three experimental set-ups examined in order to unpick the effects of accessory minerals and aperture variability on the process were:

1. *As delivered* MX80 bentonite in a variable aperture flow cell.
2. *As delivered* MX80 bentonite in a uniform aperture flow cell.
3. Purified montmorillonite in a uniform aperture flow cell.

The same hydraulic aperture as the variable aperture cell, in the order of 100 μ m, was maintained in the uniform aperture flow cells with the aid of physical spacers. Gravimetric analysis was undertaken on the effluent and the swelling pressure of the bentonite was monitored throughout for each cell. Image analysis of the extrusion process and accessory mineral ring formation was also undertaken, as illustrated in figure 1d).

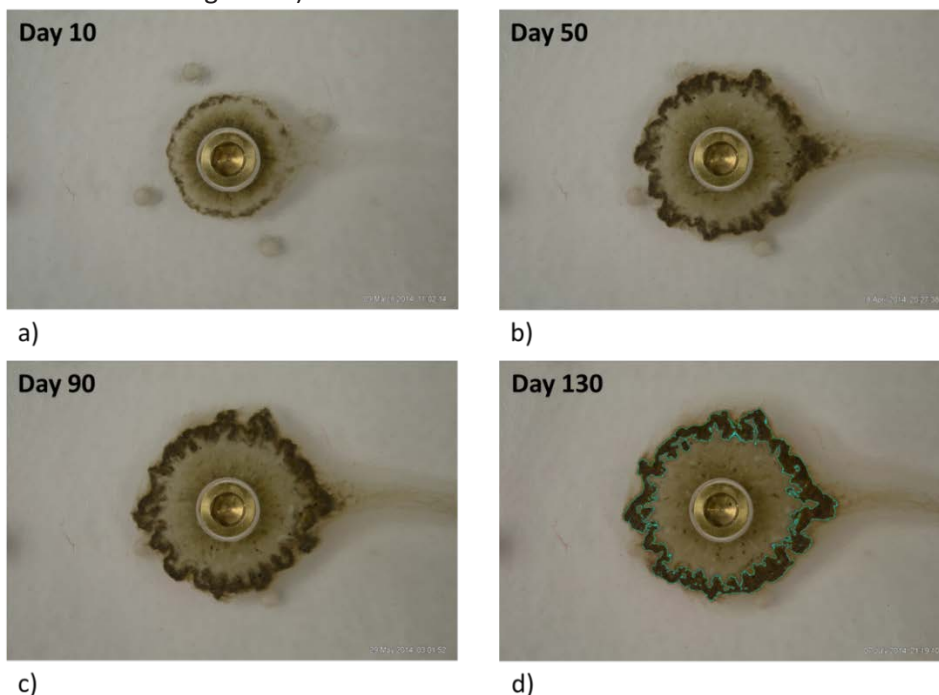


Figure 1: Evolution of MX80 extrusion over 130 erosive period with accessory mineral ring visible.

Erosion rate and image analysis data for both the variable aperture and uniform aperture cells correlated well to reveal that the accessory minerals present in MX80 do indeed provide a mitigating effect against erosion when deposited at the extruded buffer/groundwater interface. This supports a theory put forward by previous researchers that the accessory minerals, accounting for up to 25% of the buffer, may provide some mitigating effect against buffer erosion by way of filtration effects

(Richards and Neretnieks 2010). In either instance, the same thickness of accessory mineral ring (2mm) was required to be deposited in the fracture before the erosion rate started to decrease.

In both the variable and uniform aperture cell tests with MX80, subsequent to the erosion rate decreasing upon the deposition of accessory minerals; erosion rate, swelling pressure and image analysis data correlated to reveal a previously undiscovered mechanism governing the erosion process.

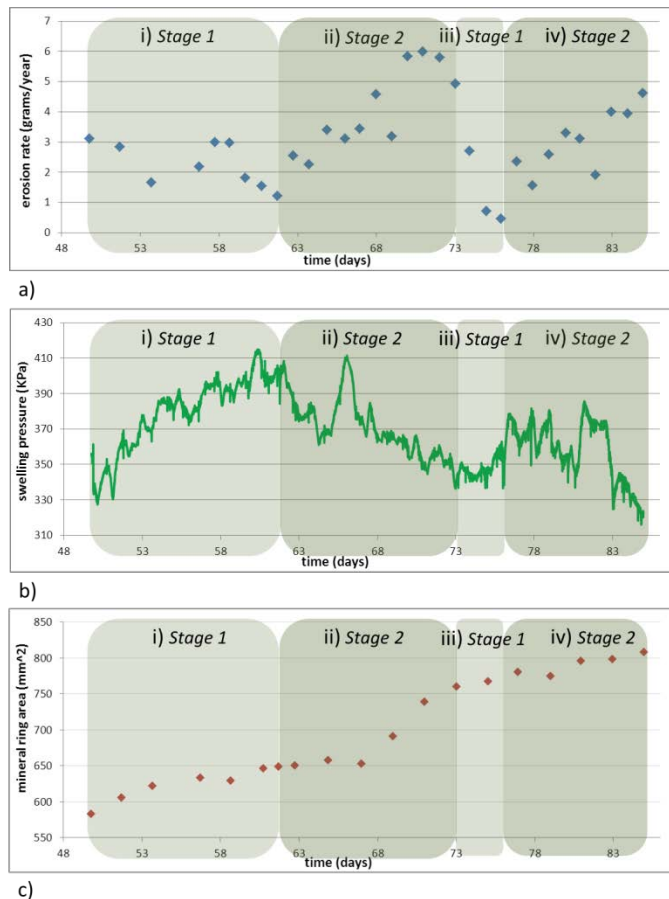
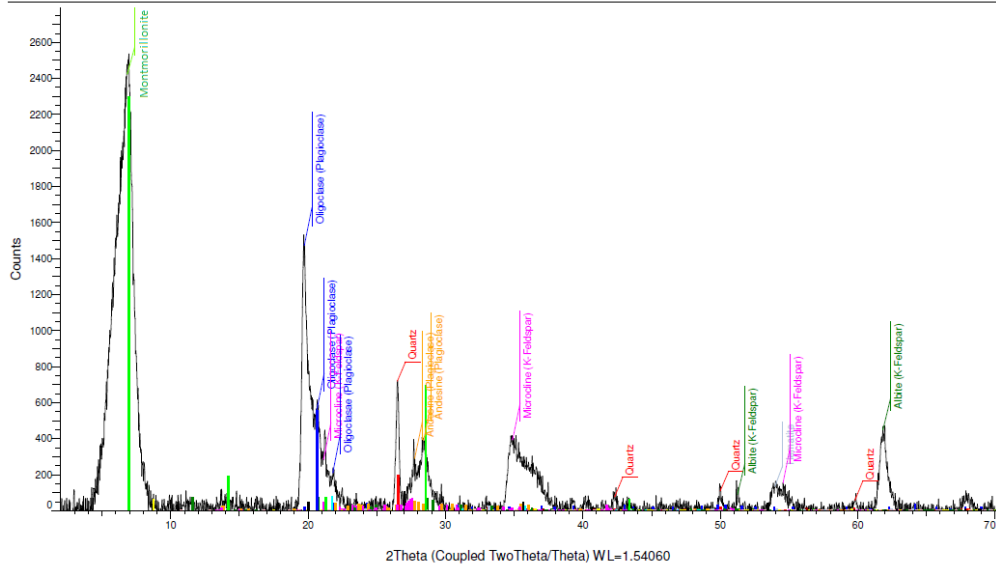


Figure 2: The 2 stage erosion cycle a) Erosion rate vs. time b) Swelling pressure vs. time c) accessory mineral ring area vs. time.

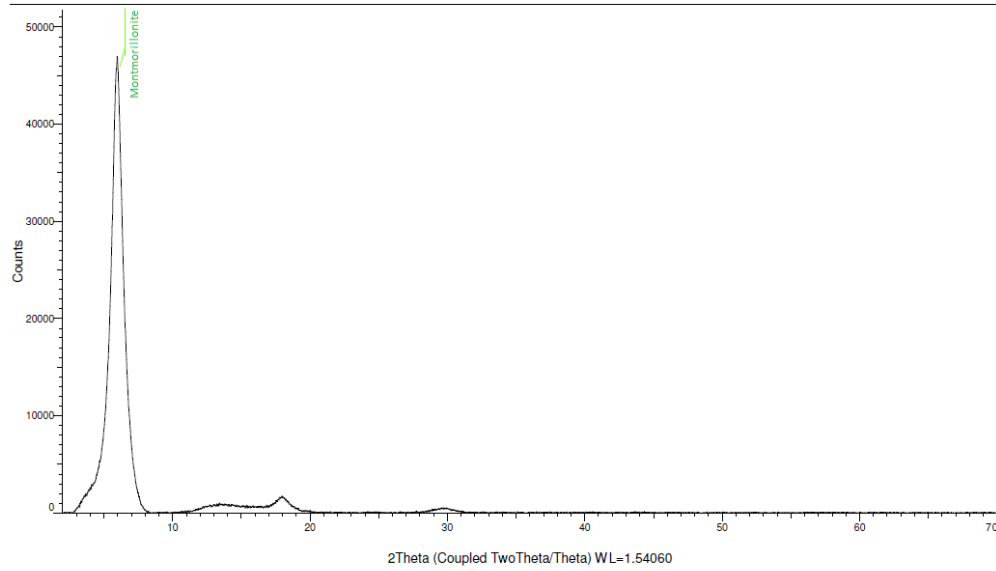
The erosion rate of buffer material exhibits a distinct cyclical nature as detailed in figure 2, governed by increases/ decreases in the swelling pressure generated by the bentonite material and the affect this has on the presence of the ring of accessory minerals at the periphery of the extruded material. During non-erosive periods (stage 1) the swelling pressure increases and the thickness of the accessory mineral ring is relatively stable. It is proposed the swelling pressure increases to the point where the accessory mineral ring is perturbed, resulting in an erosive period (stage 2). During erosive periods the swelling pressure concomitantly decreases as a consequence of mass loss and the accessory mineral ring increases in thickness, attenuating the erosion rate.

This cycle appears to repeat until such time when the accessory mineral ring is sufficiently robust to prevent further periods of erosion. This behaviour isn't as apparent for MX80 in the uniform aperture cell due to the fact there is no capacity for force chain development within the accessory mineral ring against the smooth, uniform aperture wall. In line with previous work on purified montmorillonite in uniform aperture cells, no fluctuations in erosion rate / swelling pressure was observed in this test.

a) MX-80 full sample holder



b) Filter paper MX80 variable aperture



c) Accessory minerals Sample

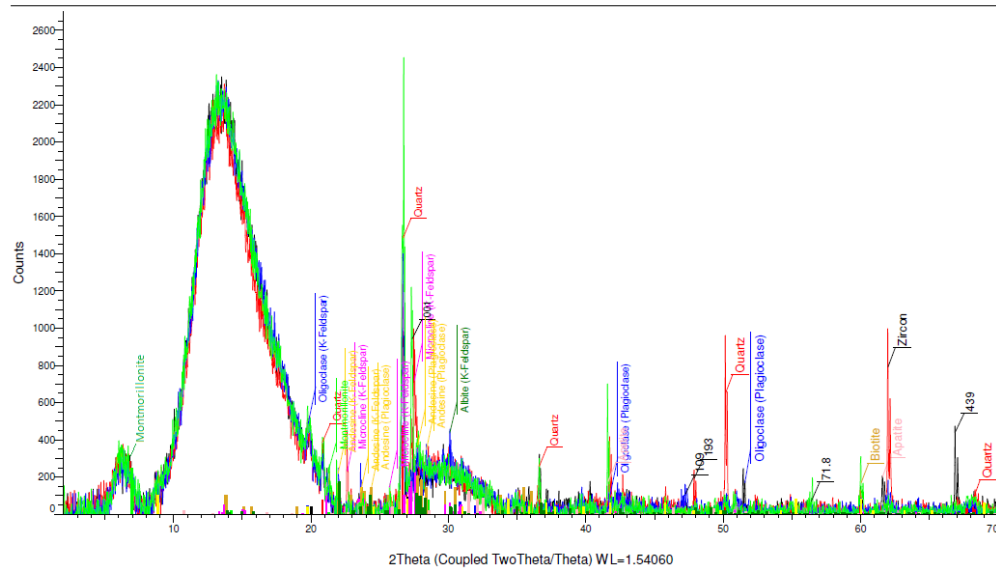


Figure 3: XRD spectra for a) *As delivered* MX80 b) Eroded material from cell c) Mineral ring sample

Post-mortem mineralogical analysis was also undertaken on the accessory mineral ring and the eroded material from test 1, MX80 in the variable aperture flow cell. In order to determine which phases were eroding and which were mitigating against erosion. As is apparent from figure 3b), only montmorillonite appeared to be eroding from the system, whereas the sample taken from the accessory mineral ring, figure 3c), appears to be dominated by the crystalline phases quartz, plagioclase and K-feldspar.

An attempt was also made at scaling the work in this thesis to the larger extents of extrusion which might be expected in a repository scenario. In terms of the mass of montmorillonite which would have to be eroded to deposit a sufficiently thick bed of accessory minerals, 2mm thick, to mitigate against erosion and the time frame this might occur over in a repository scenario. These estimations were based on the mass loss rates and extrusion distances for two repository scenarios included in SKB's 2012 safety case application, previously modelled by Neretnieks et al (2009), as detailed in table 1.

Water velocity, [m/yr]	Smectite release for 1 mm fracture aperture, [g/yr]	Penetration into the fracture at the centre, [m]
0.10	11	34.6
315.00	292	0.5

Table 1: Loss of smectite by advective flow. Neretnieks et al (2009).

Assuming the bentonite material modelled in table 1 included the same proportion of accessory minerals as the MX80 used in this experimental work, calculations were performed based on the thickness of accessory mineral bed deposited per gram of montmorillonite eroded per mm² of interfacial surface area between the extruded material and flowing groundwater. The results of which are detailed in table 2.

	Scenario 1	Scenario 2
<i>Fracture aperture</i>	1mm	1mm
<i>Water velocity</i>	0.1 m/year	315 m/year
<i>Mass loss rate</i>	11 grams/year	292 grams/year
<i>Extrusion dist.</i>	34.6 m	0.5 m
<i>Time taken for 2mm thick mineral barrier formation</i>	153841 days (422 years)	225 days
<i>Mass of montmo. Eroded to form 2mm thick mineral barrier</i>	4622 grams (4.622 kg)	180 grams

Table 2: Approximations for scaling experimental results to hypothetical repository scenarios

EVALUATION OF ACTINIDE(IV)-SILICA COLLOIDS MOBILITY UNDER REPOSITORY CONDITIONS - THE NUWAMA PROJECT

H. Hildebrand^{1,*}, S. Weiss¹, H. Zaenker¹, J. Kulenkampff¹, J. Lippmann-Pipke¹, K. Kolomáček², R. Červinka²

¹Helmholtz-Zentrum Dresden - Rossendorf, Institute of Resource Ecology, Bautzner Landstrasse 400, 01328 Dresden, Germany, *h.hildebrand@hzdr.de

²ÚJV Řež, a. s., Fuel Cycle Chemistry and Waste Management Division, Fuel Cycle Chemistry Department, Hlavní 130, Řež, 250 68 Husinec, Czech Republic

Colloidal transport in the near-field and far-field of repositories is considered as one potential pathway for migration of (radio-)toxic components in case of groundwater intrusion into a geologic nuclear waste repository. Recently, the *in-situ* formation of actinide(IV)-silica colloids ($d_p < 20$ nm) was discovered under typical conditions for nuclear waste repositories in granitic formations (Dreissig et al. (2011), Hennig et al. (2013), Husar et al. (2015)). These colloids show long-term stability over years and could therefore play a significant role in radionuclide migration since silica is an ubiquitous compound. So far, there is only limited knowledge about the reactive transport of actinide(IV)-silica colloids under repository conditions. Considering granite as one potential host rock for repository construction, mobility of these colloids in case of groundwater intrusion can't be ruled out. Within the recently started NuWaMa project, a new close collaboration between the Helmholtz-Zentrum Dresden - Rossendorf and the ÚJV Řež will be established. Joint research focused also on this problem will be intensified.

First transport experiments using packed columns with crushed granite and distilled water amended with Th(IV)-silica colloids gave hints of mobility of the colloids under certain conditions. These experiments are conducted using conventional analytics such as ICP/MS and light scattering techniques for detection of the colloids in the column effluent. In the course of the NuWaMa project, systematic studies of the mobility and stability of actinide(IV)-silica colloids will be conducted, leading to a knowledge base for prediction of significance of these colloids in a repository environment.

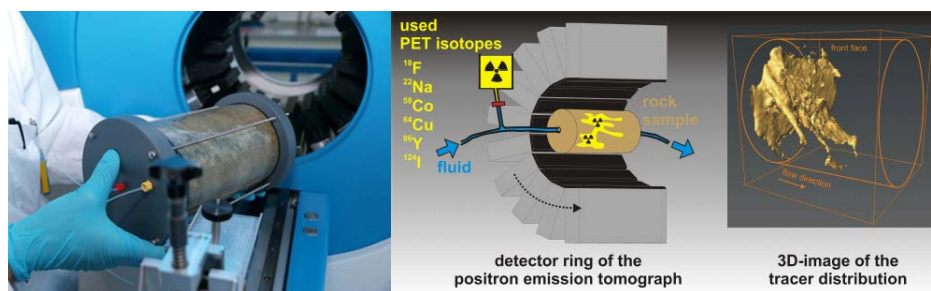


Figure 1: HZDR GeoPET scanner (left), conceptual design of flow trough experiment (centre) and exemplary result of a 3D fracture flow field obtained from GeoPET (right)

The aim of the project is also to evaluate the mechanisms of transport in more detail, including also by positron emission tomography (PET) with its unrivaled sensitivity and robustness for non-destructive quantitative spatio-temporal measurements. HZDR empowered GeoPET for its applicability in opaque/geological media (e.g. Kulenkampff et al. (2008), Kulenkampff et al. (2015), Wolf (2011), Zakhnini et al. (2013), see Fig. 1). Zirconium radionuclides (positron-emitter and analogues for tetravalent actinides) shall be used for

visualization of colloidal transport on column scale and, if applicable, also in a fractured rock sample. Using this technique, particle-mediated transport of actinides in geomaterials can be investigated in great detail and furthermore, the generated datasets can be further evaluated using reactive transport modeling.

Literature

- Dreissig, I., Weiss, S., Hennig, C., Bernhard, G., Zänker, H., 2011. Formation of uranium(IV)-silica colloids at near-neutral pH. *Geochim. Cosmochim. Acta* 75, 352–367.
- Hennig, C., Weiss, S., Banerjee, D., Brendler, E., Honkimäki, V., Cuello, G., Ikeda-Ohno, A., Scheinost, A.C., Zänker, H., 2013. Solid-state properties and colloidal stability of thorium(IV)-silica nanoparticles. *Geochim. Cosmochim. Acta* 103, 197–212.
- Husar, R.; Weis, S.; Hennig, C.; Hübner, R.; Ikeda-Ohno, A.; Zänker, H., 2015. Formation of Neptunium(IV)-Silica Colloids at Near-Neutral and Slightly Alkaline pH. *Environ. Sci. Technol.* 49, 665-671.
- Kulenkampff, J.; Gruendig, M.; Zakhnini, A.; Gerasch, R.; Lippmann-Pipke, J., 2015. Process tomography of diffusion with PET for evaluating anisotropy and heterogeneity. *Clay Minerals*, in press.
- Kulenkampff, J.; Gründig, M.; Richter, M.; Enzmann, F., 2008. Evaluation of positron emission tomography for visualisation of migration processes in geomaterials. *Physics and Chemistry of the Earth* 33, 937-942.
- Wolf, M., 2011. Visualisierung und Quantifizierung der Fluidodynamik in Bohrkernen aus dem Salinar und Deckgebirge des Raumes Staßfurt mittels Positronen-Emissions-Tomographie, dissertation, <http://nbn-resolving.de/urn:nbn:de:bsz:15-qucosa-77160>
- Zakhnini, A.; Kulenkampff, J.; Sauerzapf, S.; Pietrzyk, U., 2013. Monte Carlo simulations of GeoPET experiments: 3D images of tracer distributions (^{18}F , ^{124}I and ^{58}Co) in Opalinus clay, anhydrite and quartz. *Computers & Geosciences* 57, 183-196

Differences in crystalline swelling properties of three montmorillonites in liquid water - influence of temperature, interlayer cation and layer charge

Daniel Svensson, SKB, daniel.svensson@skb.se

This study has focused on the swelling properties of three montmorillonites with divalent interlayer cations with free access to water (Wyoming, Milos and Kutch). The swelling was studied using synchrotron XRD and SAXS. The purpose was to investigate the effects from temperature, type of interlayer cation, salt concentration and type of montmorillonite on the basal spacing. Some interesting observations were made that indirectly seem to link to important properties such as swelling pressure and osmotic swelling (chemical erosion)

SMECTITE FREE SWELLING AND EROSION IN ARTIFICIAL FRACTURES

Emelie Ekvy Hansen, Ulf Nilsson, Magnus Hedström (mh@claytech.se)

Clay Technology AB, IDEON Science Park, SE-223 70 Lund, Sweden

In this work swelling and erosion of Wyoming-type (Wy) montmorillonite extracted from MX-80 bentonite (American Colloid Co.) have been studied using artificial fractures from poly(methyl methacrylate). The montmorillonite was purified and ion-exchanged with either NaCl or CaCl₂ to homo-ionic form. Most experiments in this study have been conducted using Wy-Na. There are two major reasons for working with Wy-Na: First, Na-montmorillonite show essentially unlimited swelling below the critical coagulation concentration (CCC), i.e. it turns into a sol, which is the reason for studying the erosion process under dilute conditions in the first place. Second, Wy-Na has the highest CCC (~20 mM NaCl) of all the clays investigated within the BELBaR project. Thus erosion rates obtained using Wy-Na are pessimistic estimates, compared to the conceivable future conditions in a high-level waste repository. While Wy-Ca is not sol-forming, mixed Ca/Na-montmorillonite has been found to form sol and erode in deionized (DI) water when the Na⁺ content was >20% of the cation exchange capacity (CEC). Therefore in the present study Wy-Ca/Na montmorillonite prepared from mixing equal amount of powdered Wy-Ca and Wy-Na montmorillonite is included.

In the set of experiments reported here, two apertures, 120 μm and 240 μm have been used. The amount of eroded material was determined through turbidity measurements on the effluent. For horizontal fractures the erosion rates at salinities below the CCC were found to increase with increasing flow rates.

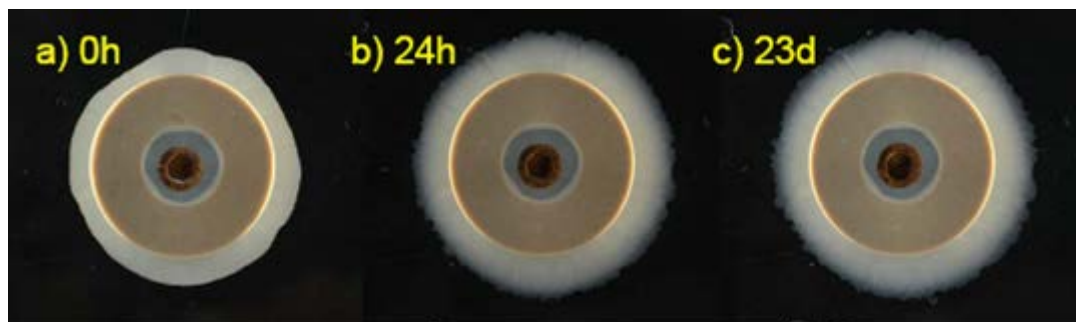


Figure 1 Top view of a 1 cm thick Na-montmorillonite disc that swells into a 120 μm fracture. The diameter of the disc (darker grey) is 35 mm. a) Initial condition. The initial extrusion of clay gel is mechanical and happened when the fracture top was mounted and thus not caused by swelling. The fracture is filled with 25 mM NaCl solution adjusted to pH >9. b) After 24h swelling. Swelling is completed and a gel is formed at the outer rim of the clay that prevents further expansion. For 10 days the solution was left stagnant. Then we let the solution flow through the fracture at various velocities. During the flowing phase the NaCl concentration in the external solution was gradually lowered. c) After 23 days. NaCl concentration has been 15 mM for the past 24 hours.

Above 20 mM NaCl erosion was not detectable, consistent with the formation of a sufficiently strong gel at the clay/water interface. Figure 1 shows the limited swelling of Na-

montmorillonite in an artificial fracture when the initial NaCl concentration is 25 mM which is above the critical coagulation concentration ~ 20 mM. The system show strong hysteresis as the ionic strength of the solution was been gradually lowered erosion did not commence until the concentration reached 5 mM.

The effect of hysteresis was further tested in experiments where first the ionic strength was increased up to the CCC and subsequently decreased. The erosion rates were substantially lower during the path of decreasing ionic strength as shown in Figure 2.

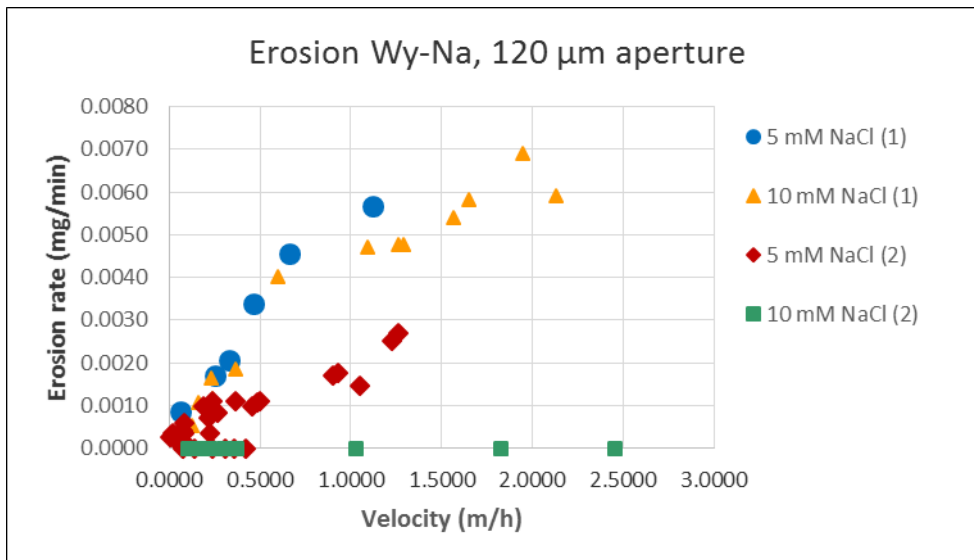


Figure 2 Erosion rates vs. flow velocity for the case where first the NaCl concentration in the flowing solution was increasing (1). After reaching 20 mM NaCl the concentration in the flowing solution was decreased (2).

Gel formation stop the swelling into the fracture, while swelling into stagnant DI water is substantial and lead to a paste/sol transition at the outer region of the clay phase. The erodible phase was found to contain up to 45 g clay/l. However the average concentrations measured in the effluent are considerably lower as most fluid passing through the artificial fracture is never in contact with the clay. Figure 3 shows the montmorillonite concentration in the effluent as a function of flow velocity for Wy-Ca/Na at NaCl concentrations from 1 to 4 mM. The clay concentration decreases with increasing velocity. This suggests that the paste-to-sol transition rate limits the erosion rate. At the higher flow velocities the concentration drops as the transfer of clay from paste to sol cannot keep up with the increased flow. The concentration dependence on velocity is reasonably well captured by a power law as showed for the 1 mM data in Figure 3. At the lowest velocity (corresponding to 850 m/yr) for the 1 mM test the unit erosion rate was evaluated to 65 kg/(m²·year). It is important to realize that this is a pessimistic rate because it is obtained at a velocity that is at least one order of magnitude higher than realistic flow velocities in a repository. Possibly this implies that horizontal fractures will not pose any problem regarding erosion.

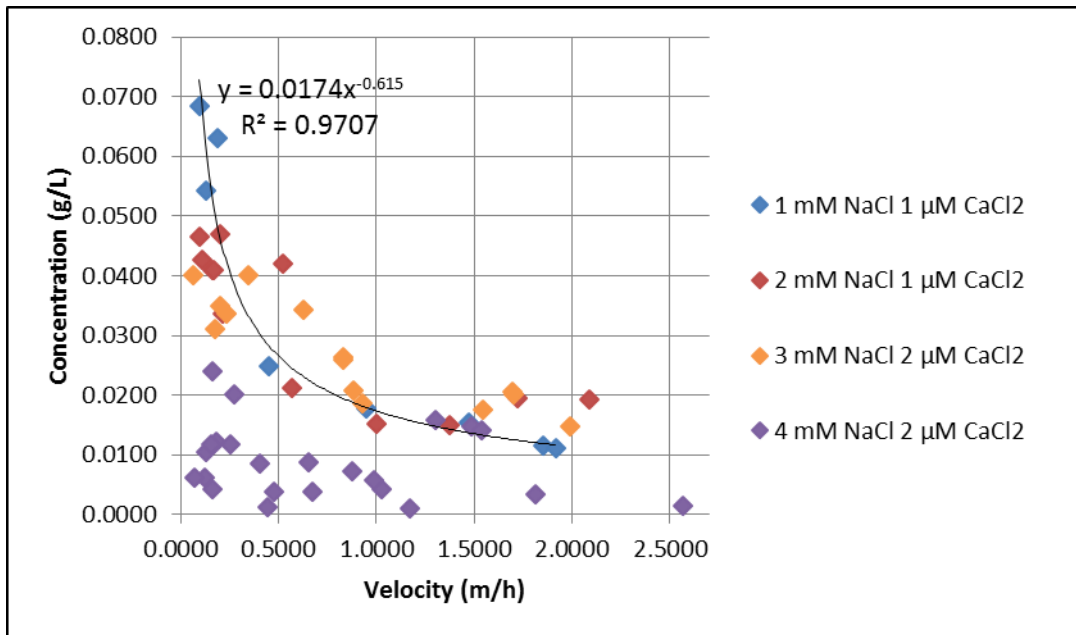


Figure 3 Clay concentration in effluent as a function of flow velocity.

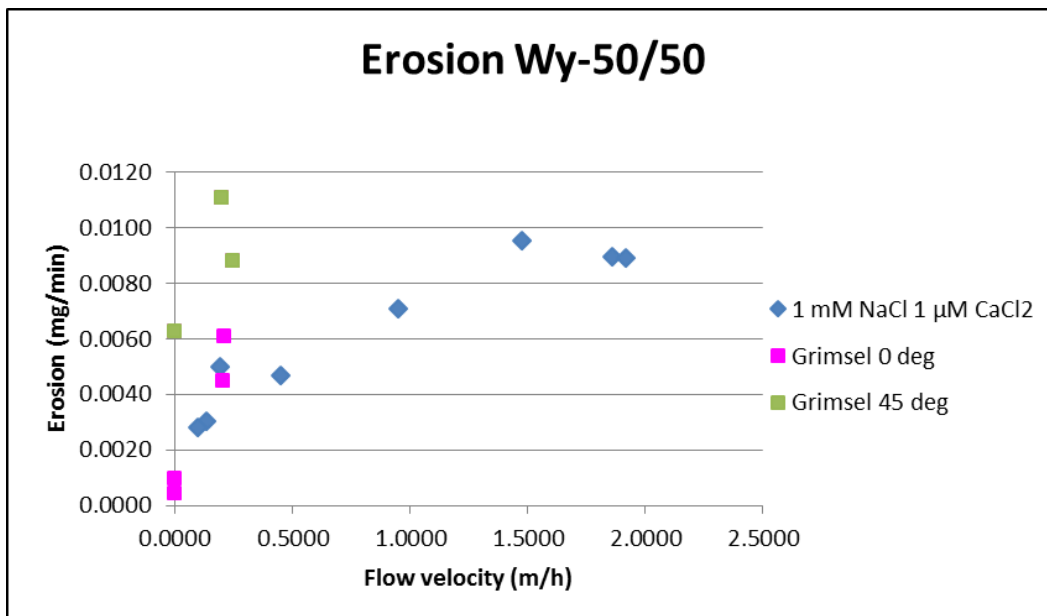


Figure 4 Erosion of Wy-Ca/Na in an artificial fracture with aperture 120 μm. Grimsel water has ionic strength of 1.12 mM which is comparable to 1 mM NaCl.

Erosion in sloped fractures was substantially higher and material was eroded even under stagnant water conditions, demonstrating the influence of gravity on the sol, which is a heavier liquid than water (Figure 4). As long as the sol is removed from the paste-sol interface, erosion was found to progress under glacial water conditions. The erosion rate obtained using Wy-50/50 montmorillonite was found to be approximately 170 kg/(m²·year) in the case of stagnant conditions but 45 degree slope angle. If one assumes a clay paste with diameter of 2 m (approximately the dimensions in a repository) and a fracture aperture of 1

mm, the erosion from a sloped fracture (slope angle 45 degrees) amounts to approximately 1 kg/yr under glacial water conditions. An aperture of 50 μm is probably more realistic for a repository. Then the buffer clay loss would be 20 times less, which over a 10 000 year period of glacial meltwater conditions would amount to 500 kg.

Acknowledgements

The research leading to these results has received funding from the European Atomic Energy Community's Seventh Framework Programme (FP7/2007-2011) under Grant Agreement no295487, the BELBaR project, and from the Swedish Nuclear Fuel and Waste Management Company (SKB).

References

Hedström, M., Ekvý Hansen, E. Nilsson, U., 2015. Montmorillonite phase behaviour. Relevance for buffer erosion in dilute groundwater. Technical report TR-15-07, SKB.

Build-up of Accessory Mineral Layers during Erosion of Buffer Material

Tim Schatz

B+Tech Oy, Laulukuja 4, 00420 Helsinki, Finland (tim.schatz@btech.fi)

It has been postulated that, following erosive loss of colloidal montmorillonite through contact with dilute groundwater at a transmissive fracture interface, accessory phases within bentonite, such as quartz, feldspar, etc., might remain behind and form a layer eventually resulting in the formation of a filter bed or cake [Neretnieks et al. 2009, Richards & Neretnieks 2010]. As more and more montmorillonite is lost, the thickness of the accessory mineral bed increases and the continued transport of montmorillonite from the emplaced source slows and possibly stops if the porosity of the filter bed is sufficiently compressed. Alternatively or concurrently, as the accessory mineral filter bed retains montmorillonite colloids, a filter cake composed of montmorillonite itself may be formed. Ultimately, depending on their extent, properties, and durability, such processes may provide the bentonite buffer system with an inherent, self-filtration mechanism which serves to limit the effects of colloidal erosion.

In order to examine whether the erosion of bentonite material through contact with dilute groundwater at a transmissive fracture interface could intrinsically result in 1) the formation of an accessory mineral filter bed and cake and/or 2) filter caking of montmorillonite itself, a series of laboratory tests were performed in a flow-through, horizontal, 1 mm aperture, artificial fracture system. Bentonite buffer material was simulated by using mixtures (75/25 weight percent ratio) of purified sodium montmorillonite and various additives serving as accessory mineral proxies (kaolin, quartz sand, chromatographic silica). The resulting mixtures were compacted into dense sample tablets with effective montmorillonite dry densities of $\sim 1.6 \text{ g/cm}^3$. Additionally, a test was performed using MX-80 bentonite washed free of soluble material and thoroughly exchanged with sodium cations providing a system in which the natural, insoluble accessory minerals remained in the sample. The fracture erosion tests were performed using a Grimsel groundwater simulant (relative to Na^+ and Ca^{2+} concentration only) contact solution at an average flow rate of 0.09 ml/min through the system.

According to Richards [2010] and Kiviranta and Kumpulainen [2011], the particle size distribution of the accessory minerals in MX-80 bentonite consists of particles with sizes less than 200 μm . Of the additive materials used in this study, the kaolin material consists of particles with sizes less than 20 μm showing a peak size of 6 μm , the chromatographic silica consists of particles with sizes narrowly distributed between 10 to 14 μm , and the sand consists of particles with sizes between 160 to 550 μm at a peak size of 280 μm .

The tests were designed to lead to the development of erosive conditions (i.e., sodium montmorillonite against a dilute solution) and, in every case, a build-up of accessory mineral layers near the extrusion/erosion interface was observed (see Figure 1). Moreover, these layers grew progressively in thickness over the course of the tests.

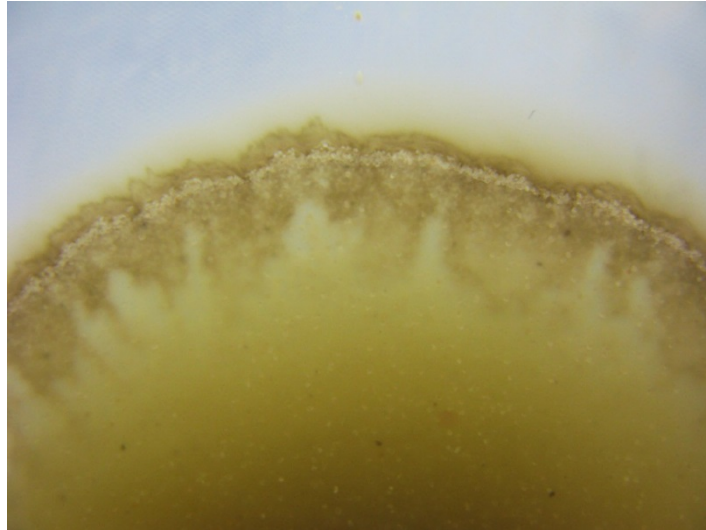


Figure 1. *Overhead photographic image of artificial fracture erosion test with a sample comprised of sand and sodium montmorillonite; sand layer formation at the extrusion/erosion interface is clearly visible.*

In order to examine whether the erosion of a more natural bentonite material would result in the observation of similar behaviour, a laboratory test was performed in a flow-through, horizontal, 1 mm aperture, artificial fracture system using MX-80 bentonite washed free of soluble material and thoroughly exchanged with sodium cations (to ensure the development of erosive conditions). In this case the natural, insoluble accessory minerals remained in the sample material. After stopping the test, samples were collected at various extrusion distances. XRD analyses were performed on the samples followed by full pattern fitting to determine mineralogical compositions. The results are presented in Figure 2.

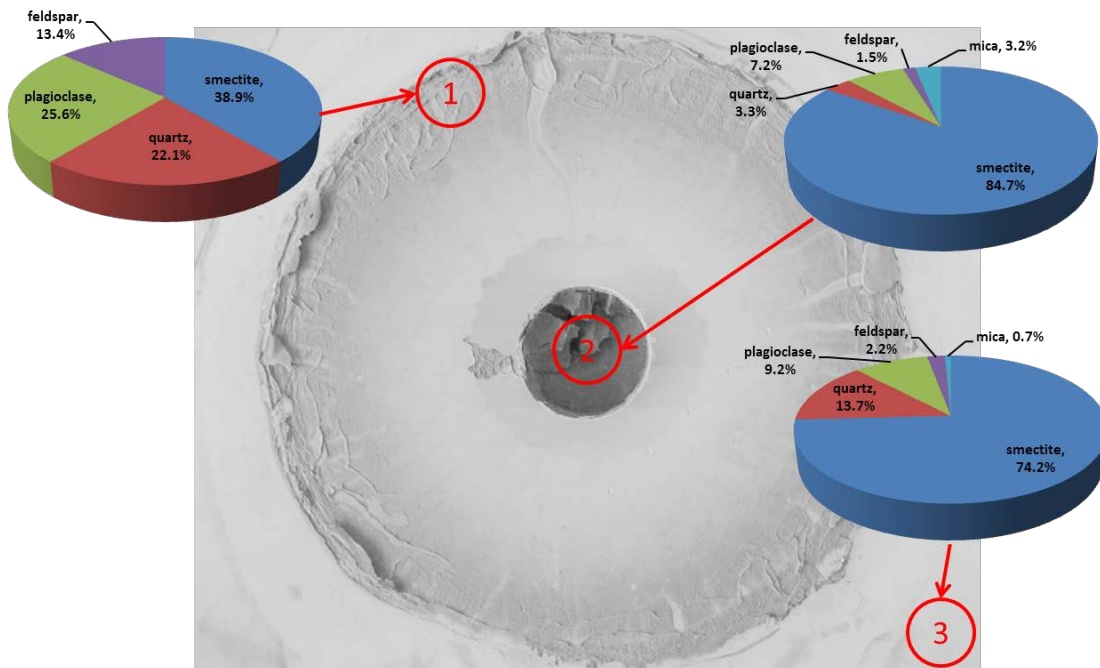


Figure 2. *Photographic image of flow-through test in artificial fracture with conditioned MX-80 after drying overlaid with mineralogical composition results from samples at the indicated positions.*

As indicated in Figure 2, the sample material at the erosion interface (1) contains a much larger fraction of accessory phases than the residual sample material (2). This result is consistent with the earlier results showing that added accessory phases remain behind and form layers near the solid/liquid interface during erosive loss of montmorillonite. The mineralogical composition of the residual sample material is essentially identical to that of the starting material. The eroding material (3) is predominantly smectite as well indicating that the clay mineral is the primary eroding phase. The presence of accessory mineral phases in sample 3 does not necessarily indicate that the interfacial accessory mineral layer was unstable to erosion during the test as partial release of these materials may have occurred as a result of tilting during post-mortem fracture transfer.

Overall these results provide evidence that, following erosive loss of colloidal montmorillonite through contact with dilute groundwater at a transmissive fracture interface, accessory phases (within bentonite) remain behind and form into layers.

References

Kiviranta, L. & Kumpulainen, S. 2011. Quality Control and Characterization of Bentonite Materials. Posiva Working Report 2011-84. Posiva Oy. Olkiluoto, Finland.

Neretnieks, I., Liu, L. & Moreno, L. 2009. Mechanisms and Models for Bentonite Erosion. SKB Technical Report TR-09-35, Swedish Nuclear Fuel and Waste Management Co., Stockholm, Sweden.

Richards, T. 2010. Particle Clogging in Porous Media, Filtration of a Smectite Solution. SKB Technical Report TR-10-22, Swedish Nuclear Fuel and Waste Management Co., Stockholm, Sweden.

Richards, T. & Neretnieks, I. 2010. Filtering of Clay Colloids in Bentonite Detritus Material. *Chemical Engineering Technology*, 33, 1303-1310.

NEPTUNIUM(V) SORPTION ONTO MONTMORILLONITE AND BENTONITE COLLOIDS AND THE INFLUENCE OF COLLOIDS ON Np(V) TRANSPORT

O. Elo (outi.elo@helsinki.fi), P. Hölttä, University of Helsinki, Department of Chemistry, Laboratory of Radiochemistry and N. Huittinen, Helmholtz-Zentrum Dresden-Rossendorf

INTRODUCTION

In Finland, the spent nuclear fuel (SNF) repository is going to be at the depth of 500 m in the crystalline bedrock in Olkiluoto at Eurajoki the site implemented by Posiva Oy. The bentonite buffer in the Engineered Barrier System (EBS) consists mainly of montmorillonite which, like other aluminosilicates is known to retain radionuclides, thus, contributing to the retention or immobilization of them. Long-lived Np-237 (2.144×10^6 a) in the pentavalent oxidation state forms a neptunyl cation NpO^{2+} , which is rather soluble, poorly sorbed and readily mobile making it highly relevant for research concerning SNF repository safety. The potential relevance of colloids for radionuclide transport is highly dependent on the formation of stable and mobile colloids in different environmental conditions and the interaction of radionuclides with the formed colloids. The aim of this work was to investigate the sorption of neptunium on montmorillonite and bentonite colloids and the influence of bentonite colloids on neptunium transport by means of batch sorption and column experiments.

EXPERIMENTAL

The materials used in this work were montmorillonite purified from MX-80 bentonite by B⁺Tech, a colloid dispersion made from MX-80 bentonite powder and crushed granitic rock. In the previous study, the interaction of neptunium with Na-montmorillonite purified from MX-80 bentonite and corundum ($\alpha\text{-Al}_2\text{O}_3$) was investigated [1]. We conducted batch sorption experiments as a function of pH (4 – 11) and neptunium concentration 1×10^{-9} to 5×10^{-6} M. Solid concentrations of 0.5 g/l and 5 g/l were used for montmorillonite, 40 g/l for crushed granite and 3.3 – 4.0 g/l for bentonite colloids. The batch sorption experiments for montmorillonite and colloids were conducted under N_2 atmosphere to exclude carbon dioxide from our samples. However, the batch sorption experiments for crushed granitic rock were conducted in ambient oxygen conditions to simulate the column experiments. The samples were made by adding Np-237 tracer, a background electrolyte (10 mM NaClO_4) and a small aliquot of concentrate montmorillonite, colloid stock solution or in the case of crushed granite rock, by weighing the desired amount of solid to 20 ml polyethylene vials. The solution was buffered to the desired pH and after one week equilibration time the solid was separated from the liquid by centrifugation and 1 mL aliquots were taken immediately for liquid scintillation counting (Perkin Elmer Tri-Carb 3100 TR liquid scintillation counter).

The effect of bentonite colloids on neptunium transport in crushed granitic rock and drill core columns [2] was studied without and with the presence of colloids. Background electrolyte (NaClO_4) was pumped through the column at different flow rates using a peristaltic pump to control the water flow rate. A tracer pulse was injected into the water flowing system using an injection loop and the out flowing tracer was collected using a fraction collector. The hydraulic properties in the columns were determined using a conservative tracer without colloids.

RESULTS

The flow conditions for each flow rate was investigated by using a non-sorbing tracer (Cl-36). Constant flow conditions in the columns were achieved with a peristaltic pump. The tracer was injected into the system through an injector of known volume and the out flowing solution from the column was collected in 20 ml polypropylene vials with a fraction collector. Experiments were conducted in drill core and crushed granite columns with different flow rates (Fig 1) where the influence of the different columns can be observed as the tracer elutes through the drill core column (closed symbols) faster than from the crushed granite column (open symbols). The longer retention time for the crushed granite column could be explained by the various flow routes, whereas for the drill core column few flow routes exist, thus, allowing the tracer elute faster through the column.

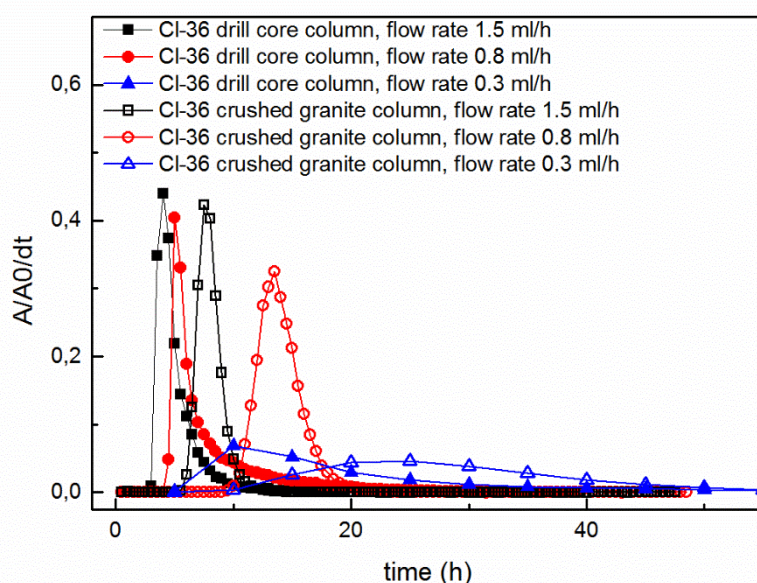


Figure 1. The break through curves of Cl-36 in drill core column (solid symbols) and crushed granite column (open symbols) with flow rates of 1.5 ml/h, 0.8 ml/h and 0.3 ml/h.

The sorption of Np-237 on montmorillonite, bentonite and crushed granite was investigated by batch sorption experiment as a function of pH (Fig 2). The neptunium(V) uptake for montmorillonite and bentonite colloids (Fig 2, left) increases at $\text{pH} > 7$ but the overall sorption percentage remains rather low over the entire investigated pH range. For both montmorillonite and bentonite colloids a constant neptunium(V) uptake of around 10 % is seen in the circumneutral to acidic pH range. However, the particle size for the bentonite colloids used in the batch sorption studies may vary significantly, which could explain the observed low Np-237 sorption capacity of bentonite colloids. For crushed granite (Fig 2, right) at pH 5 to 7 a constant sorption of around 20 % can be observed, as pH increases the sorption percentage increases slightly, however, not significantly. At the relevant pH where the column experiments were conducted only a 20 % sorption is achieved, indicating that only minority of the injected Np-237 will influence with the granite through the sorption process.

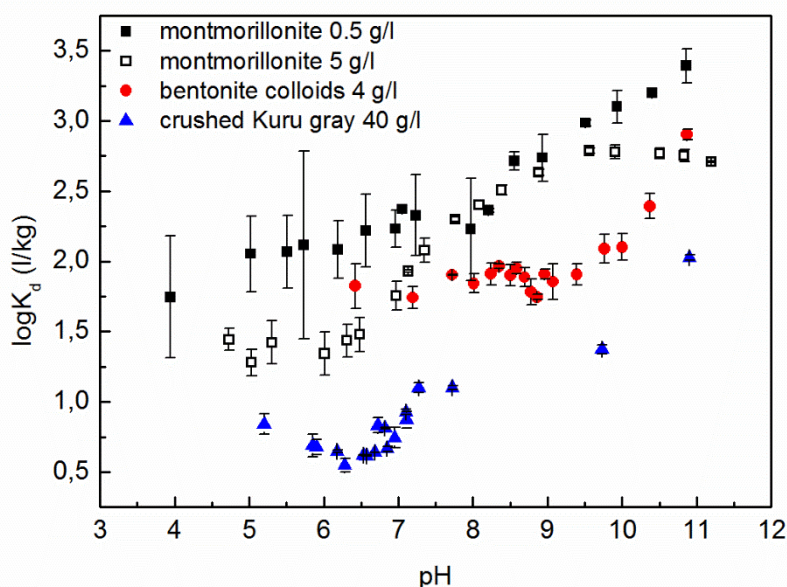


Figure 2. Np-237 sorption on montmorillonite (0.5 and 5 g/l) and bentonite colloids (4.0 g/l) (left) and on crushed Kuru Gray granite (right, particle size < 0.1 mm) as a function of pH ($c(\text{Np}) = 10^{-6}$ M) in 10 mM NaClO_4 with equilibration time of 7 days .

The effect of MX-80 bentonite colloids on Np-237 migration in the drill core and crushed granite columns was studied in the presence and absence of bentonite colloids with different flow rates (Fig 3). At first glance it seems that Np-237 elutes through the drill core column only in the presence of bentonite colloids (Fig 3, gray squares), however, in the second Np-237 column experiment with a different flow rate (Fig 3, open black squares) all of the injected Np-237 eluted through. This implies that no Np-237 was present in the column experiment with the flow rate of 1.5 ml/h and in the absence of colloids (Fig 3, open gray squares). The slight effect of matrix diffusion for Np-237 can be observed in the crushed granite column experiments with the lower flow rates (Fig 3, open dots), whereas at the presence of bentonite colloids (Fig 3, closed blue dots) matrix diffusion cannot be observed. The colloid recovery was determined from the Np-237 migration experiments, where colloid solution was pumped continuously into the water flow. Colloid concentration was determined using a derived count rate obtained PCS measurements and standard series. The recovery of colloids in the crushed granite column was 20 % and the drill core column 30 – 40 %.

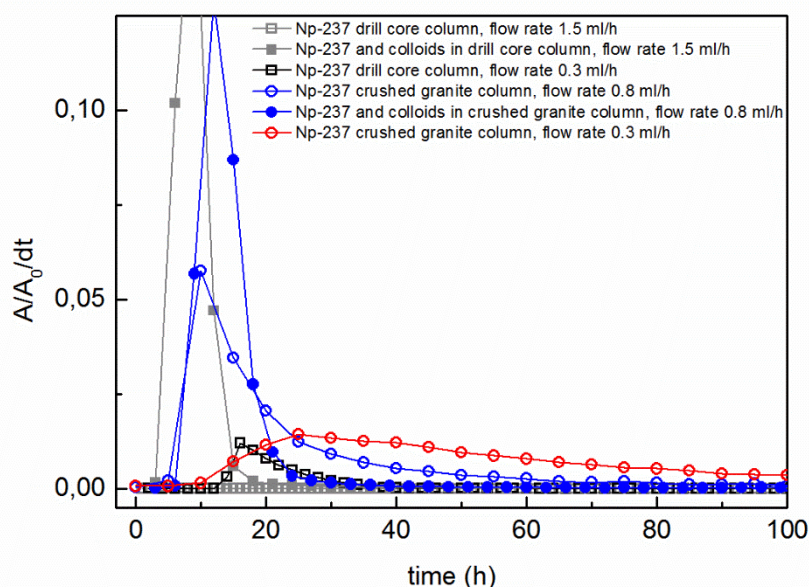


Figure 3. Measured breakthrough curves of Np-237 through drill core column (squares) and crushed granite column (dots) with flow rates of 1.5 ml/h (gray symbols), 0.8 ml/h (blue symbols) and 0.3 ml/h (open red and black symbols) in 10 mM NaClO₄. Open symbols in the absence of colloids and solid symbols in the presence of colloids.

CONCLUSIONS

The obtained results indicate that the bentonite colloids enhance the migration of Np-237. However, more information i.e. batch sorption experiments and column experiments at slower flow rates and in the presence of bentonite colloids are needed to verify these findings. In environmentally relevant conditions for SNF repository, at pH 8, montmorillonite and bentonite colloids have low and almost similar adsorption capacities for neptunium. The pH and ionic strength can have a great influence on the speciation of actinides, thus batch sorption results are an important source of data for further studies using specific methods. The results from batch sorption and column experiments will be presented and the importance of bentonite colloids on the migration of neptunium will be discussed. This research has received funding from the European Atomic Energy community's Seventh Framework Programme (FP7/2007-2011) under grant agreement n° 295487.

[1] O. Elo, K. Müller, A. Ikeda-Ohno, F. Bok, A.C. Scheinost, P. Hölttä and N. Huittinen. "Batch sorption and spectroscopic speciation studies of neptunium uptake by montmorillonite and corundum." Manuscript.

[2] P. Hölttä, A. Poteri, M. Siitari-Kauppi and N. Huittinen (2008). Phys. Chem. Earth 33, 983 – 990.

Poster:

INTERCALATION AND RETENTION OF CARBON DIOXIDE IN A SMECTITE CLAY PROMOTED BY INTERLAYER CATIONS

Jon Otto Fossum (jon.fossum@ntnu.no)

**Department of Physics
Norwegian University of Science and Technology - NTNU
Trondheim
Norway**

We have reported experiments which show that gaseous CO₂ intercalates into the interlayer nano-space of a smectite clay at conditions close to ambient causing crystalline swelling. The rate of intercalation, as well as the retention ability of CO₂ was found to be strongly dependent on the type of the interlayer cation, which in the present case was Li⁺, Na⁺ or Ni²⁺. We observed that the smectite Li-fluorohectorite is able to retain CO₂ up to a temperature of 35°C at ambient pressure, and that the captured CO₂ could be released by heating above this temperature. Our estimates indicate that smectite clays, even with the standard cations analyzed here, can capture an amount of CO₂ comparable to other materials studied in this context.

References:

X-ray Studies of Carbon Dioxide Intercalation in Na-Fluorohectorite Clay at Near-Ambient Conditions, Henrik Hemmen, Erlend G. Rolseth, Davi M. Fonseca, Elisabeth L. Hansen, Jon Otto Fossum and Tomás S. Plivelic, *Langmuir* 28, 1678-1682 (2012)

Intercalation and Retention of Carbon Dioxide in a Smectite Clay promoted by Interlayer Cations, L. Michels, J. O. Fossum, Z. Rozynek, H. Hemmen, K. Rustenberg, P. A. Sobas, G. N. Kalantzopoulos, K. D. Knudsen, M. Janek, T. S. Plivelic & G. J. da Silva, *Scientific Reports by Nature* 5, 8775 (2015) doi:10.1038/srep08775

INFLUENCE OF PHYSICO-CHEMICAL, CRYSTALLOCHEMICAL AND COMPOSITIONAL PROPERTIES OF CLAY MINERALS ON EROSION PROCESSES

Ana María Fernández (anamaria.fernandez@ciemat.es), Ursula Alonso, Tiziana Missana
(CIEMAT, Avda. Complutense 40, 28040 Madrid, Spain)

1 Introduction

An understanding of the main mechanisms of colloid and gel layer formation from compacted bentonite during bentonite erosion is one of the main objectives of the BELBAR Project. The erosion mechanisms and colloid generation process are influenced by the physico-chemical, crystallochemical and compositional properties of the clay minerals, which are analysed in this work. The settling and flocculation processes of the clay particles depends on a lot of factors, such as the size and shape of the particles, surface properties, ionic strength of the incoming water, etc. For example, smectite particles in gels and suspensions are strongly influenced by: a) decreases in dry densities of the compacted bentonite due to swelling or changes in the chemical stability of smectite (montmorillonite/bentonite volume fraction or concentration), b) pore water/groundwater chemistry: ionic strength (I), pH, chemical composition, which govern the edge charge; c) changes in cation composition at the interlayer sites (in particular the Ca/Na content), and d) crystallochemistry of the clay minerals.

In the context of nuclear waste disposal, bentonites are used as an engineering barrier for avoiding the dispersion of radioactive elements to the biosphere. This is because they are composed of smectite clay minerals comprising outstanding physical and chemical properties: swelling capacity, low permeability and large sorption capacity. Different tests about the formation and stability of colloids from compacted bentonite have shown that degree of erosion is related to the quantity of smectite in the system and, therefore, the presence of other minerals and/or different clay minerals seems to affect the erosion of bentonite (Missana et al., 2015; Alonso et al., 2015). Indeed, bentonite is defined as a naturally occurring material that is composed predominantly of the swelling clay mineral montmorillonite (>75%). However, it contains more than one type of minerals (main and accessory minerals), and other type of clay minerals can be present. Furthermore, chemical and structural heterogeneity is typical for smectites. Therefore, a study of the properties and compositional characteristics of different bentonites and clay minerals has been performed in order to identify which ones play a major role on the colloid generation process and, hence, in the bentonite erosion behavior.

Around 40 years ago few commercial high quality bentonites were acquired for the study of bentonites as buffer and backfill materials in the construction of engineering barrier systems (EBS) for the isolation of high-level radioactive waste. The natural selected bentonites are industrially processed to fabricate highly compacted bentonite blocks, which have been used in different *in situ* large-scale EBS experiments (e.g., FEBEX-*in situ*, LOT, Prototype, TBT, etc.) and Mock-Up tests. Nowadays, new reference designs for the EBS consists on compacted blocks and pellets for filling the gap between the bentonite compacted blocks and the host-rock (e.g., EB-Experiment and FE experiments at Mont Terri). A lot of tests have been performed for analyzing the properties, manufacturing, handling and long-term performance of the buffer. However, safety analyses of nuclear waste repositories deemed necessary to clarify if the bentonite backfill barrier can be eroded, under what conditions and to what extent.

2 Materials

In this work, different raw bentonites and clay materials were analysed (Fig. 1), which have different structural characteristics: 2:1 (TOT) or 1:1 (TO) layer type, Di- or Tri-octahedral sites, TOT layers with low or high layer charge, charge location at tetrahedral or octahedral sites,

dioctahedral clay minerals with cis- or trans-vacant positions. These clay minerals can be grouped as: a) Ca-Mg smectites (RO2K6-F02, FEBEX, Ibeco, S-Az2) or Na-smectites (MX-80, Nanocor, MSU, Sabil S65, B75), b) bentonites made up of low layer charge smectites: beidellite SBdI-1, Ypresian Clays from Belgium (YD40, YK38); c) bentonites made up of high layer charge smectites; d) other type of clay minerals: saponite (MCA-C, B64), nontronite (NAu-1), illite (illite du Pui, IdP-2), kaolinite (KGa-1b); and e) granular bentonite material (Pellets) used at Mont Terri Research Laboratory: GBM non activated Na-smectite (FE-Experiment) and GBM non activated Ca-Mg smectite (EB-Experiment).

3 Mineralogical Analysis

The mineralogical study of the samples was performed by DRX, SEM, TEM, FTIR, TG-DSC. The results are shown in Table 1, Figure 1, and Figure 2, where the compositional and crystallochemical features of the main clay minerals are distinguished.

Table 1. Mineralogical content of the bentonites and clay minerals and clay minerals analysed

	T. Phyllos.	Qz	Crist.	Fd-K	Plag	Calcite	Magnetite	Ankerite
Illite IdP-2	93	-	--	7	--	--	--	--
Kaolinite KGa-1b	99	1	--	--	--	--	--	--
Saponite B64	96	3	--	1	--	Tz	--	--
Saponite MCA-C	85	4	--	3	7	1	--	--
Beidellite SBdI-1	84	16	--	--	--	--	--	--
Nontronite NAu-1	95	1	--	--	--	--	4	--
Ca-Mont SAz2	98	1	--	1	--	--	--	--
FE GBM-Na Sm	92	2	2	1	2	1	--	Tz
EB GBM-Ca Sm	89	2	1	3	3	2	--	--

4 Geochemical composition

The geochemical analysis of the samples were determined by FRX, SEM and combustion. The results are shown in Table 2 and Table 3.

Table 2. Crystallochemical properties of the bentonites and clay minerals

Bentonite	Structural Formulae	$\tau\%$	$\sigma\%$	Interlayer Charge	Di-, Tri- octahedral Sm / Cis-, Trans-vacant
FEBEX	$(\text{Si}_{3.95}\text{Al}_{0.05})(\text{Al}_{1.37}\text{Fe}^{3+}_{0.21}\text{Ti}_{0.01}\text{Mg}_{0.49})\text{O}_{10}(\text{OH})_2$ (Ca _{0.09} Na _{0.10} K _{0.07})	15	85	0.66	Di-oct, cis-vacant
MX-80	$(\text{Si}_{4.00})(\text{Al}_{1.51}\text{Fe}^{3+}_{0.22}\text{Ti}_{0.01}\text{Mg}_{0.24})\text{O}_{10}(\text{OH})_2$ (Ca _{0.07} Na _{0.15} K _{0.01})	0	100	0.58	Di-oct, cis-vacant
Ibeco	$(\text{Si}_{3.90}\text{Al}_{0.10})(\text{Al}_{1.34}\text{Fe}^{3+}_{0.26}\text{Ti}_{0.05}\text{Mg}_{0.41})\text{O}_{10}(\text{OH})_2$ (Ca _{0.10} Na _{0.06} K _{0.05})	33	66	0.60	Di-oct, cis-vacant
Illite du Pui	$(\text{Si}_{3.52}\text{Al}_{0.48})(\text{Al}_{1.17}\text{Fe}^{3+}_{0.49}\text{Mg}_{0.33})\text{O}_{10}(\text{OH})_2$ (Ca _{0.04} Na _{0.12} K _{0.64})	57	43	0.84	--
Kaolinite	$(\text{Si}_{1.94}\text{Al}_{0.05})(\text{Al}_{2.01}\text{Fe}^{3+}_{0.001}\text{Fe}^{2+}_{0.003})\text{O}_{10}(\text{OH})_2$ (Mg _{0.03} K _{0.001})	--	--	0	--
Beidellite	$(\text{Si}_{3.57}\text{Al}_{0.43})(\text{Al}_{1.81}\text{Fe}^{3+}_{0.11}\text{Mg}_{0.09})\text{O}_{10}(\text{OH})_2$ (Ca _{0.185} K _{0.104})	90	10	0.47	Di-oct, Trans-v
Nontronite	$\text{Si}_{3.49}\text{Al}_{0.51}(\text{Al}_{0.15}\text{Fe}^{3+}_{1.84}\text{Mg}_{0.02})\text{O}_{10}(\text{OH})_2(\text{Na}_{0.53})$	99.0	1.0	0.53	Tri-oct
MCA-C	$(\text{Si}_{3.74}\text{Al}_{0.26})(\text{Al}_{0.26}\text{Fe}^{3+}_{0.14}\text{Mg}_{2.31})\text{O}_{20}(\text{OH})_4$ (Ca _{0.16} K _{0.65})	62	38	0.39	Tri-oct
GBM-Ca	$(\text{Si}_{3.96}\text{Al}_{0.04})(\text{Al}_{1.44}\text{Mg}_{0.38}\text{Fe}^{3+}_{0.14}\text{Fe}^{2+}_{0.05})\text{O}_{10}(\text{OH})_2$ Ca _{0.16} Na _{0.07} K _{0.04}	9	91	0.44	Di-oct Sm/ Cis-vacant

The total carbon, total inorganic carbon and sulphur content are shown in Table 3. According to XRF analyses, the Czech bentonites (S65, B75 and R02) contains a high amount of Fe-oxi-(hydroxi-)des, with respect to the other ones. Furthermore, nontronite contains magnetite. This minerals can act as colloidal particles also.

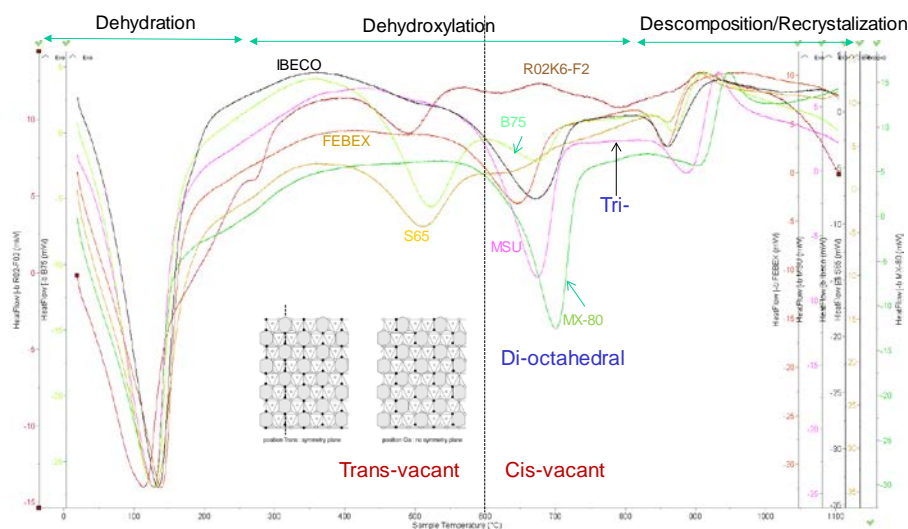


Figure 1. TG-DSC curves from some bentonite samples used in colloidal and stability studies

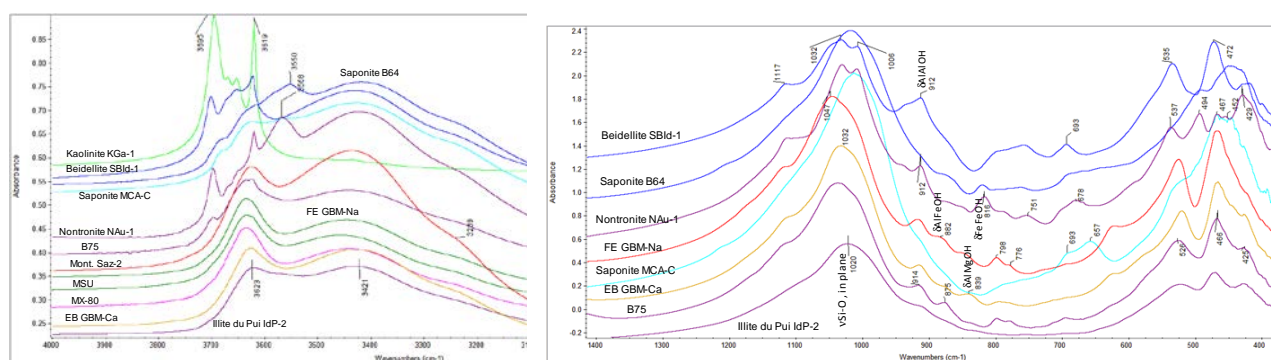


Figure 2. FTIR spectra from the bentonites and clay minerals used in colloidal and stability studies

5 Physico-chemical characteristics

Ionic exchange characteristics

One of the most important parameters for characterising the bentonite adsorption behaviour is the cation exchange capacity (CEC). This parameter is equivalent to the total negative surface charge of a clay mineral and reflects its degree of reactivity of the bentonite (absorption, swelling). The nature of interlayer cations are also an important due the cation composition affects not only the exchange properties but also the plasticity, the swelling capacity and the rheological behaviour.

The CEC (Table 3) was determined by using a complex of Cu(II) and exchangeable cations by using 0.5 M CsNO₃ buffered at pH 8.2. As expected, the lower CEC values are shown for kaolinite and illite clay minerals, as well as for Ypresian Clays, for which phyllosilicates content in the total fraction is lower than for the rest of samples. In smectites CEC is related to the smectite content.

External and Total Surface Area

The external surface area is a crucial parameter as it provides quantitative assessment of the areas available for surface reactions. On the other hand, the total surface area is an important parameter related to the water absorption and swelling capacity of bentonites. It determines the amount of water needed for hydrating all the clay particles, and therefore, it depends on the type of exchangeable cation. The lower particle size, the higher total surface area will be. The data obtained for the different clay materials analysed is shown in Table 3.

The highest values for BET external surface area are observed for illite samples. In the case of smectites, the BET value is significantly lower for mainly sodium smectites than for calcium smectites. In kaolinites, BET values depends on particle size and crystallinity, being lower for

larger and crystalline particles. Total SA is related to the main exchangeable, being higher for Na-smectites, and to the smectite content.

Table 3. Different properties of the bentonites and clay minerals used in colloidal and stability studies

Bentonite and Clay Minerals	Surface area		Ionic Exchange					Geochemical Analysis				
	BET, ext.	Total SA	CEC	Ca	Mg	Na	K	C _t	TIC	St	Cl ⁻	SO ₄ ²⁻
	m ² /g		meq/100g					wt. %			mmol/100g	
FEDEX (Mont.)	59.2 ± 0.4	700 ± 10	98.1	34.4	34.8	27.5	2.9	0.10	0.08	<0.05	2.185	1.026
MX-80 (Mont.)	39.6 ± 0.3	481 ± 1	83.6	14.6	7.2	56.1	2.2	0.30	0.08	0.24	0.246	3.804
IBECO (Mont.)	70.8 ± 0.3	611 ± 2	90.2	32.6	30.4	26.9	2.7	1.20	0.85	0.53	0.607	1.465
Sabenil 65 (Mont.)		526 ± 1	72.9	0.2	13.0	65.9	3.3	1.10	0.65	0.06	0.388	0.086
B75 (Mont.)	77.2 ± 0.6	396 ± 1	60.0	2.0	21.7	36.5	4.3	1.50	0.70	<0.05	0.322	0.112
RO2K6-F02 (M.)		573 ± 5	73.8	63.4	18.2	0.3	2.8	0.40	0.04	<0.05	0.309	0.088
Khakassiya (Mont.)		442 ± 1	68.2	0.5	2.0	76.5	2.2	1.00	0.48	0.07	1.107	< d.l
Nanacor (Mont.)	23.0 ± 0.1		86.9									
Zn-Mont.			59.3									
Illite IdP-2	135 ± 1		21.6					<0.10	<0.2	<0.10		
Illite du Pui, Na	101		24.4	--	--	24.4	--					
Kaolinite KGa-1b	38.9 ± 1.3		4.0					<0.10	<0.2	<0.10		
Saponite B64			58.6					0.28	<0.2	<0.10		
Saponite MCA-C	136	769	59.7	34.72	22.94	3.1	1.24	0.15	<0.2	<0.10		
Beidellite SBId1	33.7 ± 0.5		52.8					<0.10	<0.2	<0.10		
Nontronite N Au-1	57.8 ± 0.2		85.8					<0.10	<0.2	<0.10		
S-Az2 (Ca-Mont.)	97.4 ± 0.6		107					<0.10	<0.2	<0.10		
FE GBM-Na Sm	29.1 ± 0.1		75.9					0.38	<0.2	0.24		
EB GBM-Ca Sm	67.8 ± 0.4	526 ± 2	80.1	36.13	38.91	19.55	3.82	0.39	<0.5	0.08	1.2257	0.4801
YC-K38 (Sm)			42.1	8.57	4.22	17.86	6.68	1.10	0.94	0.29	1.6235	1.3079
YC-D40 (Sm)			31.1	5.47	5.28	20.06	4.28	0.35	0.15	0.51	5.0528	0.6617

6 Ion concentration and Pore water chemical composition

The electrical double layer behaviour is dependent on the ionic strength and salinity of the pore water. Therefore, the flocculation and dispersion of particules are affected by the pore chemistry. The pore water composition was determined by aqueous leaching (Table 3) and squeezing tests. In general, the higher chloride and/or sulphate content the higher salinity of the pore water. Therefore, Ypressian Clays at Doel site and FEBEX bentonite has the higher salinity. Other clays with high salinity are MSU, MX-80 and the two GBM-pellets samples. The ionic strength and water-type of the pore waters obtained by squeezing are 0.27, 0.33 and 0.19 M; and Cl-Na, SO₄-Cl-Na and Cl-Na for FEBEX, MX-80 and Ibeco bentonites, respectively.

7 Conclusions

Different properties and compositional characteristics of the clay materials analysed have a direct relationship with the mechanisms of colloid formation from compacted bentonite during bentonite erosion.

References

- Missana, T., Alonso, U., Fernández, A.M., Schatz, T., R. Červinka, J. Gondolli, ÚJV Řež, a. s. U., 2015. Final Report on the effects of the water chemistry and clay chemistry on erosion processes. Belbar Project. Deliverable 2.7., 25 pp. EC Contract Number: 295487.
- Alonso, U., Missana, T., Fernández, A.M., 2015. Comparison of erosion behaviour of different clays. This Volumen.

This work was supported by the EU FP7/2007-2011 program, under the EC-BELBAR Project N° 295487.

MEASURING FREE SWELLING OF MX-80 BENTONITE IN A NARROW CHANNEL USING X-RAY IMAGING

Tero Harjupatana (tero.t.harjupatana@jyu.fi), Joni Lämsä and Markku Kataja,
University of Jyväskylä, Department of Physics, Finland

Axial wetting and free swelling of compacted MX-80 bentonite samples in an aluminum tube of diameter 10 mm were studied using X-ray imaging. The experimental set-up is reminiscent of bentonite swelling into a fracture of rock surrounding the bentonite buffer in a planned nuclear waste depository. The experiments were carried out using a table-top X-ray tomographic scanner (SkyScan 1172) in a simple imaging mode (see Fig. 1). The method is based on comparison of X-ray images of the sample in the original unwetted state and in the wetted and deformed state. The measurement yields time evolution of the axial distribution of dry density and of water content during the wetting process. A typical duration of measurements with a sample of length 20 mm was four days. Three initial water contents (w_0) of the bentonite samples used were 12%, 17% and 24% while the initial dry density was fixed to 1.65 g/cm^3 . The salinity of the water used in wetting was 0.1 M (NaCl). In order to measure the local deformation of the bentonite due to swelling, the samples were doped with metallic particles. The local dry density at each instant of time was then obtained based on initial dry density and the measured displacement field. The local water content in the sample was found based on calibrated correlation to the X-ray attenuation constant and the dry density. The method is similar to that introduced recently for full tomographic reconstructions¹

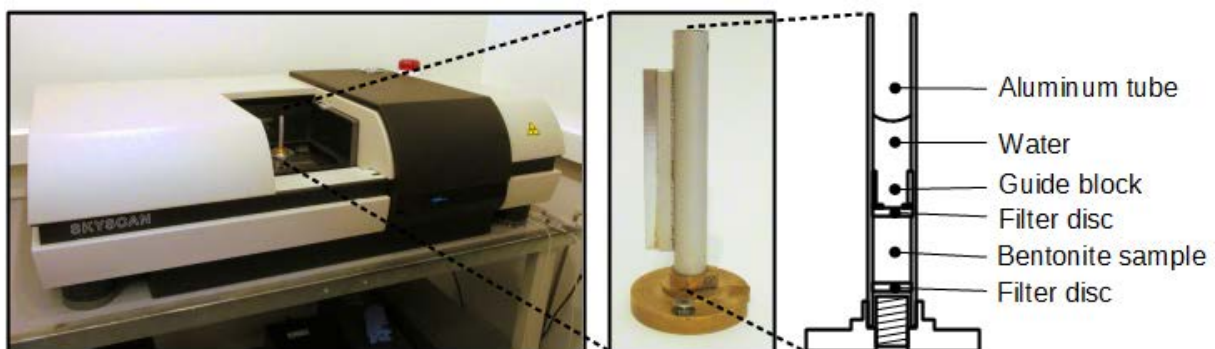


Figure 1: SkyScan 1172 X-ray Micro-CT -device and photographic image and schematic illustration of an aluminum tube used as a sample holder.

Measured and averaged displacements of iron particles are shown in Figure 2 in the initial state and at two instants of time after the beginning of wetting. Figure 3 shows the measured axial distribution of dry density and water content of bentonite during wetting at corresponding instants of time. Also shown are the original X-ray images used to obtain the measured results. The results are useful e.g. in validating models of bentonite swelling and eroding in rock fractures as well as bentonite buffer behavior in general.

¹ T. Harjupatana, J. Alaraudanjoki and M. Kataja, "X-ray tomographic method for measuring three-dimensional deformation and water content distribution in swelling clays", *Appl. Clay Sci.* 114, 386-394 (2015).

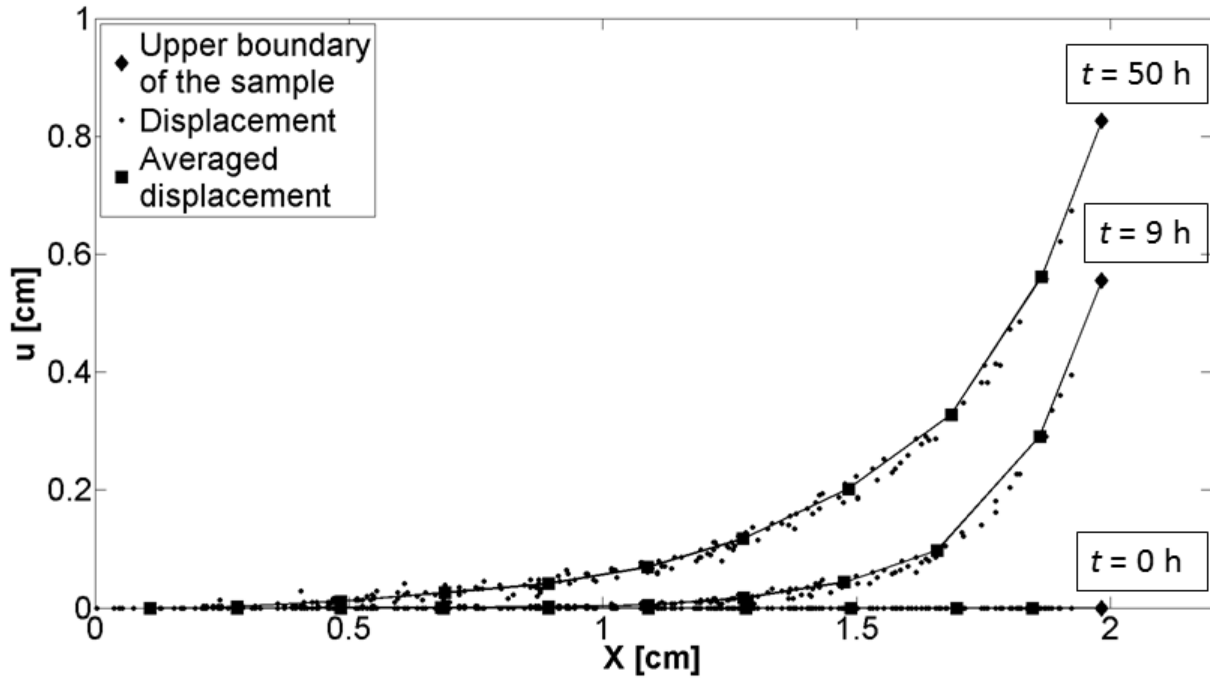


Figure 2: Measured local displacement of a bentonite sample ($w_0 = 12\%$) at three instants of time. The horizontal axis is the position of the material at $t = 0$ (undeformed state). The displacement is obtained by tracking the motion of metallic tracer particles doped in the bentonite sample.

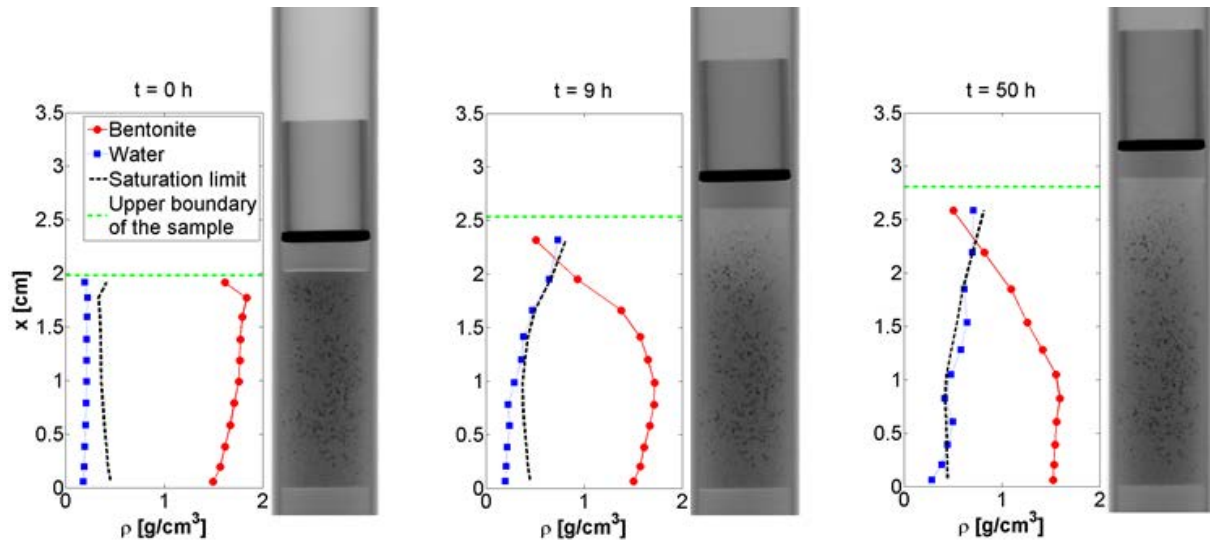


Figure 3: Measured bentonite and water content of a bentonite sample ($w_0 = 12\%$) at three instants of time. Also shown are the corresponding original X-ray images used to obtain the given data.

A NOVEL DENSITY FUNCTIONAL THEORY MODELING on CLAY COLLOIDS: INTERACTION FORCES and ION EXCHANGE

Guomin Yang (guomin@kth.se), Ivars Neretnieks, Susanna Wold

Department of Chemical Engineering and Technology and Department of Chemistry, Royal Institute of Technology (KTH), S-100 44 Stockholm, Sweden

ABSTRACT

The ionic structure of electrical double layers (EDLs)¹⁻⁴ is responsible for the electrostatic interactions between clay colloids and the ion selectivity of ion exchanger in aqueous systems, which have a great practical relevance in natural and engineered phenomena such as the coagulation of natural bentonites,⁵ the stability of colloidal dispersions,^{6,7} and cation exchange on montmorillonite clays.⁸ Theoretical studies of the interaction forces and ion exchange, therefore, play an important role in explaining these problems in surface and colloid science.⁹

To that end, a novel density functional theory (DFT) approach¹⁰ of a planar electrical double layer with the primitive model is applied to calculate the interaction forces between smectite particles (montmorillonite) and the Gaines-Thomas selectivity coefficient of the Ca/Na ion exchange equilibrium. At this point only electrical double forces are considered in this work. Other interactions, such as van der Waals forces, dispersion forces, go beyond the scope of this work.

Our modeling show that the DFT calculations are in excellent agreement with Monte Carlo simulations and experimental results from literatures.^{5,11} The results indicate that the ion size plays a significant role in force-distance relation. Due to the excluded volume effect, the osmotic pressure curve predicted by DFT is shifted towards larger separation distances with increasing the diameter of counterions. Additionally, the interaction can be switched from attraction to repulsion with increasing the diameter of counterions from standard to hydrated ionic size. The standard ionic size of 0.425 nm represents the experimental measured behavior of swelling with relevant accuracy. The quantitative characterization of the exchange of calcium for sodium at room temperature on Wyoming bentonite is investigated with the DFT approach in aqueous solutions at pH 7.0. The Gaines-Thomas convention selectivity coefficient¹² from DFT calculations is compared to Birgersson's et al. experimental results.¹¹ It is found that a significant variation of the selectivity coefficient could be observed with the interlayer separations h . For interlayer separation of 10 Å, $K_{GT} = 6.9-7.1$ M, for 14 Å $K_{GT} = 5.0-5.1$ M and for 20 Å the values are between 4.1 and 4.3 M. For the case of WyNa samples, the DFT selectivity coefficient is in excellent agreement with the ICP/AES results for dispersed clay systems where the layer separation is about 20 Å. In contrast for the cases of WyCa samples, the DFT selectivity coefficient agrees well with the ICP/AES results only when the layer separation is 10 Å. This may indicate that the interlayer distance of 10 Å in the smectite stacks better represents experimental results of free swelling for compacted Ca-bentonite in aqueous solutions. The free swelling then is between stacks and not within the layers in the stacks. Additionally, DFT predictions show that K_{GT} increases with decreasing the interlayer distance. It indicates that Ca^{2+} is preferentially taken up into the surface

exchanger for compacted clay system with smaller interlayer separation, i.e. higher compaction density.

These findings, from the newly modified DFT approach are consistent with experimental observations, which give insight into the mechanisms governing the stability and adsorption of clay colloids in aqueous solution media. The novel DFT approach that is robust enough, as a result, can be applied to model the swelling behaviour and ion exchange equilibrium of montmorillonite clay.

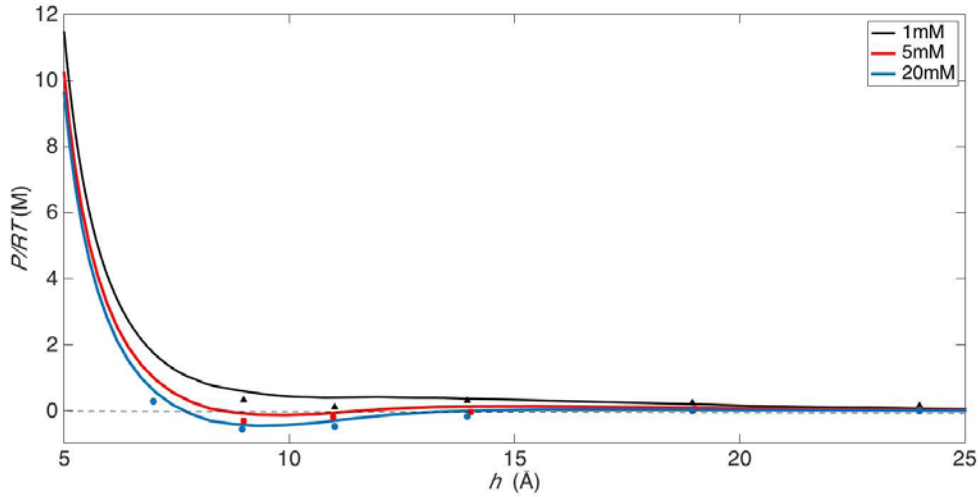


Figure 1. Net osmotic pressure as a function of separation for a mixture of bulk solutions containing NaCl and CaCl₂. The bulk concentration of NaCl electrolyte is kept constant at 100 mM, while CaCl₂ is varied as indicated in the graph. The symbols are Monte Carlo data from the literature⁵ for the surface charge density $\sigma = -0.14 \text{ C/m}^2$, the ionic diameter of 0.4 nm. The curves show the DFT calculations.

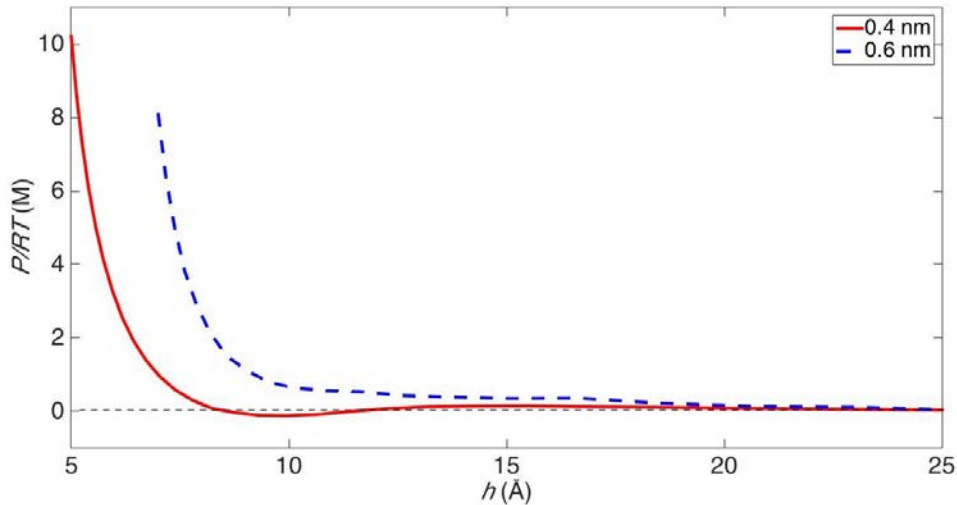


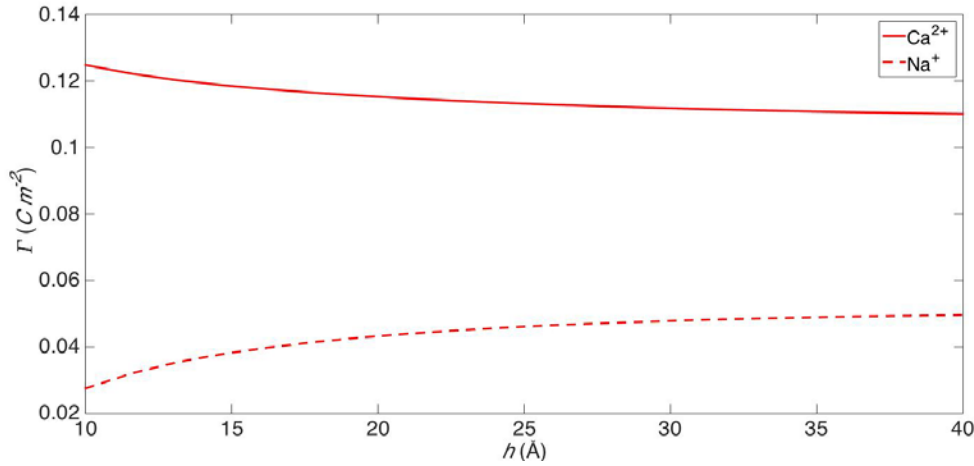
Figure 2. The DFT calculations of net osmotic pressure as a function of separation for a mixture of 100 mM NaCl and 5 mM CaCl₂ electrolytes, $\sigma = -0.14 \text{ C/m}^2$, and the

monovalent ion size is kept constant at 0.4 nm, while the divalent ion size is varied as indicated in the plot. $\epsilon_r = 78$, $T = 298$ K.

Table 1. Comparison of the selectivity coefficient from DFT calculations and experimental results from literatures¹¹ for different layer separations and compositions of the bulk solutions. $\sigma = -0.14$ C/m², $d = 0.4$ nm, $\epsilon_r = 78$, $T = 298$ K. ICP/AES indicates that ion content/concentration in both solids and solutions were determined with this method.¹¹

Samples	C _{Na} (mM)	C _{Ca} (mM)	K_{GT} (M)			K_{GT} (M)
			DFT			Experiments
			$h = 10$ Å	$h = 14$ Å	$h = 20$ Å	ICP/AES
WyNa 01	29.3	2	7.0	5.1	4.2	4.0
WyNa 02	35.8	2.1	6.9	5.0	4.1	5.5
WyNa 03	47.9	4.5	6.9	5.0	4.2	3.8
WyCa 04	28.4	3.1	7.1	5.1	4.2	6.7
WyCa 05	41.6	5.3	7.0	5.1	4.3	7.8
WyCa 06	48.2	6.9	7.0	5.0	4.3	7.0

(a)



(b)

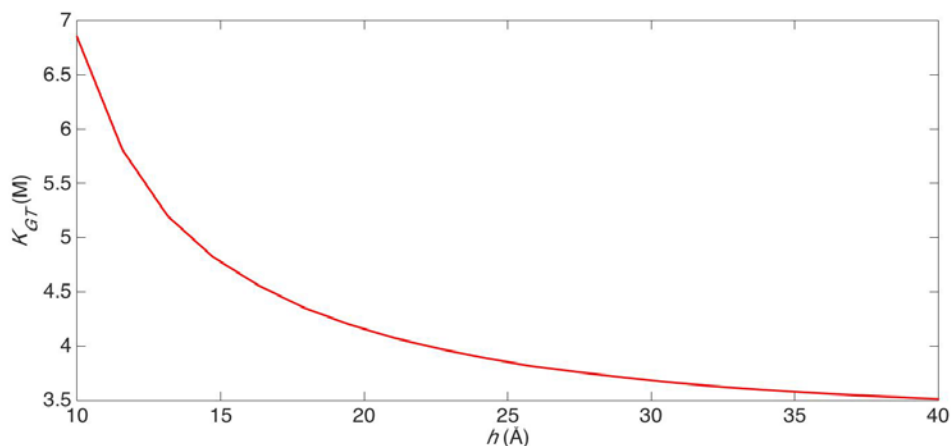


Figure 3. (a) Excess adsorption; (b) selectivity coefficient K_{GT} for WyNa 01 (see Table 1) as a function of the separations.

REFERENCE

- (1) J. O'M. Bockris and A. K. N. Reddy, *Modern Electrochemistry 1: Ionics* (Plenum Press, New York, 1998).
- (2) P. Attard, *Adv. Chem. Phys.* **92**, 1–159 (1996).
- (3) W. R. Fawcett, *Liquids, Solutions, and Interfaces* (Oxford University Press, New York, 2004).
- (4) D. Henderson and D. Boda, *Phys. Chem. Chem. Phys.* **11**, 3822 (2009).
- (5) M Segad, B Jonsson, T Åkesson, B Cabane. *Langmuir.* **26**, 5782–5790 (2010).
- (6) L. Guldbrand, B. Jönsson, H. Wennerström, and P. Linse. *J. Chem. Phys.* **80**, 2221 (1984)
- (7) Z. Tang, L. E. Scriven, HT Davis. *J. Chem. Phys.* **97**, 12 (1992).
- (8) G.Sposito, K.M. Holtzclaw, L. Charlet, C. Jouany and A.L. Page. *Soil Sci. Soc. Am. J.* **47**, 51-56 (1983).
- (9) P. Taboada-Serrano, S. Yiacoumi and C. Tsouris. *The Journal of Chmical Physics* **123**, 054703 (2005).
- (10) G. Yang and L. Liu. *J. Chem. Phys.* **142**, 194110 (2015).
- (11) M. Birgersson, L. Börgesson, M. Hedström, O. Karnland, and U. Nilsson. Bentonite erosion. SKB Technical Report TR-09-34. (Swedish Nuclear Fuel and Waste Management Company, Stockholm, Sweden, 2009).
- (12) C. A. J. Appelo and D. Postma. *Geochemistry, Groundwater and Pollution*, Second Edition. Taylor & Francis 2005. Pages 241–309.

MODELLING BENTONITE EROSION PHENOMENA BY COUPLING FINITE AND DISCRETE ELEMENT METHODS

G. Casas⁽¹⁾, J. Molinero^{(2)*}, M.A. Celigueta⁽¹⁾, E. Oñate⁽¹⁾, J. Bruno⁽²⁾

- (1) International Center for Numerical Methods in Engineering (CIMNE). Gran Capità s/n, Campus Nord UPC, Ed. C1 - 08034 Barcelona – Spain
- (2) Amphos 21 Consulting. Passeig de Garcia i Faria, 49-51. 08019 Barcelona – Spain

*jorge.molinero@amphos21.com

Bentonite barriers are crucial engineering elements to ensure the long-term safety of spent nuclear fuel repositories in several countries around the world. For example, in nuclear waste repositories of the KBS-3V type (Sweden and Finland), the nuclear waste will be contained in copper canisters and emplaced in vertical holes drilled in granitic rock at depths of about 500 m. The metallic canisters will be surrounded by compacted bentonite bricks, that will swell during the hydration process, protecting the canisters from corrosion and adding a great sorption capacity against radionuclide migration into the geosphere. However, it is known that in contact with very dilute waters, smectite particles may lose cohesion and eventually be eroded by flowing groundwater.

In this work we propose a numerical technique to study the erosion of bentonite buffer embedded in rock as it extrudes into a water-conducting fracture. Our numerical technique couples the discrete element method, used to model the colloidal particles, to the finite element method, which is used to solve the modelling equations for the suspending fluid. We focus on the sol region, where very low solid volume fractions are found. It is from this region that individual colloidal particles may be dragged away and irreversibly fall into the flowing groundwater by a combination of Brownian and hydrodynamic forces, repulsive electrostatic forces (diffuse double layer forces) and cohesive Van Der Waals forces. We model the added effect of all inter-particle interactions as a combination of a short-range inter-particle attractive force and a longer-range repulsion based on the local gradient of the volume-averaged solid fraction. Moreover, we use standard models for the hydrodynamic and Brownian forces, which we calculate for each particle based on interpolated values from the fluid phase fields. In addition to these (one-way) force exchanges, applied by the background fluid to the particles, there is also a strong dependence of the fluid's viscosity on the solid volume fraction, leading to a two-way coupled algorithm.

Diffuse double layer forces are represented as the repulsive force resulting of the local increase in the concentration of cations that takes place near the (negatively charged) surface of the smectite particles. Van der Waals forces are always attractive in the present context. Both these forces are modelled following Neretniek (2012).

The numerical implementation has been carried out within the framework Kratos Multiphysics (Dadvand et al., 2002; Santasusana, 2013). The general algorithm can be summarized as follows

1. Set the fluid and DEM initial and boundary conditions.

2. Solve for the fluid phase using a finite element implementation of the modified Navier-Stokes equations for multicomponent flows (fluid-phase only; see e.g., Zhou et al., 2010).
3. Enter the sub-stepping loop (the DEM phase is solved many times between fluid-phase solves)
 - a. Project the fluid velocity and compute the projected solid fraction onto each individual particle.
 - b. Use the data from a) to calculate the coupling forces (e.g., drag force).
 - c. Compute the contact forces using the soft-sphere approach (see Casas et al., 2015).
 - d. Go back until the sub-steps are completed.
4. Exit the substepping loop and interpolate the updated DEM data onto the fluid nodes.
5. Go back to step 2 until the simulation is completed.

The performance of the proposed algorithm will be illustrated with a realistic numerical example. The application of these models could help to describe in a more realistic way the overall effect of bentonite particles erosion and transport away from the near field of KBS-3 repositories.

REFERENCES

- Casas, G.; Mukherjee, D; Celigueta, MA.; Zohdi, TI. & Oñate, E. (2015) "A modular, partitioned, discrete element framework for industrial grain distribution systems with rotating machinery." *Computational Particle Mechanics* (2015): 1-18.
- Dadvand, P.; Mora, J.; Gonzalez C.; Arraez, A.; Ubach, P. & Oñate E. (2002) "Kratos: An object-oriented environment for development of multi-physics analysis software." *WCCM V, Fifth World Congress on Computational Mechanics*. 2002.
- Neretnieks, I, Moreno, I., Liu, L.; Olin, M.; Veli-Matti, P.; Schaefer, T; Huber, F, & Koskinen, K. (2012): Description of conceptual models and the related mathematical models to support treatment of colloids related issues in the safety case. June 2012. Belbar Project. Delivery B 5.1
- Santassusana, M. (2013). *Kratos Dem, a parallel code for concrete testing simulations using the discrete element method*. CIMNE. Barcelona
- Zhou, Z. Y., Kuang, S.; Chu, K. & Yu, A. (2010) "Discrete particle simulation of particle–fluid flow: model formulations and their applicability." *Journal of Fluid Mechanics* 661 (2010): 482-510.

RHEOLOGY MEASUREMENTS ON SMECTITE CLAY GELS

Ulf Nilsson (un@claytech.se), Magnus Hedström

Clay Technology AB, IDEON Science Park, SE-223 70 Lund, Sweden

The strength of clay gels depends on several parameters. In this study we examine the yield strength of sodium-dominated smectite and its variation with clay concentration, NaCl concentration and aging. Gel formation is the only bentonite-specific mechanism that can prevent erosion of clay at a transmissive fracture. It is therefore of importance to establish that yield strength of gels are sufficiently high to withstand the shearing forces of flowing groundwater.

Measurements have been made on two different clay concentrations and a number of NaCl concentrations in the range of 5 to 100 mM. Shear strengths were also measured at different rest time intervals. The clay fraction of Ashapura 505 bentonite was extracted by centrifugation, and subsequently oven dried, milled and then mixed with deionized water. As the origin of this bentonite is the Kutch region, India we refer to the $<2\mu\text{m}$ fraction as Kutch montmorillonite (Ku-mmt). The test samples were prepared by adding equal volumes of adequate concentration of sodium chloride solution and clay suspension. The mixtures were shaken and allowed to rest for 1 day or 1 week. The rheology of the clay gels was studied by means of rotating vane rheometry using a Brookfield Viscometer with four-bladed vanes.

It is important to distinguish between paste (sometimes called repulsive gel) and gel. Both states may exhibit yield stress. However the cause for this observation in the two systems is different. In pastes the yield stress is caused by jamming, the particles are repelling each other, whereas in gels the yield stress is an effect of attractive forces that give rise to a percolated network. A strong disturbance of a gel leads to a permanent damage as can be seen in Figure 1 that shows the disruption to the Ku-mmt gel caused by the vane. In case of pastes the indentation mark caused by the vane disappears soon after the measurement is completed. The swelling ability of pastes causes self-healing.



Figure 1. Ku-mmt, 20 g/l in 20 mM NaCl(aq) after a yield stress measurement.

Pastes with access to excess water will swell which the cause for colloidal erosion. Under gel forming conditions, salinity above a critical concentration, the bentonite/montmorillonite reach a maximum swelling.

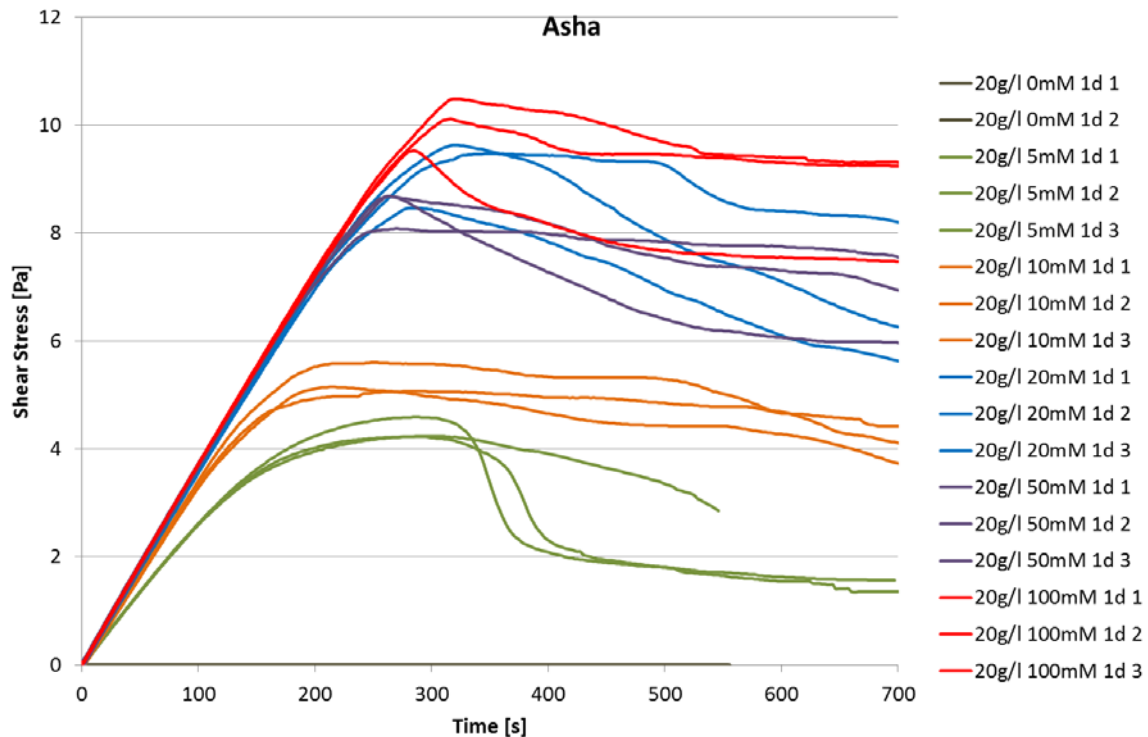


Figure 2. Shear stress vs time for Ku-mmt at a concentration of 20 g/l and different NaCl concentrations 24 hours after preparation. Note that without extra NaCl, denoted 0 mM in the legend, the suspension has no yield stress at all, and the two curves coincide with the x-axis.

Figure 2 shows the results for Ku-mmt at 20 g clay/L. With no added salt, meaning the only salt possibly present is coming from soluble minerals, the shear stress was constantly below measurement threshold. With 5 mM NaCl, which is just above the critical concentration ~ 4 mM the yield stress is substantial. Increasing the NaCl concentration further gave stronger gels and we interpret this trend as stemming from both increasing edge-face interactions and a larger role played by the van der Waals interactions at the higher salinities.

Rheological measurements were also done for more dilute gels with clay concentration 10 g/L. At a NaCl concentration of 5 mM the maximum shear stress was only 0.4 Pa compared to 4 Pa at 20 g clay/L (Figure 2). The effect of increasing clay concentration was largest for the 5 mM samples but still significant at higher NaCl concentrations, approximately following the anticipated trend with the square of the clay volume fraction (Hedström et al., 2015, Nilsson and Hedström, 2016). Even at these low volume fractions the gel yield strength is more than an order of magnitude higher than the estimated shearing forces in a future repository (Eriksson and Schatz, 2015).

One week of resting produced significantly stronger gels than those tested after 24 hours. At installation of the buffer bentonite in a future repository, the ground water conditions are such

that a gel will be formed at the swelling front and strongly limit penetration of bentonite into water-bearing fractures. These conditions will prevail at least until the next glaciation. Thus the gel, most probably will attain its maximum strength.

Acknowledgements

The research leading to these results has received funding from the European Atomic Energy Community's Seventh Framework Programme (FP7/2007-2011) under Grant Agreement no295487, the BELBaR project, and from the Swedish Nuclear Fuel and Waste Management Company (SKB).

References

- Eriksson, R., Schatz, T., 2015. Rheological properties of clay material at the solid/solution interface formed under quasi-free swelling conditions. *Appl. Clay Sci.* 108, 12–18.
- Hedström, M., Ekvý Hansen, E. Nilsson, U., 2015. Montmorillonite phase behaviour. Relevance for buffer erosion in dilute groundwater. Technical report TR-15-07, SKB.
- Nilsson U., Hedström, M., 2016. Manuscript in preparation.

SCALING OF EROSION FROM LABORATORY EXPERIMENTS TO TEMPORAL AND SPATIAL EXTENT OF A REPOSITORY

Markus Olin (markus.olin@vtt.fi), Veli-Matti Pulkkanen, Michał Matuszewicz, VTT Technical Research Centre of Finland Ltd, P.O. Box 1000, FI-02044 VTT, Finland

Why to study scaling?

Most of the erosion experiments of bentonite material to be applied in spent fuel final repositories are carried out in centimetre and month scale. However, the application scale in performance analysis is in metres spatially and centennials in temporally. Both modelling and experiments can be used in scaling. For example, showing in experiments that say total erosion flux depends on exponent of Péclet number (Pe), which is a product of length scale and velocity divided by diffusivity, gives not only the dependence but also supports the assumption that erosion is a kind diffusion process; seeing something else propose some other physical and chemical mechanisms behind the erosion.

In this work scaling is studied by modelling, because a suitable model for testing the approach was available by Neretnieks et al. (2009). There start to exist experimental data suitable for scaling, but it is pretty straightforward to add those observed numbers, when are available, for comparison with models. Both experimenting and modelling are time consuming efforts in erosion studies.

Modelling strategy

We have made a modified version of Neretnieks' model (Neretnieks et al., 2009), which was applied in these studies. The original model differs in some respects from our modified model, but being more computing friendly, at least in COMSOL Multiphysics, the modified version appears good for scaling purposes. The chosen approach was simple and straightforward: compute the steady state solution for our model version as a function of diameter and groundwater velocity. The full computing scheme is shown in Table 1.

In all examples the ionic strength of groundwater was set to 0.1 mM, and this salinity was applied over the whole system, meaning that no salt diffusion was included in the modelling. The radius (R) of the source term varied from 0.01 to 2.7 metres, and the groundwater flow velocity (v) from 0.6 to 6 000 m/a. The models were scaled so that the width (W) of the model (direction of groundwater flow) was two times the height (H) of the model, and the origin of the half circle shaped source was set to $W/2.5$ i.e. there was bit more space downstream than upstream.

The first difficulty was to maintain the relative accuracy (cell size vs. the extension of erosion profile): the W value was iterated such that the montmorillonite swelled up to about half of the H , a distance which was assumed to give enough space for the free water to flow such that the flow velocity is not affected too much. As can be seen from Table 1, there was thousand fold variations in units of radius of the model system, and three thousand fold in metres. In most the cases the system width is clearly larger than the difference between two nearby deposition holes in KBS-3 method (about 10 metres).

The second issue was long time period for the system to stabilise: this varied from weeks in small systems of high velocity to thousands of years or even more. However, every simulation took at least few days in the model and sometimes it was uncertain, if the steady was reached or not, but

due high computational costs and high number of cases still additional computations were not yet started.

Table 1. The size of computing area (W) as multiples of radius (R) and in metres.

v (m/a)	0.6	6	60	600	6000
R (m)/	W/R	W/R	W/R	W/R	W/R
0.01		4500	800	180	30
0.02		3300	500	120	21
0.05		1400	180	80	14
0.10	4000	800	200	50	10
0.3	1900	360	72	24	7
0.9	900	240	48	14	5
2.7	400	120	12	6	4

v (m/a)	0.6	6	60	600	6000
R (m)/	W (m)				
0.01		45	8	1.8	0.3
0.02		66	10	2.4	0.4
0.05		70	9	4	0.7
0.10	400	80	20	5	1
0.3	570	108	21.6	7.2	2.1
0.9	810	216	43.2	12.6	4.5
2.7	1080	324	32.4	16.2	10.8

Main findings

The major results are shown in Figure 1, where total erosion flux is in many case fitted to exponent Péclet number. The exponent is however dependent of some details in computation model. Much more results are available like the concentration profiles, but these a bit clumsy to produce by COMSOL.

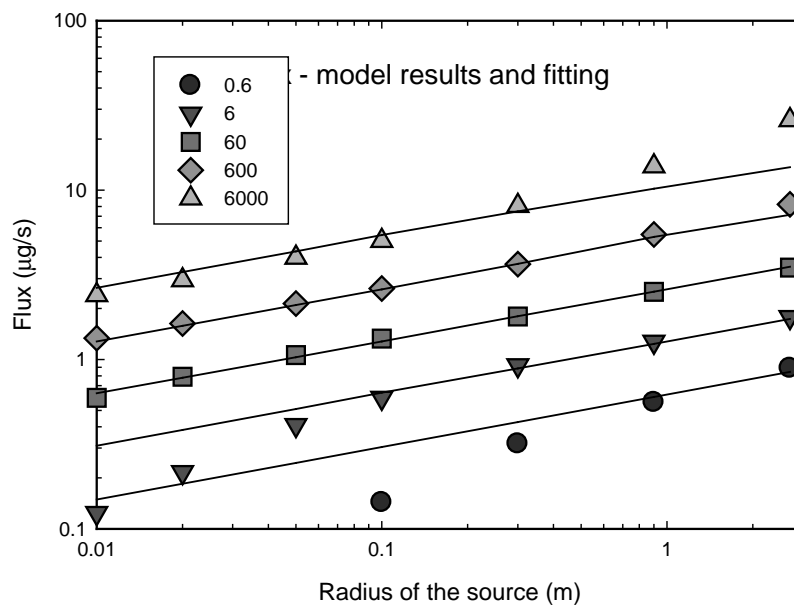


Figure 1. The total erosion flux as a function of source radius at different velocities.

Main applications and implications

This study was based on (non-validated) modelling only, but the conclusions are wider

1. Some kind of scaling is needed, and the results of that may be not self-evident
2. It is not an easy task to scale from small high velocity system to big low velocity systems as the processes governing the systems may be quite different
3. The observed salinity dependence is very weak, and erosion is taking place even at high salinity. This may be the property of VTT's implementation, but needs more studies.

References

- Neretnieks, I., Liu, L., Moreno, L. (2009). Mechanisms and Models for Bentonite Erosion. Report SKB TR-09-35, Svensk Kärnbränslehantering AB, Stockholm, Sweden
- Olin, M (2014). Tunnel Backfill Erosion by Dilute Water. Posiva Working Report 2014-07, Posiva Oy, Olkiluoto, Finland

Do montmorillonite particles form gels in aqueous suspensions?

Rasmus Eriksson (rasmus.eriksson@btech.fi), B+Tech Oy, Laulukuja 4, 00420 Helsinki, Finland

Sanna Haavisto, Spinnova Oy, Kankitie 3, 40320 Jyväskylä, Finland

Introduction

One particular clay mineral material property of interest is the mechanical response to an applied force, e.g. shear. The mechanical response depends directly on the macroscopic structure of the material as well as the interactions between particles. In general, if the solid particles form a volume-spanning network throughout the suspension, the response to a small strain deformation will be mainly elastic; otherwise the response will contain a viscous component, the magnitude of which depends on the specific physicochemical properties of the suspension. Bentonite buffer material is under stress from various sources in a KBS-3 repository environment, and therefore the structural and mechanical properties of montmorillonite (the main component of bentonite) are of interest, particularly for long-term predictions of repository evolution.

Aim of the study

This study focuses on small scale mechanical perturbation of dilute montmorillonite suspensions. A rheometer (TA Instruments DHR-2) was employed in the study and experimental details can be found in (Eriksson and Schatz 2015). The samples were subjected to small amplitude oscillatory shear at varying amplitudes and frequencies in order to gain information about sample structure and particle interactions. Particular emphasis was put on the low frequency regime, which simulates strain exerted by gently flowing groundwater. The ultimate goal is to determine the structure and the nature of the mechanical response of dilute montmorillonite suspensions to a small deformation.

Results and discussion

Strain sweep measurements on montmorillonite suspensions show the typically observed (visco)elastic response at low solids content (Fig. 1). The linear viscoelastic region (LVR) is easily identified for montmorillonite suspensions at solids contents ≥ 4 vol % as the strain amplitude range throughout which G' is constant and independent of the applied strain. Within this strain range the response of the sample is mostly elastic (phase angles vary between $\sim 1 - 5^\circ$), and therefore the suspension structure can be regarded as remaining intact. It is interesting to note that the LVR upper strain amplitude limit (or failure strain, i.e. the strain amplitude at which G' starts to drop) occurs at approximately the same strain amplitude (~ 0.005 rad) for all samples in Fig. 1, regardless of solids content (at ≥ 4 vol %) or electrolyte concentration. Similar observations have been made elsewhere (Paineau, et al. 2011). The failure strain for the montmorillonite samples in Figure 1 (~ 0.005 rad) corresponds to an effective oscillation displacement of ~ 30 μm . This indicates that domains of higher and lower density exist in these systems at roughly the same length-scale as the effective failure strain (i.e. a few tens of microns). The domains of higher density must be clay aggregates, but the size of the aggregates or the nature of interactions between these aggregates cannot be unambiguously determined from strain sweep measurements.

There are in fact indications that the failure strain is of the same order of magnitude over a wide range of solids contents. Resonant column tests (Pintado, et al. 2014) performed on highly

compacted samples with water contents ranging between approximately 17 – 26 %, display failure strains of the same order of magnitude as the low solids content samples shown in Figure 1.

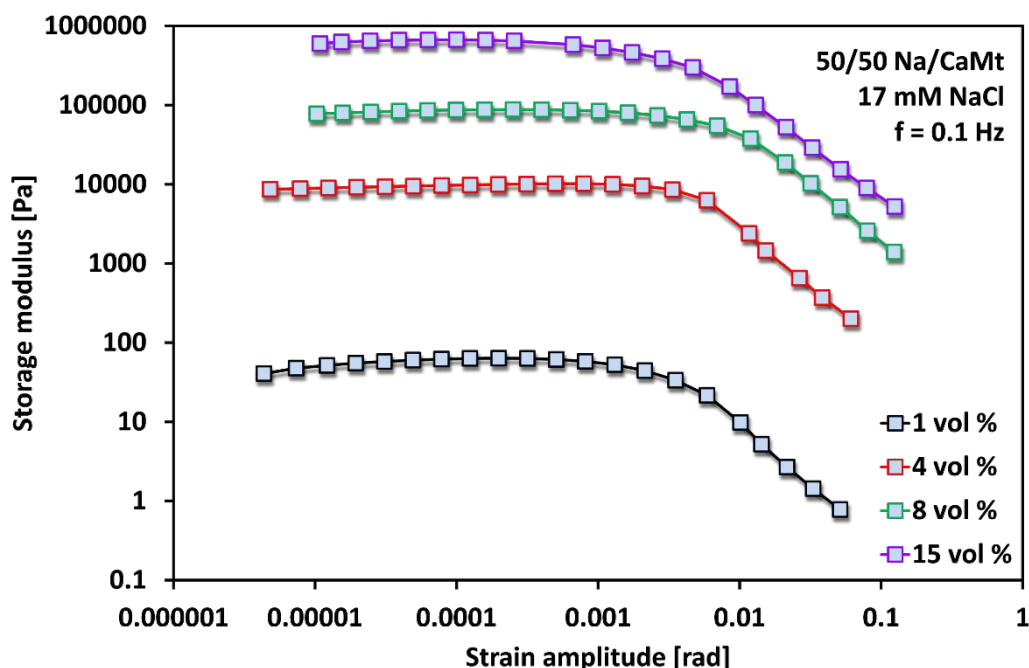


Figure 1. Strain sweep measurements on montmorillonite suspensions in 17 mM NaCl containing 50 % Na-montmorillonite and 50 % Ca-montmorillonite by weight.

Frequency dependent measurements show a gradually increasing viscous response as a function of decreasing frequency (Fig. 2), which is typical for a Maxwell viscoelastic material.

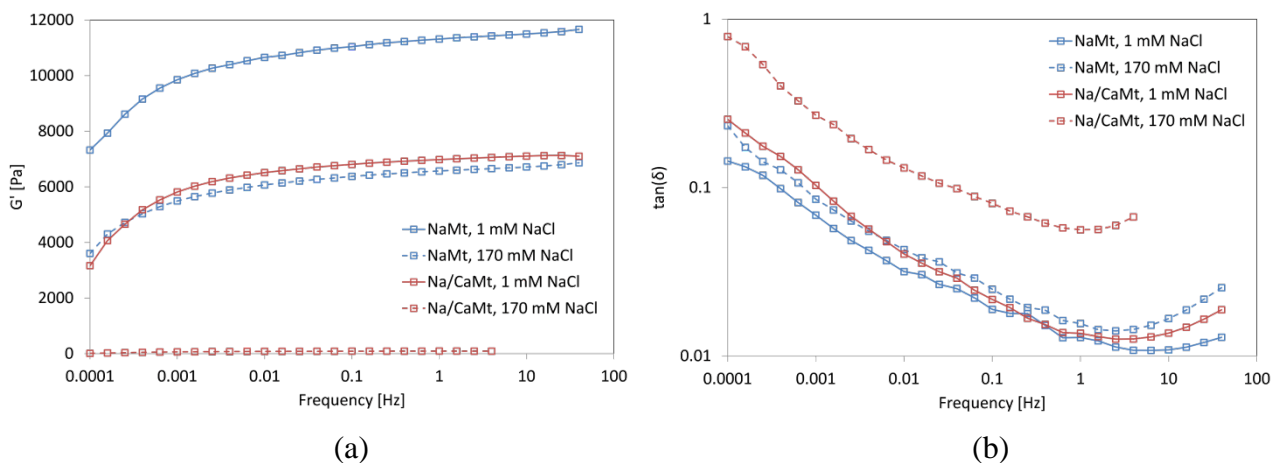


Figure 2. Frequency sweeps of 4 vol % montmorillonite suspensions at a constant oscillation displacement of 0.25 mrad. Blue curves refer to suspensions of sodium montmorillonite. Red curves refer to suspensions of 50/50 mixtures of sodium and calcium montmorillonite. The elastic modulus as a function of frequency is shown in the left chart and the corresponding loss factor is shown in the right chart.

The results shown in Figure 2 indicate that 4 vol % (~10 wt%) montmorillonite suspensions are able to relax in response to an applied strain, which is in contradiction to the common belief that montmorillonite suspensions (as well as many other clay minerals) form gels at this solids content,

and in many cases, at much lower solids content (Abend and Lagaly 2000, Michot, et al. 2004, Shalkevich, et al. 2007, Ruzicka and Zaccarelli 2011). Although the above results show that montmorillonite suspensions relax very slowly (a simple extrapolation indicates relaxation times of at least several hours), the implication is clear; montmorillonite suspensions at low solids contents should not be considered to be true gels because the structure is able to relax (i.e. rearranges) in response to a small strain.

Assuming montmorillonite suspensions consist of aggregates and/or clusters of higher density domains, a small strain deformation would lead to friction between these domains. An OCT snapshot taken during an actual measurement gives an idea of the size and shape of these aggregates in dilute suspensions (Fig. 3).

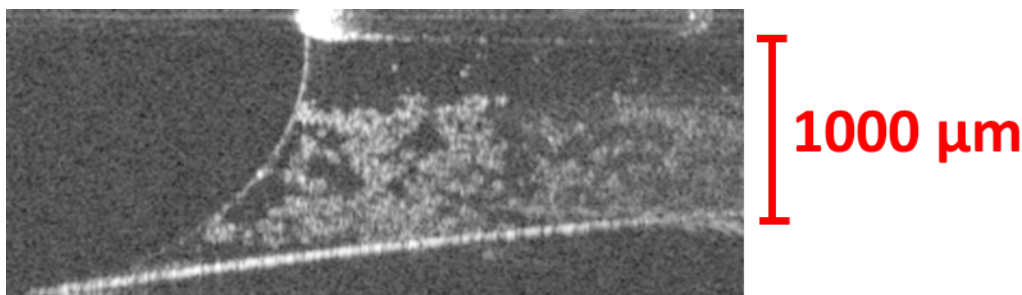


Figure 3. OCT image of 0.1 vol % NaMt in 17 mM NaCl during an actual rheological measurement. The gap between the plates is 1 mm. The lower plate appears to be curved but this is due to an optical distortion, and in reality it is perfectly flat. The white-colored areas between the plates consist of solid material (i.e. montmorillonite).

Based on the image shown in Figure 3, it seems that montmorillonite particles are able to form aggregates or clusters of considerable size (several tens of μm) even in very low solids content suspensions. At the solids content in Fig. 3 the aggregates necessarily have a very low density while, presumably, the aggregates are denser and perhaps smaller at higher solids contents. If the stress response of montmorillonite samples to a small deformation is due to friction between such aggregates (which seems likely), the relaxation process in a situation where the stress is upheld most likely involves deformation and restructuring of these aggregates. This could be a very slow process depending on the number of individual bonds that have to be broken and reformed. This process is further slowed down due to the irregular shape of montmorillonite flakes as compared to, for example, spherical particles. In any case, it appears that montmorillonite systems are dynamic (viscous) in nature rather than rigid, solid-like systems since they are able to relax in response to a very small applied strain.

Conclusion

The results presented in this work show that montmorillonite suspensions prepared under free swelling conditions are dynamic systems that will relax in response to a small applied strain, such as flowing groundwater, and therefore the system behaves like a viscous liquid rather than a gel. For buffer material performance in a repository environment this distinction is of minor consequence as long as the clay body does not disperse too easily, for example when material is extruding into rock fractures (Eriksson and Schatz 2015). However, the fundamental mechanical behavior of a material is very different between a gel and a viscous liquid, and this distinction is important for example when modeling the mechanical response of materials to strain.

An important factor to consider when discussing the structure and rheological behavior of samples is the history of the sample. Clay minerals have long been claimed to form gels in dilute aqueous

suspensions, and in a controlled lab-environment it is possible that clay suspensions exhibiting true gel-like behavior can be produced. This usually requires mechanical agitation (e.g. stirring) of the sample. A characteristic feature of a gel is that the solid material is more or less homogeneously distributed (by weight) throughout the solvent (water), and this is practically impossible to achieve when clay minerals are allowed to swell freely. It is even more unlikely for an impure mixture of minerals like bentonite, which exists in a mostly flocculated state in water. All samples in this work were allowed to swell freely for a minimum of one month, and none of them formed homogeneously distributed, gel-like suspensions. Therefore, when considering buffer material extrusion into rock fractures in a repository environment, the rheological properties of the extruding material can be compared to a viscous liquid instead of a gel, and both experimental and modeling studies on the extruding material should take advantage of this fact.

REFERENCES

- Abend, S., and G. Lagaly. 2000. "Sol-gel transitions of sodium montmorillonite dispersions." *Applied Clay Science* 16: 201-227. doi:10.1016/S0169-1317(99)00040-X.
- Eriksson, R., and T. Schatz. 2015. "Rheological properties of clay material at the solid/solution interface formed under quasi-free swelling conditions." *Applied Clay Science* 108: 12-18. doi:10.1016/j.clay.2015.02.018.
- Michot, L. J., I. Bihannic, K. Porsch, S. Maddi, C. Baravian, J. Mougel, and P. Levitz. 2004. "Phase diagrams of Wyoming Na-montmorillonite clay. Influence of particle anisotropy." *Langmuir* 20: 10829-10837. doi:10.1021/la0489108.
- Paineau, E., L. J. Michot, I. Bihannic, and C. Baravian. 2011. "Aqueous suspensions of natural swelling clay minerals 2. Rheological characterization." *Langmuir* 27: 7806-7819.
- Pintado, X., E. Romero, J. Suriol, and A. Lloret. 2014. *Small-strain stiffness of statically compacted MX-80 bentonite using resonant column tests*. TM 29/237, Helsinki: B+Tech Oy.
- Ruzicka, B., and E. Zaccarelli. 2011. "A fresh look at the laponite phase diagram." *Soft Matter* 7: 1268-1286.
- Shalkevich, A., A. Stradner, S. K. Bhat, F. Muller, and P. Schurtenberger. 2007. "Cluster, glass, and gel formation and viscoelastic phase separation in aqueous clay suspensions." *Langmuir* 23: 3570-3580.

Electrolyte-mediated dissolution of montmorillonite in alkaline environments

Rasmus Eriksson (rasmus.eriksson@btech.fi), B+Tech Oy, Laulukuja 4, 00420 Helsinki, Finland

Introduction

Dissolution and mineralogical alteration of bentonite material are interrelated processes and may, under certain circumstances, affect the performance of buffer or backfill material in a spent nuclear fuel repository. Mineralogical alteration could, for example, lead to decreased swelling pressure due to reduced swelling clay fraction, while dissolution may lead to loss of buffer (or backfill) material. At full saturation, dissolution is mainly a concern at rock fracture/buffer or rock fracture/backfill interfaces, where material can extrude into the fracture and therefore become diluted. Dissolution is not expected to occur to a significant amount in the compacted and fully saturated buffer or backfill matrices because the amount of pore water is small, and the pore water is to a large degree bound to surfaces (interlayers) and ions, which reduces its capacity to accommodate dissolved species.

Methods

A series of potentiometric and conductometric titrations on dilute Na-montmorillonite suspensions and corresponding supernatants at NaCl and CaCl₂ concentrations between 0.0001 – 1 mol/L were performed. The samples were allowed to equilibrate for 30 minutes under gentle stirring prior to analysis. The titrations were performed by first titrating the sample with 1 M NaOH to pH 11, and thereafter immediately continuing by titrating the sample with 1 M HCl to pH 4. The maximum equilibration time between titrant additions was set to 30 seconds in order to minimize the accumulated leakage from the pH electrode (a Metrohm gel electrode), which would otherwise affect the conductivity data.

Results and discussion

A comparison of initial sample conductivities (before any titrant addition) to conductivities of electrolyte solutions of equivalent concentrations (at 25 °C) reveals that montmorillonite particles are not inert materials, especially in the presence of high electrolyte concentrations (Fig. 1). The electrical conductivities of pure electrolyte solutions were calculated from literature data (Haynes 2011-2012). The conductivity values of the samples have been normalized to 25 °C assuming a 2% change per °C. In general, the relative difference in conductivity is largest at the lowest electrolyte concentrations (≤ 0.001 M, Fig. 1a,c), and the absolute difference is largest at the highest electrolyte concentrations (≥ 0.5 M, Fig. 1b,d). At the highest electrolyte concentrations the difference in conductivity is on the order of several mS/cm, which implies a significant increase in the electrolyte concentration of the aqueous phase (several tens of mM in concentration) as compared to the conductivity of the background electrolyte. Montmorillonite is the only source material available, and therefore the increase in conductivity is due to dissolving montmorillonite.

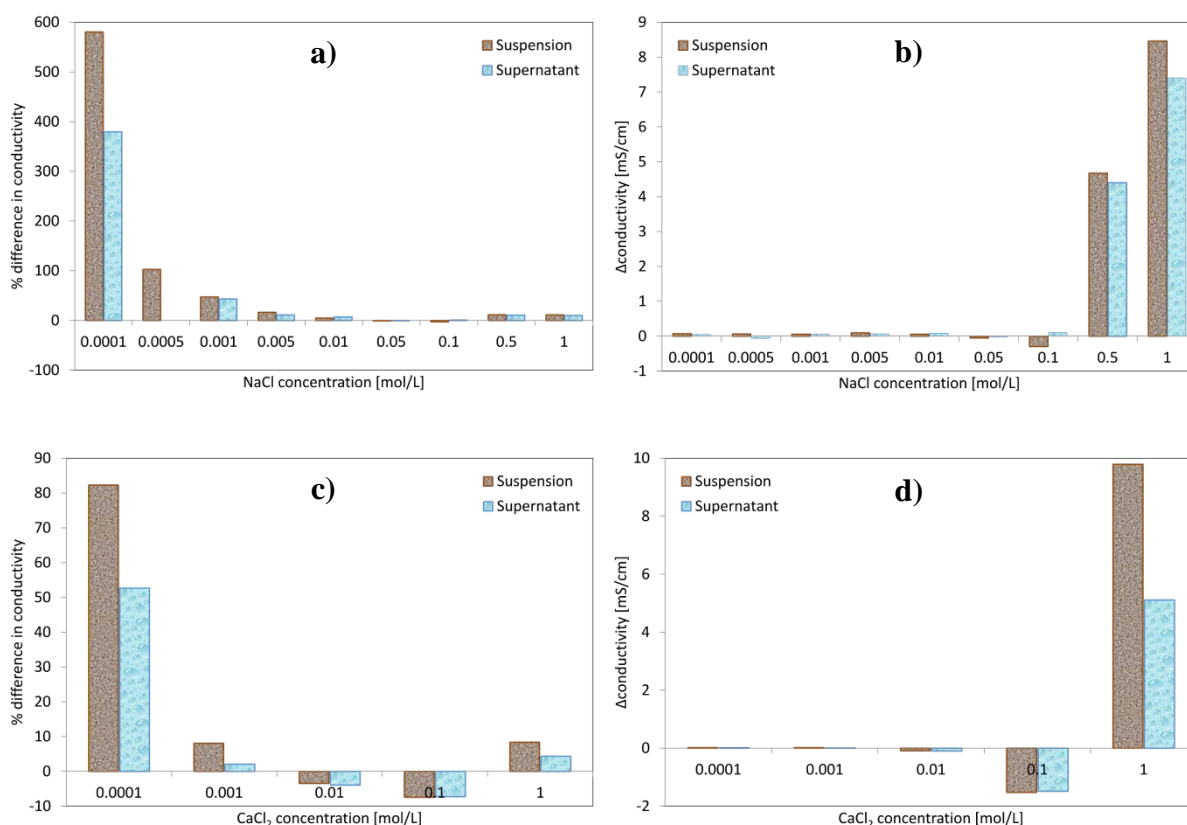


Figure 1. The difference in conductivity between 1.5 g/L Na-montmorillonite samples (suspensions and corresponding supernatants) and an aqueous solution at the same background electrolyte concentration. a,c) The relative difference (in %) for NaCl (a) and CaCl₂ (c) as background electrolyte. b,d) The absolute difference (in mS/cm) for NaCl (b) and CaCl₂ (d) as background electrolyte.

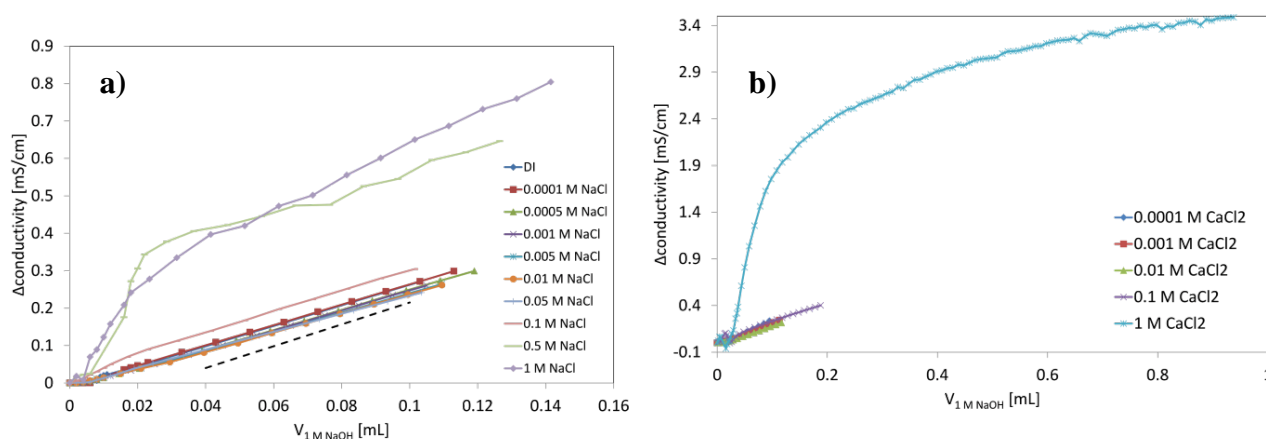


Figure 2. Conductometric titrations of 1.5 g/L Na-montmorillonite samples at different a) NaCl concentrations and b) CaCl₂ concentrations. The y-axis shows the change in sample conductivity relative to the initial conductivity.

Titrating the samples up to pH 11 shows that further dissolution is more pronounced at higher electrolyte concentrations (Fig. 2). Below an electrolyte concentration of 0.5 M, no significant dissolution is observed, while above 0.5 M, the conductivity increase is much larger than what

would be expected due to NaOH addition (Fig. 2). Montmorillonite dissolution involves reactions with water along the edge surface, but the reaction mechanism and the dissolution products have not been precisely determined. Our study suggests that the presence of electrolytes accelerates montmorillonite dissolution to a significant degree, perhaps even to a larger degree than the effect of elevated pH. As suggested by (Kubicki, et al. 2012), electrolytes may facilitate the formation of metastable surface groups that are believed to act as precursors to the actual dissolution reaction. Furthermore, dissolution has been hypothesized as being partly responsible for long-term stiffening or gelation of dilute clay mineral suspensions (Shahin and Joshi 2012, Saha, Bandyopadhyay and Joshi 2015), and therefore it may be beneficial in the sense that an increase in shear strength should decrease erosive mass loss.

REFERENCES

- Haynes, W. M., ed. 2011-2012. *CRC Handbook of chemistry and physics*. 92nd Edition. Boca Raton: CRC Press.
- Kubicki, J. D., J. O. Sofo, A. A. Skelton, and A. V. Bandura. 2012. "A new hypothesis for the dissolution mechanism of silicates." *The Journal of Physical Chemistry C* 116: 17479-17491.
- Saha, D., R. Bandyopadhyay, and Y. M. Joshi. 2015. "Dynamic light scattering study and DLVO analysis of physicochemical interactions in colloidal suspensions of charged disks." *Langmuir* 31: 3012-3020. doi:10.1021/acs.langmuir.5b00291.
- Shahin, A., and Y. M. Joshi. 2012. "Physicochemical effects in aging aqueous laponite suspensions." *Langmuir* 28: 15674-15686.

BELBaR Final Workshop - Extended Abstract

BENTONITE EROSION IN AN ARTIFICIAL FRACTURE SET-UP UNDER NEAR-NATURAL CONDITIONS

Franz Rinderknecht (Franz.Rinderknecht@kit.edu), Frank Friedrich, Stephanie Heck, Robert Götz, Florian Huber, Thorsten Schäfer

Karlsruhe Institute of Technology (KIT), Institute for Nuclear Waste Disposal (INE)

Compacted bentonite is considered to be suitable for use as geotechnical barrier in a high level radioactive waste repository in crystalline host rocks. In the Scandinavian region, for example, granite is the only possible option for the deposition of radioactive waste (SKB, 2006). Montmorillonite is a major part of most bentonites and is characterized by good swelling abilities that enable clogging of water bearing fractures and thereby safely enclosure of the containing waste (Missana et al., 2003). The outstanding sorption capacity by cationic exchange reactions and the resulting high retention capacity for many radionuclides is another key feature of the bentonite barrier. The function of the geotechnical barrier lays in the retention of the radioactive waste after the breakdown of the technical barrier as the therefore used canisters have a finite life span. In the case of a canister failure due to corrosion, radionuclides get in contact with the surrounding bentonite buffer under porewater conditions and sorption may occur (Fernandez et al., 2004). The radionuclides are safely enclosed in the geotechnical barrier as it will stay intact as long as no water enters the repository. In the example of the Scandinavian scenario glacial melt water may flow down to repository depth and intrusion to the geotechnical barrier in the course of glaciation has to be taken in account (Bath, 2011; SKB, 2011). Thereby the compacted bentonite is in the flow field of the glacial melt water which will cause swelling and gel formation at the water interface. Radionuclide bearing bentonite colloids may leave the repository due to advection which is the reason why bentonite erosion processes and the interaction of the eroded material with radionuclides play an important role in the safety assessment of a deep radioactive waste repository in crystalline host rock.

An experimental setup for the generation of colloids by bentonite erosion was build up in October, 2013. A ring shaped compacted bentonite sample is located in the middle of the setup and a spacer is placed in the centre of the ring. The parts of the housing around the bentonite ring are not in contact. Thereby a slit with an aperture of 1 mm height is formed that mimics a parallel-plate synthetic fracture around the bentonite source and allows the granitic groundwater to reach the bentonite. Natural Grimsel groundwater is pumped through this synthetic fracture with a flow rate of 50µl/min. Relatively low ionic strength (~1mM) and high pH (9.5-9.6) is characteristic for this groundwater (Schaefer et al., 2012) and makes it comparable to glacial melt water. A schematic overview of the setup is given in Figure 1. The dimensions of the compacted bentonite ring are the same as in a field experiment which started in 2014 within the Colloid Formation and Migration (CFM) project that is performed at the Grimsel Test Site (GTS, Switzerland).

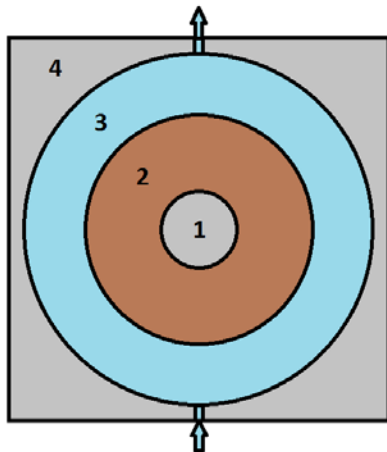


Figure 1 (left): Schematic arrangement of the bentonite erosion experiment. 1. Spacer 2. Compacted bentonite 3. Aperture of 1 mm height fracture 4. Acrylic glass in contact, seals the arrangement; Not numbered: water inlet, water outlet. (right) Glass vials containing holes on side of the ring.

Eight thin glass vials containing 220 mg (synthetic Ni-labelled) montmorillonite (as paste) spiked with 10 mg uranine in each vial as conservative tracer and the homologues Eu, Th, Hf and Tb (25 µg per vial, respectively) are emplaced in the bentonite ring (Figure 1). Due to the swelling of the clay the glass vials are supposed to break and release the labelled montmorillonite and associated tracers as well as the conservative tracer.

The experiment is continuously running since October 29th, 2013. As the bentonite used contains a high amount of swelling clay (smectite), a swelling pressure builds up in the cell as the bentonite gets water saturated due to the contact with the Grimsel groundwater. The bentonite swelling pressure evolution of the experiment is monitored by a pressure sensor (disynet XP1103-A1-100BG) (Figure 2) and the result of the first 90 days of the experiment is given in Figure 3 (left).



Figure 2 (left): Currently running bentonite erosion experiment. Pressure monitoring on top (white cable); right: Top view of the bentonite ring in the swelling stage.

Within the first 10 h after the start of the experiment the swelling pressure rose up to 2500 kPa. During the following days the pressure decreased to a constant value between 1700 to 1800 kPa (Figure 2 (left)) implying steady state conditions. The pressure drop coincided with the bentonite swelling into the fracture. Water samples of the reactor effluent were taken daily

before May, 2014 and weekly afterwards for analysis of elemental composition, fluorescence, pH, colloid size and concentration.

The colloidal size distribution and concentration obtained during the first weeks of the experiment is depicted in Figure 3 (right). During the first days a high colloid concentration was detected (initially ~10 mg/l) that was explained by the release of accessory minerals and loosely aggregates during the initial saturation of the set-up followed by a decrease of colloid concentration to values around 0.2 to 1 mg/l after 50 d which coincided with increased Ca^{2+} -concentrations above the critical coagulation concentration (CCC) in the effluent. This trend was monitored by optical LIBD, s-curve LIBD and ICP-MS measurements. The colloid concentrations obtained by ICP-MS and optical LIBD increase after 150 days which goes along with a decrease of Ca^{2+} under the CCC that leads to higher colloid stability.

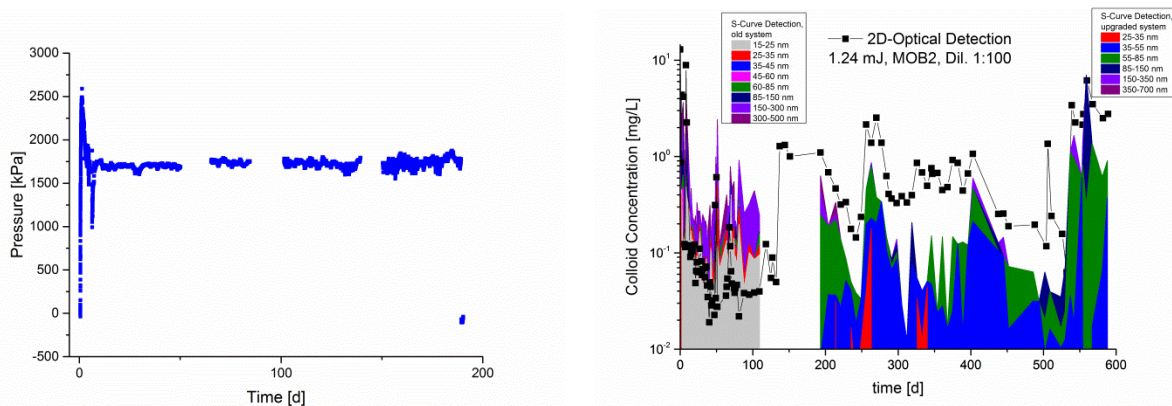


Figure 3 (left): Pressure flow of the experiment, measured on top of bentonite ring. (right) Colloidal concentration measured by ICP-MS and LIBD and colloidal size distribution measured by s-curve LIBD.

Erosion rates are calculated and normalised for the contact area between the rim of the bentonite's swelling zone and the contacted groundwater. Two different rates are calculated for (i) the early stage ($5\text{d} < t < 150\text{d}$) in which the colloid mobility is limited by increased Ca^{2+} concentrations and calculates to a bentonite loss rate of $R_d = 8.3 \text{ g}/(\text{a} \cdot \text{m}^2)$ and (ii) the period of unhindered erosion under GW conditions without increased Ca^{2+} concentrations ($t > 150\text{d}$). The latter case leads to a bentonite loss rate of $R_{BE} = 109.9 \text{ g}/(\text{a} \cdot \text{m}^2)$.

REFERENCES

- Bath, A., 2011. Infiltration of dilute groundwaters and resulting groundwater compositions at repository depth. Swedish Radiation Safety Authority.
- Fernandez, A.M., Baeyens, B., Bradbury, M., Rivas, P., 2004. Analysis of the porewater chemical composition of a Spanish compacted bentonite used in an engineered barrier. *Physics and Chemistry of the Earth* 29, 105-118.
- Missana, T., Alonso, U., Turrero, M.J., 2003. Generation and stability of bentonite colloids at the bentonite/granite interface of a deep geological radioactive waste repository. *Journal of Contaminant Hydrology* 61, 17-31.

Schäfer, T., Huber, F., Seher, H., Missana, T., Alonso, U., Kumke, M., Eidner, S., Claret, F., Enzmann, F., 2012. Nanoparticles and their influence on radionuclide mobility in deep geological formations. *Applied Geochemistry* 27, 390-403.

SKB, 2006. Long-term safety for KBS-3 repositories at Forsmark and Laxemar - a first evaluation; Main report of the SR-Can project. SKB Technical report TR-06-09, Svensk Kärnbränslehantering AB, Stockholm, Sweden.

SKB, 2011. Long-Term Safety for the Final Repository for Spent Nuclear Fuel at Forsmark, Main Report of the SR-Site Project. SKB technical report TR -11-01. Svensk Kärnbränslehantering AB.

BELBaR Final Workshop - Extended Abstract

BENTONITE EROSION AND COLLOID MEDIATED TRANSPORT OF RADIONUCLIDES IN A NATURAL SHEAR ZONE AT THE GRIMSEL TEST SITE

Franz Rinderknecht (Franz.Rinderknecht@KIT.edu), **Stephanie Heck, Robert Götz, Cornelia Walschburger, Frank Geyer, Stefanie Hilpp, Markus Fuß, Florian Huber, Thorsten Schäfer, Horst Geckeis, Karlsruhe Institute of Technology (KIT), Institute for Nuclear Waste Disposal (INE)**

Andrew Martin, Ingo Blechschmidt, NAGRA, Wettingen, Switzerland

Bill Lanyon, Fracture Systems Ltd., St. Ives, UK

The multi-barrier system of a deep geological nuclear waste repository in crystalline host rocks consists basically of the technical, the geotechnical and the geological barrier. The backfill material forms the geotechnical barrier and surrounds the canister. Compacted bentonite is considered to be suitable for this purpose due to (a) its swelling properties that seal potential void space which in turn (b) limits radionuclide transport by diffusion and (c) its high sorption capacity which effectively retains radiotoxic elements.

In the case of canister corrosion or an earlier failure, radionuclides can get in contact with the compacted bentonite and sorption on the bentonite surface will take place in the pore spaces [1]. During future glaciation periods, dilute melt water may intrude down to repository depths and come into contact with the compacted bentonite. Under this condition, a gel layer can form in the contact zone and successive bentonite erosion might occur, releasing colloid associated radionuclides to the repository far-field.

In recent years, a lot of effort has been put on bentonite erosion experiments in artificial fractures (parallel plates) on the lab scale [2] and migration tests of radionuclide bearing bentonite colloids in the natural system [3, 4].

In the course of the Colloid Formation and Migration experiment (CFM; see <http://www.grimsel.com/gts-phase-vi/cfm-section/cfm-introduction>) a bentonite source was emplaced consisting in total of 16 compacted bentonite rings with 12 rings consisting of pure Febex bentonite and 4 rings emplaced directly in contact with a water conducting feature. The bentonite is a 10% admixture of synthetic Zn-labeled montmorillonite [5] doped with a cocktail of radionuclides (^{45}Ca , ^{75}Se , ^{99}Tc , ^{137}Cs , ^{233}U , ^{237}Np , ^{241}Am , ^{242}Pu) and a conservative tracer (Amino G). The packer system was emplaced in the shear zone at the Grimsel Test Site (GTS) in May 2014. The purpose of this experiment is to determine bentonite erosion rates under glacial melt water geochemical conditions in a real fracture and hydraulic conditions comparable to the repository post closure phase. Another aspect is the mobilization of bentonite derived colloids and radionuclides being in contact over considerable time with the bentonite source. This experiment combines for the first time in-situ colloid generation with radionuclide interaction and migration in an advective naturally occurring shear zone under low flow controlled conditions.

Hydrogeological conditions are monitored constantly on-site regarding volumetric flow velocity, pH, E_h , conductivity, swelling pressure of the bentonite source and fluorescence signal of the effluent (conservative tracer) which is sampled from the outflow of the shear zone at the tunnel wall and from an observation borehole close to the bentonite source (distance: ~10 cm).

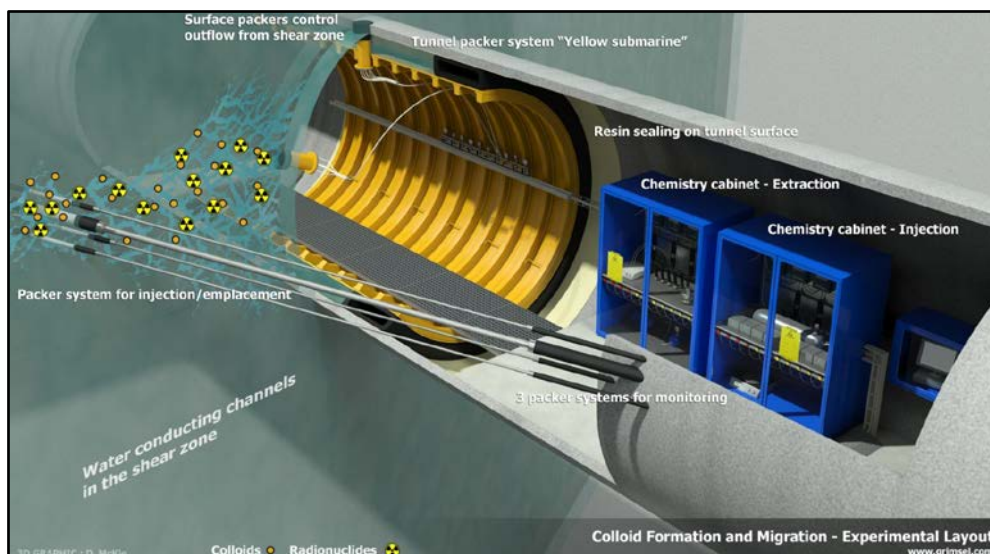


Figure 1 Schematic experimental set-up at the GTS. The radionuclide bearing bentonite sample is emplaced into the shear zone (www.grimsel.com).

The focus of the work presented here is on the KIT/INE off-site analytics of samples taking from the observation borehole with a volumetric flow rate of $50\mu\text{L}/\text{min}$ with a fraction collector emplaced inside an Argon glovebox to keep the Eh/pH conditions constant. The sampled effluent is sealed in head-space vials from the observation borehole close to the bentonite sample, transferred and analyzed to monitor changes in pH, conductivity, fluorescence, colloid mean size, colloid concentration (laser induced breakdown detection; LIBD) and colloid size distribution (s-curve LIBD), chemical (ICP-MS) and radiochemical composition (ICP-MS, SF-ICP-MS, LSC and γ -spectroscopy).

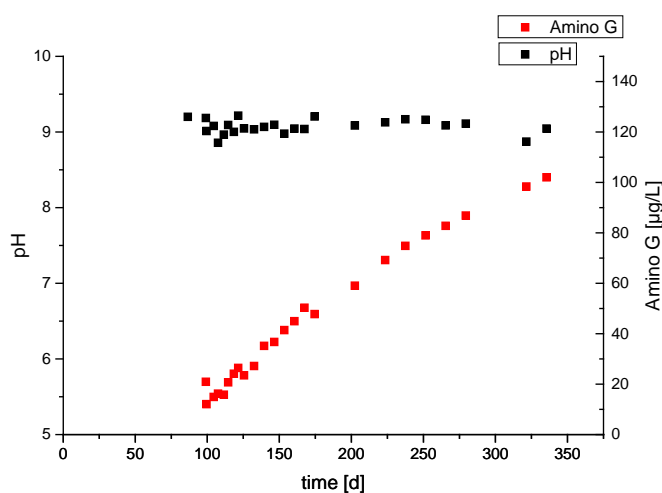


Figure 2 Off-site pH and fluorescence measurements.

After 100 days, the conservative tracer (Amino G) was detectable by fluorescence measurements and its concentration steadily increased while pH was constant at 9.1 (Figure

2). Both parameters presented in Figure 2 (pH and fluorescence) are very comparable to the in-line on-site measurements stored by the data acquisition system (not shown here).

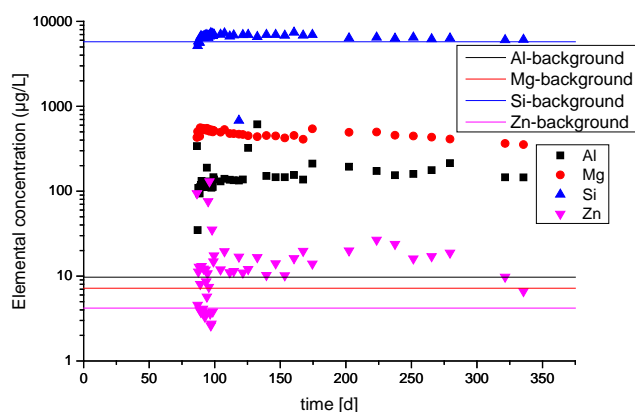


Figure 3 Chemical composition (ICP-MS)

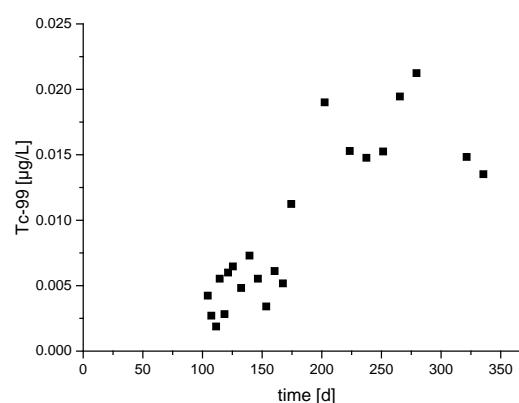


Figure 4 Rising ⁹⁹Tc concentration (SF-ICP-MS)

Assuming that the Zn and Al concentrations above the background level (Figure 3) are directly originating from bentonite colloids, the excess can be translated to colloid concentrations between 1-2 mg/L colloids (Al signal) and 1.5-3 mg/L colloids (Zn signal) in the effluent samples. Increased colloid concentration has also been validated by LIBD while the mean colloid size is around 60 nm and rising. Disproportionately high Mg concentrations and reversed Mg/Al-ratios in the effluent samples compared to the background level that go along with decreasing Ca concentrations suggest a cation exchange reaction of Mg with Ca in the smectite interlayer. A constant elevated sulphate release of ~15 mg/L over the last 350 days implies that a significant influence of sulphate reducing bacteria that could decrease the concentration range of sulphate has not been active so far. Radiochemical investigations only found ⁹⁹Tc in the effluent samples (Figure 4). Due to the high mobility of the spiked ⁹⁹Tc(VII) in the source, the evolution of its concentration with time is in line with the detection of the conservative tracer and the Eh/pH conditions still present in the near-field.

References

1. Fernandez, A. M.; Baeyens, B.; Bradbury, M.; Rivas, P., Analysis of the porewater chemical composition of a Spanish compacted bentonite used in an engineered barrier. *Physics and Chemistry of the Earth* **2004**, *29*, (1), 105-118.
2. *Posiva Buffer Erosion in Dilute Groundwater*; Posiva: Olkiluoto, 2013.
3. Geckeis, H.; Schafer, T.; Hauser, W.; Rabung, T.; Missana, T.; Degueldre, C.; Mori, A.; Eikenberg, J.; Fierz, T.; Alexander, W. R., Results of the colloid and radionuclide retention experiment (CRR) at the Grimsel Test Site (GTS), Switzerland - impact of reaction kinetics and speciation on radionuclide migration. *Radiochimica Acta* **2004**, *92*, (9-11), 765-774.
4. Möri, A.; Alexander, W. R.; Geckeis, H.; Hauser, W.; Schäfer, T.; Eikenberg, J.; Fierz, T.; Degueldre, C.; Missana, T., The colloid and radionuclide retardation experiment at the Grimsel Test Site: influence of bentonite colloids on radionuclide migration in a fractured rock. *Colloids Surf. A* **2003**, *217*, (1-3), 33-47.
5. Reinholdt, M.; Mieke-Brendle, J.; Delmotte, L.; Tuilier, M. H.; le Dred, R.; Cortes, R.; Flank, A. M., Fluorine route synthesis of montmorillonites containing Mg or Zn and characterization by XRD, thermal analysis, MAS NMR, and EXAFS spectroscopy. *Eur. J. Inorg. Chem.* **2001**, (11), 2831-2841.

Modelling the impact of fracture geometry on bentonite erosion

F.M. Huber^{1*}, M. Trumm¹, A. Wenka², D. Leone¹, I. Neretnieks³, L. Moreno³ and T. Schäfer¹

¹*Karlsruhe Institute of Technology (KIT), Institute for Nuclear Waste Disposal (INE), P.O. Box 3640, D-76021 Karlsruhe, Germany.*

²*Karlsruhe Institute of Technology (KIT), Institute of Micro Processing Engineering (IMVT), P.O. Box 3640, D-76021 Karlsruhe, Germany.*

³*Department of Chemical Engineering and Technology, Royal Institute of Technology, Stockholm, Sweden*

*corresponding author: florian.huber@kit.edu

Natural fractures are characterized by complex spatial geometries and heterogeneous (mostly normal to lognormal) aperture distributions (e.g. (Adler and Thovert, 1999)). The question addressed in this study aims on the assessment of a potential impact of fracture geometry (= flow field heterogeneity) on the bentonite erosion. Since aperture or hydraulic conductivity distributions of field scale fractures are not available random lognormal aperture distributions were generated and used in the simulations.

Moreno et al. presented model calculations on bentonite erosion using the “KTH model” ((Moreno et al., 2011; SKB, 2009)). A parallel plate fracture geometry with a constant aperture of 1 mm is assumed in these calculations. The simulations covered a range of mean velocities in the fracture of 1e-5 m/s up to 1e-8 m/s. To model the flow they used constant hydraulic conductivities in the Darcy law. To study the effect of flow field/fracture heterogeneity on the bentonite erosion the model by Moreno et al. (2011) was used including lognormal distributions of apertures with a mean value of 1mm and standard deviations of 0 mm (no random field; constant aperture as used by Moreno et al. (2011)), 0.1 mm and 0.3 mm. By application of the “cubic law” ((Witherspoon et al., 1980)) the hydraulic conductivities are derived from the aperture field distributions and used in the model simulations.

Results of the simulations will be presented and compared to the results given by Moreno et al. (2011).

Adler, P.M., Thovert, J.-F., 1999. Fractures and fracture networks. Theory and applications of transport in porous media ; 15. Kluwer, Dordrecht [u.a.], XII, 429 S. pp.

Moreno, L., Liu, L., Neretnieks, I., 2011. Erosion of sodium bentonite by flow and colloid diffusion. *Physics and Chemistry of the Earth, Parts A/B/C*, 36(17–18): 1600-1606.

SKB, 2009. Mechanisms and models for bentonite erosion. SKB Technical report TR-09-35, Svensk Kärnbränslehantering AB, Stockholm, Sweden.

Witherspoon, P.A., Wang, J.S.Y., Iwai, K., Gale, J.E., 1980. VALIDITY OF CUBIC LAW FOR FLUID-FLOW IN A DEFORMABLE ROCK FRACTURE. *Water Resources Research*, 16(6): 1016-1024.

MICROSTRUCTURE OF BENTONITE AND DILUTE WATER EROSION

Michał Matuszewicz (michal.matuszewicz@vtt.fi), Veli-Matti Pulkkanen, Markus Olin, VTT Technical Research Centre of Finland Ltd, P.O. Box 1000, FI-02044 VTT, Finland

Why to study microstructure?

MX-80 bentonite clay is the reference buffer material in planned repository of spent nuclear fuel in Finland [1]. Repository design imposes strict requirements for the buffer material. Bentonite is one of the materials fulfilling those requirements. Its beneficial properties are based on the high fraction of montmorillonite mineral, the properties of which, in turn, result from its complicated nano- and micrometre scale structure. The montmorillonite could be even called a “native nanomaterial”. Studying the microstructure of compacted bentonite or compacted pure montmorillonite starting from the initial highly compacted state in the disposal and moving towards lower densities gives knowledge about changes in the structure of the material before the erosion process begins. It is necessary to understand these changes in the structure of the bentonite leading to erosion to fully understand the erosion process itself and to build the model predicting the bentonite behaviour.

An evaluation of bentonite applicability as the buffer material will finally be based on macroscopic experiments and modelling. However, as almost all beneficial properties of bentonite are based on the microscopic properties, it is essential to know how macroscopic properties relate to microscopic ones, for example, by characterising both scale properties before and after the experiments. Otherwise, apparently similar macroscopic bentonite samples may be totally different at the microscopic scale. At least some of the observed controversial experimental results may be caused by these types of differences.

Materials and methods

The microstructure of bentonite is studied using a set of complimentary methods. Small-angle X-ray scattering (SAXS), nuclear magnetic resonance (NMR), ion exclusion (IE) and transmission electron microscopy imaging (TEM) are used to characterize the samples' structure. Our approach included state of the art preparation of the frozen and embedded samples for TEM using high pressure freezing (HPF) method and novel NMR measurements in low temperatures.

The materials studied were pure calcium [2] and sodium montmorillonites and MX-80 bentonite. The influence of different procedures of preparation of water-saturated, compacted bentonite samples was tested [3]. The information on microstructure has been collected from the range of different compaction levels and different salinity conditions.

Main findings

The TEM studies showed a clear difference in the microstructure of the MX-80 bentonite and the montmorillonite obtained by the purification of MX-80. Apart from removing the accessory minerals, clusters and aggregates of clay layers have been destroyed and montmorillonite layers organized in a different way. As can be seen in the Figure 1 the platelets seem to be more oriented in the purified clay, whereas in the MX-80 their orientation

appears to be more random. This effect could be caused by the sedimentation after the purification process or the uniaxial compression method used to prepare the sample [4].

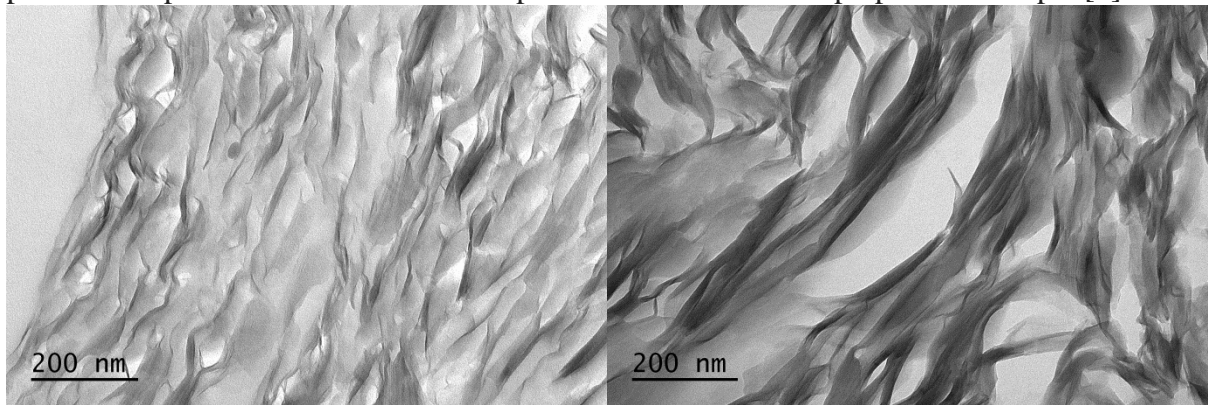


Fig. 1 TEM micrograph of Na-montmorillonite (left) and MX-80 bentonite (right) magnified 23 000 times. Both samples have the bulk dry density of 0.7 g/cm^3 and have been saturated with 0.1 M NaClO_4 solution.

Combining the information from SAXS, NMR and IE quantification of the volume of the slit-like pores between the clay layers (interlamellar (IL) pores)) has been made and compared with the total pore volume. Figure 2 shows the plot of the volume of IL pores in Ca-montmorillonite and in MX-80 bentonite based on the SAXS calculation as a function of dry density of the clay. A clear tendency of forming larger stacked structures is visible for the calcium montmorillonite than for the predominantly sodium MX-80 bentonite.

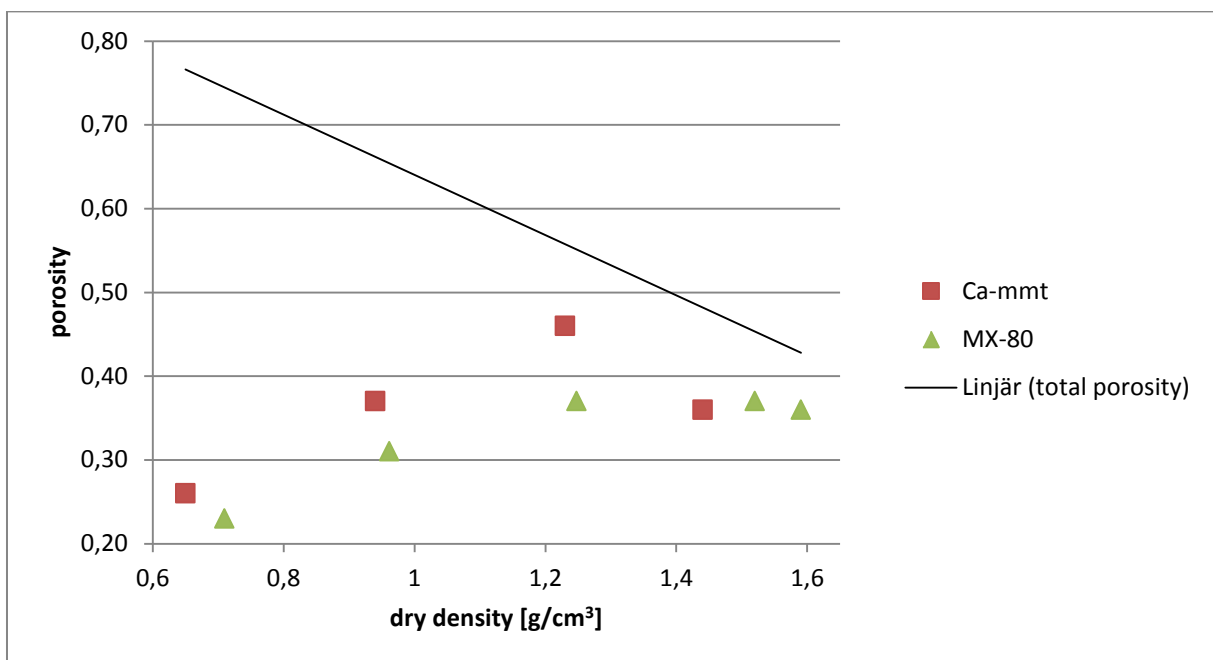


Fig. 2 Estimation of the interlamellar porosity calculated basing on SAXS patterns of the Ca-montmorillonite and MX-80 samples saturated with MilliQ water. The solid line corresponds to the total porosity of the sample

Main applications

The knowledge acquired by the investigation of the microstructure is used to increase the basic understanding of the material and for bentonite model development. Especially, this knowledge is needed to understand the evolution of bentonite structure to a state where bentonite can erode. Consequently, it is an important contribution to ensure the safety of a deep geological disposal of high-level nuclear waste.

References

- [1] M. Juvankoski, "Buffer Design 2012. Posiva Report 2012-14," 2013.
- [2] M. Matuszewicz, K. Pirkkalainen, V. Liljeström, J.-P. Suuronen, A. Root, A. Muurinen, R. Serimaa, and M. Olin, "Microstructural investigation of calcium montmorillonite," *Clay Miner.*, vol. 48, no. 2, pp. 267–276, 2013.
- [3] M. Matuszewicz, V.-M. Pulkkanen, and M. Olin, "Influence of the sample preparation on MX-80 bentonite microstructure," accepted manuscript, *Clay Miner.*
- [4] J.-P. Suuronen, M. Matuszewicz, M. Olin, and R. Serimaa, "X-ray studies on the nano- and microscale anisotropy in compacted clays: Comparison of bentonite and purified calcium montmorillonite," *Appl. Clay Sci.*, vol. 101, no. 0, pp. 401–408, 2014.

BENTONITE EROSION EXPERIMENTS UNDER DYNAMIC CONDITIONS

M. Bouby (muriel.bouby@kit.edu), S. Heck, F. Geyer, T. Schäfer, Karlsruhe Institute of Technology (KIT), Institute for Nuclear Waste Disposal (INE), P.O Box 3640, D-76021 Karlsruhe, Germany

Introduction

Compacted bentonite is considered to be suitable for use as geotechnical barrier in a high level radioactive waste repository in crystalline host rocks. The radionuclides are safely enclosed in the geotechnical barrier if it stays intact, i.e. as long as no water enters the repository. Considering for example the Scandinavian glacial cycles scenario (SKB, 2011), melt water may flow down to repository and enter in contact with the compacted bentonite inducing its swelling and a gel formation at the water interface. Accordingly, the bentonite erosion processes and the interaction of the eroded material with radionuclides may play an important role in the safety assessment of a deep radioactive waste repository in crystalline host rock which has to be fully understood (Missana et al., 2003). To simulate erosion processes under dynamic conditions is the aim of this work. The results obtained will be compared with other ones obtained with different or same bentonite material. This is greatly useful to validate and select the data which can be further used for performance assessment (PA).

Material And Methods

The experimental set-up used to perform bentonite erosion experiments in this study is adapted from (Seher, 2011), see Figure 1. The bentonite used in these experiments is the Volclay bentonite MX80. The brand name MX-80 represents a western, or Wyoming, sodium dominated bentonite supplied by the American Colloid Company. The montmorillonite content is ~ 82 %. The raw material is the one used in two other recent studies (Norrfors et al., 2015; Norrfors et al., 2016). The raw material is first sieved and the fraction < 63 μm is used to prepare Na- and Ca- homo ionic MX80.

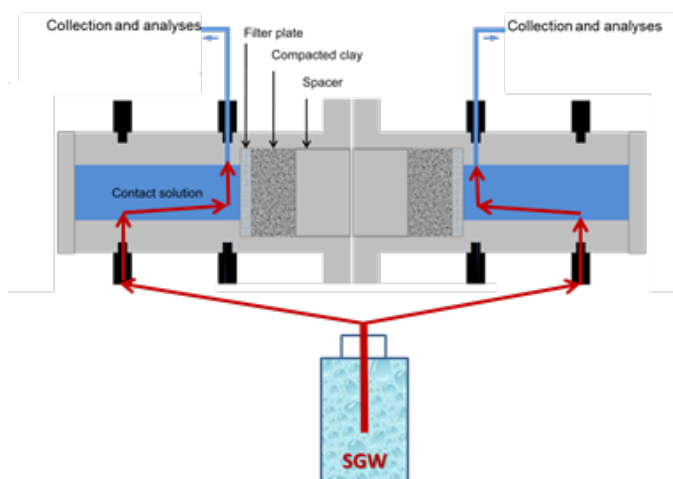


Figure 1: Scheme of one of the double-side reactor used for the erosion experiments.

Raw, Na- and Ca-exchanged MX80 bentonite samples or mixture of both have been compacted in pellets at a density of 1.6 g/cm^3 and placed in 4 double-side reactors. Erosion experiments are conducted by using a synthetic low ionic strength carbonated water (SGW) to simulate the potential effect of glacial melt water on the bentonite

stability (see Table 1 for details). Main and trace elements were analyzed over time in the collected SGW. The element compositions were determined by Ion Chromatography (IC, ICS-3000), ICP-OES (Optima 2000 DV, Perkin elmer) or ICP-MS (X-Series 2, Thermo Scientific, Germany). This allows to plot the breakthrough curves (BCs) for each elements of interest. The BCs represent the evolution of the elemental mass concentrations. The presence of clay colloids is revealed by the detection of their main or trace constituents. This may be confirmed via the calculation of the experimental mole ratios which can be compared to the theoretical ones obtained from the structural formula (see Table 1). Finally, one can follow any mineral dissolution (especially NaCl and CaSO₄).

Results

Samples are regularly taken and analyzed since the beginning of the experiment running now for almost 3 years. The present data summarize the results of the first 2.5 years (907 days), see Table 1. The results are very reproducible. The pH (8.3 ± 0.3) and flow rate (3.0 ± 0.1) $\mu\text{L}\cdot\text{min}^{-1}$ remain constant over the investigated time period.

Some material is clearly produced (detached) and identified as clay according to the concentrations of Si, Al, Mg and Fe recorded (see Figure 2). A clear effect of the initial bentonite pellet composition is evidenced.

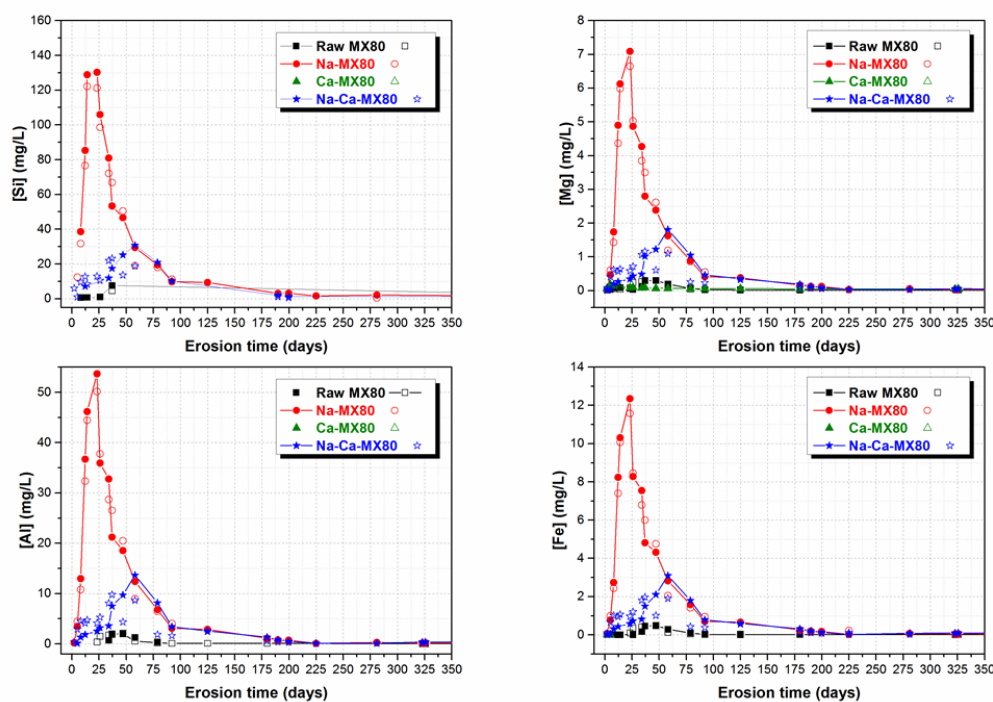


Figure 2: Si, Al, Mg and Fe breakthrough curves (BCs) over the first 9 months

The highest erosion occurs for the Na-exchanged MX80 pellets while (almost) no erosion is observed when using Ca-exchanged ones and it is much more limited when using raw MX80 or the Na-Ca-MX80 pellets. When effective, the colloid production presents maxima after ~25 or 50 days to reach a colloid concentration up to ~ 500 mg/L (for Na-exchanged MX80 compacted pellets). Afterwards, the clay colloid concentration is decreasing to level off after 6 months at ~ < 2 mg/L.

These data are used to determine the mass loss rates (MLR) and average mass loss rates (AMLR) under those specific conditions (see Table 1).

BELBAR PROJECT - WP2 – Final Report- Summary-Erosion experiments- M. Bouby

The sizes of the eroded material collected after ~ 1 month were determined by PCS and presented Table 1. They agree with the sizes already previously reported for clay colloids extracted by centrifugation (Missana et al., 2003; Bouby et al. 2011; Norrfors et al., 2015).

		CLAY PELLET NAME			
		Raw MX80	Na-MX80	Ca-MX80	Na-Ca-MX80
Pre - conditioning		No	Homo ionization in NaCl (1M)	Homo ionization in CaCl ₂ (1M)	Mixture
Mass	g	4.90 and 4.88	4.25 and 4.45	4.90 and 4.89	4.80 and 4.81
Dry Density	g/cm ³	1.6			
Na- or Ca-MX80 percentage in pellet	%	100 % of raw material	100 % Na-MX80	100 % Ca-MX80	50:50 % Na- : Ca- MX80
		EROSION CONDITIONS			
Synthetic carbonated ground water (SGW)		pH = 8.4 ± 0.1 and E _{h(SHE)} = +0.35 ± 0.05 V			
Composition		[Na ⁺] = 1.2 mM, [Ca ²⁺] = 0.05 mM, [F ⁻] = 0.1 mM, [Cl ⁻] = 0.074 mM, [SO ₄ ²⁻] = 0.04 mM, [HCO ₃ ⁻] = 1.0 mM, Si traces			
Ionic Strength		1.6 mM			
Volume		11.6 mL in the reactor (see Fig.1)			
Dynamic conditions (time)		907 days (2.5 years)			
Test duration	hours	21768			
Flow		(3.0 ± 0.1) μL / min 2.3 10 ⁻⁴ m/s			
Sloped	Angle	no			
Free Swelling		no			
Confined		yes			
Fracture dimensions	cm ²	Stainless Steel Porous filter: 20 μm; Surface area: 2.86 cm ² ; porosity 29.4%. frit volume 134.7 μL. real surface contact area: 0.842 cm ²			
Extrusion Distance (Filter Thickness)	cm	0.16			
		RESULTS			
		Raw MX80	Na-MX80	Ca-MX80	Na-Ca-MX80
pH		8.3 ± 0.3	8.3 ± 0.3	8.3 ± 0.3	8.3 ± 0.3
Mass Eluted (colloids)	mg	5.5 ± 0.1	77.8 ± 2.1	none	31.2 ± 6.3
Mass Loss/initial mass	%	0.11 ± 0.01	1.8 ± 0.1	none	0.6 ± 0.1
Mass loss	kg/m ²	0.065 ± 0.001	0.92 ± 0.2	none	0.37 ± 0.07
Average mass loss rate (AMLR)	kg/(y·m ²)	0.026 ± 0.005	0.37 ± 0.01	none	0.15 ± 0.03
		Time used for AMLR calculations 21768 hours / 907 days			
Mass loss rate (MLR)	kg/(y·m ²)	0.051 ± 0.007	1.01 ± 0.02	none	0.37 ± 0.08
		Time used for MLR calculations 7800 hours / 325 days			
		CLAY COLLOIDS CHARACTERIZATION			
Size: hydrodynamic diameter		Raw MX80	Na-MX80	Ca-MX80	Na-Ca-MX80
PCS. f(I)	nm	162 ± 32	131 ± 3	-	132 ± 7
PCS. f(V)	nm	131 ± 98	93 ± 52	-	83 ± 40
Mean Mole ratios (325 days)	Theoretical				
Si/Al	2.49	-	2.54 ± 0.04	none	2.8 ± 0.6
Al/Mg	6.62	5.6 ± 1.2	6.75 ± 0.02	none	6.66 ± 0.01
Al/Fe	7.57	10.2 ± 2.5	8.93 ± 0.13	none	9.0 ± 0.1

Table 1: Results of the dynamic erosion experiment performed in double-sided reactors

A Cs, Eu and U sorption test was performed with the eroded material. Cs is not sorbed. No U sorption can be demonstrated which agrees with our latest results



(Norrfors et al., 2016). As only a partial removal of the clay colloids was possible in this single test (centrifugation at 16192 x g), one can only state that a minimum of 20 % up to 40 % of Eu is sorbed under the present conditions, with apparently a lower sorption on the eroded material obtained from the raw MX80 pellets. Further work is in progress to obtain a more precise Eu sorption quantification as done in (Bouby et al., 2011).

Interestingly, in agreement with literature data and other works (Norrfors et al., 2015), instant releases of sodium, sulphate and chloride are clearly evidenced and attributed to the dissolution of accessory minerals present in the raw bentonite (like gypsum or halide) followed by cationic exchange process.

For the first time, the release of Cs, Th and U have been quantified additionally. Cs behaves, as expected as a cationic exchanger. Th and U BCs behave like the Al ones and can thus be considered as clay trace components. This is very interesting as these elements are more easily detectable by ICP-MS. In the present case, it permits to detect the non-expected erosion occurring for the Ca-MX80 compacted clay pellet. The Cs, Th and U amounts released have been calculated and normalized (see Table 2). It is thus possible to take into account the potential amount of natural radionuclides released by the backfill material itself. This has probably to be consider in PA.

CATION RELEASES					
		Raw MX80	Na-MX80	Ca-MX80	Na-Ca-MX80
Cs	Days (d)				
Mass Released ($\mu\text{g/g}$) ($\mu\text{g/g/y}$)	907	0.04 ± 0.02	0.036 ± 0.002	1.58 ± 0.05	0.4 ± 0.1
Mass Rate Release (kg/m^2) ($\text{kg/m}^2/\text{y}$)		0.017 ± 0.008	0.015 ± 0.001	0.64 ± 0.02	0.14 ± 0.05
		$(2.4 \pm 1.2) 10^{-6}$ $(9.7 \pm 4.7) 10^{-7}$	$(1.87 \pm 0.02) 10^{-6}$ $(7.53 \pm 0.07) 10^{-7}$	$(9.2 \pm 0.3) 10^{-5}$ $(3.7 \pm 0.2) 10^{-5}$	$(2.0 \pm 0.7) 10^{-5}$ $(8.1 \pm 2.7) 10^{-6}$
Th					
Mass Released ($\mu\text{g/g}$) ($\mu\text{g/g/y}$)	907	0.056 ± 0.003	0.53 ± 0.02	0.012 ± 0.004	0.21 ± 0.05
Mass Rate Release (kg/m^2) ($\text{kg/m}^2/\text{y}$)		0.023 ± 0.001	0.21 ± 0.01	0.005 ± 0.002	0.08 ± 0.02
		$(3.3 \pm 0.2) 10^{-6}$ $(1.32 \pm 0.08) 10^{-6}$	$(2.73 \pm 0.02) 10^{-5}$ $(1.1 \pm 0.01) 10^{-5}$	$(7.2 \pm 2.4) 10^{-7}$ $(2.9 \pm 0.9) 10^{-7}$	$(1.2 \pm 0.3) 10^{-5}$ $(4.8 \pm 1.2) 10^{-6}$
U					
Mass Released ($\mu\text{g/g}$) ($\mu\text{g/g/y}$)	907	0.07 ± 0.02	0.154 ± 0.005	0.13 ± 0.07	0.07 ± 0.02
Mass Rate Release (kg/m^2) ($\text{kg/m}^2/\text{y}$)		0.026 ± 0.007	0.062 ± 0.002	0.05 ± 0.03	0.029 ± 0.006
		$(3.8 \pm 1.0) 10^{-6}$ $(1.5 \pm 0.4) 10^{-6}$	$(8.0 \pm 0.02) 10^{-6}$ $(3.21 \pm 0.01) 10^{-6}$	$(7.8 \pm 4.0) 10^{-6}$ $(3.1 \pm 1.6) 10^{-6}$	$(4.2 \pm 0.9) 10^{-6}$ $(1.7 \pm 0.4) 10^{-6}$

Table 2: Cs, Th and U releases during the dynamic MX80-bentonite erosion experiments.

References

- (SKB, 2011) Long-Term Safety for the Final Repository for Spent Nuclear Fuel at Forsmark, Main Report of the SR-Site Project. SKB technical report TR -11-01. Svensk Kärnbränslehantering AB.
- (Missana et al., 2003) Missana, T., Alonso, U., Turrero, M.J., 2003. Generation and stability of bentonite colloids at the bentonite/granite interface of a deep geological radioactive waste repository. J. Cont. Hydrol., 61, 17-31.
- (Seher, 2011) Seher, H. Influence of colloids on the migration of radionuclides, PhD thesis, University of Heidelberg, Faculty of Chemistry and Earth Sciences.
- (Norrfors et al., 2015) Norrfors, K.K., Bouby, M., Heck, S., Finck, N., Marsac, R., Schäfer, T., Geckeis, H., Wold, S. (2015) Montmorillonite colloids: I. Characterization and stability of dispersions with different size fractions. Applied Clay Science, 114, pp. 179-189.
- (Norrfors et al., 2016) Norrfors, K.K., Marsac, R., Bouby, M., Heck, S., Wold, S., J. Lützenkirchen, J.; Schäfer, T., (2016) Montmorillonite colloids: II. Colloidal Size Dependency on Radionuclide Adsorption, under Revision, Applied Clay Science.
- (Bouby et al., 2011) Bouby, M.; Geckeis, H.; Lützenkirchen, J.; Mihai, S.; Schäfer, T. (2011) Interaction of bentonite colloids with Cs, Eu, Th and U in presence of humic acid: a Flow Field-Flow Fractionation study. GCA, 75, 3866-3880.



MONTMORILLONITE COLLOIDS. I: CHARACTERIZATION AND STABILITY OF DISPERSIONS WITH DIFFERENT SIZE FRACTIONS. II: DEPENDENCY OF COLLOIDAL SIZE ON SORPTION OF RADIONUCLIDES. III: INFLUENCE OF COLLOIDAL SIZE ON THE SORPTION REVERSIBILITY OF RADIONUCLIDES

K.K Norrfors^{1,2,3}, (norrfors@kth.se), M. Bouby¹ (muriel.bouby@kit.edu), R. Marsac¹, J. Lützenkirchen¹, S. Heck¹, N. Finck¹, S. Wold², T. Schäfer¹, ¹: Karlsruhe Institute of Technology (KIT), Institute for Nuclear Waste Disposal (INE), P.O Box 3640, D-76021 Karlsruhe, Germany, ²: School of Chemical Science and Engineering, Applied Physical Chemistry, KTH Royal Institute of Technology, Teknikringen 30, SE-10044 Stockholm, Sweden, ³: Present address, ÅF, Frösundaleden 2A Stockholm, 169 99 Sweden.

Introduction

Bentonite is envisaged as a suitable hostrock/backfill material in most designs of high level radioactive waste repositories. The main component of the bentonite (for example the montmorillonite) belongs to the smectite group. Smectites are 2:1 phyllosilicates which are intrinsically small nanoparticles, i.e. particles of 1 nm-1 µm in at least one dimension, which hydrate and swell in contact of water, leading to a gel formation. Under specific (ground-)water conditions, the gel can take a *sol* character (SKB, 2011). The clay colloids potentially generated in the nuclear waste repository near-field from the bentonite-buffer/backfill material might be stable under geochemical conditions prevailing in the fractured rock far-field and could be a carrier of radionuclides (Bouby et al., 2011). Colloid mobility is strongly depending on fracture geometry (aperture size distribution and fracture surface roughness) as well as chemical heterogeneity induced by the different mineral phases present in the fracture filling material and the chemistry of the matrix porewater. The mobility of clay colloids will not necessarily enhance the mobility of strong sorbing radionuclides (RNs) if the sorption is reversible. Strong radionuclide clay colloid sorption reversibility kinetics have frequently been observed, but the reasoning for the observed kinetics is still pending.

The aim of this work is to complete the actual knowledge regarding clay colloid facilitated transport of RNs by studying the influence of the bentonite colloid size on the radionuclide sorption and its reversibility.

I: Characterization and stability of dispersions with different size fractions

The bentonite used in these experiments is the Volclay bentonite MX80. The brand name MX-80 represents a sodium dominated, Wyoming bentonite, supplied by the American Colloid Company. The montmorillonite content is ~ 82 %. A protocol for size fractionation of clay colloids was developed by sequential and direct centrifugation, in the presence and in the absence of organic matter. Seven colloidal fractions are obtained (S0, S1, S2, S3, S3.5, S3.5^{UC}) ranging, when considering the mean equivalent hydrodynamic sphere diameter, from ~ 950 nm down to ~ 85 nm. When applying mathematical treatments and approximating the clay particles to regular disc-shaped entities, the mean surface diameters varies from ~1.5 µm down to ~190 nm. Detailed characterization of the colloidal fractions is done by XRD, IC and ICP-OES, and they present the same chemical composition. The total number of edge sites (aluminol and silanol) is estimated (in mol/kg) for each colloidal fraction according to literature data and is found to vary significantly between the different size fractions. In addition,



stability studies of the colloidal fractions are performed by addition of NaCl, CaCl₂ or MgCl₂, in the presence or in the absence of organic matter, like fulvic acids (FA), where no differences in stability between the different clay colloidal size fractions are found. All the results are presented in details in (Norrfors et al., 2015).

II: Dependency of colloidal size on sorption of radionuclides

In this work, radionuclides (Th(IV), U(VI), Np(V), Tc(VII) and Pu(IV)) sorption onto size fractionated montmorillonite colloids is experimentally studied in a synthetic, carbonated groundwater (SGW) at pH 8.4 and low ionic strength (IS) < 2. 10⁻³ M and predicted by modeling as well. U(VI), Np(V) and Tc(VII) do not sorb to the montmorillonite colloids in the present SGW. The uptake of Th(IV) ($K_D = 6.4 \pm 0.5$ dm³/kg) and Pu(IV) ($K_D = 5.7 \pm 0.5$ dm³/kg) to montmorillonite colloids is high and does not appear to be significantly affected by the colloidal mean size. In the presence of organic matter during fractionation of clay colloids, sorption of Th and Pu is reduced significantly. These results are illustrated for two colloidal clay suspensions (mean size < 250 nm) with or without FA in Figure 1 below. All the results are presented in details in (Norrfors et al., 2016a).

In conclusion, the size of the colloids does not seem to play a role on the RNs sorption retention process. Small clay colloids can thus be considered as miniatures of bigger ones. **MAIN IMPLICATION:** Based on the results, implementation of an “average log K_D ” (i.e. average distribution coefficient) for all colloidal sizes in reactive transport modelling codes would be acceptable.

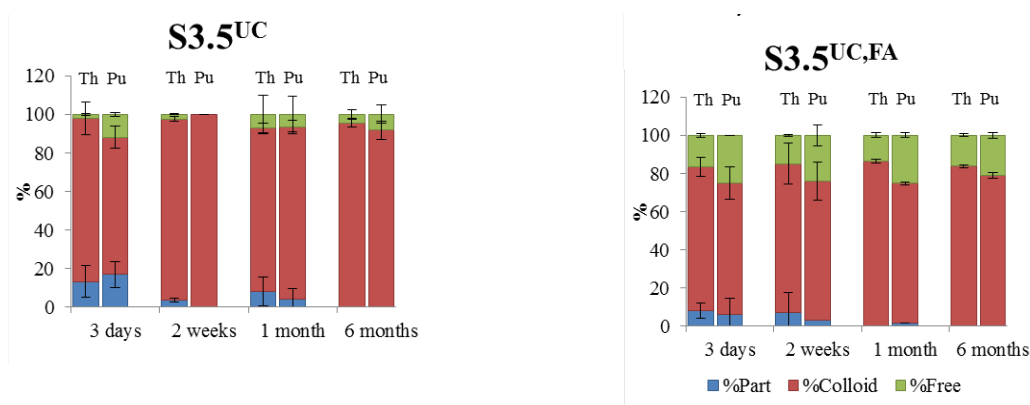


Figure 1: Th (left histogram) and Pu (right histogram) distribution in % for each equilibration time (x-axis) between clay particulates (%Part, blue), stable clay colloids (%Colloid, red) or soluble species (%Free, green) for two clay dispersions (mean size < 250 nm), with or without FA present. In the presence of FA (S3.5^{UC,FA}), no distinction between soluble RNs and FA-RN complexes is possible. The values presented are mean values of duplicates with its standard error.

III: Influence of colloidal size on the sorption reversibility of radionuclides

This part of the work examined the radionuclides’ sorption reversibility, or progression, onto the size-fractionated montmorillonite colloids (see part I and II) after i) decreasing the pH, ii) increasing the ionic strength (IS), iii) adding crushed bed rock material (CBM) or iv) fulvic acids (FA) as competing ligand. This is investigated for various contact times (3 days, 2 weeks, 1 month, 6 months) between the clay suspensions and the RNs added before the desorption/reversibility test starts.

i. pH decrease: 1 week at pH 7.5 and 1 year at pH 2.7



Np is unaffected, whatever the initial contact time, and remains “free”(i.e. as aqueous species) in suspension.

Tc remains free after 1 week at pH 7.5, however after 1 year at pH 2.7 the free Tc fraction is > 80%, the rest is found in the particulate phase (i.e. eigen-colloids-and/or Tc-associated to sedimented clay colloids).

U is sorbed onto the different montmorillonite size fractions after 1 week at pH 7.5 as the competition with carbonates is lower at that pH **except in** the suspension containing FA during fractionation, since FA compete with the clay colloids for the U sorption. After 1 year at pH 2.7, the U is found 100 % free in suspensions. **The U sorption is reversible at that rather low pH.**

Th is initially sorbed (> 95 %) to all clay colloidal fractions, even in the presence of FA (> 80 %). This does not change after decreasing the pH during 1 week at 7.5 except that it strengthens the competition with FA (~ 10 % more Th-FA complexes). After 1 year at pH 2.7, whatever the initial sorption contact times, 80 ± 5 % of Th are desorbed from the clay colloids. The remaining Th clay sorbed fraction should be further characterized. **The Th sorption is partly reversible at rather low pH.**

Pu: whatever the contact times 85 up to 100 % Pu are sorbed to the clay colloidal fractions. In the presence of FA it reduces down to ~ 70%. After one week at pH 7.5 without FA present the results remain unchanged. In the presence of FA, at that pH, only 40-60 % of Pu remains associated to clay colloids. After 1 year at pH 2.7 and in the absence of FA, surprisingly, only 10 to 15 % of Pu is free, the rest is found under particulates state which should be further characterized. In the presence of FA, 40-50 % Pu is found free or FA-complexed. **Thus, in the absence of FA, the Pu remains associated to clay material at that rather low pH while the presence of FA increases the labile Pu fraction.**

ii. Ionic strength (IS) increase: 0.5 M IS CaCl₂ at pH 7.4

At 0.5 M IS CaCl₂, the clay colloids are unstable and sediment.

Np and Tc: are unaffected and remain free in suspension. **U** remains in suspension. As this contradicts the results found by a decrease in pH to 7.5, it indicates the higher strength of the Ca-U(VI)-CO₃ complexes compared to the U(VI)-clay colloid-bound species.

Th and Pu initially sorbed remain associated with the clay colloids which sediment. **In conclusion,** at 0.5 M IS CaCl₂ and under the present water conditions, Np, Tc and U remain free in suspension. Th and Pu sorbed prior to the addition of CaCl₂ remain associated with the colloids which sediment. Thus, they do not present any sorption reversibility.

iii. Addition of CBM: solid:liquid ratio is 1:4

The clay colloids do not interact with the CBM.

Np is transferred to the particulate phase whatever the colloidal size fraction investigated after addition of CBM. This is kinetically controlled: 50 ± 10 % of Np are transformed after 1 week and ~100 % after 1 year. This might be attributed to the slow reduction of Np(V) to Np(IV) accompanied by the formation of Np(IV)-eigen colloids. The reduction can be explained by the presence of iron into the granidiorite. **Tc** behaves similar to Np.

U is sorbed onto the CBM (~ 60 to 80 %) after 1 week. This percentage is reduced after 1 year which might be due to the competition with carbonates or the release of natural U from the CBM.



Th is initially mainly sorbed to the clay colloids. After 1 week of desorption in contact with the CBM, the results are the same. But after 1 year, drastic changes are observed where the contact time prior to the addition of the CBM and the clay colloidal size fractions play a role. A longer sorption contact time reduces the desorption in favour of the CBM, and the smaller clay colloid sized fractions (mean size < 250 nm) keep better sorbed the **Th**. **Pu**: behaves like **Th**.

In conclusion, in the presence of CBM, under the present water conditions, **Np**, **Tc** and **U** are mainly sorbed and immobilized. **Th** and **Pu** sorption to clay colloids is partly reversible in the presence of CBM, it is lower for increasing sorption contact time before desorption, and significantly reduced for the smallest sized clay colloidal fraction.

iv. Addition of FA (5 mg.L⁻¹) with a delay, i.e. after different contact time

Tc, **Np** and **U**: are unaffected and remain as aqueous species in suspension.

Th: no strong desorption (not more than 10 % after 1 year), whatever the mean clay colloidal size.

Pu: For shorter sorption contact times before the addition of FA, the desorption/complexation by the FA is higher and can reach up to 20%. In addition, a higher desorption/FA-complexation is observed for the smallest clay colloid size fraction (<250 nm). Nevertheless, even after 1 year desorption time, the reversibility is not 100%. More details can be found soon in (Norrfors et al, 2016b).

In conclusion, the reversibility is not guaranteed in this colloidal systems and when it occurs it greatly depends on the geochemical parameters (pH, IS, competing material).

MAIN IMPLICATION: This contradicts a statement previously formulated in the treatment of the colloids in the SAFETY CASE. The position when the BelBar project started was “Reversible, linear sorption of radionuclides onto colloids has been assumed”.

References

(SKB, 2011) Long-Term Safety for the Final Repository for Spent Nuclear Fuel at Forsmark, Main Report of the SR-Site Project. SKB technical report TR -11-01. Svensk Kärnbränslehantering AB.

(Bouby et al., 2011) Bouby, M.; Geckeis, H.; Lützenkirchen, J.; Mihai, S.; Schäfer, T. (2011) Interaction of bentonite colloids with Cs, Eu, Th and U in presence of humic acid: a Flow Field-Flow Fractionation study. GCA, 75, 3866-3880.

(Norrfors et al., 2015) Norrfors, K.K., Bouby, M., Heck, S., Finck, N., Marsac, R., Schäfer, T., Geckeis, H., Wold, S. (2015) Montmorillonite colloids: I. Characterization and stability of dispersions with different size fractions. Applied Clay Science, 114, pp. 179-189.

(Norrfors et al., 2016a) Norrfors, K.K., Marsac, R., Bouby, M., Heck, S.; Wold, S.; Lützenkirchen, J.; Schäfer, T.(2015) Montmorillonite colloids: II. Colloidal size dependency on radionuclide adsorption. Applied Clay Science, 2016, under revision.

(Norrfors et al., 2016 b) Norrfors, K.K., Bouby, M., Heck, S., Finck, N., Marsac, R., Schäfer, T., Geckeis, H., Wold, S. (2015) Montmorillonite colloids: III. Influence of colloidal size on the sorption reversibility of radionuclides. Applied Clay Science, 2016, under preparation.

This work was carried out entirely at KIT-INE by Mrs K.K. Norrfors, in the frame of her PhD. We have accordingly contributed to a “training education”.



INFLUENCE OF ORGANIC MATTER (FULVIC ACIDS, FA) ON THE (LONG TERM) STABILITY OF CLAY COLLOIDS PREPARED UNDER DIFFERENT CHEMICAL CONDITIONS

M. Bouby (muriel.bouby@kit.edu), Y. Heyrich, S. Heck, S. Hilpp, T. Schäfer; Karlsruhe Institute of Technology (KIT), Institute for Nuclear Waste Disposal (INE), P.O Box 3640, D-76021 Karlsruhe, Germany

Introduction

Bentonite is envisaged as a suitable hostrock/backfill material in most designs of high level radioactive waste repositories. The main mineral component in bentonites belongs to the smectite clay group. Smectites are 2:1 phyllosilicates. If they enter in contact with the water coming from the geological formation where the repository is placed, they will hydrate and swell. A *gel* will form able to penetrate all available pore spaces (open rock fissures, joints, ...). Under specific (ground) water conditions, i.e low concentration of dissolved ions (like those found in low saline waters such as fresh age ice waters), the gel can take a *sol* character (SKB, 2011). Erosion processes can thus occur at the gel front and colloidal particles can be released if the geochemical conditions ensure their stability. In the worst case, this will lead to a decrease of the mass of the bentonite barrier available with strong consequences (like for example a loss of the expected and desired diffusion control). As clay colloids released could be carriers of radionuclides, their stability and transport may have a significant impact on the radionuclide dissemination in the geosphere. Clay colloid stability is thus one of the key question for predicting their potential influence on the migration of radionuclides (Missana et al., 2003). This is greatly dependent of the geochemistry of the environmental medium and in particular of chemical parameters like the pH, the ionic strength, the ionic composition and the natural presence of in/organic complexing agents among with the humic substances (humic and fulvic acids). According to our previous work (Bouby et al., 2011), performed over a 3 years period, the clay colloids undergo a continuous agglomeration process even in natural ground water where conditions were first thought to be ideal for clay colloid stabilization: high pH (8-9) under low ionic strength conditions. The water chemistry and mainly the Ca^{2+} concentration were thought to determine the colloid size distribution. The aim of this additional experimental work program is to examine in more details the individual effects of 1) specific cations (CO_3^{2-} , Ca^{2+} , Na^+ , ...) and 2) the addition of fulvic acids, as a potential source of dissolved organic carbon (DOC), on the clay colloid stability over a short (fast coagulation experiments) or a long time period (suspensions ageing), since FA is known to stabilize montmorillonite colloids (Furukawa and Watkins, 2012).

Material and methods

The MX80 bentonite colloid stability is examined systematically under different chemical conditions, starting from a delaminated bentonite clay suspension.

The raw material is first sieved and the fraction $< 63 \mu\text{m}$ is used. Clay suspensions (6 x 1L) are prepared at 10 g/ L in LiCl 1M. After 1 week, the suspensions are centrifuged, rinsed and re-suspended in 6 different aqueous media simulating natural waters at low ionic strength ($\text{IS} = 1.3 \cdot 10^{-3} \text{ M}$). These rinsing aqueous media consist in 1) ultra pure water (MQ) at pH 5.7, 2) NaCl $1.3 \cdot 10^{-3} \text{ M}$ at pH ~ 5.7 , 3) CaCl_2 $0.433 \cdot 10^{-3} \text{ M}$ at pH ~ 5.7 ; 4) NaHCO_3 10^{-3} M at pH ~ 8.4 , 5) a SGW at pH ~ 8.5 and 6) a SGW at pH ~ 5 .



The acronym SGW is used for Synthetic Ground Water as it is supposed to simulate a glacial melt water with Na^+ , Ca^{2+} , SO_4^{2-} , Cl^- , F^- , trace of Si and with or without HCO_3^- resulting in 2 different pHs (see Norrfors et al., 2015 for the detailed composition). The colloidal suspensions obtained after the fourth centrifugation/rinsing/re-suspension step become the colloidal clay stock suspensions.

Results

The results of the first analysis (obtained from IC, ICP-OES and PCS) of the 6 clay colloidal stock suspensions are summarized in Table 1. It appears clearly that the composition of the SGW strongly influenced the clay colloidal production.

	Aqueous media	[Colloids] 4 th supernatant	pH 4 th supernatant	Size range nm (PCS)
1	MQ (pH 5.7)	1.95 g.L ⁻¹	9.9	270-300
2	NaCl 1.3 10 ⁻³ M (pH 5.7)	1.38 g.L ⁻¹	9.9	240-300
3	CaCl ₂ 0.433 10 ⁻³ M pH 5.7	1.56 g.L ⁻¹	9.9	240-350
4	NaHCO ₃ 10 ⁻³ M pH 8.5	1.59 g.L ⁻¹	9.6	270-310
5	SGW pH ~ 8.5	0.92 g.L ⁻¹	9.3	290-350
6	SGW ~ pH 5.7	0.87 g.L ⁻¹	9.7	270-320

Table 1: Characterization of 6 clay colloidal stock suspensions after preparation

i) Fast coagulation experiments

These studies are performed using PCS measurements according to the experimental protocol described in Behrens et al., 2000; Czigány et al., 2005; Holthoff et al., 1996; Kretzschmar et al., 1998.

In this study, the clay colloid concentration is fixed to 10 mg/L by prior dilution in the corresponding aqueous media (1 to 6) with or without additional fulvic acids (FA) at 2.5 mg/L (1,5 mg/L NPOC). The ionic strengths (IS) examined were 0.1 M, 1M and 3 M set by using the electrolytes NaCl, CaCl₂ or MgCl₂.

The pHs are indicated Table 2. They are comparable to those of the aqueous media used for the clay colloid stock suspensions.

The initial intensity-weighted hydrodynamic mean diameter is first measured during 45 s and the corresponding values are reported Table 2. Note that in presence of CaCl₂ (aqueous media number 3), the clay colloids present a mean hydrodynamic diameter significantly larger than in the other aqueous media, due to the calcium ion acting slowly as a coagulant, even at low concentration. The presence of FA might have slowed down this process (see Table 2). This has to be further investigated.

The evolution of the hydrodynamic diameter of the clay colloids is monitored, after affecting the suspension by simultaneous addition of concentrated electrolyte aliquots (NaCl, CaCl₂ or MgCl₂).

All samples are measured up to between 10 and 40 min after addition of the electrolyte, with measurements of 15 s each.

The initial agglomeration rates were presently not determined and the data were only examined qualitatively. The main observations are summarized below:



Suspensions	pH	t=0	NaCl			CaCl ₂			Mg		
		∅ nm	IS 0,1 M	IS 1 M	IS 3 M	IS 0,1 M	IS 1 M	IS 3 M	IS 0,1 M	IS 1 M	IS 3 M
1	6.5±0.1	280 ± 22	yes	yes	yes	yes	yes	yes	yes	yes	yes
1FA	6.4±0.1	269 ± 9	no	yes	yes	yes	yes	yes	yes	yes	yes
FA effect			stabilisation	no	no	no	no	no	no	no	no
2	6.1±0.1	255 ± 16	yes	yes	yes	yes	yes	yes	yes	yes	yes
2FA	6.2±0.1	257 ± 20	no	yes	yes	yes	yes	yes	yes	yes	yes
FA effect			stabilisation	no	no	no	no	no	no	no	no
3	6.1±0.1	431 ±50	yes	yes	yes	yes	yes	yes	yes	yes	yes
3FA	6.2±0.1	381 ±33	no	yes	yes	yes	yes	yes	yes	yes	yes
FA effect			stabilisation	no	no	no	no	no	no	no	no
4	8.5±0.1	307 ± 62	yes	yes	yes	yes	yes	yes	yes	yes	yes
4FA	8.4±0.1	250 ± 30	no	yes	yes	yes	yes	yes	yes	yes	yes
FA effect			stabilisation	no	no	no	no	no	no	no	no
5	8.4±0.1	320 ± 28	yes	yes	yes	yes	yes	yes	yes	yes	yes
5FA	8.3±0.1	292 ± 20	yes, reduced	yes	yes	yes	yes	yes	yes	yes	yes
FA effect			kinetic	no	no	no	no	no	no	no	no
6	6.3±0.1	268 ± 30	yes	yes	yes	yes	yes	yes	yes	yes	yes
6FA	6.4±0.1	249 ± 27	yes, reduced	yes	yes	yes	yes	yes	yes	yes	yes
FA effect			kinetic	no	no	no	no	no	no	no	no

Table 2: Main observations during the coagulation experiments followed by PCS, yes: agglomeration detected, no: no agglomeration detected in the experimental time frame, FA effect observed: no: none, stabilization or kinetic effect

In CaCl₂ and MgCl₂ media and [IS] = 0.1 M, 1 M and 3 M, the clay colloids agglomerate immediately and already significantly in the first 15 s. This is also the case in NaCl media at [IS] = 1 M and 3 M. These observations are true whatever the aqueous media and their pH which indicates that the IS value is the key parameter under those conditions tested. In addition the additional presence of 2.5 mg/L FA (1.5 mg/L NPOC) does not influence the results and does not prevent the fast agglomeration of the clay colloids.

In NaCl medium at 0.1 M IS, the results are different. First, in absence of FA, the clay colloids agglomerate but with a lower rate as that observed at 1 or 3 M IS. In presence of FA, the colloids do not agglomerate anymore in four of the aqueous media tested: 1, 2, 3 and 4 (see Table 1 for details) and the agglomeration is kinetically hindered in the SGW prepared with or without NaHCO₃.

This observation is consistent with the one reported by Cervinka et al. in the frame of the BelBar project (see deliverable D4.6), working under conditions corresponding to our aqueous medium number 1 (ultrapure water alone) and testing the coagulation kinetics of clay dispersion in NaCl electrolyte in presence or not of organic matter (humic acid (HA)). Accordingly, the results are very similar independently of the source of the OM.

This shows in addition that one or a combination of the other ions present in the SGW counterbalances the prevention of the clay colloids agglomeration induced by the presence of FA. This point calls for further investigations.

Conclusions of the fast coagulation study: whatever the aqueous media in which the clay colloids are obtained, they present the same coagulation behavior at moderate to

high IS (0.1 M, 1 M and 3 M) in NaCl, CaCl₂ or MgCl₂ electrolytes. In 0.1 M NaCl nevertheless, the coagulation rate is slowed down. The presence of FA only prevents or disturbs the clay colloids coagulation in 0.1 M NaCl but in none of the other conditions tested. Interestingly, those results are comparable with previously reported ones performed with clay colloids and organic matter of different origins.

ii) Long term study

A great number of batch samples have then been prepared from these 6 colloidal clay suspensions to study the colloid stability over a long time period, at least 4 years, which means beyond the end of the project.

They consist finally in suspensions at different colloid concentration (1, 5, 10 and 100 mg/L) in each of the 6 pre-cited electrolytes. The influence of organic matter (OM) is examined in parallel by preparing the batch samples once again after adding, prior to the dilution, 2.5 mg/L fulvic acids (FA-573, Gorleben site, Lower Saxony, Germany) in each of the pre cited electrolytes. This represents 1.5 mg/L NPOC. The samples are stored in the laboratory (at ~ 21-22°C) but preserved from the light.

Exemplarily, two of them from the set number 6, containing FA have been analysed. These preliminary investigations are very promising.

The samples were first examined prior to any shaking. The pH remains constant at respectively 6.4 ± 0.1 in these two samples and they present a mean effective intensity-weighted clay colloids diameter of (205 ± 16) nm. Shaking the samples has no influence on the pH values but significant differences in the colloid sizes are then reported, with a value > 310 nm in both cases. It agrees with the colloidal concentrations measured before and after shaking which reveal a gradient. Actually the upper part of the samples contains only 60 up to 71 % of the colloids. This indicates that under the present experimental conditions representative of a glacial melt water at quasi-neutral pH (SGW at pH 6.4 and low IS) the clay colloids undergo a slow agglomeration process even in the presence of organic matter (2.5 mg/L FA representing 1.5 mg/L NPOC). These measurements have to be continued systematically which will allow a very interesting comparison between different experimental conditions over a long time period.

References

- (SKB, 2011): Long-Term Safety for the Final Repository for Spent Nuclear Fuel at Forsmark, Main Report of the SR-Site Project. SKB technical report TR -11-01. Svensk Kärnbränslehantering AB.
- (Missana et al., 2003) Missana, T., Alonso, U., Turrero, M.J., 2003. Generation and stability of bentonite colloids at the bentonite/granite interface of a deep geological radioactive waste repository. *J. Cont. Hydrol.*, 61, 17-31.
- (Bouby et al., 2011) Bouby, M.; Geckeis, H.; Lützenkirchen, J.; Mihai, S.; Schäfer, T. (2011) Interaction of bentonite colloids with Cs, Eu, Th and U in presence of humic acid: a Flow Field-Flow Fractionation study. *GCA*, 75, 3866-3880.
- (Norrfors et al., 2015) Norrfors, K.K., Bouby, M., Heck, S., Finck, N., Marsac, R., Schäfer, T., Geckeis, H., Wold, S. (2015) Montmorillonite colloids: I. Characterization and stability of dispersions with different size fractions. *Applied Clay Science*, 114, pp. 179-189.
- (Behrens et al., 2000) Behrens, S.H., Christl, D.I., Emmerzael, R., Schurtenberger, P., Borkovec, M., 2000. Charging and Aggregation Properties of Carboxyl Latex Particles: Experiments versus DLVO Theory. *Langmuir* 16, 2566-2575.
- (Czigany et al., 2005) Czigány, S., Flury, M., Harsh, J.B., 2005. Colloid Stability in Vadose Zone Hanford Sediments. *Environmental Science & Technology* 39, 1506-1512.
- (Holthoff et al., 1996) Holthoff, H., Egelhaaf, S.U., Borkovec, M., Schurtenberger, P., Sticher, H., 1996. Coagulation Rate Measurements of Colloidal Particles by Simultaneous Static and Dynamic Light Scattering. *Langmuir* 12, 5541-5549.
- (Kretzschmar et al., 1998) Kretzschmar, R., Holthoff, H., Sticher, H., 1998. Influence of pH and Humic Acid on Coagulation Kinetics of Kaolinite: A Dynamic Light Scattering Study. *Journal of Colloid and Interface Science* 202, 95-103



(Furukawa and Watkins, 2012) Furukawa, Y., Watkins, J.L., 2012. Effect of Organic Matter on the Flocculation of Colloidal Montmorillonite: A Modeling Approach. *J. Coast. Res.* 28, 726-737



THE SURFACE PROPERTIES AND CS ADSORPTION OF NATURAL AND ACID-MODIFIED MONTMORILLONITES

V.V. Krupskaya (krupskaya@ruclay.com), S.V. Zakusin, Lomonosov Moscow State University, Institute of Ore Geology, Petrography, Mineralogy, and Geochemistry (IGEM) RAS, O.V. Dorzhieva, Institute of Ore Geology, Petrography, Mineralogy, and Geochemistry (IGEM) RAS, Geological Institute RAS, M.S. Chernov, Lomonosov Moscow State University (MSU), E.A. Tyupina, Mendeleev University of Chemical Technology of Russia (RHTU)

Bentonite (montmorillonite) clay is widely used in various industries, including nuclear power and particularly radioactive waste management as a component of engineered barrier systems for the radioactive waste disposal (Sellin and Leopin, 2013). The main component of bentonite clay is a dioctahedral smectite — montmorillonite. Due to of isomorphic substitutions in the 2:1 layer it obtains charge, which is compensated by hydrated interlayer cations. Features of the montmorillonite structure determine specific properties of bentonite clays, especially its high sorption capacity, specifically for heavy metals and radionuclides. During a long term operation of radioactive waste disposal site, engineered barriers based on bentonite may be exposed to thermochemical effects, which, for instance, can be modeled by brief treatment with nitric acid solutions at an elevated temperature (90°C).

The aim of this research is to assess the mechanism of montmorillonite's structure and the adsorption properties transformation in the process of the long-term interaction with a nitric acid solution. Natural clay samples from Dashkovsky deposit (Moscow region) and Tagansky deposit (Kazakhstan) have been used as objects for the study. Structural features were studied using X-ray diffraction and infrared spectroscopy, particle interaction in bentonite suspension — with scanning electron microscopy, modification of surface properties was assessed by specific surface area estimation, changes of adsorption properties — by evaluation of the cation exchange capacity and the adsorption of Cs-133 and Cs-137.

The suit of methods allows us to simulate the mechanisms of structural transformations of montmorillonite as a result of exposure to nitric acid, which are expressed in the leaching of interlayer cations, partial interlayer protonation (substitution of interlayer cations to oxonium ion), leaching octahedral cations of the positions, partial destruction of the layer 2:1 structure. It was noted by other authors (Timofeeva et al., 2015, and others) that Fe and Mg are less stable to leaching than Al. Thus, montmorillonites with mainly Al in octahedral sheet and a small amount of Mg substitution, are more resistant to thermochemical treatment compared to montmorillonites with a significant degree of Fe to Al substitution. Lack of octahedral cations results in a change of the layer charge, which is noticeably manifested when processing Taganskiy montmorillonite compared with Dashkovskiy montmorillonite which is generally shows greater stability to acid exposure. A significant reduction in the charge layer leads to the formation of pyrophyllite-like structures with a layer charge close to 0. These structural changes are traced according results of X-ray diffraction and infrared spectroscopy methods (Fig. 1). Transformation of structural characteristics, and, primarily, reduction of the charge and its redistribution between tetrahedral and octahedral sheets resulting thermochemical effects modifies the interaction of montmorillonite particles in pore space.

This transformation can be visualized by changes of the bentonite suspension microstructure using a scanning electron microscope (Fig. 2). The described reduction of the Tagansky montmorillonite layer charge is already noticeable after 1 hour of treatment with nitric acid, and by increasing the exposure time up to 5 hours montmorillonite particles completely lose their ability to interact with each other. In turn, the Dashkovsky montmorillonite particles retain the ability to form microaggregates which are characteristic for smectites even after 5 hours of treatment. The

absorption capacity of the interlayer is determined mainly by the layer charge and its distribution between the octahedral and tetrahedral sheets. Montmorillonite is typically characterized by localization of the layer charge in octahedral sheets due substitution of Al to Mg, Fe, and others.

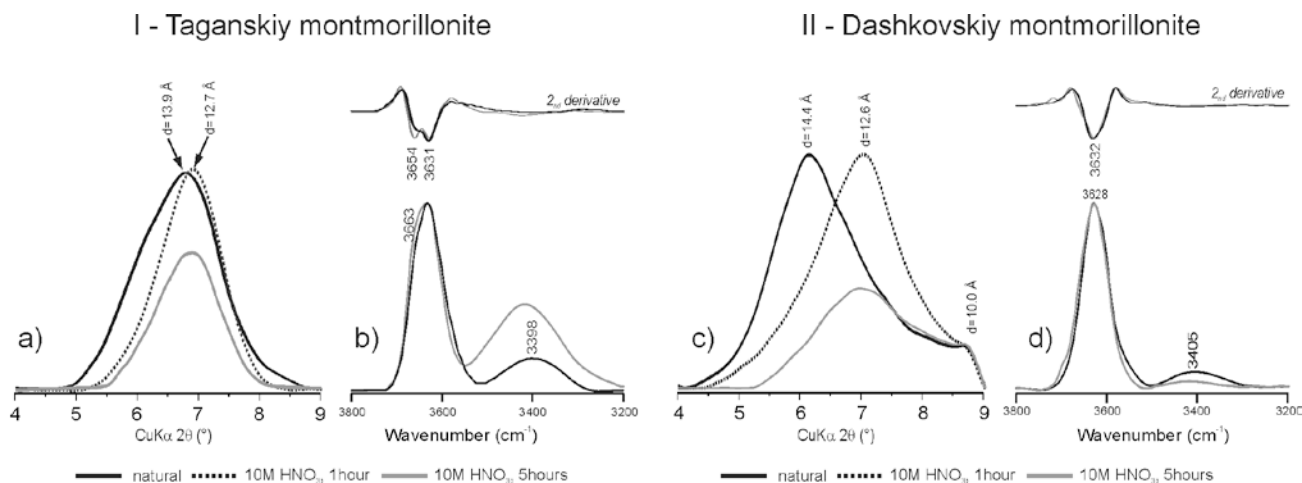


Fig. 1. Fragments of XRD patterns (a, c) and FTIR spectra of Tagansky (I) and Dashkovskiy (II) montmorillonites. Changes from 13.9 to 12.7Å and 14.4 to 12.6Å demonstrates substitution of interlayer cations to oxonium ion. Appearance of the bond at 3654cm⁻¹ indicates pyrophyllite-like structure formation.

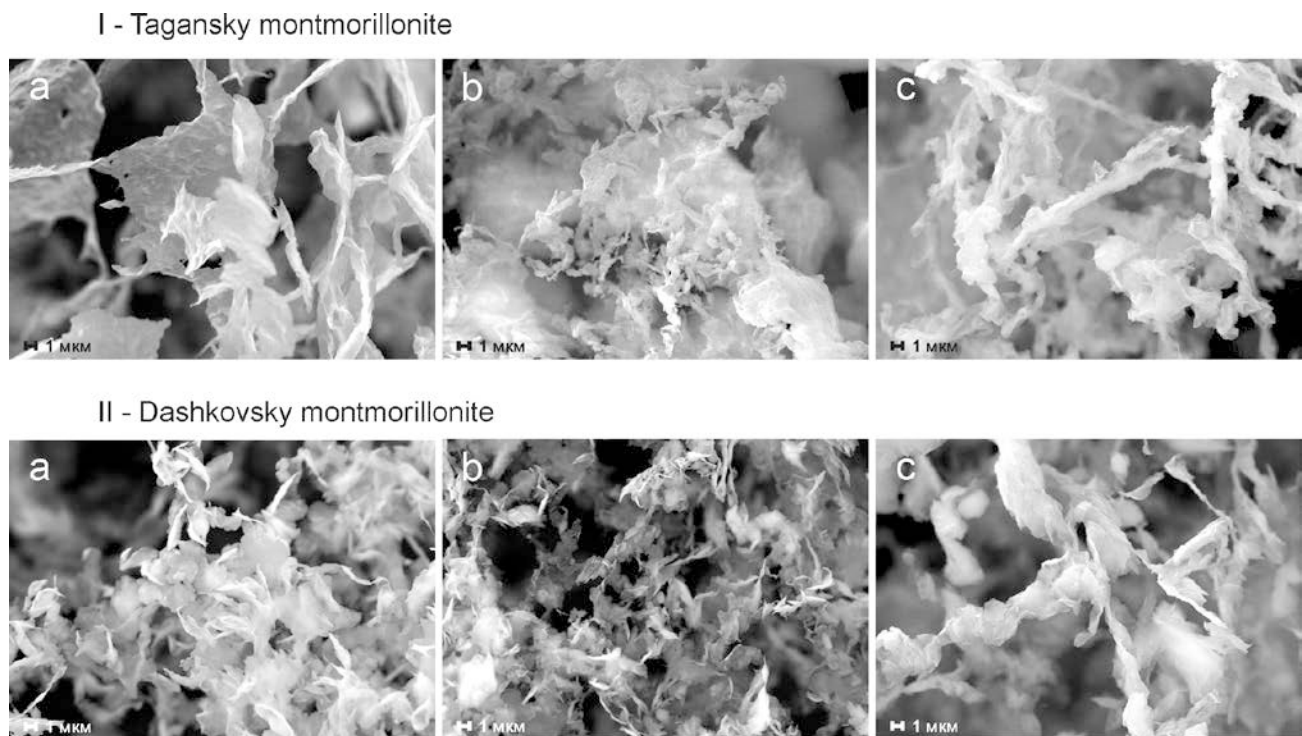


Fig.2. Bentonite microstructure of Tagansky (I) and Dashkovskiy montmorillonite obtained by scan electron microscope: a – natural state, b – after HNO₃ treatment, c – Cs-montmorillonite.

Tagansky montmorillonite belongs to this type. In some cases, a small proportion of isomorphous substitutions of Si to Al gives rise to a tetrahedral charge, respectively. Overall, the amount substitutions of this kind for montmorillonite is low, but very important for the adsorption of cations, in particular Cs⁺. The obtained data on the adsorption of Cs-137 shows that at low concentrations, the process is mainly determined by the absorption of Cs into tetrahedral sheets,

creating a stronger field near the layer surface. Thus, the adsorption capacity for Cs-137 is larger for Dashkovsky montmorillonite which has about 20-30% of the tetrahedral charge whereas Tagansky has the layer charge localized in octahedral grids and therefore the lower adsorption capacity for Cs-137. However, the total amount of adsorbed Cs-133 is determined by the overall cation exchange capacity, which is higher for Tagansky montmorillonite due to a lower layer charge. Partial protonation of the bond couple of octahedral Al^{3+} converts it from 4 to 6-coordinated (He et al., 2015), together with leaching of the octahedral cations when exposed it creates a specific pore structure, associated with an appearance of nano-porosity and increasing micro and meso-porosity. In conjunction with the partial destruction of the structure which was also observed using a scanning electron microscopy, this leads to a significant increase of the specific surface area (up to 150-200% of the initial value). At the same time, as described earlier leaching of the octahedral cation, leads to a reduction of the layer charge, which results in decrease of cation exchange capacity. The mechanism of the cesium adsorption on montmorillonite after a thermochemical impact differs significantly from the natural montmorillonite. The main reason appears to be related to changes of the layer charge and a partial interlayer protonation. Cesium substitutes oxonium than Ca and Mg. Thus, as indicated above, the total amount of the adsorbed cesium is determined by capacitive abilities of montmorillonite and thus is reduced after a long-term treatment with nitric acid solutions.

In summary, this research demonstrates that even after a very aggressive impact that would not be achieved in the radioactive waste isolation site, montmorillonites retain their ability to adsorb cations, including Cs, at a very high level. Such values of the adsorption of the vast number of radionuclides cannot be achieved with other insulation materials. The research results can be used in modeling the transformation of the montmorillonite structure and stability of bentonite barriers properties. Experimental studies have been partially performed on equipment purchased by the Moscow State University Development Programme (X-ray diffractometer Ultima-IV, Rigaku and scanning electron microscopy (Carl Zeiss, LEO 1450VP). The research was carried in a framework of the public contract № 0136-2014-0009 (72-3).

Sellin P. and Leopin OX The use of clay as an engineered barrier in radioactive-waste management - a review. *Clays and Clay Minerals*, Vol. 61, No. 6, 477-498, 2013

Timofeeva MN, Volcho KP, Mikhalchenko OS, Panchenko VN, Krupskaya VV, Tsybulya SV, Gil A., Vicente MA, Salakhutdinov NF Synthesis of octahydro-2H-chromen-4-ol from vanillin and isopulegol over acid modified montmorillonite clays: Effect of acidity on the Prins cyclization. *Journal of Molecular Catalysis A: Chemical* 398 (2015) 26-34. Ref. No. : MOLCAA-D-14-00920

He H., Guo J I., Xie X., Lin H. AND Li L. A microstructural study of acid-activated montmorillonite from Choushan, China. *Clay Minerals* (2002) 37, 337-344

DETACHMENT OF COLLOIDAL PARTICLES FROM BENTONITES IN WATER

S. Kaufhold, R. Dohrmann

*BGR Bundesanstalt für Geowissenschaften und Rohstoffe, LBEG Landesamt für Bergbau,
Energie und Geologie, Stilleweg 2, D-30655 Hannover, Germany*

Bentonites are currently investigated as geotechnical barrier for sealing radioactive waste e.g. in HLRW repositories (HLRW =high level radioactive waste). Their favourable properties are low hydraulic permeability, cation exchange capacity as well as swelling capacity in contact with aqueous solutions. The pre-requisite for this application is the stability of bentonite under the conditions expected. Accordingly, several studies are available dealing with different scenarios of possible alteration processes (e.g. high pH, high salinity, extensive drying). In most of the studies either only a few different bentonites are investigated or a number of bentonites are compared based on only a few parameters. Different bentonites perform rather different in most fields of applications. These differences cannot always be explained by the dominating exchangeable cation only. Therefore, comparative studies considering various different bentonites sometimes allow for the identification of relations between properties and performance.

This study was conducted in order to identify the differences of stability (detachment of colloidal particles and/or dissolution) of bentonites in contact with deionized water, representing the simplest aqueous solution. Some of the bentonites release ultrafine colloidal particles upon shaking of suspensions which cannot be centrifuged even by using an ultracentrifuge with 46,000 g. After centrifugation the supernatant containing the colloidal particles was separated. ESEM, XRD, and IR prove that the colloidal particles are mainly montmorillonites. Considering the stoichiometrical composition of montmorillonites suggests that approximately 10% of the elemental concentration measured in the supernatant stems from dissolution of octahedral sheet. However, detachment of colloidal particles was found to be the dominating mechanism. As expected, the amount of released colloidal particles strongly depends on the amount of exchangeable Na⁺. However, in the present study we show that exchangeable Na⁺ and pH show a good correlation. In a separate test the facilitating effect of alkalinity (at a given Na⁺ content) on detachment of colloidal particles was proved. This can be either due to the increase of solubility of aluminosilicates at pH10 and/or due to the stabilization of the dispersion. In advance of this study it was expected, that bentonites showing a high degree of intergrowth of the fine constituents (e.g. montmorillonite intergrowth with relict volcanic glass) do not release the same amount of colloidal particles at a given exchangeable Na⁺ content and pH compared to bentonites showing a loose microfabric. This was not confirmed in this study.

We, conclude that alkaline Na⁺ bentonites generally are less suitable for the application as geotechnical barrier in HLRW repositories since the probability that colloidal particles are released is higher than in the case of pH neutral Ca²⁺ bentonites. It is conceivable that such colloidal particles are able to transport strongly adsorbed radionuclides. On the other hand detachment of colloidal particles reduces the thickness of the geotechnical barrier itself.

Keywords: Bentonite; Radioactive waste disposal; Detachment of colloidal particles; Erosion stability

The BELBaR project has received funding from the European Atomic Energy Community's (EURATOM) 7th Framework Programme (FP7/2007-2011) under the grant agreement No. 295487

